THE ROLE OF SUBCHONDRAL CIRCULATION IN THE PHYSIOLOGY OF LOAD TRANSMISSION

A DISSERTATION SUBMITTED TO THE UNIVERSITY OF OXFORD



IN PARTIAL FULFILMENT OF THE REQUIREMENTS FOR THE DEGREE OF

DOCTOR OF PHILOSOPHY

BY

MICHAEL BEVERLY

ST PETER'S COLLEGE

TRINITY TERM 2018

ACKNOWLEDGEMENTS

Nothing can adequately express my gratitude for this opportunity to complete a DPhil at Botnar on ideas that first occurred to me in 1985. A host of people have helped me on the way. Specifically I would wish to thank the Wellcome Trust who funded my first year as a research registrar. I thank those supervisors who then left me free to explore the wonders of bone and joint circulation, MRI, isotopes, microbubbles, angiography and more. Joseph Pflug offered a chance to test IOP in his conscious patients in Germany. Robert Mathie at the RPMS and Barbara Sandin at Northwick Park helped with lab work and radiography. Murray Brookes at Guy's and Harry Crock at the Hammersmith personally offered useful advice. Little was published.

Decades passed but the original ideas did not fade. When retirement from the NHS beckoned, my research proposal was turned down by all - save for Oxford. Afsie Sabokbar went out of her way to encourage my application. I am grateful for being accepted and supervised by Jill Urban at DPAG, Peter Winlove in the University of Exeter Physics department and David Murray and OOEC in the Botnar Research Centre.

Barbara Marks and her team made me welcome and patiently assisted with the endless cycle of paper submissions and revisions. Hemant Pandit offered help and MRI data. Various students one third of my age assisted with general computing, Word, Excel, PowerPoint and EndNote. Thomas Cranshaw rebuilt my old Mac and Gil Stamm collaborated with the first 60 MRI study. Simon Hook x-rayed feet and Claudio Pereira produced 200 pairs of X-ray and MRI scans. Two fine Oxford FHS medical students helped, Robert Hyder-Wilson with the second 200 MRI group and Eleanor Vickers did a great job on histology, guided by James Edwards. David Wilson explained MRI technology and Nick Athanasou's lab helped with histology.

After struggling with horse fetlocks in Exeter, a move to calf feet from F. Drury and Sons near Wootton Bassett saved my project. The abattoir men's language, body decoration and tea break chat were a revelation. But I am left with great respect for the physical hard work done by Simon and his men in the hidden world of mass animal slaughter. Back at the lab Jim Dunford's practical help in obtaining kit and chemicals

was very useful. I was kindly offered space in a large lab to play with the bones. It has been a privilege to be accepted as a non-funded senior student and allowed to research my own ideas. Pete Salmond and Jim Busby patiently resurrected lost computer connections on several occasions. Thanks are also due to my fellow students and lab members James Kennedy, Louise Strickland, Hasan Mohammed, Thomas Hamilton, Gulraj Matharu and Stephen Mellon. All have helped with their stats and research experience at different times.

Most of all I have been grateful for challenge and advice from my supervisors Jill Urban and David Murray. When at times it was tempting to just walk away from it all, David's calm approach and immediate grasp of the orthopaedic issues in a new field of physiology, together with his unfailing encouragement, were of fundamental importance. His ability to see the wood for the trees and to improve papers at a glance has been wonderful. Throughout the journey Barbara Marks has been a constant friend with oversight and political and practical advice. She has patiently re-read frequently changing texts and put up with my failure to master Twitter. And to Jo Brown, many thanks for the 'Tweet of the day' mornings, coffee warnings and for your amazing organisation of this work into a thesis.

Finally and above all I am grateful to my wife Celia who has put up with my absence, excuses and delays for long enough. This thesis is dedicated to her.

I formally thank The Wellcome Trust who in 1985 funded my early work (Grant 12425/1.5/SC). I formally acknowledge that the tissue samples obtained from the Oxford Musculoskeletal Biobank and were collected with donor consent in full compliance with national and institutional ethical requirements, the United Kingdom Human Tissue Act, and the Declaration of Helsinki (HTA Licence 12217 and Oxford REC C 09/H0606/11). I acknowledge the OA Pathogenesis Centre whose work has been supported by the Arthritis Research UK Centre for Osteoarthritis Pathogenesis (Grant 202).

ABSTRACT

THE ROLE OF SUBCHONDRAL CIRCULATION IN THE PHYSIOLOGY OF LOAD TRANSMISSION

Michael Beverly **Doctor of Philosophy**
St Peter's College **Trinity Term 2018**

Although the blood supply of bone at rest is well defined, the way in which skeletal activity might affect perfusion under active joints has received little attention. Intraosseous pressure (IOP) has been studied for several decades and was thought to be raised in osteonecrosis, arthritis and bone pain but there has been difficulty in defining IOP and using it for clinical purposes. This work aims to explore subchondral physiology during loading and to seek supporting evidence for a specialised subchondral circulation adapted to load transmission.

Originally in 1985 IOP was studied in an animal model. IOP at rest was found to be variable and sensitive to measurement technique. It had underlying cardiac, respiratory and circulation waves. It was correlated with blood pressure and had a proportionate pulse pressure (PP). Subchondral IOP was raised by proximal venous occlusion and loading. Steroid treatment increased IOP, probably by reducing intraosseous fat volume.

For this thesis in 2014 an in vitro calf foot model was developed and used to further investigate IOP at rest and with combinations of perfusion. The model was then used to study different patterns of loading. Load was found to be transferred partly by hydraulic forces from subchondral to cortical bone through high pressure tolerant tissues. There appeared to be a one way valve within the bone.

Previously undescribed upper tibial vascular marks were found on MRI scans. 60 pairs of scans were scored against osteoarthritis (OA) by Kellgren-Lawrence grade on plain x-rays. Vessels were reduced or lost in early OA. A second study of 200 paired X-ray and MRI scans confirmed the initial results and examined the femoral subchondral vascular marks.

Axial subchondral histology in animal and human tissue showed the presence of subchondral vessels. The subchondral vascular network was found to be present in healthy bone but absent in osteoarthritis. A subcortical valve like structure appears to exist that might allow high pressure hydraulic force transmission without vascular damage. Finally, other evidence in support of the thesis is advanced.

IOP measurement is only a reflection of perfusion conditions in the blood pool at the needle tip. A new understanding of IOP and its use in exploring bone perfusion by a subtraction technique is offered. Load is transferred partly by hydraulic force from the subchondral bone to the cortical shaft. Histologically there are subchondral vessels with possible valves in the subcortical region. A fine subchondral capillary plexus exists under healthy cartilage. Subchondral tissues support hydraulic pressure transmission during weight bearing. Vessels are lost in early OA. Osteoarthritis may be due to failure of vasculo-mechanical circulation in the subchondral region.

TABLE OF CONTENTS

1. INTRODUCTION AND LITERATURE REVIEW.....1

1.1. Bone Circulation - history and literature review 1

1.2. Intraosseous Pressure - history and literature review 6

1.3. In vivo perfusion - literature review 12

1.4. In vivo loading - literature review 13

1.5. In vivo steroids - literature review.....14

1.6. In vitro foot perfusion - literature review 15

1.7. In vitro foot loading - literature review 16

1.8. XR and MRI Study - literature review.....17

1.9. Anatomy and histology - literature review 19

1.10. Clinical background to this work.....20

1.11. Contemporary state of knowledge in 2014.....22

1.12. Thesis – Overview 23

1.13. Hypothesis 26

2. PRELIMINARY IN VIVO STUDY [1] 27

2.1. Background.....27

2.2. Part 1: Introduction - in vivo perfusion 28

2.3. Method.....28

2.4. Part 2: Introduction - in vivo loading.....31

2.5. Method.....31

2.6. Part 3: Introduction - in vivo steroids 34

2.7. Method.....35

2.8. Results.....37

2.8.1. PART 1 Perfusion (Experiments 1-7) 37

2.8.2. PART 2 Loading (Experiments 8-10) 46
2.8.3. PART 3 Steroids (Experiments 11-14) 52
2.9. Discussion (1-14) 55
3. CALF FOOT IN VITRO MODEL FOR IOP AND PERFUSION 72
3.1. Background 72
3.2. Development of the experimental set up 72
3.3. Method 78
3.4. Results (1-7) 84
3.5. Discussion (1-7) 93
3.6. Conclusion 101
4. CALF FOOT IN VITRO MODEL FOR IOP WITH LOADING 102
4.1. Background 102
4.2. Development of set up and methods 102
4.3. Results Part 1 – Static loading 110
4.4. Results Part 2 - Dynamic loading 115
4.5. Discussion 119
4.6. Conclusion 126
5. UPPER TIBIAL VASCULAR MARKS, K-L GRADE AND OA [2] 127
5.1. Introduction – Part 1 127
5.2. Method – Part 1 129
5.3. Results - Part 1 134
5.4. Introduction - Part 2 142
5.5. Method – Part 2 142
5.6. Results – Part 2 147
5.7. Discussion - Part 1 153

5.8. Discussion - Part 2 157

6. SUBCHONDRAL BONE ANATOMY AND HISTOLOGY 162

6.1. Background 162

6.2. Objectives 162

6.3. Method 163

6.4. Results 166

6.5. Discussion 175

6.6. Conclusion 181

7. SUPPORTING EVIDENCE 182

8. CONCLUSION 198

8.1. The Problem 198

8.2. The Hypothesis 198

8.3. The Objectives 198

8.4. The Findings 199

8.5. Research Relevance 206

8.6. Clinical Relevance 206

8.7. Treatment of Painful Bone 207

8.8. The Future 207

8.9. Summary 210

TABLE OF FIGURES

Figure 1.1 Currently accepted pattern of osseous blood flow taken from Gray's Anatomy, 41st Edition 2016. The arterial and venous paths are after Brookes. They seem curiously symmetrical. 5

Figure 1.2 Upper tibial subchondral vessels described by Nelson (left) and Crock (right). 18

Figure 1.3 An upper tibial axial PD_SPAIR MRI scan showing the radiating white marks which appeared to be vascular. 19

Figure 2.1 Diagram showing position of vascular clips and intraosseous needles. 29

Figure 2.2 Experimental set up. The spring loaded pusher covers the foot and prevents flexion and extension while using a longitudinal one body weight load (4520-5400 g). 33

Figure 2.3 Graph showing variation in resting or basal IOP between subjects (mean 22.4 mmHg, SD 13.7) and within subjects (mean 25.9 mmHg, SD 6.8) in 21 subjects at 44 different sites. Blue – femoral head, Red – femoral condyle, Green – upper tibia. 38

Figure 2.4 A representative trace from a typical experiment showing the effect of a 0.5 ml saline bolus flush injection with about 8 minutes to recover followed by aspiration with recovery in less than 30 seconds. A second bolus flush injection and slow recovery follows. Large square = 0.5 cm or 30 secs. 39

Figure 2.5 A representative IOP recording at a faster chart speed of 100 mm/min shows the cardiac pulse and a superimposed respiratory wave. In this section recorded for approximately 40 seconds some 9 respiratory waves and approximately 100 cardiac waves are seen. Large squares = 0.5 cm or 3 secs. 40

Figure 2.6 Systemic administration of anaesthetic agents such as diazepam and fentanyl affected the IOP as in this representative trace. Diazepam appears to have an immediate sedative effect for about 90 seconds. Fentanyl has an excitatory effect with a double circulation time wave pattern each of about 90 seconds. Large square = 0.5 cm. 41

Figure 2.7 Effect of blood pressure on IOP. Intraosseous pressure was measured at 13 sites among five subjects. Pearson correlation r=0.829. 42

Figure 2.8 Pulse pressure (mmHg) with IOP (mmHg) for 44 separate sites among 21 subjects. Pearson Correlation r=0.788. 43

Figure 2.9 Recording showing the effect of clamping and releasing the proximal femoral artery (left half) and clamping and releasing the proximal femoral vein (right side). Large square = 0.5 cm. 44

Figure 2.10 Blue – IOP, Red – PP. Initial or basal IOPb and PPb, arterial clamp IOPa and PPa, venous clamp IOPv and PPv and difference in IOP (IOPv-IOPa) and PP (PPv-PPa) for the perfusion range at the needle tip, n=31 individual records among 14 subjects, error bars SD. 45

Figure 2.11 Showing the effect of loading alone with one body weight. Upper trace - femoral head, middle trace - femoral condyle and lower trace - proximal tibia.

All traces show basal IOP, loading by one body weight for two minutes, rest for six minutes and load for three minutes. The changes in IOP appeared to be simultaneous at all three sites. Vertical scale 0 - 100 mmHg for each trace, trace speed 12.5 mm/min. 47

Figure 2.12 The upper trace is from the femoral head, middle trace femoral condyle and lower trace proximal tibia. From left to right the traces show the effect of arterial occlusion, arterial occlusion with loading, load removal and arterial clamp removal. The second part shows changes at the same sites after venous occlusion, venous occlusion with loading, removal of load and removal of the occluding clamp. The IOP changes are seen to be similar at all three sites and simultaneous. Vertical scale 0 - 100 mmHg for each trace, trace speed 12.5 mm/min. 48

Figure 2.13 Basal IOP during perfusion at rest (IOPb), an increase in IOP with loading by one body weight (IOPb+Ld) $p<0.0002$; IOP during proximal arterial occlusion (IOPa) and with loading during arterial occlusion (IOPa+Ld) $p<0.002$ and IOP during venous occlusion (IOPv) and loading during venous occlusion (IOPv+Ld) $p<0.003$. N=5 subjects, 12 IOP needle sites. Error bars are SEM. 49

Figure 2.14 Left: Injection (between arrows) at the femoral head caused a rise in IOP at the femoral condyle but not the proximal tibia. Centre: Injection at the femoral condyle caused a rise in IOP at the femoral head but not the proximal tibia. (Some artefactual shake is seen on the femoral condyle trace during injection). Right: Injection at the proximal tibia had no effect on the femoral head or femoral condyle IOP. Vertical scale 0 - 100 mmHg on all traces, trace speed 12.5 mm/min. 51

Figure 2.15 The Steroid treated (Red) IOP had higher IOP at basal ($p<0.002$) and with artery ($p<0.03$) and venous ($p<0.05$) occlusion than the non-steroid treated (Green), controls. N=6 steroid, 15 controls. The subtraction values (IOPv-IOPa) remained similar, $p=0.59$. Error bars SD. 52

Figure 2.16 Photograph of femora post angiography and decalcification. Top row steroid treated bones are whiter due to more barium retention. Bottom row controls are darker and contain less barium than the steroid treated femora. . 53

Figure 2.17 showing examples of femoral angiogram microradiographs. The left radiograph shows a pair of femora from a control barium angiogram. The right femoral pair were from a steroid treated subject and demonstrate better barium filling. 54

Figure 3.1 Left - upper tibial articular surface in man and right - proximal metacarpal articular surface of calf. The calf has no menisci. 73

Figure 3.2 Calf feet with radial artery catheter inserted prior to wash out with Krebs-Henseleit saline. 74

Figure 3.3 Experimental set up with serum in Mariotte flask at 150 cm above foot in water bath. 77

Figure 3.4 Experimental set up showing foot in water bath with attached IOP needles and pressure transducers. 78

Figure 3.5 Metacarpal following intra-arterial perfusion of serum with 1% Evans Blue showing penetration throughout the bone. 80

Figure 3.6 Averaged IOP values in 15 feet at 150 cm perfusion pressure after 60 seconds. Blue - fresh feet less than 4 hours old, Red - feet more than 4 hours old. 84

Figure 3.7 Difference in IOP at 60 seconds perfusion at the different sites tested, Blue - MCD - metacarpal diaphysis, Red - MCS - metacarpal subchondral, Green - PPD - proximal phalanx diaphysis. Error bars SD. 85

Figure 3.8 Left pair - perfusion of dye through the artery gives general filling. Centre pair - dye injected into epiphysis, right pair dye injected into metaphysis. There is little cross flow over the epiphyseal plate. 86

Figure 3.9 Rise in IOP with time among 15 subjects at different perfusion pressures, Blue - perfusion at 150 cm, Red - perfusion at 100 cm and Green - perfusion at 50 cm pressure. Error bars SEM. 87

Figure 3.10 Additional rise in IOP with a proximal tourniquet for 60 seconds and the effect of removal of the tourniquet after a further 60 seconds during steady perfusion of serum at 150 cm pressure. Error bars SEM. 88

Figure 3.11 Perfusion at 50, 100 and 150 cms serum pressure after 60 seconds within each individual site. Pearson correlation R2=0.9993. Error bars SD, n=15 feet. 89

Figure 3.12 Relative rates of rise and fall with perfusion at 150 cm serum, n=15 Error bars SEM. 90

Figure 3.13 For fresh feet IOP peaked at about one minute with no further increase up to 100 seconds (t-test $p<0.4$). Blue=150 cm, Red=100 cm, Green=50 cm perfusion pressure, N=8, Error bars SEM. 91

Figure 3.14 Older feet had a different filling curve profile with continued perfusion. They become increasingly oedematous with no obvious IOP end point. Blue=150 cm, Red=100 cm, Green=50 cm perfusion pressure, N=7, Error bars SEM 92

Figure 3.15 The different patterns in filling curves for fresh and old feet at different perfusion pressures. Red – eight fresh feet perfused at 50 cm, 100 cm and 150 cm pressure: Blue – seven older feet perfused at 50 cm, 100 cm and 150 cm pressure. Error bars SEM 92

Figure 4.1 Calf feet with various arrangements of fixator screws and IOP needles in position. 103

Figure 4.2 X-ray of calf feet above showing bifid metacarpal, phalanges and hoof and typical location of Ex-fix screws and IOP needles. 104

Figure 4.3 Calf foot in water bath with scissor type Ex-fix applied. Fixator held by transverse screws through distal third of metacarpal and middle phalanx. IOP needles in metacarpal diaphysis, distal subchondral epiphysis and diaphysis of proximal phalanx. 105

Figure 4.4 showing the posture during ‘standing’ load. (External fixator screws are seen in the mid metacarpal and proximal phalangeal positions and the intraosseous needles are seen in the metacarpal diaphysis, metacarpal subchondral epiphysis

and proximal phalanx positions). The line of weight bearing passes from the tip of the hoof to the carpal joint centre. At the MCP joint the line lies approximately 3 cm in front of the centre of rotation of the MCP joint marked by a red star. 106

Figure 4.5 Radiograph showing the transverse external fixator screws in the metacarpal diaphysis and the IOP needles in the metacarpal metaphysis, subchondral epiphysis and middle of the proximal phalanx. A centimetre scale is seen above and the manual compression loading pusher is seen below with its calibrated internal spring..... 108

Figure 4.6 (Foot 187) showing IOP with standing type loading of 10 kg for 10 seconds with 10 seconds intervals x 3 during perfusion with a tourniquet, removal of the tourniquet at 5 minutes, loading during perfusion alone at 7 minutes, removal of perfusion at 12 minutes, and loading non-perfused at 15 minutes. Blue - serum perfusion pressure, Red - metacarpal diaphysis IOP, Green - metacarpal epiphyseal IOP. 110

Figure 4.7 showing the effect of a 10 kg static load on IOP. Blue no load, Red 10 kg load, n=9. Error bars SEM 111

Figure 4.8 (Foot 143) Blue - perfusion pressure, Red - Metacarpal diaphysis IOP, Green - Metacarpal epiphysis IOP. Perfusion for 60 seconds, then Ex-fix type loading for 10 seconds at each weight, 5, 10, 15 and 20 kg with 10 seconds between as between blue arrows, perfusion off for 60 seconds and repeat load pattern. 112

Figure 4.9 showing that the IOP is proportional to the applied load whether the bone is perfused (Blue) or not perfused (Red)..... 112

Figure 4.10 The change or gain in IOP is well correlated with the applied load in both non-perfused (Red) and perfused (Blue) bone, Pearson correlation R^2=0.984, n=22..... 113

Figure 4.11 (Foot 186) showing an example of IOP with standing type loading during perfusion (left group), with perfusion and tourniquet (central group) and perfusion alone (right group). Blue – serum perfusion pressure, Red – metacarpal diaphysis IOP, Green – metacarpal epiphysis IOP. Each group shows the effect of a static load of 10 kg applied for 10 seconds with 10 second intervals x 3. The tourniquet was applied at 6 minutes and removed at 12 minutes (dotted red line). 114

Figure 4.12 (Foot 177) Example showing effect of three sets of 10 kg static standing type load for 10 seconds with 10 second intervals. Left group - perfused with tourniquet, tourniquet removed at 5 minutes, central group - perfused only and right group - non-perfused. Blue – serum perfusion, Red – metacarpal diaphysis, Green – metacarpal epiphysis. There is a progressive fall in IOP with repeat load in all three perfusion states. 115

Figure 4.13 (Foot 142b) showing a typical dynamic Ex-fix type load trace. Left side non-perfused, right side perfused. Left side 5, 10, 15, 20 kg load x 10 steps in 10 seconds, right side 20 kg x 10 steps in 10 seconds, three groups. Blue – perfusion pressure 0 - 150 cm, Red – metacarpal diaphysis IOP, Green – metacarpal subchondral IOP, Purple – proximal phalanx diaphysis IOP. 116

Figure 4.14 (Foot 141b) showing the effect of dynamic Ex-fix type loading on IOP. Each set of steps is of 20 kg load x 10 steps in 10 seconds. The sequence shows

from the left three sets of 20 kg x 10 steps in 10 seconds during perfusion at 150 cms. Perfusion was stopped at 80 seconds and a further three sets of 20 kg x 10 steps in 10 seconds follows. The load applied at 180 seconds was a steady 20 kg for 20 seconds. Blue – perfusion pressure, Red - metacarpal diaphysis IOP, Green - metacarpal epiphysis IOP, Purple - proximal phalanx diaphysis IOP. 117

Figure 4.15 IOP fluctuation with loading, Blue – 5 Kg, Red – 10 Kg, Green – 15 Kg, and Purple - 20 Kg loads, 10 steps in 20 seconds and associated drop in IOP post exercise for perfused and non-perfused feet, n=25 sites in 11 feet, error bars SEM. 118

Figure 5.1 Left upper tibial PD_SPAIR MRI scan. Third slice down from tibial surface. 128

Figure 5.2 A typical MRI left upper tibial PD_SPAIR slice at level of third slice from upper tibial plateau. Radial vascular marks are evident in all quadrants. The popliteal artery contents are dark while the superficial veins, periosteal veins and proximal tibio fibular joint fluid are bright. 130

Figure 5.3 Kellgren-Lawrence grade reference sheet. These are computer generated teaching images from the internet (osteoarthritis classification WikiDoc). They give more uniform scoring examples rather than clinical radiographs. 131

Figure 5.4 showing the same level 3 MRI slice seen in Figure 5.2 with scoring marks. This slice scored 5, 0, 2, 3 for Anteromedial, Posteromedial, Posterolateral and Anterolateral quadrants. 132

Figure 5.5 The distribution of K-L grades among 56 subjects by severity and side, Blue medial, Red lateral. There was more osteoarthritis medially, $p<0001$, n=56. 135

Figure 5.6 Example of six consecutive axial PD_SPAIR MRI slices from one upper tibia showing vessel frequency and distribution. 137

Figure 5.7 Vascular marks by layer for the first six axial layers below the upper tibial articular surface. Scans slices were 3.0 mm thick and 0.3 mm apart giving a depth of 16.5 mm from the middle of slice 1 to the middle of slice 6 or total depth of 19.5 mm. Error bars SEM, N=56. 137

Figure 5.8 The distribution of vascular marks was as shown with most in the anterolateral quadrant and fewest in the posteromedial quadrant, $p<0.001$ for all. 138

Figure 5.9 showing the reduction in vascular marks with increasing K-L grade. There were insufficient numbers for comparison in grades 3 and 4. 140

Figure 5.10 showing a typical right upper tibial MRI slice at level 3 of the right knee with K-L grade 2 osteoarthritis medially and K-L grade 0 laterally on plain x-ray. The medial vascular marks have been lost while the lateral marks remain. 141

Figure 5.11 Left upper tibial axial slice showing the radiating vascular marks (red arrows) in a typical PD_SPAIR scan at layer 2. 142

Figure 5.12 Left femoral PD_SPAIR slice sixth from joint surface showing vascular marks as indicated. 143

Figure 5.13 Six sequential PD_SPAIR MRI slices from the upper tibia of a right knee. Vascular marks are evident from slice 1 to slice 5.....145

Figure 5.14 An example of a left distal femoral axial slice at level 5 showing 2 transverse white lines medially and 5 laterally. 146

Figure 5.15 Average vascular mark numbers by layer from the upper tibial surface on the medial and lateral sides, Blue – medial, Red – lateral. The distance from the centre of layer 1 to the centre of layer 6 is 16.5 mm. Error bars are SEM....148

Figure 5.16 There was a loss in vascular marks medially with increasing K-L grade, p<0.001. Error bars =SD. 150

Figure 5.17 There was a loss in vascular marks laterally with increasing K-L grade, p<0.002. Error bars=SD. 150

Figure 5.18 The tibial average total vascular marks decreased with increasing K-L grade, p<0.0001, error bars=SD. 151

Figure 5.19 The first 10 axial slices from the distal femur showing the average numbers of vascular marks by layer and medial (blue) or lateral (red) side. The total depth covered is 30 mm. There were more vessels laterally p<0.0001. Error bars=SEM. 152

Figure 5.20 Vascular mark numbers by K-L grade and medial (Blue) or lateral (Red). Error bars = SD. 152

Figure 6.1 Left - human upper tibial articular surface and right - calf proximal metacarpal articular surface. The calf metacarpal is a fused third and fourth metacarpal. (This example was perfused with Evans blue). 166

Figure 6.2 Calf metacarpal after arterial injection with Evans Blue. Subchondral capillary vessels filling is evident. 167

Figure 6.3 Calf metacarpal injected with dilute Evans Blue and squeezed in a vice. The subchondral plexus oozes Evans blue stained blood..... 167

Figure 6.4 Slice of normal human upper tibia showing radiating vascular marks as in an equivalent PD_SPAIR MRI scan. 168

Figure 6.5 Slice of human normal distal femur showing transverse vascular marks as in an equivalent PD_SPAIR MRI scan. 168

Figure 6.6 Photograph of decalcified subchondral section of human upper tibia prior to tissue processing and embedding. Cortical surface left edge in all images. Specimen size 1 x 3 cm. 169

Figure 6.7 Left - calf axial subchondral proximal metacarpal bone. Stain Van Gieson trichrome, x 20 Right – calf axial subchondral proximal metacarpal bone. Goldner's, x 20. Subchondral vessels running towards the juxta articular cortex which is still cartilaginous in the calf at this age. Cortex to the left in all images. 169

Figure 6.8 Low power human subchondral bone in the axial plane. Cortex to left in all images. Axial plane - vein and artery pairs are seen. 170

Figure 6.9 A composite image from three calf axial subchondral proximal metacarpal low power H&E images demonstrating the length of the vessel bundle of

approximately 2 cm running in the subchondral plane. The vascular channels run straight towards the cortex but bend or kink at the margin..... 171

Figure 6.10 Both images show calf axial subchondral proximal metacarpal bone, H&E, x 20 showing vessels angulating as they exit the medulla and enter the cartilaginous cortex. 171

Figure 6.11 The image shows calf axial plane subchondral proximal metacarpal bone, H&E, x 20. Example of vascular channels traversing the cartilaginous cortex. 172

Figure 6.12 Both slides show normal human upper tibial axial subchondral longitudinal vessels running towards the cortex. As the vessels approach the cortex they become convoluted and distorted. Left - Van Gieson trichrome. Right - Goldner's, x 20. 172

Figure 6.13 Both images show axial subchondral vessels reaching the cortex in normal human upper tibial slices. Complex angulation and distortion develops. Left - H&E, Right – Goldner's, x 20. 173

Figure 6.14 Both images show axial subchondral vessels reaching the cortex in normal human upper tibial slices. Complex angulation and distortion develops. Left - H&E, Right – Masson's trichrome, x 20..... 173

Figure 6.15 Higher power view of normal human upper tibia axial plane sections with vascular distortions at the cortex. Left Masson's trichrome, right H&E x 40. 174

Figure 6.16 Two sections of healthy human articular surface cartilage in sagittal section showing fine capillaries in the subchondral region. H&E x 20. 174

Figure 6.17 Section of human upper tibia with early osteoarthritis in sagittal section showing a lack of subchondral vascular features, unhealthy overlying cartilage and early surface fibrillation beginning. H&E x 20. 175

Figure 7.1 Volunteer walking during measurement of pressure in dorsal foot vein, subcutaneous calf tissue and upper tibial intraosseous pressure. 183

Figure 7.2 IOP trace showing upper tibial IOP recording from subject taking 10 slow steps, 20 fast steps, running on the spot and 10 slow steps, each with 20 second rest interval between exercises. Vertical scale 0 - 500 mmHg. Large square 0.5 cm or 3 secs. 183

Figure 7.3 Images of femora from the internet (anatomycorner.com) showing the articular margin holes which may be venous exit channels. 185

Figure 7.4 Left – 90 ° capillary/arteriole junction with thickened cuff of cells at junction. Gomori x 560. Right – cortical bone surface showing vein with circular muscle constriction. Gomori x 150. Taken from Burkhardt 1975... 193

TABLE OF TABLES

Table 2.1 showing values for IOP (mmHg) at 12 sites among five subjects. Columns are for basal IOP at rest (IOPb), with only loading (IOPb)+Ld (difference $p<0.0002$), proximal arterial occlusion (IOPa), arterial occlusion with load (IOPa)+Ld (difference $p<0.002$), venous (IOPv) occlusion and venous occlusion and load (IOPv)+Ld (difference $p<0.003$). 49

Table 3.1 At 150 cm perfusion pressure the fresh feet showed no significant difference in IOP from 60 to 100 seconds (32.4 mmHg to 29.8 mmHg, $p= 0.4$). 90

Table 5.1 Distribution of patients at each K-L grade. There was proportionately more osteoarthritis medially. There were more patients in the lower grades..... 136

Table 5.2 showing the vascular marks score for the above six slices by layer and medial or lateral side. 145

Table 5.3 There was a significant difference in average vascular mark numbers between the medial and lateral sides of the tibia at all levels as set out above. 149

ABBREVIATIONS

3Rs of animal research	Replace, Refine, Reduce
AVN	Avascular Necrosis
BMI	Body Mass Index
DDH	Developmental Dysplasia of the Hip
DHS	Dynamic Hip Screw
DIPJ	Distal Inter Phalangeal Joint
IOP / IOPb	Intraosseous Pressure / IOP basal
IOPa	IOP with arterial occlusion
IOPv	IOP with venous occlusion
K-L	Kellgren-Lawrence grade of osteoarthritis
MCPJ	Metacarpo-phalangeal Joint
mmHg	Millimetres of Mercury
MPa	Mega Pascal
MRI	Magnetic Resonance Imaging
OA	Osteoarthritis
ON	Osteonecrosis
OUH	Oxford University Hospitals NHS Foundation Trust
PET	Positron Emission Tomography
PD_SPAIR	Proton Density Spectral Attenuated Inversion Recovery
PIPJ	Proximal Interphalangeal Joint
PP	Pulse Pressure
R&D	Research & Development
SD	Standard Deviation
SEM	Standard Error of the Mean
SLE	Systemic Lupus Erythematosus
T2	T2 MRI scan for water bright image
X-Ray	Radiograph

1. INTRODUCTION AND LITERATURE REVIEW

1.1. Bone Circulation - history and literature review

[Details of the methods used for the following literature searches are set out in Appendix 1]

Early investigation

Mankind has long had an interest in bone, perhaps initially finding its structure useful for weapons or tools and the marrow good to eat. Early Egyptian orthopaedic interest is recorded in the treatment of fractures. Subsequent civilisations continued to focus mainly on the treatment of injuries and on bone disease rather than on the nature of the organ itself (Brorson 2009). Hippocrates of Kos (460 - 370 BC), the 'Father of Medicine' and perhaps of ethical medical behaviour, is credited with the idea that illness has a cause, rather than being due to fate or the Gods. He linked disease to the four humours – black bile, yellow bile, blood and phlegm but tempered this approach with more useful orthopaedic advice (Livingston 1988). Galen of Pergamum (120 - 217 AD) followed Hippocrates' teaching and influenced Western medical thought for the next 1,300 years (Ponseti 1991). Leonardo da Vinci (1452 - 1519) the Renaissance polymath, produced some 13,000 pages of notes and drawings during his lifetime often displaying a strong interest in the cardiovascular and orthopaedic systems (Burrows 1952). Blood was thought to ebb and flow along vessels until William Harvey (1578 – 1657) was credited with the discovery of the circulation (Harvey 1628, Keynes 1966).

It was not until the invention of the microscope by van Leuwenhoek (1632 – 1723) that it became possible to observe, in strong sunlight, cellular detail and the capillaries of

different tissues (van Leeuwenhoek 1700). Clopton Havers (1657 – 1702) described in Latin the ‘canaliculi’ in cortical bone and also ‘medullary oil’ whose function is discussed further in Chapter 6 and 7 (Havers 1691). Albinus in 1754 combined skill as an injector of blood vessels in the dissecting room with macroscopic observation of split long bones. He suggested that the cortex depended on a dual blood supply from the medullary cavity and the periosteum (Albinus 1761).

John Hunter (1728 – 1793) based his career on a detailed study of anatomy, both animal and human (Hunter 1861). Surgery then was often crude or fatal but he recognised the importance of the blood supply to a limb. Hunter also described a ‘vascular mesentery’ or rich capillary plexus in the immediate subchondral region which might be of nutritional value to the cartilage. Hunter’s vascular mesentery has attracted little attention subsequently but is considered again in Chapters 6 and 7 (Lemperg 1978). Astley Cooper (1768 – 1841) was another early Victorian surgeon with vascular and orthopaedic interests. Though much of his anatomy school material was perhaps obtained by grave robbers, his work describing the blood supply to bone and to the hip has endured (Cooper 1973). Others followed a similar path. James Paget (1814 – 1899) was a distinguished late Victorian anatomist and pathologist. At that time the hardness and opacity of bone caused the blood supply within to remain obscure (Paget 1966).

Radiology

The discovery of x-rays by Roentgen in 1895 allowed internal bone structure to be clearly seen (Roentgen 1959). Bony vascular anatomy was then described in more detail, for example, by Lexer (Lexer 1904). He injected the arterial systems of new-born and adult post-mortem subjects with a mercury-turpentine emulsion and took stereoscopic radiographs of the specimens. Spalteholz (1861 - 1940) proposed a method

for calcified tissue clearance by acid (Steinke 2001). Since 1911 his technique has frequently been employed using dilute acid to slowly dissolve the opaque calcium from bone. The protein matrix and vessels left behind form a soft pliable model of the original bone. That may then be x-rayed or sectioned to show injected vascular pathways which have retained their barium or other casting material. Barclay, a radiologist working in Oxford in the late Forties, explored intraosseous bone circulation. He used barium sulphate emulsion injected into arteries under pressure then examined on fine grained x-ray film. He later used cine radiography (Barclay 1947).

Arterial supply

Much of the early interest in bone circulation was focussed on the question of centrifugal or centripetal flow within long bones and to what extent there was periosteal, cortical and medullary supply. Joseph Trueta, also in Oxford, used Barclay's techniques to study the finer details of intraosseous circulation particularly around the hip and femoral head. He was interested in the differences between the juvenile and adult circulation and changes in relation to growth. His paper describes detailed capillary anatomy together with vessels penetrating the articular bone-cartilage junction to supply cartilage. He suggested that slow flow in the subchondral capillary loops might favour the precipitation of bacteria or metastatic tumour. He was interested in the differences in circulation between red and fatty marrow and concluded that the vascular pattern remained the same but that the capillaries enlarged with haemopoiesis (Trueta 1964).

Harry Crock from Australia wrote extensively on the blood supply of bone (Crock 1962). He clearly described radiating subchondral vessels in the upper tibial axial plane as did Nelson (Nelson 1960) but their work did not trigger any interest in the possibility that there was a functional reason for those vascular patterns.

Nelson and Crock seem to have been among the only authors to take an interest in the axial or subchondral plane. Almost all others have examined bone circulation in longitudinal, sagittal or coronal sections. Murray Brookes spent a lifetime studying the blood supply of bone (Brookes 1998). He too used barium sulphate, Indian ink or plastic injection of animal and human bones combined with microradiography, electron microscopy and photographic enlargement to produce detailed studies of the osseous circulation. It is those images that form the basis of our current understanding of bone circulation depicted in Gray's Anatomy. More recent anatomists appear to have re-discovered the trans-cortical capillaries previously identified by Albinus in 1761, Brookes and others since (Grüneboom 2019).

Venous drainage

While it has been possible to explore the arterial blood supply to bone, the venous circulation has proved more awkward. It is a relatively simple matter to inject a limb artery under reasonable pressure with a dye or filler and to decalcify and examine the results radiologically or histologically in minute detail. The venous system is more difficult to define. The average limb has one or two supplying arteries but many superficial and deep draining veins. Those vessels are thin walled and do not tolerate much pressure for retrograde injection without leaking or bursting. There are valves preventing retrograde flow. Veins do not mirror the arterial supply but often form a web of anastomosing and dividing pathways communicating between deep and superficial layers with sinuses, loops and bypasses.

Others have injected the bone itself with contrast or latex and observed the emerging venous pathways. That may well delineate the extra osseous drainage but can hardly give an accurate idea of the intraosseous venous pattern (Handley 1991). In addition

there appear to be possible valves at the bone subcortical level, described in Chapter 6, which may prevent retrograde intraosseous flow. Unfortunately the result has been that anatomists generally assumed that there is a reciprocal tributary pattern to the venous drainage which is a mirror image of the arterial supply. This is as illustrated in the current edition of Gray's Anatomy (Standring 2016) as in Figure 1.1.

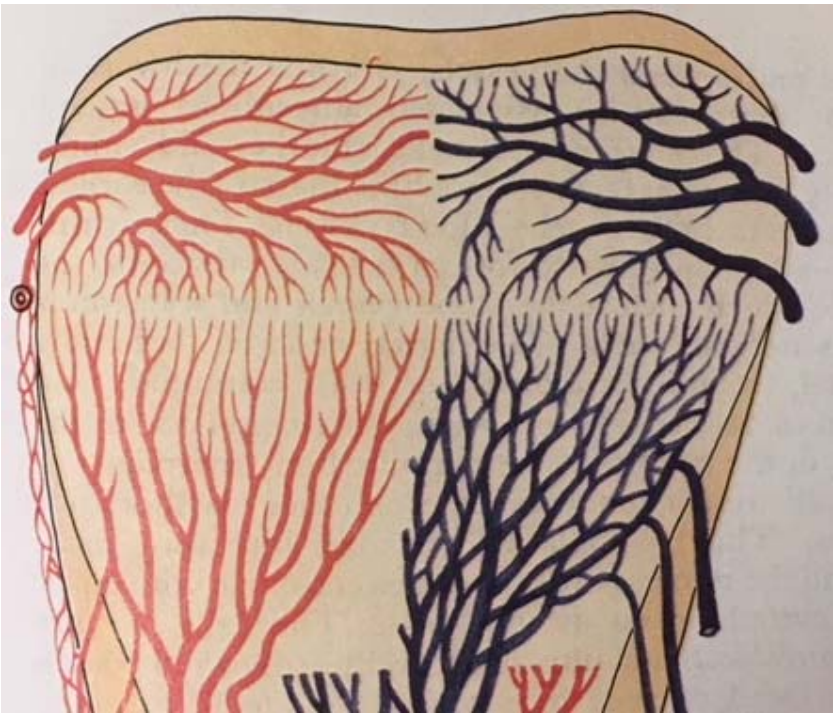


Figure 1.1 Currently accepted pattern of osseous blood flow taken from Gray's Anatomy, 41st Edition 2016. The arterial and venous paths are after Brookes. They seem curiously symmetrical.

The authors mentioned above have generally approached the subject from a 'vessel chasing' perspective. They begin at a larger vessel and follow it as far as their techniques allow. Their work has usually been in static, post mortem or isolated bone. Few of the anatomical studies to date are based on bones or joints which are exercising or weight bearing at the time of injection (Prisby 2017).

1.2. Intraosseous Pressure - history and literature review

Intraosseous pressure (IOP) has been of interest to orthopaedic surgeons since the early 20th century. For much of that time it was assumed to be connected in some way with bone circulation and the development of osteonecrosis. This work explores IOP and introduces a potentially new field of subchondral physiology.

Intraosseous pressure (IOP) might be defined as that pressure found within the cancellous substance of a bone. It is usually measured by the insertion of a needle and trochar or cannula directly into the area of interest. The needle would then be connected to a manometer or pressure recorder. What exactly causes the pressure remains controversial. In the past it has been assumed to be either a reflection of venous back pressure, or due to tissue turgor or fat and soft tissue swelling. As early as 1938 Larsen showed that drugs which changed the systemic blood pressure produced a similar but reduced effect on IOP. He also recognised that high pressure injection of saline into bone, for example to clear an intraosseous needle, could later cause osteonecrosis (Larsen 1938). Yet the intraosseous injection habit persists (Ficat 1985, Frascone 2007, Taylor 2011, Suominen 2015).

More interest in IOP is reported in the 1950s and 60s. Azuma produced a classic paper on IOP in 1964. He recognised that the marrow was a semi-closed space and thought that IOP would be a good indicator of bone perfusion. He sought to explore the effects of various systemic drugs on IOP and showed that there was great individual variation in IOP. He found that nerve stimulation and cardiovascular stimulants altered IOP proportionately. There was a change in IOP with altered flow to the limb. He found regional variations in IOP together with pulsatile and respiratory wave forms. He also

described but could not explain IOP ‘undulations’ without systemic pressure change (Azuma 1964).

Since his paper there has been little progress in understanding the physiology of intraosseous perfusion. Keck carried out IOP measurement after various arterial and venous ligation experiments but was chiefly interested in the subsequent growth arrest patterns (Keck 1965). Arnoldi combined IOP studies with intraosseous phlebography and found a raised IOP in bone pain and osteoarthritis (Arnoldi 1972). It was recognised that relieving bone pressure by drilling might treat pain in osteoarthritis (Åström 1975). Wilkes and Visscher measured venous pressure and IOP through a small endosteal bone window. They found them to be comparable and so assumed that IOP was due to venous back pressure (Wilkes 1975). Interest in the effects of decompression on the treatment of osteoarthritis continued (Termansen 1976, Hietala 1977).

In the mid-70s there was an epidemic of corticosteroid induced osteonecrosis. Several papers discussed IOP measurement and animal experiments with steroid induced osteonecrosis at that time (Glade 1982, Boskey 1983, Wang 1983, Kawai 1985, Matsui 1992) and some of that interest has continued to the present (Miyanishi 2002, Drescher 2004, Sen 2012).

There was further interest in IOP with the development of the North Sea oil industry in the 1970s as a result of which divers with caisson disease were seen. At the same time it became possible for tunnellers to work in high pressure air to reduce flooding such as during the construction of the Mersey and Dartford tunnels. They too suffered decompression accidents and caisson disease but in a pattern quite different from the divers. A registry was kept in Newcastle (Davidson 1975, McCallum 1984) but interest seems to have waned with the decline of commercial diving. There was an unexplained twelve-fold difference in femoral head osteonecrosis between the two groups but the

difference in their patterns of osteonecrosis attracted little attention (Beverly 1987, Beverly 1987).

Subsequently organ transplantation and head injury management used large doses of steroids with corresponding increases in osteonecrosis and associated research (Inoue 2003).

In more recent times those mainly involved with IOP work have included Arnoldi who described IOP changes with joint position and intraosseous phlebography (Arnoldi 1980), and Arlet, Ficat and Hungerford whose book 'Bone Circulation' summarised the state of knowledge in 1984 (Arlet 1984). In 1985 Ficat described his technique for the 'functional exploration of bone' in osteonecrosis but there has been little take up or interest since (Ficat 1985, Petty 1986).

Several authors have reported their dissatisfaction with the measurement of IOP (Camp 1986, Petty 1986, Warner 1987, Lausten 1990). Yet as early as 1964 Azuma recognised that IOP did not have a fixed value but varied with the individual tested, the specific site within a bone, the bone blood flow and venous occlusion. It is surprising that the many investigators since have not materially advanced this view (Azuma 1964, Salzman 2017).

Contemporary understanding of osteoarthritis.

Originally osteoarthritis was considered to be a disease of ageing and natural wear and tear. More recently it has been regarded as a 'whole joint' disease involving all structures around the affected joint (Sharma 2008). Others regard the osteoarthritic process as one of the most chronic health disorders in the western world and one which becomes particularly common with advanced age. The joints most commonly affected by OA include the knees, hips, ankle, elbow, shoulder, hand, wrist and spine. Risk

factors that may increase the risk of developing OA are age, gender, joint injury or overuse caused by physical labour or sports, obesity, joint alignment, and heredity. Symptoms of OA may appear well after disease onset. Such symptoms include joint pain, limitation of motion and stiffness after inactivity, tenderness, crepitus, and joint enlargement. While previously characterized as a disease of progressive articular cartilage degradation, OA pathophysiology involves all of the tissues that form the synovial joint which are the subchondral and metaphyseal bone, synovium, ligaments, joint capsules, and the muscles acting across the joint. Subchondral bone remodelling, osteophyte formation, synovial inflammation, ligamentous laxity (loose ligaments), and the weakening of periarticular muscles exemplify several joint structure alterations observed. Chondrocytes, the only cell types present in the articular cartilage, are responsible for maintaining an equilibrium between the anabolic and catabolic activities in the extracellular matrix (ECM). The trigger of OA is unclear; however, it may begin with tissue damage from mechanical injury, infiltration of inflammatory mediators from the synovium into the cartilage, or defects in cartilage metabolism/homeostasis. Chondrocytes attempt to repair cartilage damage/degradation by increasing the production of ECM macromolecules. As degeneration continues, catabolic mechanisms overpower the anabolic capabilities of chondrocytes and the homeostatic balance is tipped resulting in progressed cartilage breakdown (Loeser 2012, Barr 2015).

Osteoarthritis and Osteonecrosis

Blood supply in osteoarthritis has been analysed with various scans, Tc99 MDP isotope scans, PET/CT scans and MRI scans, with and without contrast, but the results vary. Some authors point to increased blood flow with increasing osteoarthritis and others the converse. Several different types of bone scans have been used in osteoarthritis. While

there is clear evidence that osteoarthritis and degenerative vascular disease are linked, the literature finds both increased and reduced uptake in osteoarthritis. It is not always clear if the increased uptake is in fact within the osteoarthritic bone or in surrounding tissues which may have inflammation and an enhanced blood flow as a reaction to the osteoarthritis (Findlay 2007, Temmerman 2013, Dyke 2015, Savic 2016, Kim 2017, Park 2017). Isotope bone scans have been used in osteoarthritis but the results are confused. While Park found increased uptake (Park 2017) others have found he results less reliable (Yoon 2013).

In any event there is little doubt that osteoarthritis is epidemiologically linked to degenerative vascular diseases (Conaghan 2005, Fernandes 2015).

Intraosseous pressure has been extensively studied in the clinical assessment of ischaemic necrosis of bone otherwise known as avascular necrosis (AVN) or osteonecrosis (ON). Most authors report a raised IOP in early arthritis (Arnoldi 1972, Solomon 1981), with osteonecrosis and in alcohol and steroid treated subjects, in systemic lupus erythematosus (Conklin 1983, Learmonth 1990, Breusch 2000), in anterior knee pain (Hejgaard 1984) and in early pre-scintigraphic change cases of osteonecrosis (Morscher 1984).

Ficat claimed that in the ‘functional exploration’ of avascular change in bone the IOP and its response to a ‘saline bolus stress test’ were at higher pressures than in normal bone. In fact, most reported techniques of IOP measurement rely on an intraosseous injection of some volume to clear the needle before pressure readings begin. The consequences of this method of measurement are explored in Figure 2.4, Chapter 2.

The picture is complicated by the work of several authors who have attempted to produce animal models of avascular necrosis of bone either with steroids (Gold 1978, Kenzora 1978, Wang 1985, Jones 2004) by joint capsule tamponade, by direct vascular

occlusion, or by microspheres, cryotherapy, heating and other techniques outlined in a review by Jones (Jones 2011). Recently there have been further attempts to understand the association between bone and fat or adipocytes. None appears to consider that there might be an interesting mechanical or hydraulic relationship to the semi-liquid fat and the delicately aligned trabecular network (Rendina-Ruedy 2017).

Influence of loadbearing on IOP

Bone is obviously designed to have a role in locomotion. It is surprising therefore that so little attention has been paid to the possibility that the anatomy and blood supply might be better interpreted in terms of the function of the organ or that they might be modified in any way to cope with the forces likely to be present at joints. Other than the work of Tondevold who used microspheres and showed a general increase in cortical and cancellous blood flow after two hours of exercise in dogs, there is very little research analysing blood flow in bone during exercise (Lemperg 1978, Tondevold 1983, Stabley 2014).

Denham and others had recognised some time ago that up to five times body weight might be transferred across the hip joint during walking, yet virtually no research pursued this to examine how the tissues might bear such potentially destructive forces at the joint and subchondral level (Denham 1959, Afoke 1987). In the sixties Swanson, Freeman and others did consider the possibility that bone might be hydraulically strengthened. They carried out experiments using dry bones saturated in grease or used isolated cancellous bone plugs in testing jigs struck by weights (Swanson 1966, Hwa 2004). Hwang in 2008 looked at the ‘hydraulic conductance’ or flow of saline under pressure across isolated bone cores in normal and arthritic bone (Hwang 2008). These far from physiological studies concluded that there was no hydraulic effect in weight

bearing. The matter does not otherwise appear to have been much considered (Beverly 1987, Beverly 1987, Beverly 2012, Beverly 2015). Only very recently has Simkin suggested that marrow fat may play a part in energy distribution at the subchondral level with load stretching the elastic trabecular walls (Simkin 2018). If there is a dynamic aspect to the circulation and physiology of blood flow around actively loaded joints it has been comprehensively ignored.

1.3. In vivo perfusion - literature review

In preliminary unpublished clinical work from 1983 to 1985, we measured IOP in man prior to forage, osteotomy or decompression, in anaesthetised and conscious walking subjects (Gardner 1989). The findings were variable. An intraosseous pressure approach was used because a raised intraosseous pressure had been associated with bone pain in osteoarthritis and osteonecrosis and in vascular diseases such as osteonecrosis and Perthes' disease of the hip in children (Ikeuchi 2015). Osteonecrosis was a clinically important condition at that time for several other reasons. Embolic bone diseases such as sickle cell disease, caisson disease and the storage diseases such as Gaucher's have been reported to have a raised IOP (Mukisi 2009). Alcoholism, corticosteroid use and diabetes have also been associated with a raised IOP (Zizic 1986). Osteonecrosis incidence varies across cultures but is said to affect 10 - 20,000 new patients a year in the USA. Worldwide, osteoarthritis affects the majority of the ageing population (Allen 2015). It had usually been thought that IOP had a static or fixed value which was due to venous back pressure, intramedullary or interstitial pressure (Arnoldi 1972). IOP had been measured experimentally in animals and in man. Steroid induced models of avascular necrosis have been developed in order to study IOP and its treatment

(Drescher 2002, Miyanishi 2002). Ficat and others developed a technique for the 'functional exploration' of bone in patients with early osteonecrosis (Ficat 1985).

The rationale for the initial in vivo study in 1985 was therefore to explore the physiology of IOP in healthy subchondral cancellous bone at rest in an animal model. The rabbit was chosen because of its availability in the RPMS animal laboratory, Home Office licensing requirements and because much of the previous literature had used the rabbit as a model. The factors that controlled IOP at rest and during activity and the physiology of subchondral bone circulation remained largely unknown. It seemed appropriate to develop an animal model which would allow IOP to be explored on a more scientific basis than occasional attempts to measure it in theatres as part of forage.

1.4. In vivo loading - literature review

As the musculoskeletal system is clearly designed for weight bearing, studies of intraosseous pressure should be not only under static conditions but also under conditions of loading or during activity in vivo (Day 1975, Afoke 1987). There has been very little published on IOP during joint weight bearing in vivo (Beverly 1987), (Beverly 2016). Denham and others calculated that a considerable force, perhaps five or more times body weight, is transmitted through weight bearing joints in use (Denham 1959, Klenerman 1967, D'Lima 2012). Previous authors have explored the possibility that bone might be hydraulically strengthened but those tests used non-physiological techniques such as grease saturated dry bones or bone plugs in mechanical testing jigs or tests of trans-osseous perfusion (Swanson 1966, Bryant 1983, Kafka 1983, Hwang 2008). The physiological relationship between subchondral intraosseous pressure, loading and blood supply in normal healthy bone had received little attention. The

hypothesis was that loading forces might be transmitted by hydraulic pressure through bone fat and marrow from the subchondral region to the trabeculae and on to the cortical shaft during weight bearing. The effect of physiological loads on subchondral IOP was therefore studied in the animal model together with the effects of load combined with vascular occlusion. Compartmentalisation within and between bones was also tested by selective saline injections.

1.5. In vivo steroids - literature review

Corticosteroids are recognised to be associated with the development of avascular bone disease or osteonecrosis. Steroids are thought to cause intraosseous fat cell swelling. Other conditions including alcoholism, diabetes, chemotherapy, radiotherapy and a variety of embolic bone diseases, for example, sickle cell anaemia and caisson disease, trauma, atherosclerotic vascular disease, storage diseases such as Gaucher's and lupus have also been implicated in osteonecrosis (Zizic 1989, Liu 1991, Kerachian 2009, Mukisi 2009, Cooper 2010, Fukushima 2010, Han 2010, Sheng 2013).

In children, Perthes' disease of the hip and perhaps osteochondritis dissecans may have a vascular basis. Many cases are idiopathic with no obvious cause. Iatrogenic osteonecrosis has occurred with excessive abduction force in infant hips with DDH and after forced saline injection (Taylor 2011).

Experimental models for osteonecrosis have included a variety of different animals and birds from rats to pigs and geese to emus (Gosling 1987, Holm 1990, Boss 2003, Drescher 2004, Drescher 2006, Goetz 2008, Yang 2009, Wang 2010, Tian 2013). Models used have included vascular obliteration, freezing, chemicals and radiation and steroids in various dosage regimes. The rabbit has frequently been used as a steroid

treated model for femoral head osteonecrosis and to assess treatments which may be of use in man (Keck 1965, Gronlund 1984, Shih 1991, Yang 2009, Tian 2013). The results of testing IOP in a steroid treated in vivo model were therefore explored.

1.6. In vitro foot perfusion - literature review

In terms of in vitro models for the study of IOP perfusion both at rest and with weight bearing there is very little previous literature. Intraosseous pressure and bone blood flow have been studied by authors interested in bone circulation, bone diseases and bone pain for more than 70 years in animal models such as the rabbit (Azuma 1964), and dog (Wilkes 1975) and in children with Perthes' disease (Green 1982) and Liu (Liu 1991) measured IOP. In man IOP was studied by Arnoldi, Lempberg, Termansen, Ficat and others. Measurement techniques have varied and there has been difficulty in establishing reliable values for IOP (Azuma 1964, Bourne 1972, Bouteiller 1983, Bryant 1983, Hungerford 1985, De Lorenzo 2014, Frascone 2015, Salzman 2017). It is has generally been assumed that IOP is due to a background venous or intrinsic tissue pressure (Zizic 1986, Zhang 1998, Miyanishi 2002, Mukisi 2009, Pasley 2015) and that the same pressure is present throughout the bone. There has been limited progress in understanding IOP perfusion since Azuma reported IOP fluctuation in a rabbit model in 1964 (Azuma 1964).

IOP has generally been found to be raised in bone diseases such as osteonecrosis and after steroid use (Cruess 1975, Chryssanthou 1978, Glade 1982, Aglietti 1983, Bouteiller 1983, Boss 2003, Miyanishi 2005, Kuribayashi 2010). A raised IOP has been associated with pain in osteoarthritic joints, chondromalacia patellae and with cartilage degeneration (Kofoed 1986, Ho 2014). IOP may also be important in driving fluid

through canaliculi, hence governing osteocyte activity and bone turnover (Cardoso 2013, Verbruggen 2014). Clinical measurement of IOP in man has offered variable results (Salzman 2017). Ficat developed a technique for the 'functional exploration' of bone in patients with early osteonecrosis but this has not been widely adopted (Ficat 1985).

However, the factors that control IOP at rest and the physiology of subchondral bone circulation remained largely unknown. Although intraosseous pressure had been of historic interest in osteonecrosis, osteoarthritis and bone pain it was of limited practical clinical value. The earlier in vivo studies in Chapter 2 showed that IOP is not a constant but fluctuates predictably with systemic vascular pressure changes and loading. The calf foot in vitro model was therefore developed in order to comply with the 3Rs of research, to confirm the earlier in vivo findings and to act as a model for possible further work on changes in IOP with weight bearing.

1.7. In vitro foot loading - literature review

It was previously generally assumed that IOP was due to venous back pressure or an intrinsic tissue pressure. Long ago it was recognised that joints were loaded in vivo with huge forces several times body weight. The possible fluid and mechanical stresses at quite low loads have been considered in mathematical models of joint loading (Dabiri 2013). Cadaveric hip joint forces have been measured (Downey 1988) and (Day 1975) and forces in active knees (D'Lima 2012). Others have shown that weight bearing may not be associated with development of osteonecrosis (Okazaki 2012). However, there are few if any accounts of IOP recording during loading in physiological conditions (Downey 1988, Simkin 2018). The calf foot model was used to pursue IOP changes with different patterns of loading.

1.8. XR and MRI Study - literature review

It is well known that osteoarthritis (OA) of the knee is a significant economic cost to society with morbidity affecting much of the ageing population (Hunter 2014). Diagnosis is traditionally by clinical and radiological examination. The aetiology of primary osteoarthritis is usually thought to be multifactorial with age related wear and tear, overload, trauma, genetic factors and systemic disease being recognised as major contributors. Vascular disease has not usually been considered a significant factor (Abramson 2009).

John Hunter described a subchondral vascular 'mesentery' in the 18th century and Nelson and then Crock in described a further subchondral plexus of vessels in the upper tibia (Nelson 1960, Crock 1962). They used Indian ink and latex with decalcification. Figure 1.2 shows images from their papers. Little interest has otherwise been directed at subchondral blood vessel patterns underweight bearing joints. It seems that when detailed vascular anatomy is considered it is usually in the longitudinal sagittal or coronal plane rather than in the subchondral or axial plane. It is also evident that much of the vascular and histological interest has focused on the cartilage / bone interface rather than on the deeper subchondral vascular plexus described by Nelson and Crock and shown in Figure 1.2.

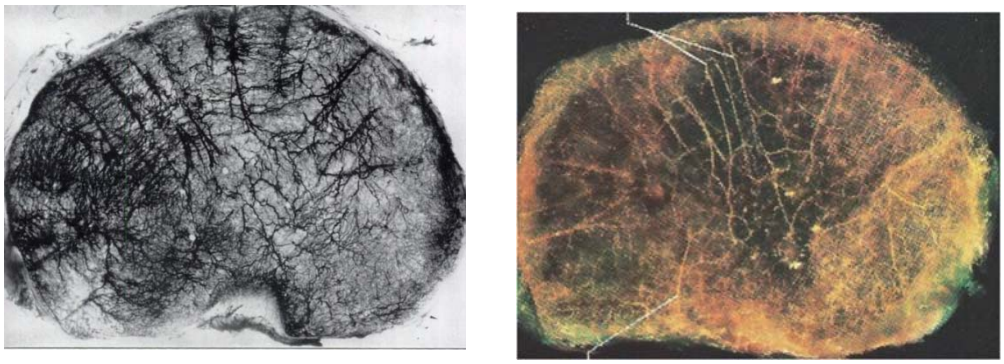


Figure 1.2 Upper tibial subchondral vessels described by Nelson (left) and Crock (right).

Although MRI has been available for some time and is capable of quantifying change in cartilage at the molecular level (Bashir 1999) and in combination with PET scanning can offer information on the metabolic processes in cartilage (Kogan 2017), the macroscopic appearances of certain obvious, possibly vascular features, seen on routine water bright MRI scans has escaped attention. The marks are shown in Figure 1.3.

In terms of scoring plain x-rays, the Kellgren-Lawrence system, though relatively crude, has stood the test of time and was used here because of its direct applicability to the plain x-rays available and because of its ease of use where large numbers of films were to be scored (Kellgren 1957, Kiapour 2019).

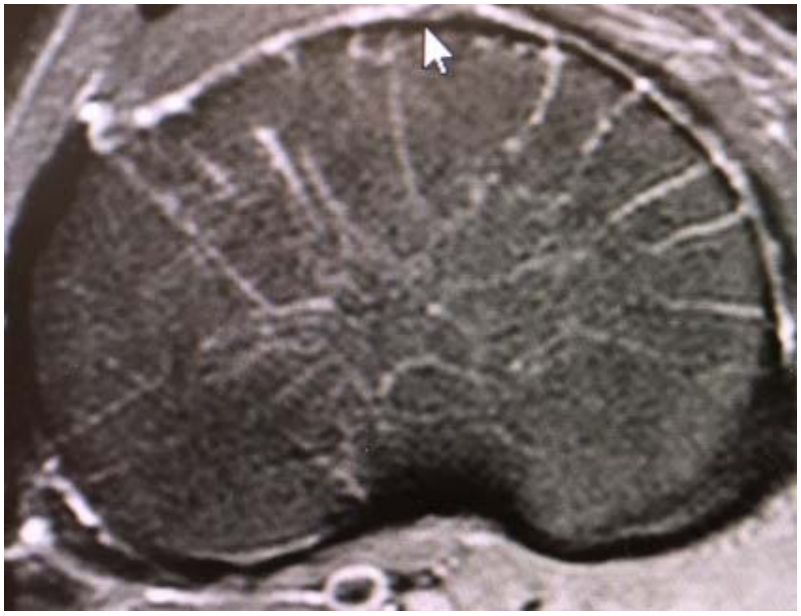


Figure 1.3 An upper tibial axial PD_SPAIR MRI scan showing the radiating white marks which appeared to be vascular.

Radiological opinion was that the marks were vascular and probably venous. This was based on their longitudinal appearance, water enhancement, combination with the superficial periosteal vessels and tributary-like appearance on some slices. A literature search failed to provide any previous description using key words including MRI, tibia, subchondral, blood vessel, vascular, venous and vein in various combinations.

1.9. Anatomy and histology - literature review

References dealing with the history of bone circulation and anatomy and histology are listed in preceding sections. In 1975 Burkhardt, a bone histologist interested in bone and haematological malignancies, identified several unusual features in his description of normal anatomy (Burkhardt 2012). These include possible capillary choke valves, 90 degree branching at the capillary junctions and possible exit vein periosteal muscular

valves. He did not consider their possible role in weight bearing. Other authors have not really considered the nature of adipocytes and the viscosity of bone blood fat or how they might be of structural importance in active load bearing joints (Kremer 2015). Literature searches combining the key words bone fat, viscosity, adipocyte, weight bearing and hydraulic produced no evidence of previous research in the field of this hypothesis. Anatomical and histological work in the subchondral plane was therefore carried out.

1.10. Clinical background to this work

At the Hammersmith Hospital and Royal Postgraduate Medical School in West London in the 70s and 80s many patients received large doses of corticosteroids to manage their difficult immunological or rheumatological conditions, such as in SLE or to suppress rejection after organ transplantation. Consequently there were significant numbers of patients who developed side effects from corticosteroids including painful osteonecrosis or collapse of bone in their weight bearing joints (Saag 1994, Hirano 2007, King 2007). In the mid-80s most orthopaedic surgeons were aware that there was a measureable pressure within bones. It was generally termed intraosseous pressure (IOP) and was thought to be a reflection of venous back pressure or some form of intrinsic tissue or fat cell pressure or tissue turgor (Dieppe 1999, Simkin 2004). IOP appeared to be raised in certain diseases such as osteoarthritis and osteonecrosis and also with bone pain (Laroche 2002).

With the post war increase in obesity, alcoholism and diabetes there was a further increase in patients presenting with painful joints due to osteonecrosis (Aaron 2013). Another group was identified among those who had experienced embolic microvascular

problems. These included the divers and tunnellers mentioned above and also patients with sickle cell disease which caused a form of embolic occlusion of bone blood vessels and had become more commonplace in London with an increase in the Afro-Caribbean population.

Orthopaedic surgeons have long known that osteotomy (cutting) or forage (drilling) of bone was often effective in relieving bone pain. It was assumed that the IOP was somehow relieved by this simple procedure (Koshino 1982, Baksi 1991, Pedersen 1995).

As orthopaedic registrars in the early 1980s, we were often called upon to carry out drilling or 'forage' of painful osteonecrotic lesions. A typical patient would have developed bone and joint pain over a few months often preventing walking. X-rays or in those days, early MRI scans, would show bone oedema or collapse at the ankle, knee or hip and sometimes the shoulder. Under image intensifier control each area would be drilled with a ¼ inch drill. Accurate placement of the drill could be achieved with a guide wire and cannulated screw or DHS type drill for the femoral head. The effects were dramatic. Following a day case procedure many patients were completely pain free, required no analgesics and asked for other joints to be similarly treated. In steroid treated patients the effects were long lasting but in pure osteoarthritis the effects lasted only for several months. At that time the reasons were not clear (See chapter 7 page 196).

In conjunction with forage, we often tried to measure IOP. The anaesthetic machine arterial pressure channel was usually available. In contrast to the success of the surgery, efforts at measuring IOP were dismal. There was no clear pattern to the pressures obtained and no obvious correlation with pre or post-operative pain.

1.11. Contemporary state of knowledge in 2014

Since the mid -1980s there had been little interest in IOP. Most textbooks accepted the view of bone circulation illustrated in Gray's Anatomy. Most surgeons accepted that IOP was present in all bone and measured about one third of systemic blood pressure or about 30 mmHg. They accepted that IOP was raised in certain painful bone conditions and was probably due to a raised venous back pressure or tissue and fat cell swelling or tissue turgor. Osteonecrosis still occurred but could be treated by forage-type drilling in some patients and perhaps osteotomy in others. Otherwise most patients would in due course come to joint replacement which was becoming increasingly successful. In any event, the problem had diminished with better steroid control and new immunological treatments. Bone circulation was no longer controversial.

It was widely believed that the cancellous bone trabeculae bore weight directly from loads applied to the articular surface and that trabeculae transferred that weight to the cortical shaft. Osteoarthritis was considered to be mainly a disease of wear and tear. This was confirmed because the wear appeared to begin with fibrillation on the cartilage surface.

It was generally accepted that cartilage derived much of its nutrition from synovial fluid. The evidence for this view was that cartilage covered bony loose bodies within the knee remained viable. Tritiated hydrogen H_3 introduced into a joint rapidly crossed the cartilage into underlying bone so presumably other nutrients would move in the same way (Amiel 1986). With respect to osteonecrosis, publications concentrated mainly on the treatment of osteonecrosis by a range of medical and surgical means such as in recent text books and reviews (Babhulkar 2013, Koo 2014).

The research effort had moved to a mainly genetic and molecular focus to identify cellular level problems. Immunological fixes for various molecules found in degrading cartilage were sought. It seemed that orthopaedic interest had moved from delineating the vascular anatomy to replacing joints with only a passing glance at intraosseous pressure on the way. The orthopaedic and rheumatological worlds had largely ignored the vascular supply to bone and joints and never really considered the hydrodynamic forces that might be involved in joints as they perform their primary function.

1.12. Thesis – Overview

In 1985 I was given a Wellcome Trust grant (Grant 12425/1.5/SC) to study IOP in a standardised animal model (Royal Postgraduate Medical School, Home Office licence ELA 24/4994). Although that work developed a usable model in the rabbit, it failed initially to establish what a normal IOP might be. The measurement of IOP varied even with apparently similar experiments. Then it became obvious that IOP was not a fixed parameter but depended on a wide range of experimental conditions and perfusion at the needle tip (Beverly 2016). IOP as previously measured was therefore of little clinical value. Nevertheless, it was possible to use that new understanding to further logically explore subchondral perfusion by applying selective vascular occlusion, subtraction and loading tests to the apparently random IOP values.

During that year experimental work also included studies using the Lixiscope, a hand held isotope powered radiological screening device, Tc99 MDP bone scans and blood flow studies in vivo, MRI studies for bone oedema in animal and man and further intraosseous pressure studies in man, both anaesthetised and walking (Gardner 1989).

A microbubble study with blood saturated at different pressures and with different gasses was also carried out (Beverly 1987, Beverly 1987). Those studies combined to offer an enhanced understanding of the physiology of subchondral bone circulation, decompression sickness and possibly a fresh insight into osteoarthritis. Many years later this was pursued in the present study, now submitted for a DPhil thesis.

All the original needles, catheters, intraosseous pressure transducers, four channel amplifiers and chart recorders were retained. All the original chart records, experimental notebooks, diaries, x-rays, bone scans and other data had been preserved and remained available. Originally, the data had been loaded onto a Minitab spread sheet but the results had never been fully analysed and the system was no longer available. The data was therefore re-loaded into Excel. On conducting that analysis in Oxford for this DPhil thesis in 2014, it became apparent that the early work covered three main areas, namely the basic resting perfusion studies, the studies of loading with vascular occlusion and the studies made in a group of animals given steroids.

Chapter 1 offers an overview of the literature.

Chapter 2 describes and re-analyses that animal work from 1985. The data analysis is new. Those studies showed that there were IOP changes with circulatory manipulation and loading and that steroid treatment also raised IOP, apparently by fat shrinkage rather than fat cell swelling.

Chapter 3 documents how, as a result of the early work, it seemed reasonable in 2014 to revisit IOP but this time to use an in vitro model in order to comply with the 'three Rs' of animal research - Replace, Refine, Reduce (Tannenbaum 2015).

The earlier static perfusion findings were confirmed.

Chapter 4 used the new model to explore different patterns of loading in terms of type, duration and frequency. It became apparent that load was transferred through

subchondral bone partly by hydraulic force rather than solely through the trabeculae. It also became apparent that there was evidence of a valve influencing subchondral blood flow during brisk exercise as opposed to static loading.

In Chapter 5 the presence of commonly seen but previously ignored marks on MRI scans was explored. The marks which were thought to be vascular were present on upper tibial MRI scans. They were counted and compared with the grade of osteoarthritis on contemporary x-rays using the Kellgren-Lawrence system. A second larger study of 200 pairs of x-rays and MRI scans was made and included the distal femur.

In Chapter 6 anatomical and histological evidence for a specialised subchondral circulation was sought. Bone from the calf and from man was examined for blood vessels and other structures which might confirm the presence of vascular arrangements to support joint load transfer by hydraulic forces.

In Chapter 7 a number of observations are listed and referenced which collectively support the thesis. In defence of a thesis or hypothesis it is not always possible to offer a single definitive experimental proof. That applies in this case. A number of experiments have been carried out as listed in Chapters 2 - 6 above which collectively support the central hypothesis. But there is a further body of supporting evidence. This is presented in Chapter 7 together with the associated references.

Chapter 8 summarises the findings and points to future areas for research.

1.13. Hypothesis

There is a specialised vasculo-mechanical subchondral environment which allows load to be transferred partly by hydraulic force. Subchondral anatomy is modified to cope with high pressures. Vessels are lost in early osteoarthritis. Osteoarthritis may be a partly vasculo-mechanical disease.

OBJECTIVES

Chapter 1 – sets out the background literature

- Chapter 2 - explores and re-analyses previous in vivo IOP studies.
- Chapter 3 - develops an in vitro model to test IOP during different perfusion regimes.
- Chapter 4 - uses that model to test IOP with different loading regimes.
- Chapter 5 - analyses subchondral vascular marks on MRI scans of knees and compares them with Kellgren-Lawrence grading for osteoarthritis.
- Chapter 6 - explores subchondral upper tibial anatomy and vascular histology.
- Chapter 7 – presents further referenced evidence in support of the thesis.
- Chapter 8 – summarises results and suggests areas for future work.

2. PRELIMINARY IN VIVO STUDY [1]

2.1. Background

This in vivo study was carried out in 1985 as part of a Wellcome Trust funded research project (Grant 12425/1.5/SC) to study IOP in a standardised animal model at the Royal Postgraduate Medical School under a Home Office licence ELA 24/4994). Although a raised intraosseous pressure (IOP) had been found in osteoarthritis and osteonecrosis, the normal physiology of subchondral circulation was poorly understood. In an animal model the physiology of subchondral perfusion at rest, during loading and with vascular occlusion was explored. Corticosteroids are recognised to have side effects which include osteonecrosis. The effects of steroids on IOP and bone perfusion were studied. The chapter falls into three parts covering experiments numbered 1-14 with the results presented in that order. Part 1 (experiments 1-7) deals with perfusion at rest. Part 2 (experiments 8-10) deals with loading and Part 3 (experiments 11-14) explores steroid effects.

Work in this chapter has been published in the following peer reviewed publications

1. Factors affecting intraosseous pressure measurement. **Beverly M**, Murray D. J Orthop Surg Res. 2018 Jul 28; 13(1):187. doi: 10.1186/s13018-018-0877-z. PMID:30055642

1. Intraosseous pressure during loading and with vascular occlusion in an animal model. **Beverly M**, Mellon S, Kennedy JA, Murray DW. Bone Joint Res. 2018 Sep 15;7(8):511-516. doi: 10.1302/2046-3758.78.BJR-2017-0343.R2. eCollection 2018 Aug. PMID:30258570

2.2. Part 1: Introduction - in vivo perfusion

A rabbit animal model was developed and studied to establish baseline IOP values during perfusion, with and without arterial and venous tourniquets and at different sites and under different perfusion conditions.

2.3. Method

IOP was measured experimentally using intraosseous needles at 44 sites in the subchondral cancellous bone of the femoral head, femoral condyle and proximal tibia of 21 adult New Zealand White rabbits (Royal Postgraduate Medical School, Home Office licence ELA 24/4994). The rabbits were anaesthetised through an ear vein with intravenous Sublimaze (fentanyl, Janssen-Cilag Pty Ltd, NSW, Australia) and Valium (diazepam, Genentech Inc., San Francisco, CA). Induction of anaesthesia was by IV Sublimaze (fentanyl) 2 ml of 0.05 mg/ml solution depending on the size of animal with top up IV infusion of Valium (diazepam) 0.5 ml of 5 mg/ml solution alternating with Sublimaze (fentanyl) 0.5-1.0 ml given slowly on approximately a half hourly basis. The initial recordings were mainly from the right femoral head with later recordings mainly from the femoral condyles and proximal tibia as in Figure 2.1. These were more reliable. There were 44 different IOP recordings, six at the femoral head, seven from the femoral condyles and 31 from the proximal tibiae. The femoral head was approached by dissection anteriorly through the femoral triangle. A saline filled 21G (n=13) or 23G (n=31) venesection needle was pushed by hand into the femoral head subchondral bone by rocking the needle through a 5 to 10 degree arc along the line of the bevel of the needle. The needles were placed under direct vision in the approximate centre of the

subchondral region within a few millimetres of the subchondral surface. For the femoral condyle, insertion was a few millimetres proximal to the visible and palpable surface. The same applied to the proximal tibia. In 14 subjects the right femoral artery and vein were selectively clamped at the inguinal ligament. The needles were connected by saline filled lines to pressure transducers (Druck PDCR75, Druck Ltd, Leicester, UK) and to a four channel chart recorder (Lectromed MX4P-31, Lectromed Ltd, Jersey, Channel Islands). The transducers were calibrated on a 0 - 100 mmHg scale. In five animals the arterial blood pressure was measured by cannulating the left femoral artery and recording pressure using the same transducer system. The experimental set up was as illustrated in Figure 2.1.

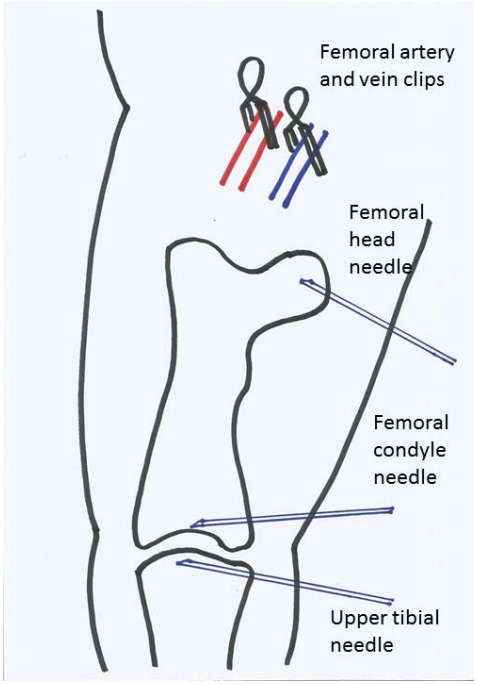


Figure 2.1 Diagram showing position of vascular clips and intraosseous needles.

Experimental Plan (1-7)

A series of experiments were undertaken to investigate the following:

Experiment 1 Baseline IOP variability

The normal IOP was measured at all 44 sites among the 21 subjects and the influence of factors relating to the animal including gender, weight, site and size of needle were explored.

Experiment 2 Method of measuring IOP

The Ficat method in which a 0.5 ml clearance bolus of saline was injected was compared with a method using needle clearance by aspiration. An example trace was recorded.

Experiment 3 IOP wave forms

IOP wave forms were explored at different chart speeds, 12.5 mm/sec and 12.5 mm/min. The traces were compared with the directly visible pulse and respiratory waves. The chart speed was 12.5 mm/min in subsequent experiments. An example trace was recorded.

Experiment 4 Drug administration on IOP

The effect of a bolus drug administration of Valium (diazepam 2.5 mg) or Sublimaze (fentanyl 0.05 mg) on IOP was recorded. An example trace was recorded.

Experiment 5 Blood pressure and IOP

The relationship between systemic blood pressure and IOP in 13 sites among five subjects was explored.

Experiment 6 IOP and pulse pressure (PP)

The relationship between IOP and the associated pulse pressure was explored at 44 sites among all 21 subjects. The pulse pressure was taken to be the difference between the top and bottom of the wave on the IOP tracing at that point.

Experiment 7 Vascular occlusion and IOP

The effect on IOP of clamping the femoral artery or femoral vein was recorded in 31 sites among 14 subjects. The clamps were small 'bulldog' sheathed vascular clips. They were applied to the proximal femoral artery or vein under direct vision. An example trace was recorded.

2.4. Part 2: Introduction - in vivo loading

Using the rabbit model, IOP was tested under loading and with and without vascular occlusion. The IOP was also measured at several point simultaneously along the limb and with selective saline injections in order to assess the degree of compartmentalisation between bones.

2.5. Method

For the loading and vascular occlusion study IOP was measured experimentally in the subchondral bone of the femoral condyle and proximal tibia of five anaesthetised adult New Zealand White rabbits using the technique described above. The transducers were

calibrated on a 0 - 100 mmHg scale. For each set of recordings the pressure transducers were zeroed to air, calibrated and maintained level with the site being measured.

Loading was carried out using a reversed spring pusher. A weighing spring and its calibration scale were mounted in concentric tubes, one end attached to the inside of each tube such that longitudinal compression of a set force could be applied. The inner tube contained and controlled the foot preventing collapse into a flexed posture. The tube prevented movement of the hind limb and avoided direct squeezing of limb muscle. The subject was supine with the leg extended. A steady load of one body weight (between 4520 and 5400 g) was applied down the limb as in Figure 2.2. The loading recordings were carried out with the leg in an extended position and the pusher in place without limb movement in flexion or extension. Example traces were recorded.

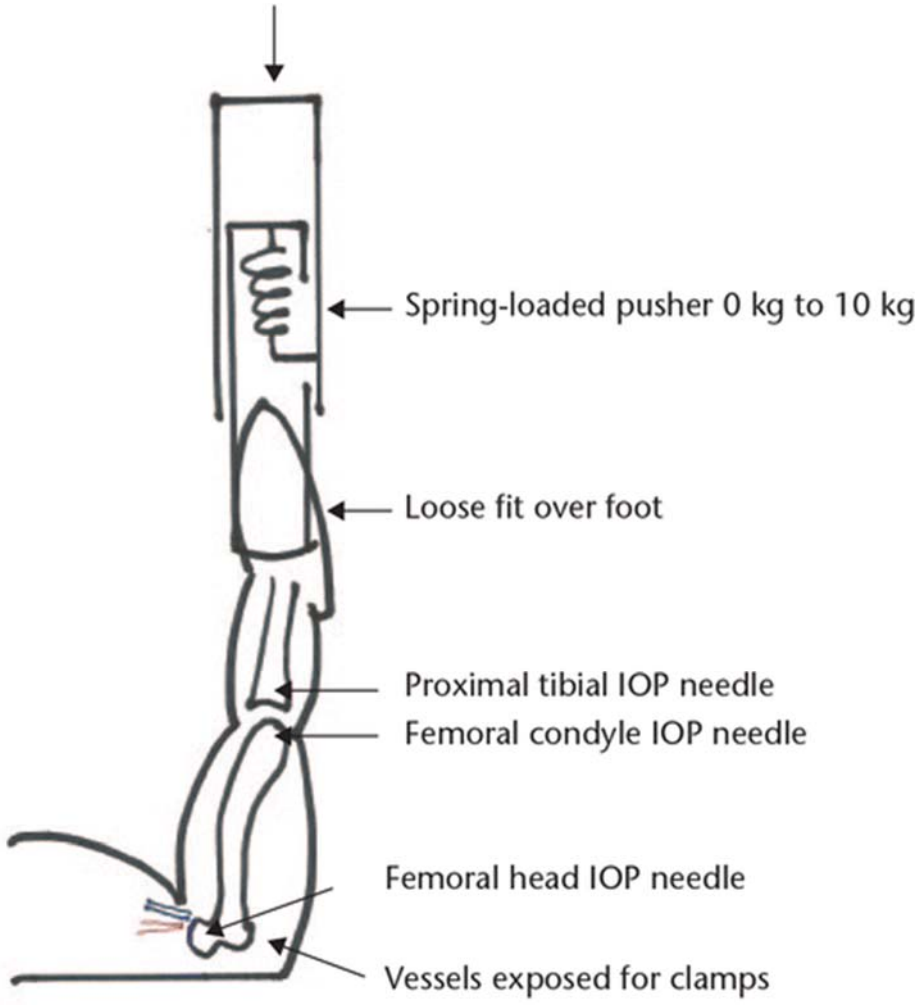


Figure 2.2 Experimental set up. The spring loaded pusher covers the foot and prevents flexion and extension while using a longitudinal one body weight load (4520-5400 g).

Experimental Plan (8-10)

A series of experiments were undertaken to investigate the following:

Experiment 8 IOP with loading and vascular occlusion

IOP recordings from five femoral condyles and seven proximal tibiae in five subjects were obtained.

(a) The effect on basal IOP (IOPb) of a load of one body weight (IOPb+Ld) was measured.

(b) The effect on IOP of arterial occlusion (IOPa) then loading of one body weight (IOPa+Ld) was measured.

(c) The effect on IOP of venous occlusion (IOPv) then loading by one body weight (IOPv+Ld) was measured.

Experiment 9 IOP at different sites

An additional experiment was undertaken in one subject in which IOP was recorded simultaneously at the femoral head, femoral condyle and proximal tibia during vascular occlusion and loading. This required placement of an additional needle in the femoral head. An example trace was recorded.

Experiment 10 IOP compartment injection study

A further experiment was carried out in one subject to assess the qualitative effect on IOP of saline bolus injection at the femoral head, femoral condyle and proximal tibia in turn while recording at the other sites. An example trace was recorded.

2.6. Part 3: Introduction - in vivo steroids

From the in vivo perfusion work it was evident that IOP was not a single value parameter but varied depending on the measurement technique used and conditions in the needle tip microvascular pool. The vascular occlusion and loading experiments showed that the IOP was affected in a predictable way both by loading and vascular control. But the possible effect of steroids on the basic physiology was not known. The previous assumption was that the steroids caused an effect by fat cell swelling leading to a raised IOP and possible infarction or osteonecrosis. The effect of a large dose of

long acting steroid was therefore assessed in the animal model to explore the effect on the perfusion. Micro-angiography was used to assess the extent of possible infarction or fat cell swelling as set out in the next section.

2.7. Method

One ampoule of methyl prednisolone or 80 mg (Sigma Aldrich, Dorset, UK) was administered intravenously through an ear vein to six animals three weeks before the experiment. That represents a large dose of long acting corticosteroid. There were 15 untreated controls. The rabbits were anaesthetised three weeks later through an ear vein as above. A saline filled 23G venesection needle was pushed into the upper tibial subchondral bone by rocking the needle through a 5 to 10 degree arc along the line of the bevel of the needle. The needles were placed in the approximate centre of the subchondral region within a few millimetres of the subchondral surface. Vascular clips were placed on the proximal femoral vessels alternately and the change in IOP and PP was recorded after 30 seconds.

The aorta was opened immediately post mortem and 200 ml dilute 50% barium sulphate suspension in water (Microcat 50 mg/ml, Guerbet Laboratories Ltd, Avon House, 435 Stratford Road, Shirley, Solihull, UK) was infused. The femora were dissected out, fixed in 10% formalin and decalcified over a period of 72 hours in 5 % nitric acid. Photographs were made of the femora and micro-angiograms were carried out using fine grain film at 40 kV, 100 mA, 100 cm tube-target distance with a 20 second exposure.

Experimental Plan (11-14)

A series of experiments were undertaken to investigate the effect of steroids on:

Experiment 11 Basal IOP and pulse pressure

Experiment 12 IOP with proximal occlusion

Experiment 13 IOP subtraction difference

Experiment 14 Photography and micro angiography

Statistical Analysis

Experimental time for the basal IOP perfusion studies varied from about 30 minutes to over two hours. Intraosseous pressure and the associated pulse pressure (PP) were measured at all 44 sites. Pulse pressure was taken as the difference between the top and bottom of the IOP trace on each occasion. For the loading and occlusion study experimental duration varied between 30 minutes to two hours. Basal IOP (IOPb) was measured on three occasions (early, middle and late) for each site during each experiment and the readings were averaged. The occlusion and loading experiments lasted for a few minutes only. IOP responses were recorded only once after approximately 30 seconds. Results were expressed as means, standard deviations and ranges. Student's t-test was used to determine if there were significant differences. When each subject was used as its own control, paired tests were used. Otherwise

unpaired tests were used. The Pearson test was used to assess correlations. $P<0.05$ was considered to be statistically significant.

2.8. Results

This chapter falls into three parts covering experiments 1-14 with the results presented in that order. Part 1 experiments 1-7 deal with perfusion at rest, part 2 experiments 8-10 deal with loading and part 3 experiments 11-14 cover steroids.

2.8.1. PART 1 Perfusion (Experiments 1-7)

Experiment 1 Baseline IOP variability

Basal intraosseous pressure was measured at 44 sites among 21 subjects as in Figure 2.3. At each site the early, middle and late IOP were averaged. The averaged IOP at different sites varied considerably (mean 23.4 mmHg, SD 13.7, range 3 - 55).
Gender (female n=14, male n=7) had no effect on IOP (t-test p=0.537). Weight (2,920 g – 5,560 g) had no effect on IOP (Pearson correlation p=0.368). Needle size 21G (n=13) and 23G (n=31), t-test p=0.14, had no effect on IOP.

Several subjects had two or more sites measured. There was variation between subjects (SD 11.5 mmHg) and variation between sites within subjects (SD 6.8 mmHg). Where paired measurements were available (n=7) there was no difference (t-test p=0.52) between the femoral condyle (mean 9.8, SD 3.6, range 5 -16) and proximal tibia (mean 12, SD 7.4, range 5.7 - 16.7). There were insufficient paired data for femoral head comparisons.

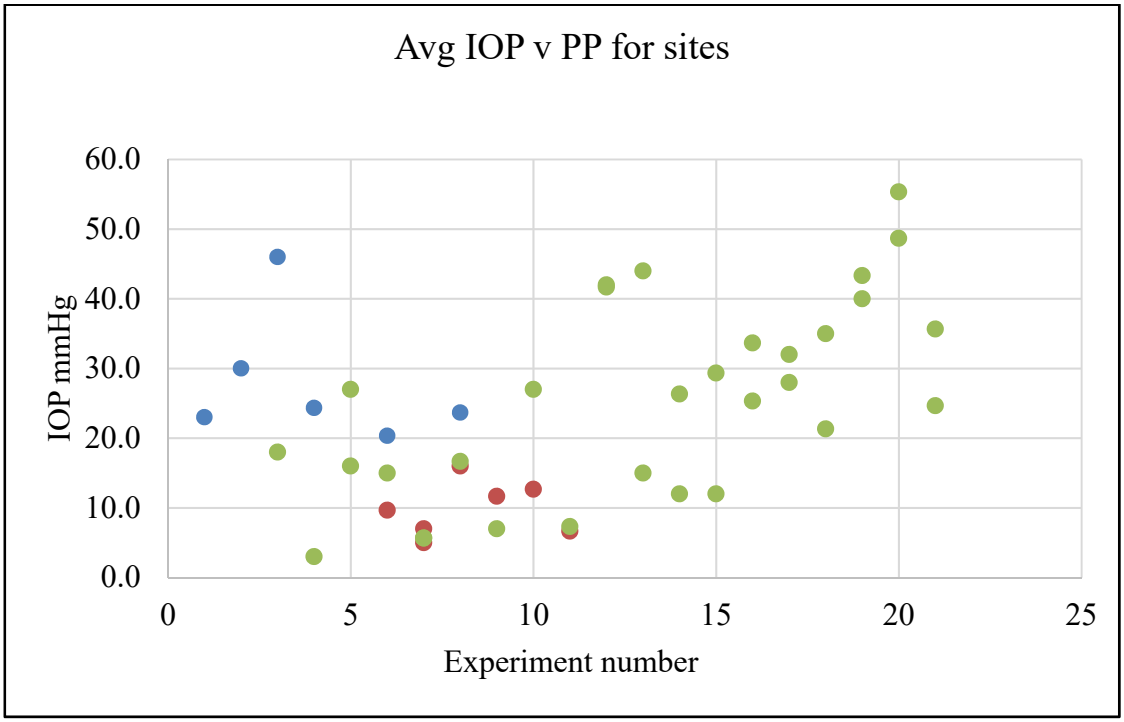


Figure 2.3 Graph showing variation in resting or basal IOP between subjects (mean 22.4 mmHg, SD 13.7) and within subjects (mean 25.9 mmHg, SD 6.8) in 21 subjects at 44 different sites. Blue – femoral head, Red – femoral condyle, Green – upper tibia.

Experiment 2 Method of measuring IOP

Previous investigators have used a saline bolus or 'clearance' injection (Ficat 1985) before recording IOP. We found that in healthy bone this caused a marked fall in IOP which was followed by a gradual recovery taking up to 10 minutes. Aspiration was followed by faster recovery which took less than 1 minute as in Figure 2.4.

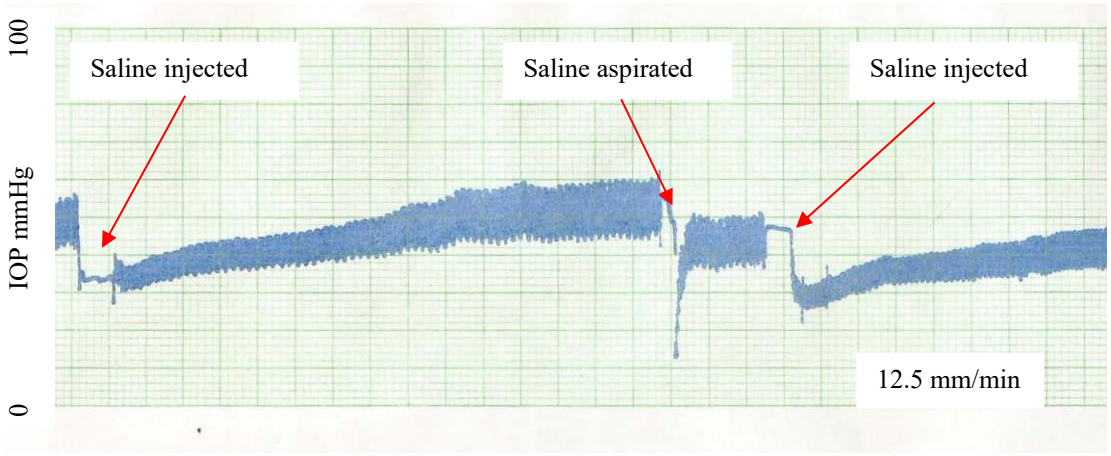


Figure 2.4 A representative trace from a typical experiment showing the effect of a 0.5 ml saline bolus flush injection with about 8 minutes to recover followed by aspiration with recovery in less than 30 seconds. A second bolus flush injection and slow recovery follows. Large square = 0.5 cm or 30 secs.

Experiment 3 IOP wave forms

The majority of recordings showed a pulsatile wave form. At a faster chart speed of 100 mm/min the primary wave was seen to be synchronous with the cardiac arterial pulse by direct observation. An underlying slower wave form was observed. This wave was seen to be synchronous with respiration by direct observation as in Figure 2.5.

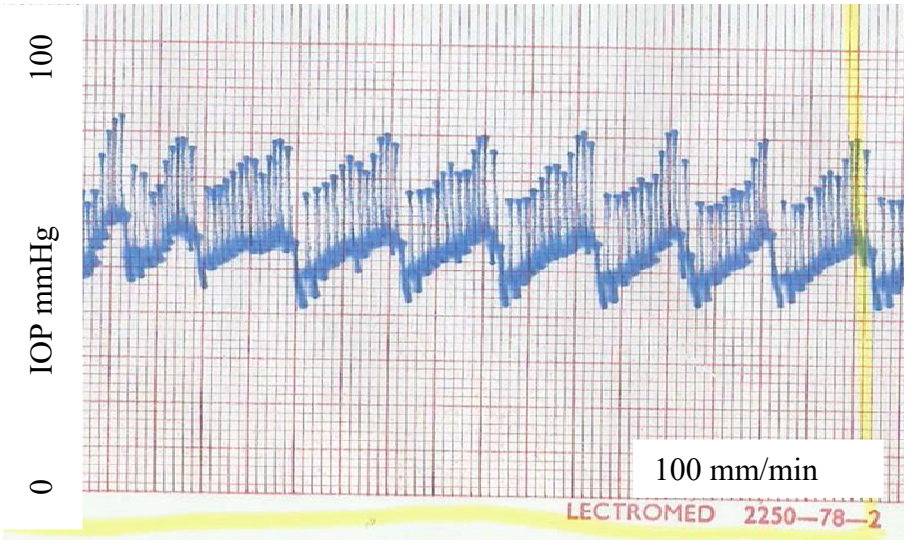


Figure 2.5 A representative IOP recording at a faster chart speed of 100 mm/min shows the cardiac pulse and a superimposed respiratory wave. In this section recorded for approximately 40 seconds some 9 respiratory waves and approximately 100 cardiac waves are seen. Large squares = 0.5 cm or 3 secs.

Experiment 4 Drug administration on IOP

Systemic administration of anaesthetic agents affected the IOP. For example, in the representative trace shown, the administration of an intravenous bolus of Valium (diazepam 2.5 mg) lowered the IOP and PP waves for about 90 seconds. Sublimaze (fentanyl 0.05 mg) caused a variable effect. In this representative trace there was an excitatory effect. The IOP and PP rose for about 90 seconds with another lesser peak following. This double wave pattern corresponds to the expected circulation time of the drug bolus as in Figure 2.6.

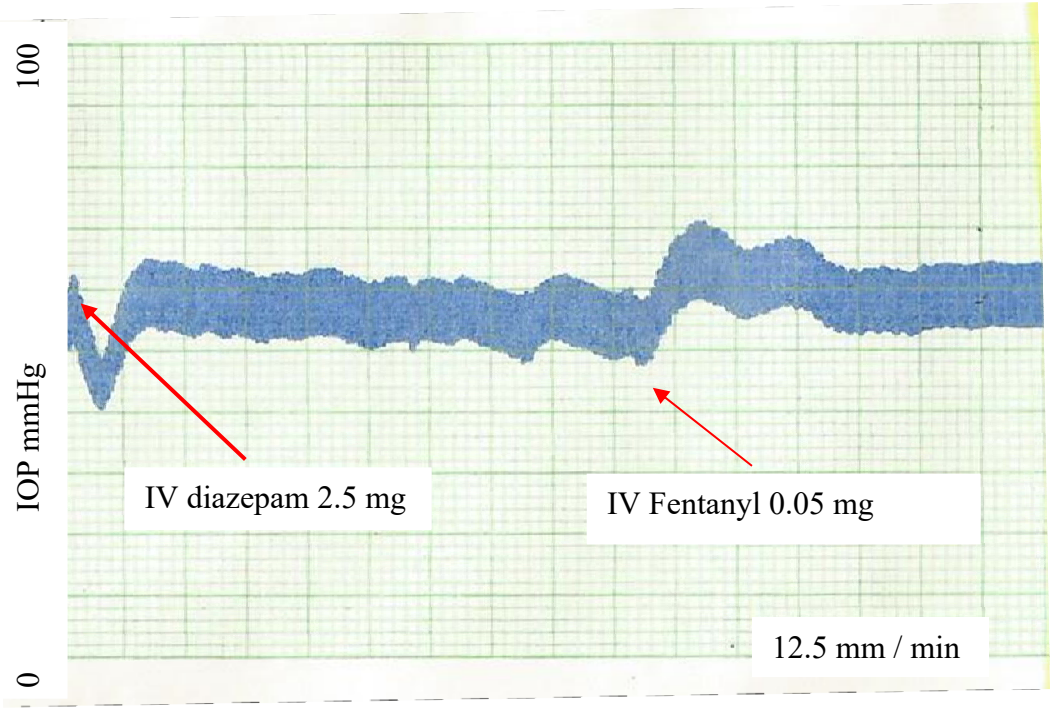


Figure 2.6 Systemic administration of anaesthetic agents such as diazepam and fentanyl affected the IOP as in this representative trace. Diazepam appears to have an immediate sedative effect for about 90 seconds. Fentanyl has an excitatory effect with a double circulation time wave pattern each of about 90 seconds. Large square = 0.5 cm.

Experiment 5 Blood pressure and IOP

Arterial blood pressure (BP) was measured in the left femoral artery in 5 animals using a pressure transducer. The mean BP was 62.8 mmHg, SD 8.2, range 55 - 73. Intraosseous pressure was measured at the same time at 13 different sites among the five subjects. The mean IOP was 11.7 mmHg, SD 7.2, range 5 - 27. There was a significant relationship ($p<0.0005$) between blood pressure and IOP, Pearson correlation 0.829 as in Figure 2.7.

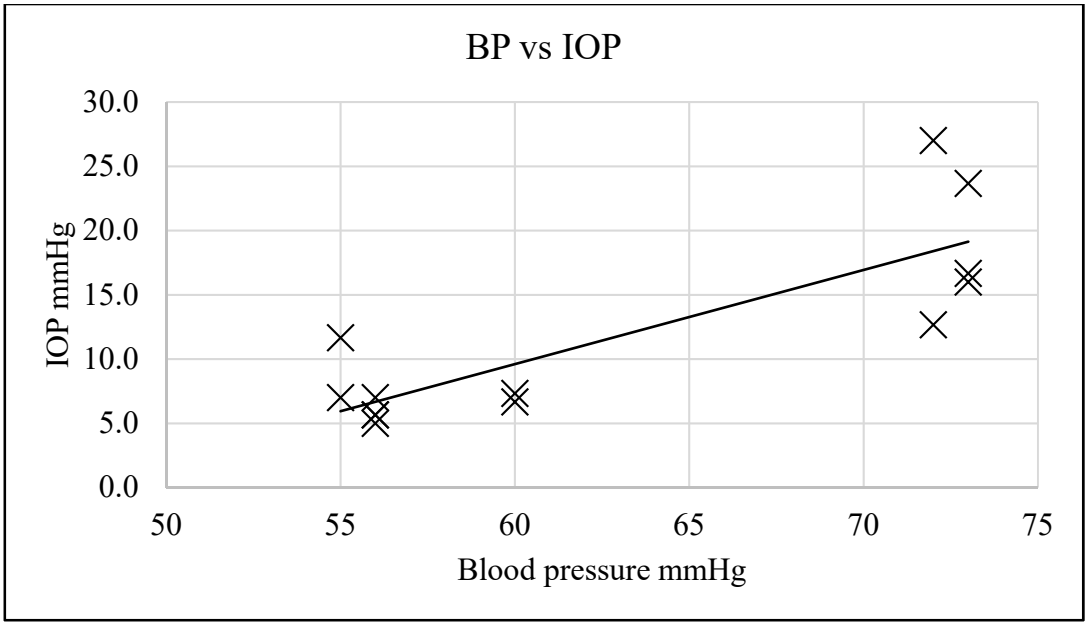


Figure 2.7 Effect of blood pressure on IOP. Intraosseous pressure was measured at 13 sites among five subjects. Pearson correlation r=0.829.

Experiment 6 IOP and Pulse pressure

IOP was compared with the associated pulse pressure (PP) at all sites (n=44) among the 21 subjects. The pulse pressure was taken as the difference between the top and bottom of the IOP trace wave. There was a significant correlation ($p<0.0001$) between IOP and the associated PP, Pearson Correlation 0.788 as in Figure 2.8.

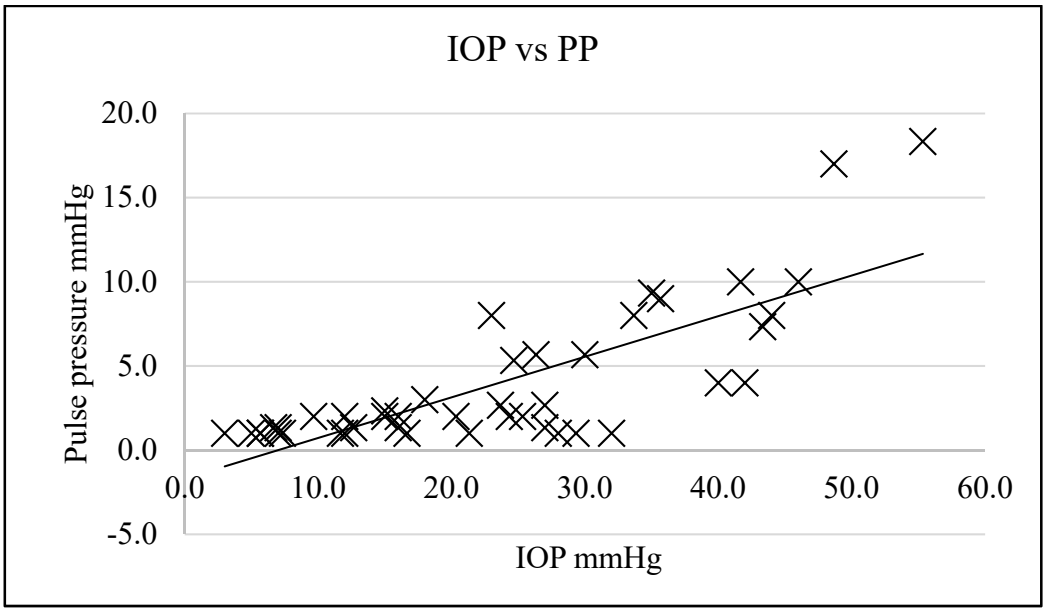


Figure 2.8 Pulse pressure (mmHg) with IOP (mmHg) for 44 separate sites among 21 subjects. Pearson Correlation r=0.788.

Experiment 7 Vascular occlusion and IOP

In 14 subjects (31 sites) when the proximal femoral artery was clamped at the inguinal ligament there was a fall in IOP with loss of the pulse pressure immediately. IOP stabilised within about one minute as in Figure 2.9. Recovery in IOP and restoration of the pulse pressure wave following release of the arterial clip was seen after less than one minute. When the proximal femoral vein was clamped the IOP rose and the pulse pressure was preserved as in Figure 2.9. With clamping the proximal femoral vein there was a pressure rise taking up to 30 seconds to stabilise and a similar time after venous release before the IOP returned to normal. During proximal venous clamping the pulse pressure or respiratory wave was preserved. The period during which the clamp was applied was typically 2 - 3 minutes as shown in the representative traces in Figure 2.9.

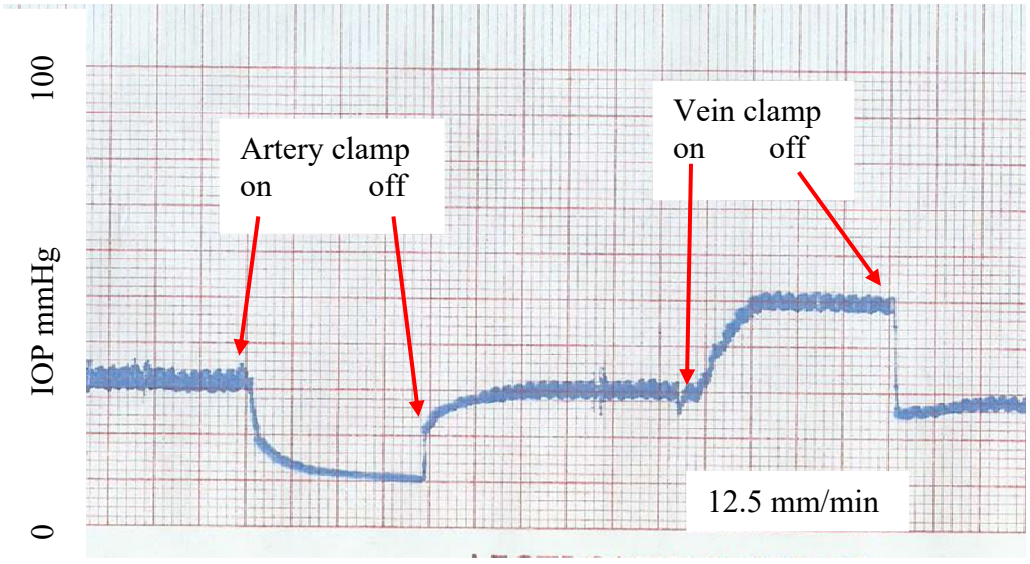


Figure 2.9 Recording showing the effect of clamping and releasing the proximal femoral artery (left half) and clamping and releasing the proximal femoral vein (right side). Large square = 0.5 cm.

With proximal arterial occlusion the IOP fell from 23 mmHg (SD13.6 mmHg) to 7.6 mmHg (SD 4.4 mmHg, p<0.0001) and PP fell from 4 mmHg (SD 4.2 mmHg) to 1 mmHg (SD 0) mmHg, p<0.0001). With proximal venous occlusion the IOP rose to 29.1 mmHg (SD12.2 mmHg, p<0.09) and PP rose to 3.3 mmHg (SD 3.2 mmHg, p<0.41). The difference between the venous occlusion IOPv and arterial occlusion IOPa was 15.0 mmHg, SD13.6 mmHg (p<0.0001) and the difference PPv - PPa was 1.7 mmHg (SD 3 mmHg, p<0.0002) as in Figure 2.10.

The difference between IOPv and IOPa or perfusion range obtainable at the needle tip blood pool with alternate arterial and venous clamping was significant n=14, p<0.0001.

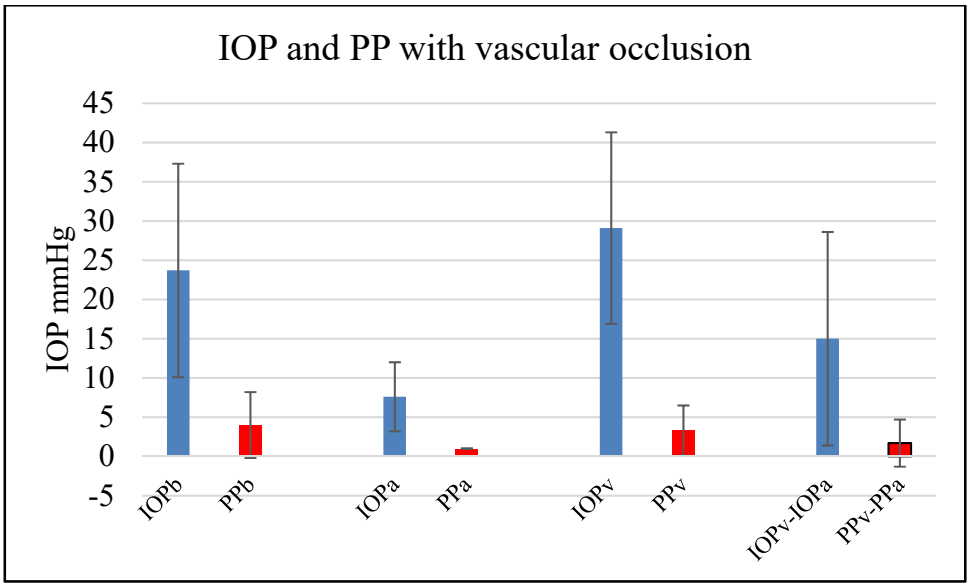


Figure 2.10 Blue – IOP, Red – PP. Initial or basal IOPb and PPb, arterial clamp IOPa and PPa, venous clamp IOPv and PPv and difference in IOP (IOPv-IOPa) and PP (PPv-PPa) for the perfusion range at the needle tip, n=31 individual records among 14 subjects, error bars SD.

2.8.2. PART 2 Loading (Experiments 8-10)

Experiment 8a IOP with loading and vascular occlusion

When the limb was loaded by one body weight there was a rise in IOP as demonstrated in the example shown in Figure 2.11. When a load of one body weight was applied longitudinally without moving the limb the IOPb (mean 11.7 mmHg, SD 7.1 mmHg) rose to IOPb+Ld (17.9 mmHg, SD 8.1 mmHg) n=12, $p<0.0002$ as in Figure 2.13.

The basal IOP at the femoral condyle and proximal tibia was compared. There was a wide range of values but no significant difference (t-test $p=0.159$) between them. The tibial and femoral results were therefore pooled.

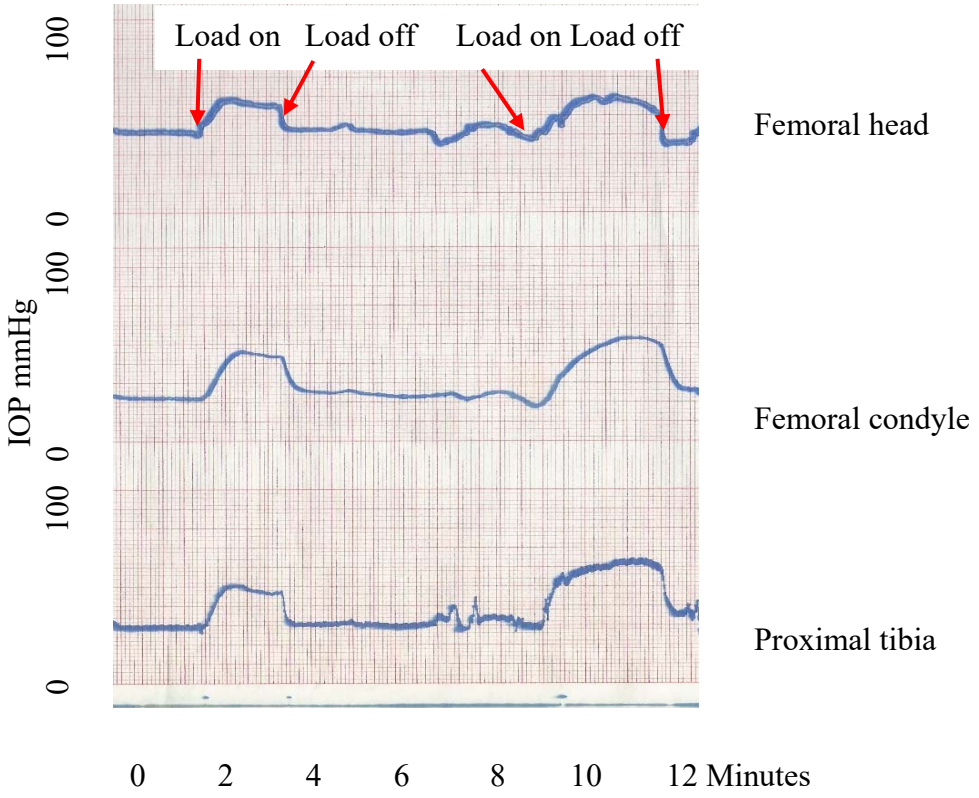


Figure 2.11 Showing the effect of loading alone with one body weight. Upper trace - femoral head, middle trace - femoral condyle and lower trace - proximal tibia. All traces show basal IOP, loading by one body weight for two minutes, rest for six minutes and load for three minutes. The changes in IOP appeared to be simultaneous at all three sites. Vertical scale 0 - 100 mmHg for each trace, trace speed 12.5 mm/min.

Experiment 8b The effect of arterial occlusion then loading

When a clip was applied to the proximal femoral artery there was a fall in IOP (IOPb mean 11.7 mmHg SD7.1 mmHg) to IOPa (mean 5.3 mmHg, SD 4.1 mmHg) n=12, $p<0.005$. The fall in IOP was proportional to the initial or basal IOPb (Pearson correlation 0.81). Loading the limb under these conditions caused a small rise in IOPa to IOPa+Ld (mean 7.6 mmHg, SD 4.5 mmHg) n=12, $p<0.002$ as in Figure 2.12, Table 2.1 and Figure 2.13.

Experiment 8c The effect of venous occlusion and loading

When the femoral vein was clamped there was a rise in IOPb (mean 11.7 mmHg, SD 7.1 mmHg) to IOPv (20.2 mmHg, SD 5.8 mmHg) n=12, $p<0.0001$. The rise in IOP was

inversely proportional to the starting IOPb (Pearson correlation -0.57). The addition of a one body weight load caused a further rise in pressure to IOPv+Ld (26.3 mmHg, SD 6.3 mmHg) n=12 p<0.003 as in Figure 2.12, Table 2.1 and Figure 2.13.

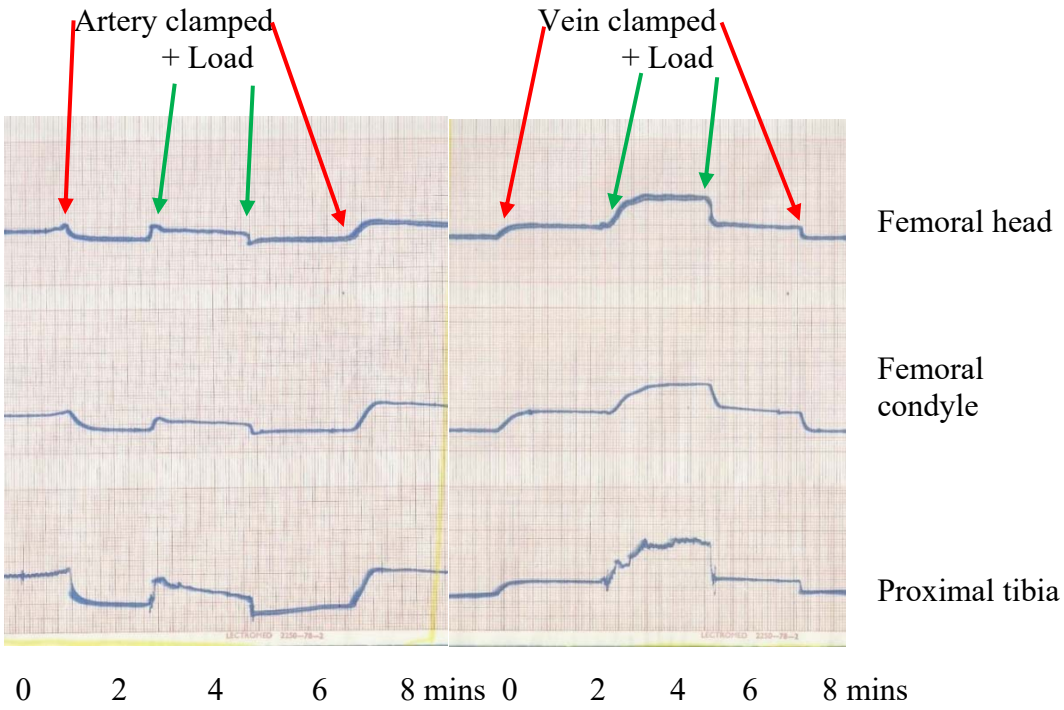


Figure 2.12 The upper trace is from the femoral head, middle trace femoral condyle and lower trace proximal tibia. From left to right the traces show the effect of arterial occlusion, arterial occlusion with loading, load removal and arterial clamp removal. The second part shows changes at the same sites after venous occlusion, venous occlusion with loading, removal of load and removal of the occluding clamp. The IOP changes are seen to be similar at all three sites and simultaneous. Vertical scale 0 - 100 mmHg for each trace, trace speed 12.5 mm/min.

N=12 for all	IOPb mmHg	IOPb+Ld mmHg	IOPa mmHg	IOPa+Ld mmHg	IOPv mmHg	IOPv+Ld mmHg
Mean	11.7	17.9	5.3	7.5	20.2	26.3
SD	7.1	8.1	4.1	4.5	5.8	6.3
Range	5-27	7-30	2-17	4-18	14-35	16-34

Table 2.1 showing values for IOP (mmHg) at 12 sites among five subjects. Columns are for basal IOP at rest (IOPb), with only loading (IOPb)+Ld (difference $p<0.0002$), proximal arterial occlusion (IOPa), arterial occlusion with load (IOPa)+Ld (difference $p<0.002$), venous (IOPv) occlusion and venous occlusion and load (IOPv)+Ld (difference $p<0.003$).

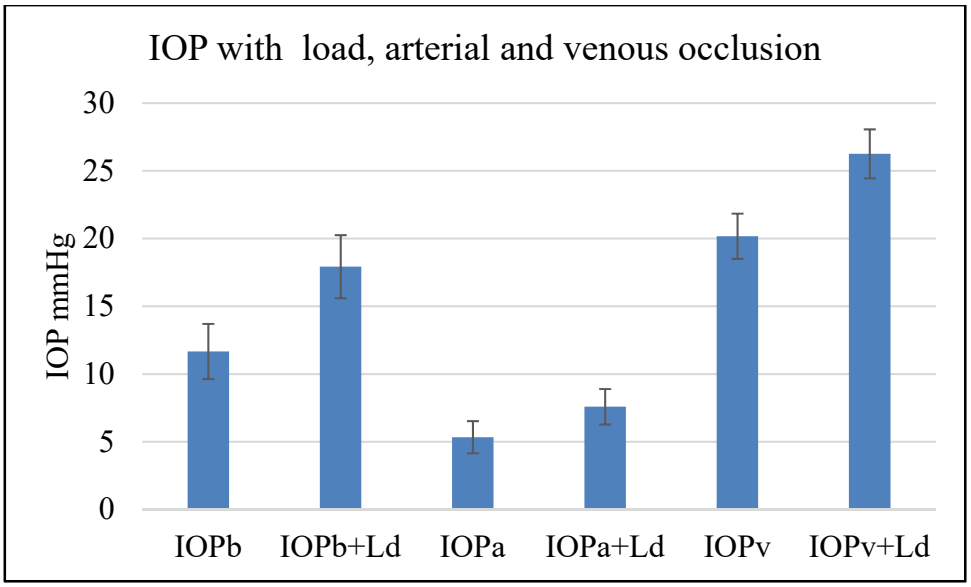


Figure 2.13 Basal IOP during perfusion at rest (IOPb), an increase in IOP with loading by one body weight (IOPb+Ld) $p<0.0002$; IOP during proximal arterial occlusion (IOPa) and with loading during arterial occlusion (IOPa+Ld) $p<0.002$ and IOP during venous occlusion (IOPv) and loading during venous occlusion (IOPv+Ld) $p<0.003$. N=5 subjects, 12 IOP needle sites. Error bars are SEM.

Experiment 9 IOP at different sites

When simultaneous records were made in one subject at the femoral head, femoral condyle and proximal tibia the effect of loading was to raise IOP at all three sites simultaneously as in Figure 2.11. With vascular occlusion and loading the effect was seen to be present at all three sites simultaneously as demonstrated in Figure 2.12.

Experiment 10 IOP compartment injection

Saline 0.5 ml was injected into the femoral head, femoral condyle and proximal tibia in turn. Pressure could not be recorded at the injection site itself during injection but pressure was recorded at the other two IOP needles. There was a pressure rise in the femoral condyle when the femoral head was injected and vice versa. Neither caused a rise in proximal tibial pressure. Proximal tibial injection caused no rise across the knee joint in the femur as seen in Figure 2.14.

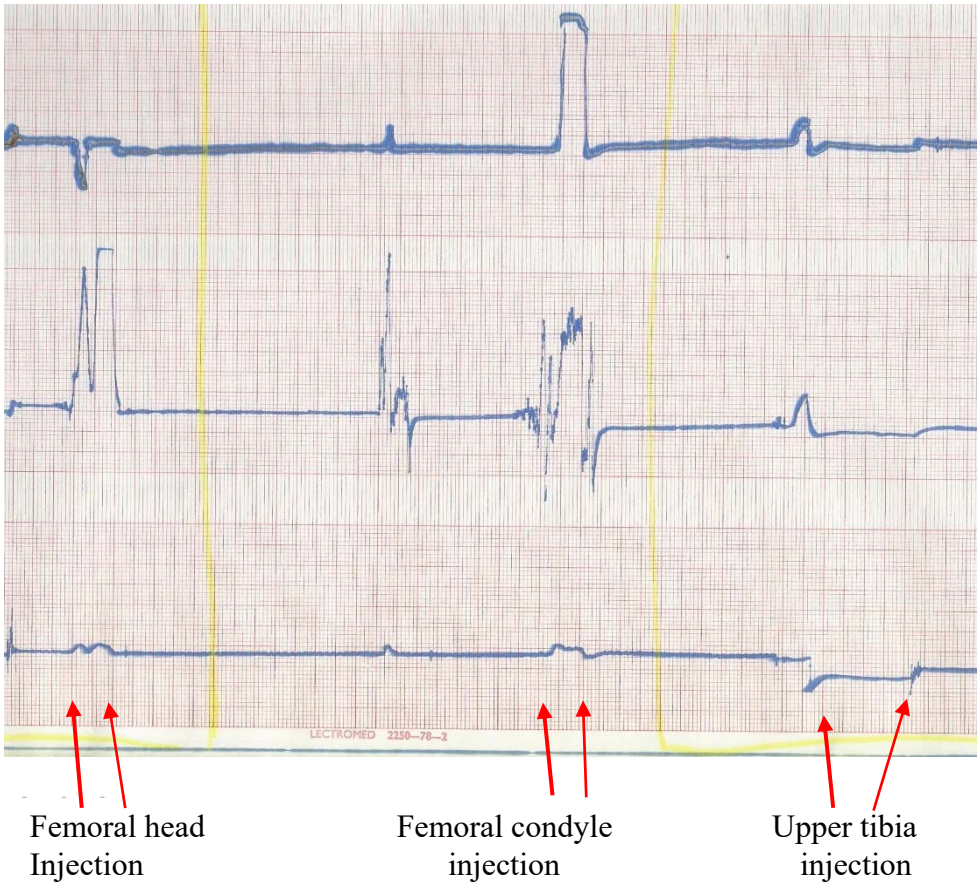


Figure 2.14 Left: Injection (between arrows) at the femoral head caused a rise in IOP at the femoral condyle but not the proximal tibia. Centre: Injection at the femoral condyle caused a rise in IOP at the femoral head but not the proximal tibia. (Some artefactual shake is seen on the femoral condyle trace during injection). Right: Injection at the proximal tibia had no effect on the femoral head or femoral condyle IOP. Vertical scale 0 - 100 mmHg on all traces, trace speed 12.5 mm/min.

2.8.3. PART 3 Steroids (Experiments 11-14)

Five females and one male received steroids. Steroid treated subjects became visibly thinner and weighed less (3965 g vs 4610 g, t-test $p<0.003$).

Experiment 11 Basal IOP and pulse pressure

The effect of steroids for three weeks was to increase the IOPb from 19.6 mmHg in the 15 controls (SD 2.9 mmHg) to 33.5 mmHg in the six treated subjects (SD 6.9 mmHg, $p<0.002$) as in Figure 2.15.

Experiment 12 IOP with proximal occlusion

The venous occlusion value IOPv rose from 23.5 mmHg (SD 7.3 mmHg) to 37.5 mmHg (SD14.4 mmHg, $p<0.05$) and the arterial occlusion value IOPa also increased in the steroid treated group from 6 mmHg (SD 4.3 mmHg) to 11 mmHg (SD 5.9 mmHg, $p<0.03$) as in Figure 2.15.

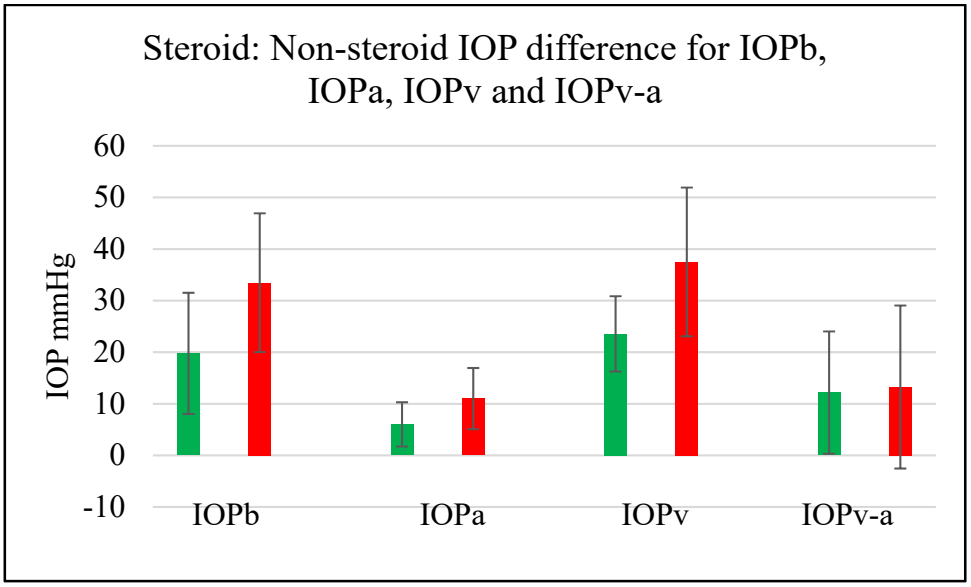


Figure 2.15 The Steroid treated (Red) IOP had higher IOP at basal ($p<0.002$) and with artery ($p<0.03$) and venous ($p<0.05$) occlusion than the non-steroid treated (Green), controls. N=6 steroid, 15 controls. The subtraction values (IOPv-IOPa) remained similar, $p=0.59$. Error bars SD.

Experiment 13 IOP subtraction difference

The difference in perfusion range at the needle tip determined by subtraction IOPv - IOPa remained relatively stable (p=0.6) between the non-steroid treated group 12.2 mmHg (SD 11.9 mmHg) and the steroid treated group 13.3 mmHg (SD 15.8 mmHg) as in Figure 2.15.

Experiment 14 Photography and micro angiography

Barium was injected into the descending aorta and the femora were removed, decalcified and photographed. The steroid treated femora were noticeably whiter than the controls as in Figure 2.16



Figure 2.16 Photograph of femora post angiography and decalcification. Top row steroid treated bones are whiter due to more barium retention. Bottom row controls are darker and contain less barium than the steroid treated femora.

Micro radiographs were carried out after decalcification. They showed that the steroid treated bones contained more barium than the controls as in Figure 2.17.

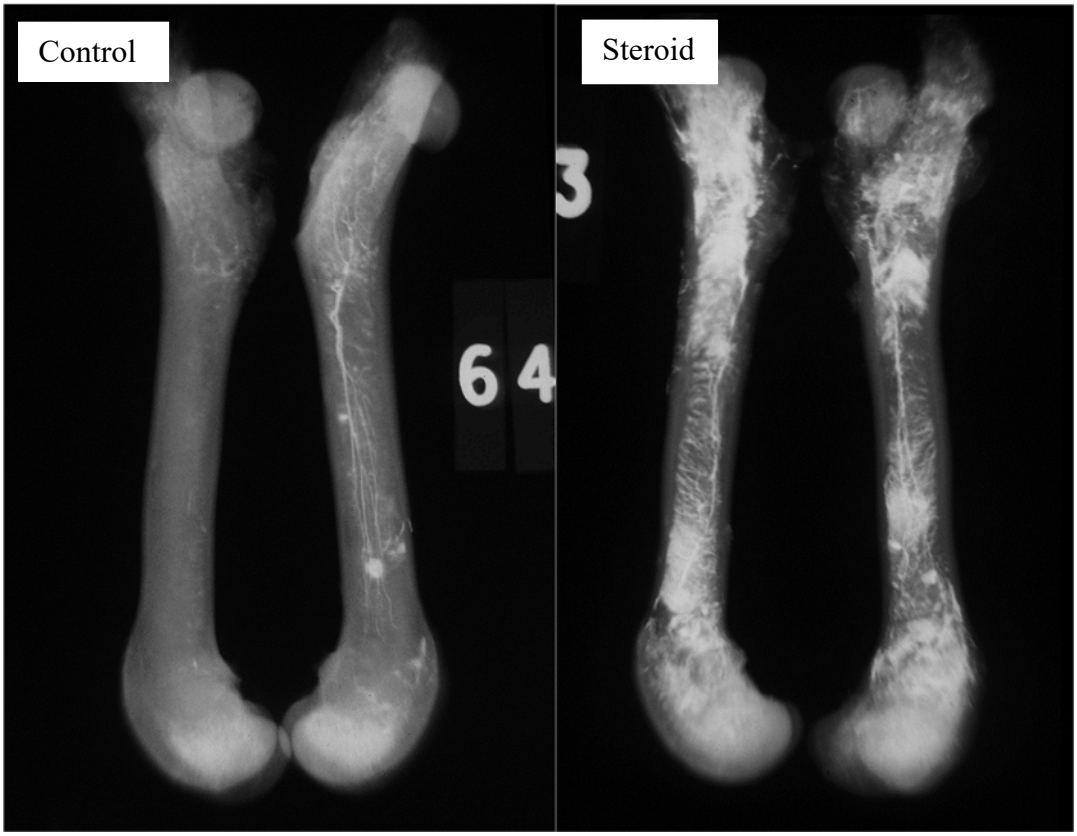


Figure 2.17 showing examples of femoral angiogram microradiographs. The left radiograph shows a pair of femora from a control barium angiogram. The right femoral pair were from a steroid treated subject and demonstrate better barium filling.

2.9. Discussion (1-14)

This discussion follows the same order as the experiments 1-14 described above.

1 Baseline IOP variability

Needles placed in cancellous bone generally record a pressure. Previously the assumption was made that in normal bone this would have a repeatable, stable or fixed value. It has generally been supposed that in healthy bone IOP would be around 30% of systolic BP or 30mmHg. In reality most authors have had some difficulty in establishing a stable or repeatable measure of IOP and there remains disagreement as to the value that might be considered a normal IOP even in healthy volunteers (Salzman 2017). It was initially frustrating to find that the IOP varied so much even in carefully controlled studies in apparently similar healthy subjects. There was significant variation both within and between subjects. Reasons for the variation in terms of gender, weight, needle site and needle size were sought but none could be found. It was not until later in the series when there was a reasonable number of recordings that it became apparent that in fact there was no single value for IOP. There was a wide spectrum of values rather than a narrow band of 'normal' values. That led to questioning of the previous understanding of the measurement of IOP itself. This point is discussed more fully in sections 6, 7, 8 and 12 of the discussion below.

2 Method of measuring IOP

While setting up recordings it was noted that the IOP was dependent on the needle clearance technique used. It seemed that the injection of even small 'clearance' volumes of heparinised saline together with the associated blood, fat, bone and other debris backwards into the delicate cancellous bone vascular tree was a major physiological

insult. The IOP usually took 10 or more minutes to recover from a small injection whereas aspiration was followed by a rapid recovery in around 30 seconds. From that point on forced injection of saline into bone was avoided. Previous reports linking IOP with the type and timing of needle clearance are not available. Ficat popularised a technique for the 'functional exploration 'of bone which included deliberate saline injection (Ficat 1985). This work calls into question the validity of that technique. Others have reported on the dangers of intraosseous perfusion and the risk of it leading to amputation in infants (Larsen 1938, Taylor 2011). The exact clearance technique used by previous authors is not always clear (Jones 2011). It now seems possible that they may have been damaging the local microcirculation and recording a low IOP as a result. Alternatively they may have been blasting or tearing into larger vessels so that once the initial circulatory shock had passed the effective needle tip blood pool was enlarged thereby giving a higher chance of contacting larger blood vessels and a higher IOP. It is equally possible that clinicians have in the past injected saline into osteonecrotic or diseased bone thereby directly causing a pressure rise in poorly drained bone that they then took to be a raised IOP (Ficat 1985).

3 IOP wave forms

Previous authors have reported a pulsatile IOP (Azuma 1964). Pulsatility synchronous with the observed cardiac pulse was present in most of the traces in this study. The respiratory wave only became evident with slower trace recording speeds. The wave was then observed to be synchronous with the observed respiration of the subject. At first sight it seems remarkable that a respiratory wave could be found in a pressure recording from a needle tip buried deep in cancellous bone. But there is no other reasonable explanation for the wave seen in virtually all these recordings at slower

speeds. For this work there was no access to anaesthetic monitoring equipment. As experience was gained it became evident that the most effective means of controlling the anaesthetic was by observation of the IOP recording for pulse and respiration. Previous reports of intraosseous pressure being used for monitoring anaesthetic control do not appear to exist in the literature.

4 Drug administration on IOP

The anaesthetic technique involved intermittent bolus injections of diazepam or fentanyl. It became obvious that there was a direct effect on the IOP record. Furthermore it was seen that after around 90 seconds the IOP returned to the previous level with diazepam but that with fentanyl there was a second smaller wave of a similar 90 second duration as in Figure 2.6. It appears that 90 seconds is equivalent to one 'circulation time' and that diazepam is cleared in one cycle. Fentanyl is less rapidly cleared and produces a second circulation time wave. Previous reports of IOP registering circulation times could not be found in the literature.

5 Blood pressure and IOP

Blood pressure (BP) was measured directly by catheterising the opposite left femoral artery in five subjects. The catheter was connected to a pressure transducer. There was clearly a correlation between BP and IOP with a Pearson correlation of R=0.829. Other authors have recently described a falling IOP in exsanguinating pigs (Frascone 2013). Collectively these observations confirm that IOP is mediated more by the arterial supply side rather than being a measure of venous back pressure as had generally been supposed. Any measurement of IOP should therefore perhaps be compared with or

described as proportional to the systemic circulation pressure. This point does not appear to have been considered in previous IOP work.

6 IOP and pulse pressure

Although previous authors have shown graphs with an appreciable wave depth or pulse pressure (PP) this work appears to be the first to observe a correlation between the IOP and PP. It is not entirely clear what the ‘pulse pressure’ is. Here it has been taken as the difference between the top and bottom of the recorded IOP wave. It probably represents the capillary level systolic to diastolic pressure difference with a superimposed ‘respiratory wave’ component. In any event it was the correlation between the IOP and the PP that first indicated why a single IOP measurement might be so variable.

It would appear likely that within any bone there is a vascular tree. Inserting a needle randomly into that vascular tree records pressure only in the blood pool at the needle tip. On some occasions the needle tip would strike a larger arteriole with a higher pressure and larger pulse volume. At other times the needle would encounter only smaller vessels or veins, fat and other lower pressure tissues. It seems that the variable placement of a needle into the cancellous bone vascular tree might explain the variable nature of the IOP recorded. If this explanation holds true it calls into question the validity of previous IOP work and the value of measuring or using IOP measurement in bone at all (Jones 1993). This is explored further in section 11 below.

7 Vascular occlusion and IOP

Arterial occlusion

In the past it has been considered that IOP was very largely a reflection of a venous back pressure or tissue swelling or turgor. In all these recordings the application of a clamp to the proximal artery caused a fall in IOP over the course of 20 to 30 seconds to a stable, low and entirely pulseless IOP. Both the loss of pressure and the loss of pulsatility indicate that IOP is predominately a measure of capillary arterial supply pressure at the needle tip and not a venous back pressure.

Venous occlusion

When the proximal vein was clamped, in every case there was a rise in IOP and the pulse pressure wave was retained. If IOP was a retrograde pressure phenomenon a clamp on the draining vein would not have been expected to allow pressure to increase, nor to retain the pulse volume wave.

Further observations

The majority of the pressure in any single measurement of IOP in vivo is seen to be mainly due to the arterial supply. The loss in IOP seen with proximal arterial clamping is usually more than the rise seen on proximal venous clamping. Similarly the fall seen on removing a proximal venous clamp is proportionately less than the rise seen on removing proximal arterial occlusion. It is therefore evident that the IOP seen after clamping the proximal arterial supply (IOPa) probably represents the lowest possible drainage pressure achievable at the needle tip. This appears to be a novel observation or

at least a new definition for IOP. In fact, it is probably the only means of measuring a true or background 'IOP' if not a particularly useful one from a clinical point of view.

Similarly the raised IOP recorded with a proximal venous clamp in position (IOPv) probably represents the best capillary supply pressure achievable at the needle tip. The vascular system is not a perfectly frictionless hydrodynamic model. One would not expect the lowest pressure IOPa in vivo ever to be zero. Neither would one expect the highest pressure with a clamp IOPv ever to reach full systolic arterial pressure.

Reynolds and Burkhardt both described right angled capillary divisions which might be associated with greater 'stepping down' in cancellous bone capillaries or alternatively some form of back flow choke or flow prevention mechanism (Reynolds 1948, Burkhardt 2012). The nature of the stepping down in pressure at each junction of the arterial and capillary tree and the converse venous tree and back pressure allows one to say that for the blood pool at the needle tip the difference IOPv - IOPa is probably as close to a repeatable bone perfusion pressure range or 'bandwidth' obtainable.

If this is to be used clinically it would be preferable if a fixed small size bolus be used to prime or clear the needle tip and adjacent blood pool. Perhaps an even better method would be to use a needle and trochar, remove the trochar and aspirate to establish the IOP with minimal damage to the bone. Heparinisation would probably be required.

While neither the initial IOP nor the two clamped values are likely to be of clinical importance individually, it is proposed that the subtraction value (IOP with a proximal venous clamp minus the IOP with a proximal arterial clamp) or IOPv - IOPa gives a more useful value than a single IOP measurement. It gives a perfusion pressure range or 'bandwidth' achievable at the needle tip deep in cancellous bone.

This concept does not seem to have been previously reported. Literature searches reveal no useful previous references. McQueen described a 'differential' pressure by

measuring diastolic blood pressure minus the compartment pressure in tibial fracture compartment syndromes but this is quite a different concept (McQueen 1996). In many clinical situations it would be possible to apply an arterial or venous pressure cuff above the bone in question rather than needing surgical exposure of the vessels to apply clamps.

Compartment syndrome

There may well be wider practical clinical applications for the measurement of perfusion in other organs (Elliott 2003). For example, this approach could be used clinically to study perfusion problems such as compartment syndromes. If a catheter or needle is placed in the affected calf muscle and then shows little change in pressure with differential proximal tourniquet application at arterial and venous pressures, then, irrespective of the starting value, there is a poor perfusion range at the needle tip. Decompression would be advisable no matter what the actual intra-muscular pressure. A wider perfusion pressure or 'bandwidth' range would indicate that there is better perfusion at the needle tip and that surgical intervention is not urgently required, again no matter what the initial intramuscular pressure.

Experiment 8 IOP with loading and vascular occlusion

As the skeleton is obviously designed for activity it seems surprising that IOP has not previously been measured during activity. Historically it has been assumed that bone was perfused by blood both at rest and during activity in a fairly steady manner. Tondevold showed that cancellous blood flow increased slightly with activity (Tøndevold 1983). There had been attempts by previous authors such as Swanson and Freeman to see if bone was hydraulically strengthened (Swanson 1966). They used

grease saturated dry bones or cancellous bone plugs in jigs with impact testing. The conclusion from those non-physiological experiments was that there was no hydraulic strengthening of bone.

It has long been recognised among orthopaedic surgeons that certain bone diseases were caused by failure of the blood supply. Some were obviously post traumatic such as femoral neck fractures or after slipped epiphyses of the femoral neck. Some were embolic bone diseases such as sickle cell osteonecrosis and caisson disease Others appeared developmental such as Perthes and perhaps osteochondritis dissecans (Osunkwo 2013, Marti-Carvajal 2016, Mallet 2018). Some were iatrogenic, for example compression ischaemia of the femoral head caused by forced abduction of paediatric hips being treated for developmental dysplasia.

Osteoarthritis itself has not generally been thought of as a vascular disease (Termansen 1981, Fernandes 2015). This work shows that IOP fluctuates with vascular changes. It was therefore important to arrange to load the bone without compressing soft tissue or obstructing the blood supply. This simple experiment aimed to do this as far as possible by enclosing the bony part of the foot in a loose fitting tube. That controlled movement and allowed longitudinal weight bearing down the axis of the limb without altering limb position or squeezing soft tissue or interfering with blood flow. It was found that with loading of one body weight there was a consistent increase in IOP.

It was also evident that the IOP change occurred immediately as the load was applied rather than slowly as with the vascular occlusion studies. The raised IOP persisted while the load was applied indicating that the bone was being constantly compressed rather than it being a perfused tissue, like a sponge or balloon which ‘emptied’ within a few seconds of a load being applied.

The loading was repeated with and without vascular occlusion. The reduced effect on IOP in the arterial clamped limb and increased IOP with the venous clamp in place suggest that cancellous bone is a perfused tissue that has additional hydraulic pressure transferred through its substance with loading. The IOP is greater in perfused or charged bone and less in bone that is not prefilled or charged by the arterial supply. This experiment therefore appeared to confirm that there is immediate transmission of load by hydraulic pressure through the substance of the cancellous bone.

It becomes apparent that in effect there are two fluid systems in operation. The first is the normal circulation. This operates at the usual systolic and diastolic pressures and can be interrupted on the arterial or venous side with entirely predictable slow filling and emptying effects on IOP as might be expected in any other perfused organ.

The second system is one specific to subchondral bone in which the load is transferred through soft cartilage onto the slightly flexible thin bone of the subchondral plate and into the fatty tissues below the subchondral plate. Subchondral fat cells are fragile with thin walls. They contain lipid which is liquid at body temperature. This appears to be the only fat in the body which is liquid at body temperature. This is a personal observation for which no references could be found. Most orthopaedic surgeons recognised that bone fat pours out of fractures or sprays from power tools whereas other body fats do not. The delicate fat cells are soft but constrained within the cancellous bone matrix. Collectively, together with haemopoetic tissues these soft, flexible but incompressible tissues allow the transmission of weight bearing force by means of hydraulic pressure to the trabeculae. The trabeculae in turn are aligned so as to transfer the force onwards to the cortex and so down to the next metaphysis and joint where the process is reversed.

Simple estimates of the possible subchondral pressures in the system indicate that pressures are likely to be up to 20,000 mmHg (Fukubayashi 1980). Such pressures if unconstrained would be damaging to fat cells, capillaries, red cells and other fine tissues in the subchondral region. Significant bone bruising would be expected. Subchondral pressures are likely to be very much higher than those in the circulating system where pressures of 250 mmHg at a maximum and perhaps around 30 mmHg in bone capillaries may be expected. Hwang describes increased 'hydraulic conductance' or less resistance to pressurised saline flow across isolated cores of osteoarthritic bone compared to normal bone. She suggested that in OA there may be more vessels penetrating or weakening the subchondral layer. That is not a physiological test and in any event is not something addressed in this work (Hwang 2008).

Evidence for structures which allow great pressures to be tolerated yet which do not prevent the low pressure circulation from functioning should be sought (see Chapter 6).

Experiment 9 IOP at different sites

The question arises as to the distribution of the IOP changes in the loaded bone. This experiment appears to show that the pressure is present simultaneously at more than one point within a femur and in the adjacent upper tibia. The changes in the example shown demonstrate again that the effects of proximal vascular obstruction are present throughout the bony chain or at least at both bone ends and that the same applies when loaded.

Experiment 10 IOP compartment injection study

The injection of a small bolus of saline into either end of the femur and the upper tibia by turns appears to show that IOP is capable of being transferred throughout the length

of the bone but not across the knee joint. This lends further support to the idea that each bone is a relatively enclosed space and that the joint is a hydraulic barrier. It is not claimed that this crude injection study is evidence that in vivo the IOP is equal throughout the bone or that in reality any IOP is transferred from the end of one bone to the other. It merely demonstrates that the bone is a relatively closed space and that the joint itself is an absolute hydraulic barrier.

As described above it seems more likely that in vivo the load is dissipated by hydraulic force stepping down from the immediate subchondral area with an IOP that diminishes with distance from the joint as the trabeculae take up the load and transfer the force to the cortical shaft. That might be a distance of a few centimetres in a large joint like the knee or a few millimetres in a finger. The reverse would happen at the far end of the loaded long bone. The cortical shaft transmits force onto the trabeculae and they in turn are slightly flexible and compress soft fatty subchondral tissue transferring the load into the endplate and cartilage above and so on across the joint and along the bony chain.

Experiment 11 Basal IOP and pulse pressure with steroids

The primary object of this part of the work was to test the effect of steroids on IOP. The study confirmed that steroid treatment raised IOP as previous authors have found. However, it was surprising to find that there remained a wide range of IOP values in both steroid treated and control groups. For several decades IOP has been measured in an attempt to understand bone pathology and to explore bone perfusion in pain, osteonecrosis and other diseases. Previous authors have considered IOP to have a static or constant value. This is said to increase in osteonecrosis, with steroids and with bone pain.

However, the logic behind IOP testing itself needs to be questioned. No other solid organ has had pressure measured in this way. Generally if pressures and blood flow are to be measured elsewhere in the body it is done by inserting a needle into an artery or into a hollow organ such as the brain ventricle, spinal CSF space or bladder. It is surprising that for so long orthopaedic surgeons may have assumed that there might be a constant or fixed pressure within bone, no matter where the needle is placed. No such approach has been considered elsewhere or for any other organ. No other author appears to have raised this objection to the use of IOP in bone perfusion studies.

Experiment 12 IOP with steroids and proximal occlusion

This work repeats and confirms that with or without steroid treatment and even with a repeatable technique, a wide range of IOP values is obtained by putting a needle into bone. The spread of those values and their correlation with the associated PP appears to support the concept that the IOP is nothing more than a reflection of local perfusion conditions in a small blood pool at the needle tip. Any single IOP measure is therefore of limited value. The loss in both IOP and the PP with proximal arterial occlusion together with the augmentation in IOP and preservation of the PP with proximal venous occlusion further supports the argument that the IOP merely reflects perfusion conditions in a blood pool at the needle tip.

Experiment 13 IOP subtraction difference with steroids

The significant fall in IOP with arterial occlusion (IOPb – IOPa, 23.8 mmHg to 7.6 mmHg, $p<0.0001$) and the relatively modest rise in IOPb to IOPv (23.8 mmHg to 29.1 mmHg, $p<0.09$) indicates that the majority of the recorded IOPb is due to the arterial supply side rather than being a venous back pressure. One would expect the IOP needle to record only pressure from the largest or highest pressure vessel at the needle tip blood pool. It is probable that the best supply pressure achievable at the needle tip would be that seen during proximal venous occlusion. Similarly any underlying back or venous drainage pressure at the needle tip would be that seen when there is proximal arterial occlusion.

In this experiment no significant difference between the steroid treated and control subtraction results were found even though there was clearly a difference in the other absolute values. This may confirm that IOPv - IOPa is a better measure of bone

perfusion at the needle tip than IOP alone. The logic of these assumptions needs to be tested further. Nevertheless, this appears to be a novel concept which may have further application in the study of the effects of disease, drugs and surgery on bone perfusion.

Experiment 14 Photography and micro angiography

The steroid treated controls lost weight and were visibly cachexic. Surprisingly the angiograms appeared to show that steroids allowed increased barium uptake in bone. It seemed that steroids at these doses in this particular model caused the intraosseous fat space to shrink rather than fat cells swelling as previously described. If it is assumed that bone is a relatively closed space, manipulation of the soft tissue or fat volume within the space might have an effect on the IOP. The barium uptake, colour photographs and micro angiograms together with the cachexia and weight loss point to the intraosseous volume decreasing. It remains possible that the haemopoetic tissue volume falls rather than the fat cell volume but the same logic applies. Other authors have shown that fat cell volume is preserved or even relatively increased in starvation (Bathija 1979, Devlin 2015) but it seems more likely in this model that the rise in IOP with steroids was due not to an increased back pressure from fat cell swelling but to reduction of the bone fat space and therefore a better supply pressure at the needle tip.

There are several possible limitations in this work. The animals were not identical in terms of age or weight. Needle placements could never be identical. X-rays were not available for needle placement but under direct vision hand placement of the needle tip was to within a few millimetres of the subchondral surface. Anaesthesia without specialised equipment in these subjects is recognised to be brittle. As the duration of each experiment varied, an average value for IOPb from early, middle and late in each recording was used. The vascular occlusion and loading values were recorded once only

at the steady state achieved within 30 seconds of applying the clamp or load. For the main loading study there were five subjects with a total of 12 IOP recordings, from the femoral condyle and the proximal tibial. Although there was a wide range of values for IOP at both sites there was no statistical difference between the femoral condyle and the proximal tibia. Data from both the femoral condyle and the proximal tibial was therefore pooled. This reflects the clinical situation where IOP may be measured at virtually any site. Corticosteroids are known to raise systemic blood pressure and that may have caused an indirect rise in IOP. The subtraction difference was not affected. No histology was carried out. Several of the figures demonstrate traces from individual subjects such as the compartment injection tests and the results can only be qualitative.

In summary this work was carried out in 1985. Further analysis in 2014-18 offers the following conclusions, several of which appear to be novel observations. Collectively they offer a fresh view of subchondral perfusion physiology in active joints.

1 There is a wide range of IOP values in healthy bone rather than there being a single value.

2 IOP is not much affected by weight, gender, site or size of needle used.

3 IOP is significantly affected by the method of needle clearance.

4 Intraosseous saline injection appears damaging and lowers IOP for several minutes. Needle clearance by aspiration may be better.

5 IOP records demonstrate cardiac, respiratory and circulation time waves.

6 IOP fluctuates with systemic circulation pressure changes.

7 IOP is proportional to BP.

8 PP is proportional to IOP.

9 Proximal arterial occlusion reduces IOP to IOPa and obliterates the PP.

10 Proximal venous occlusion increases IOP to IOPv with preservation of the PP.

11 A better means of assessing needle tip perfusion might be by subtraction IOPv - IOPa.

12 This technique could probably be used to assess other perfusion problems such as compartment syndromes.

13 Physical loading instantly increases IOP to IOP+Ld.

14 Loading during arterial occlusion instantly gives a small rise from IOPa to IOPa+Ld.

15 Loading during proximal venous occlusion instantly gives an augmented rise from IOPv to IOPv+Ld.

16 Load is transferred through subchondral bone and fat to the trabeculae instantly, probably by hydraulic pressure, whereas perfusion changes are slower.

17 Each bone is a relatively enclosed space.

18 Joints act as hydraulic pressure barriers.

19 Steroids increase IOP, PP and the occlusion and loading pressures.

20 Steroids have little effect on needle tip perfusion range by the subtraction method.

21 Steroids in this model raise IOP by reducing fat cell volume thereby improving perfusion pressures at the needle tip.

22 Two fluid systems exist, one for low pressure circulation and one for higher pressure hydraulic force transfer.

23 There must be anatomical and histological modifications to cope with both fluid systems.

24 In conclusion subchondral perfusion physiology requires further research.

In summary, this work indicates limits to the usefulness of IOP as a measure of bone perfusion. A fresh interpretation of subchondral bone perfusion and IOP measurement is offered. A new means of assessing perfusion in bone at the needle tip by a subtraction technique is suggested. The subtraction technique may have clinical applications in other perfusion problems. Load appears to be transferred partly by hydraulic pressure from the subchondral region to the cortical shaft. An alternative view of the effect of steroids in raising IOP in this particular model is proposed. The work opens the door to a new vasculo-mechanical understanding of the physiology of subchondral bone circulation.

A further study was therefore undertaken in Chapter 3 and Chapter 4 to develop an in vitro model to confirm these findings and to explore more effectively the dynamics of IOP during joint loading.

3. CALF FOOT IN VITRO MODEL FOR IOP AND PERFUSION

3.1. Background

Intraosseous pressure (IOP) has been of historic interest in osteonecrosis, osteoarthritis and bone pain but of limited practical clinical value. Earlier in vivo studies showed that IOP is not a constant but fluctuates with systemic vascular pressure changes and loading. In this study a new in vitro calf foot model was developed to confirm the earlier in vivo work. IOP would be tested by altering perfusion pressures and with a tourniquet to establish parameters for later testing of IOP with loading.

3.2. Development of the experimental set up

Choice of location and animal

Initially the work began in the Physics department at the University of Exeter where there was previous experience with vascular studies and nutrient transfer across the horse fetlock. Abattoir material from Taunton consisted of a variety of horses and wild ponies of differing breeds, weights and ages. The horse fetlock metacarpal and phalanx must be one of the hardest bones in the animal kingdom and one capable of taking a force of several tons when at a gallop. Drilling such bone and inserting an intraosseous needle proved awkward. To load the bone physically might require a force of several hundred kilos in a jig. Nevertheless some fetlocks were processed.

The Taunton abattoir closed and the decision was made to use the Swindon (Wootton Bassett) abattoir and the more readily available calf foot. The experimental work moved to the OOEC labs at the Botnar Research Centre at the Nuffield Orthopaedic Centre in Oxford. In the UK most male calves are culled at around 1 - 2 weeks of age. Their feet are regarded as a waste product. Several hundred calves are culled on a weekly basis throughout the year. The proximal metacarpal articular surface is remarkably similar in shape to the upper tibia in man as in Figure 3.1.

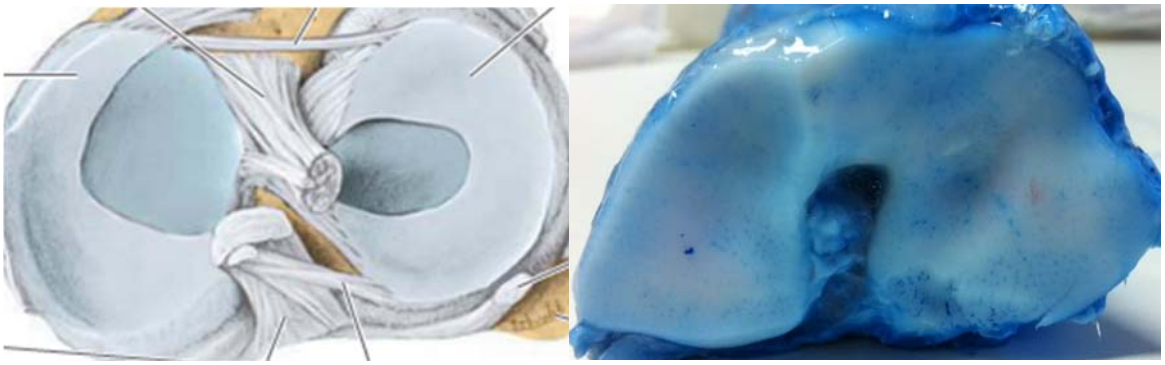


Figure 3.1 Left - upper tibial articular surface in man and right - proximal metacarpal articular surface of calf. The calf has no menisci.

The metacarpal itself is a fused remnant of the 3rd and 4th metacarpals but becomes bifid from the mid metacarpal shaft down. The metacarpo phalangeal joint, the phalanges and the hoof are bifid in the ungulate. The calf effectively walks on the third and fourth finger nails. The specimen is equivalent in size to a small human forearm as in Figure 3.2. The weight of the animals was 50 - 80 kilos.



Figure 3.2 Calf feet with radial artery catheter inserted prior to wash out with Krebs-Henseleit saline.

The animal is culled by a shot or bolt to the brain, suspended at a height by one hind leg and exsanguinated by cutting the major neck vessels. Their blood for serum preparation is available in large quantities. The calf feet were obtained fresh within a few minutes of being culled. The forefoot was sectioned just above the carpus or wrist. It was possible to collect feet, catheterise, rinse out and return to the lab in Oxford within an hour or two of culling. Calf feet are of a roughly similar size and age, are readily obtainable and have softer bone than the horse fetlock. Each foot is in many ways a paired organ being nearly bifid. That might have allowed for paired or control individual ray loading experiments.

Anatomy

Essentially one radial artery supplies the equivalent of the human hand from the distal radius onwards. In the calf it is a thick walled muscular tube adjacent to a large median nerve equivalent and several veins. Once found it is easily dilated and catheterised as in Figure 3.2. Occasionally the anatomy was anomalous or the level of amputation was too low and the artery could not be found.

Choice of perfusion fluid

Saline, phosphate buffered saline and Krebs-Henseleit solutions were tried. The tissues became oedematous. Bovine serum albumin is obtainable but expensive. Egg albumin for fishing bait was tried but was difficult to dissolve. Cow derived gelatin is available as granules for sports diet supplements. The gelatin dissolved in warm water but solidified too easily and osmotic pressure measured by depression of the freezing point varied. Whole blood perfusion was considered but collection, anticoagulation, cleaning, warming, oxygenation and glucose replacement would not be possible. Calf blood was freely available. It was centrifuged in 500 ml containers, six at a time. The serum was filtered and stored frozen at - 80 °C. It was rewarmed, filtered and perfused without further difficulty. Each experiment used around one litre of serum. Calf serum proved a reliable fluid for this work.

Choice of pump or static perfusion

Normal circulation down to capillary level is pulsatile. A peristaltic pump was available. By adjusting the tube diameter and pump speed a reasonably physiological arterial pulse type of perfusion could be obtained. It proved difficult to manage in reality because pressure would fluctuate significantly with minor changes in pump speed or with movement of the limb. Furthermore with a pump much larger quantities of serum were used.

A static height of perfusion was therefore used with a Mariotte flask. A Mariotte flask employs a syphon to maintain a constant height or head of pressure as the fluid level in the supply descends. The Mariotte flask was filled with re-warmed serum and placed on a step ladder at known heights above the limb. The distance from the tip of the syphon to the limb was controlled and tests were carried out at different pressure heights from 50 cm to 250 cm. The connecting tube was a drip or IV line with the last several centimetres of the line, the attached side arm, the pressure transducer and the arterial line itself all resting in the same 37 °C water bath as the experimental foot. This is illustrated in Figure 3.3.

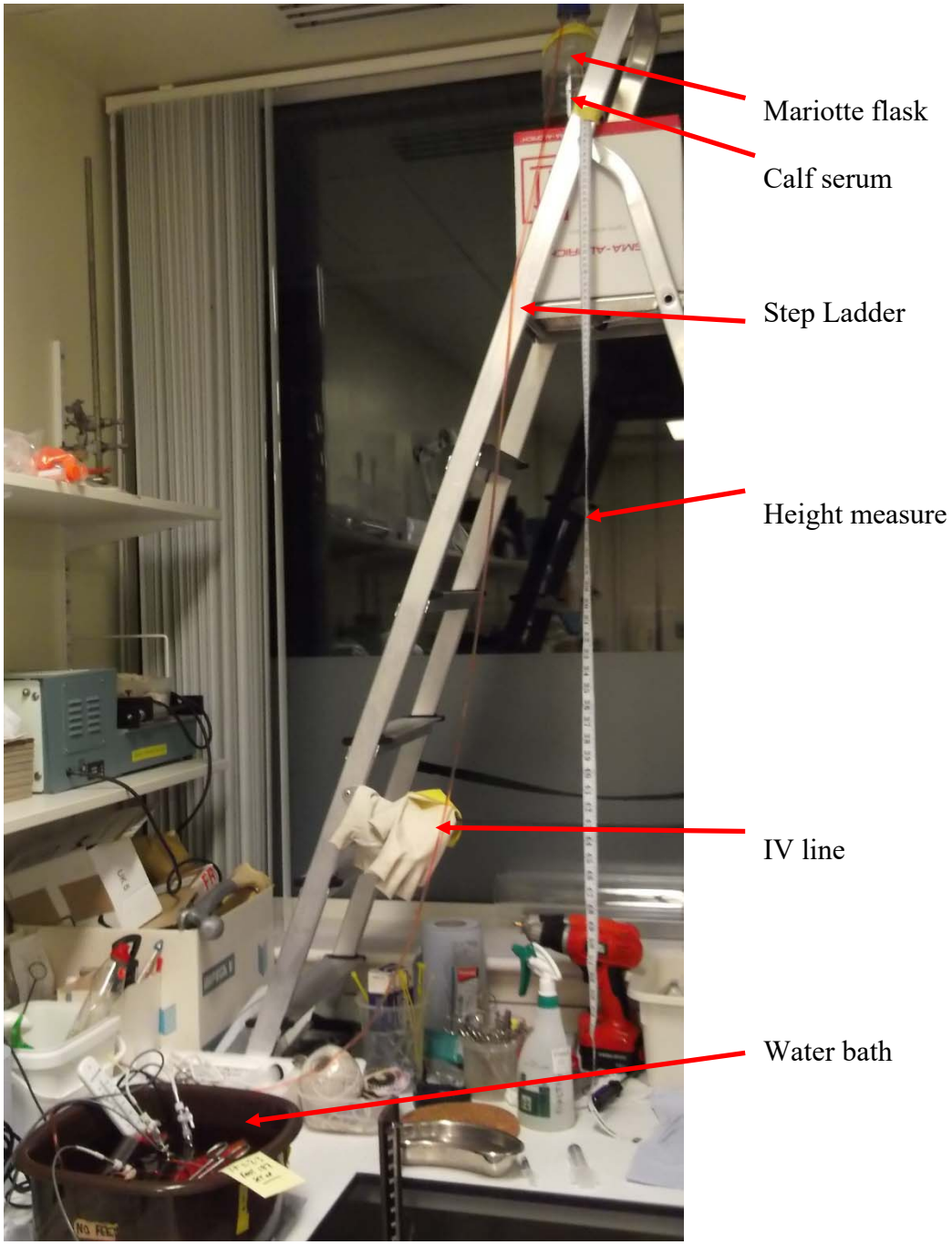


Figure 3.3 Experimental set up with serum in Mariotte flask at 150 cm above foot in water bath.

Choice of incubator or water bath

An enclosed air incubator for the feet was tried but though of adequate size could not be maintained at 37 °C during the experiment. A water bath proved better. This was

open but easily maintained temperature with a heater and pump allowing free access to the foot as in Figure 3.4.

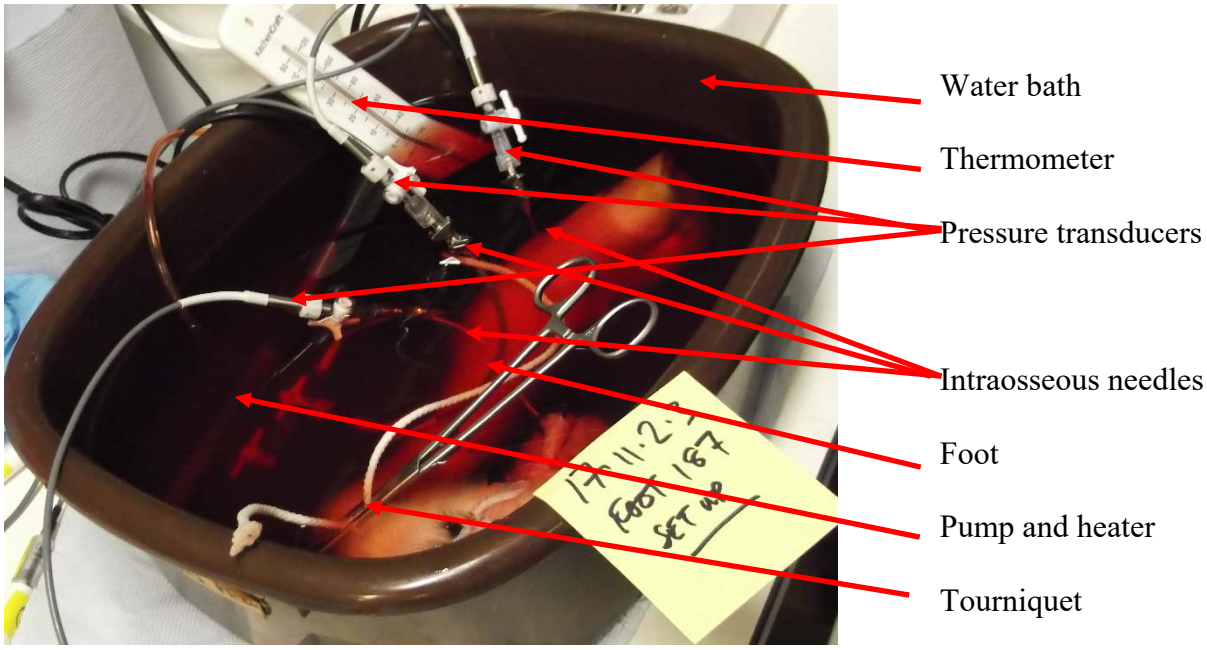


Figure 3.4 Experimental set up showing foot in water bath with attached IOP needles and pressure transducers.

3.3. Method

Model preparation

Fore feet from freshly culled Friesian male calves 1 - 2 weeks of age and weighing 50 - 80 kg were used. They were collected from an abattoir (F Drury and Sons Ltd, Swindon, UK). The fore feet were sectioned immediately post mortem above the carpus. The radial artery was catheterised with a 12" Teflon 16G catheter (E-Z Cath, Desert Pharmaceutical, Sandy, Utah) inserted for about 6 - 8" to approximately the mid metacarpal point and tied in with a linen thread. The limb was flushed with 2 x 60 ml of warm 37 °C Krebs-Henseleit (K-H) solution (Sigma Pharmaceuticals PLC, HD

House, Imperial Way, Watford.) The feet were set up in a water bath at 37 °C within one to two hours of culling. These were referred to as 'fresh feet'. Some feet were kept at room temperature until later the same day or overnight at 5 °C or frozen at - 80 °C with rewarming in a water bath for two hours before being used. These were termed 'old feet'.

The water bath was an open bowl with a circulating pump (Fluval FLU.U1 model C-48020 from Rolf C. Hagen UK Ltd, Whitwood Industrial Estate, Castleford, UK) and a heater to maintain the temperature at 37 °C (Aqua One 100 Watt IPX8 from Aqua Pacific UK Ltd, Southampton). A room thermometer confirmed that the temperature remained stable within a degree for the duration of the experiment. A doubled string tourniquet was applied and tensioned by twisting in forceps. It could be applied and released without moving the foot in the water bath.

Serum was prepared by collecting fresh calf blood, centrifuging at 10,000 rpm for 10 minutes at 4 °C and taking the supernatant fluid though a filter into plastic one litre storage bottles. Serum was kept in a fridge at - 80 ° C fridge. The serum was re-warmed and passed through an IV line which lay in the water bath at 37 °C before entering the foot. The warmed calf serum was perfused from a fixed height above the foot using a one litre Mariotte flask at 50, 100 or 150 cm. These heights equate to pressures of 37, 74 and 110 mmHg. Injection of the arterial catheter with 1 % Evans Blue in serum were carried out to assess distribution of perfusion as shown in Figure 3.5.

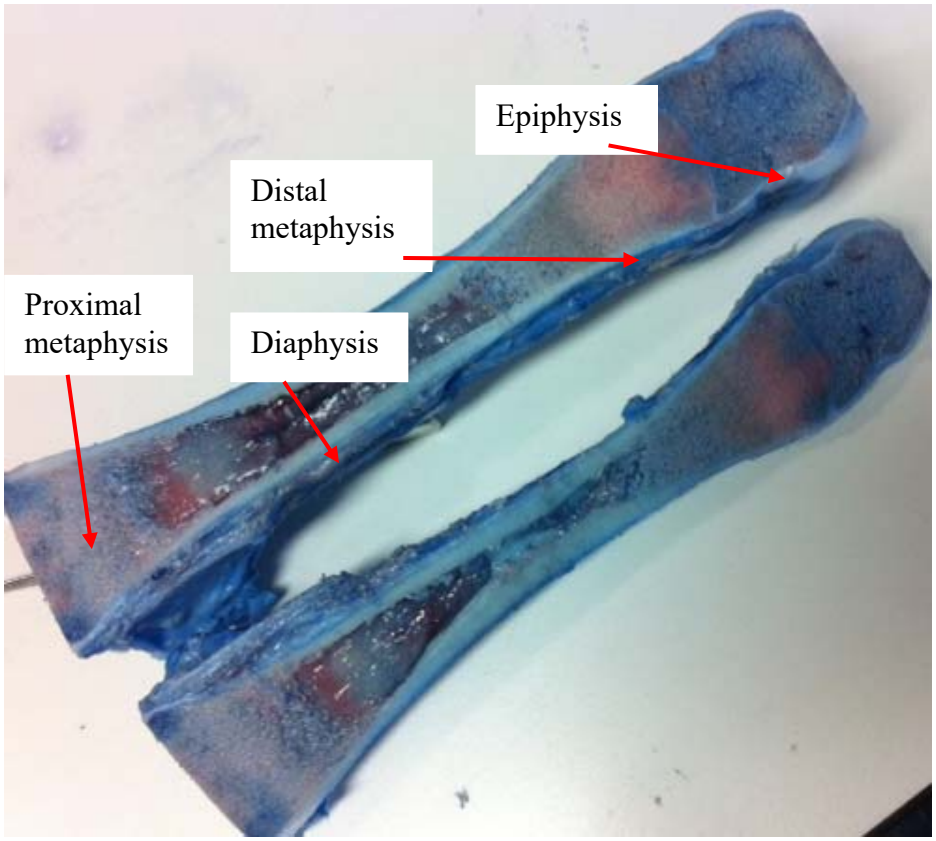


Figure 3.5 Metacarpal following intra-arterial perfusion of serum with 1% Evans Blue showing penetration throughout the bone.

Experimental setup

The Mariotte flask containing serum for perfusion was mounted on a step ladder 150 cm above the foot in the water bath as in Figure 3.3.

Pressure transducers

Previous work had used standard hypodermic Blue 21G needles. For this work stronger reusable needles with trochars were obtained. These were Luer lock bone biopsy needles with a bevelled trochar (Rosenthal Bone Marrow Biopsy Needle Luer lock fitting 16 swg 1.6 mm x 35 mm from Dixons Surgical Instruments Ltd, Wickford, UK). Insertion was by hand using direct percutaneous puncture at the relevant site. The

needles were placed in the approximate centre of the cancellous bone or within a few millimetres of the subchondral surface. The trochar was withdrawn and the needle was filled with Krebs-Henseleit (K-H) saline and connected to a three way tap. Care was taken to avoid forced saline injection during 'clearance' of the needles. One arm of the saline charged three way tap was connected to the bone needle and one to the pressure transducer (Gaeltec TT Luer lock catheter tip pressure transducer, Gaeltec Devices Ltd, Dunvegan, Isle of Skye). The third port could be used for irrigation or aspiration purposes. The general set up was as shown in Figure 3.4. Before each experiment the pressure transducers were zeroed and calibrated against a sphygmomanometer inflated to 100 mmHg. The four pressure transducers were connected to a Gaeltec S7d (version 4.3) transducer amplifier. That in turn connected to a Picolog ADC20 Data Logger and to a standard Hewlett Packard Prodesk PC. After a learning curve and trial and error it was found that the optimal settings were for results to be recorded for all four channels at one per second for up to an hour. The pressure transducers were zeroed at the start of each run. The range was set at 2500 uV full scale deflection for all transducers. At the end of each run the data was saved to an individual Picolog file. Hand written notes were kept during each experiment to record the various perfusion and loading events and their timing. Graphs of the entire run or desired portions could be printed off on an HP Deskjet1510 colour printer. The Picolog '.plw' data file was saved and later transferred into a '.txt' file which could be saved into Excel.

For analysis the Excel data was loaded to a separate file. The IOP values were recorded on a scale whereby zero pressure was at 1000 uV. A pressure of 150 cm water or 110 mmHg gave a value of 1330 uV. The values recorded were converted from uV to mmHg by the formula:

IOP mmHg = (uV – 1000)*110/330

Relevant parts of the data were saved to a separate file and converted from uV to mmHg. Graphs were then produced in Excel at an appropriate scale. This allowed specific IOP values and times to be read directly either from the data set or from the graphs themselves looking at the appropriate time or IOP. Those result were loaded onto an Excel spreadsheet for analysis.

Four pressure transducers and channels were available. Channel one was always used for recording the perfusion pressure at the point of entry to the arterial catheter. The other three channels were connected to needles in the metacarpal diaphysis, distal metacarpal epiphysis, subchondral metacarpal or proximal phalanx as required.

Recordings were made from up to three intraosseous needle channels at one per second for up to an hour. A total of 188 feet were collected. For this part of the study eight feet were tested fresh that is within two hours of culling. Seven feet were tested after more than four hours. These were known as old feet. In addition to the perfusion studies the effect of a tourniquet was explored in nine feet, six fresh and three old.

Experimental plan (1-7)

After initial trials to develop the model, experiments were conducted to establish the IOP response to static perfusion at different sites, times and pressures in fresh and old feet, with and without a tourniquet.

Experiment 1 Baseline IOP

Eight fresh feet and seven old feet were perfused at 150 cm pressure for 60 seconds to assess baseline IOP.

Experiment 2 Site differences

Among the 15 feet 40 separate IOP recordings at three different sites were made to assess site variation in IOP. In three feet dye injections were made to assess inter compartmental flow.

Experiment 3 Perfusion pressures

Perfusion at different pressures was carried out.

Experiment 4 Tourniquet effects

A proximal venous tourniquet was used to assess IOP increase and elastic recovery.

Experiment 5 Individual site response

The variation in IOP with increased perfusion at individual sites was tested.

Experiment 6 IOP rise and fall with perfusion

The IOP rise and fall with perfusion and cessation of perfusion was assessed.

Experiment 7 IOP filling curves in fresh and old feet

The difference in IOP filling curves with fresh and old feet at different pressures was explored.

Statistics

Results were expressed as means, standard deviations and ranges. Student's t-test was used to determine if there were significant differences. When each subject was used as its own control, paired t-tests were used. Otherwise unpaired t-tests were used. The Pearson test was used to assess correlations with $p<0.05$ considered to be statistically significant.

3.4. Results (1-7)

Experiment 1 Baseline IOP

Under similar perfusion conditions there was a wide range of basal IOPs. There were 15 subjects with 40 separate site IOP recordings. Where a subject had two or more recordings these were averaged. After 60 seconds of perfusion at 150 cm pressure there was a mean IOP of 30.0 mmHg (SD 14.4, range 7.6 mmHg to 52.7 mmHg) as in Figure 3.6. There was no significant difference between the fresh and old feet, t-test p=0.513.

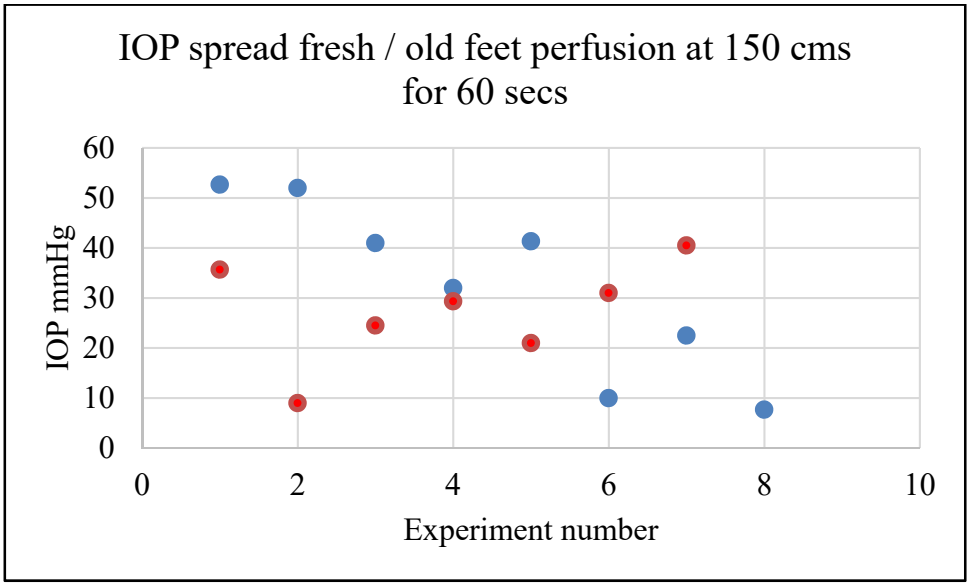


Figure 3.6 Averaged IOP values in 15 feet at 150 cm perfusion pressure after 60 seconds. Blue - fresh feet less than 4 hours old, Red - feet more than 4 hours old.

Experiment 2 Site differences

There was no significant difference in IOP between the sites tested. Forty different IOP recordings were obtained from three different sites in 15 calf feet under the same perfusion conditions (50, 100 and 150 cm serum for 60 seconds). At each pressure there were ten separate metacarpal diaphysis recordings (MCD), 18 metacarpal subchondral recordings (MCS) and 12 from the diaphysis of the proximal phalanx (PPD) as in Figure 3.7. There were no significant differences between the sites at 150 cm pressure perfusion for 60 seconds. The t-test results for the MCD to MCS was p=0.54, MCS to PPD was p=0.124 and MCD to PPD was p=0.051.

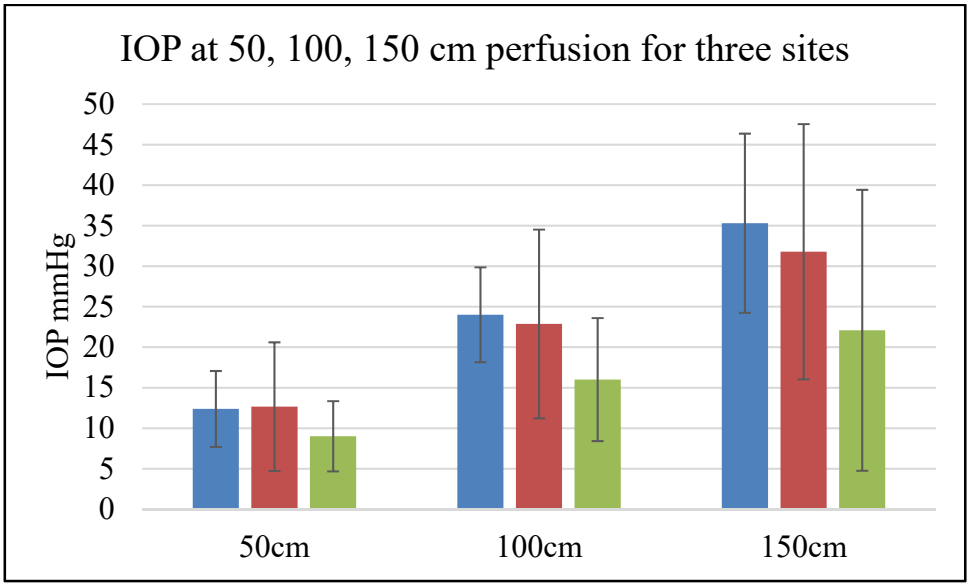


Figure 3.7 Difference in IOP at 60 seconds perfusion at the different sites tested, Blue - MCD - metacarpal diaphysis, Red - MCS - metacarpal subchondral, Green - PPD - proximal phalanx diaphysis. Error bars SD.

Figure 3.8 shows three split metacarpals. The first had been perfused with Evans blue into the supplying radial artery, the next bone also received an injection of 2 ml dilute Evans blue in the epiphysis and the third received the same injection in the distal metaphysis. There is perfusion to the whole bone through the artery but little cross over between the diaphysis and epiphysis in either direction.



Figure 3.8 Left pair - perfusion of dye through the artery gives general filling. Centre pair - dye injected into epiphysis, right pair dye injected into metaphysis. There is little cross flow over the epiphyseal plate.

Experiment 3 Perfusion pressures

IOP increases with perfusion pressure and with time. Initial IOP was always zero both in freshly prepared and older feet. There was no intrinsic or background IOP. IOP rose with perfusion as shown. With perfusion at higher pressures there were proportionately higher pressure filling curves as in Figure 3.9.

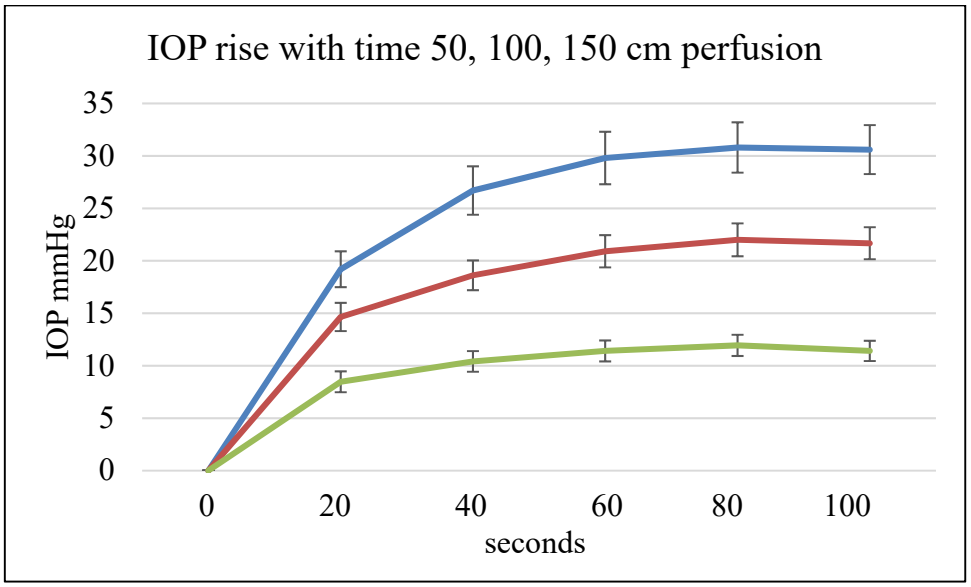


Figure 3.9 Rise in IOP with time among 15 subjects at different perfusion pressures, Blue - perfusion at 150 cm, Red - perfusion at 100 cm and Green - perfusion at 50 cm pressure. Error bars SEM.

Experiment 4 Tourniquet effects

In a group of nine subjects (6 fresh and 3 old feet) after perfusion at 150 cm serum for 60 seconds the IOP was a mean of 15.14 mmHg (SD 11.3 mmHg). When a venous tourniquet was applied proximally while perfusion at 150 cm continued, the IOP rose to 44.9 mmHg ($P<0.0001$) after a further 60 seconds. On removal of the tourniquet but with continuing perfusion at 150 cm serum the IOP fell back to a mean of 14.1 mmHg (SD 11.1) after 60 seconds ($p<0.0001$) as in Figure 3.10.

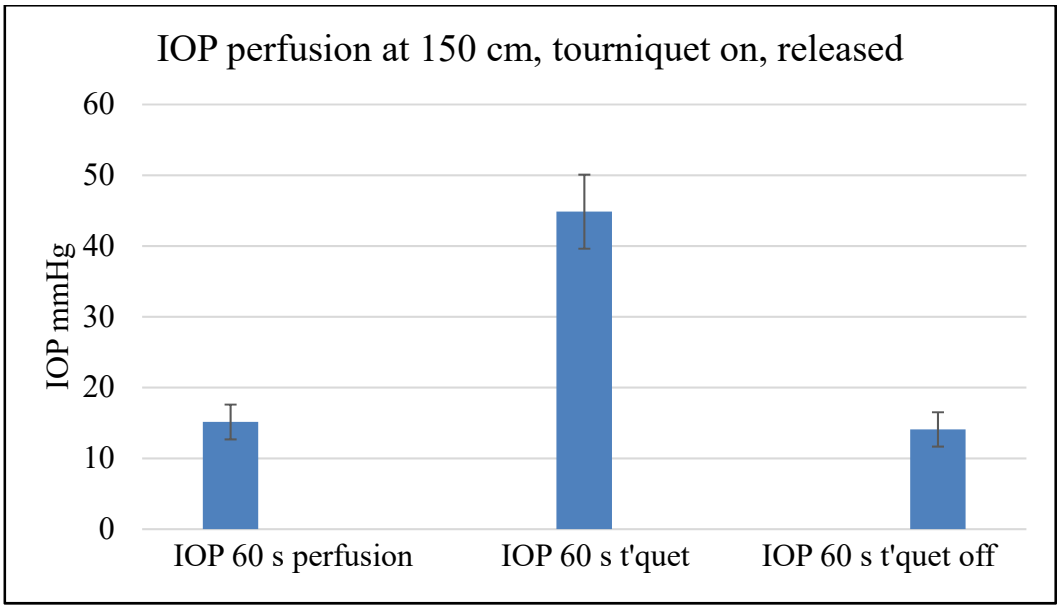


Figure 3.10 Additional rise in IOP with a proximal tourniquet for 60 seconds and the effect of removal of the tourniquet after a further 60 seconds during steady perfusion of serum at 150 cm pressure. Error bars SEM.

Experiment 5 Individual site response

Within each individual site IOP was strongly correlated with perfusion pressure. At each site individually perfusion with serum at 50 cm, 100 cm and 150 cm pressure for 60 seconds resulted in proportionately higher IOP as in Figure 3.11.

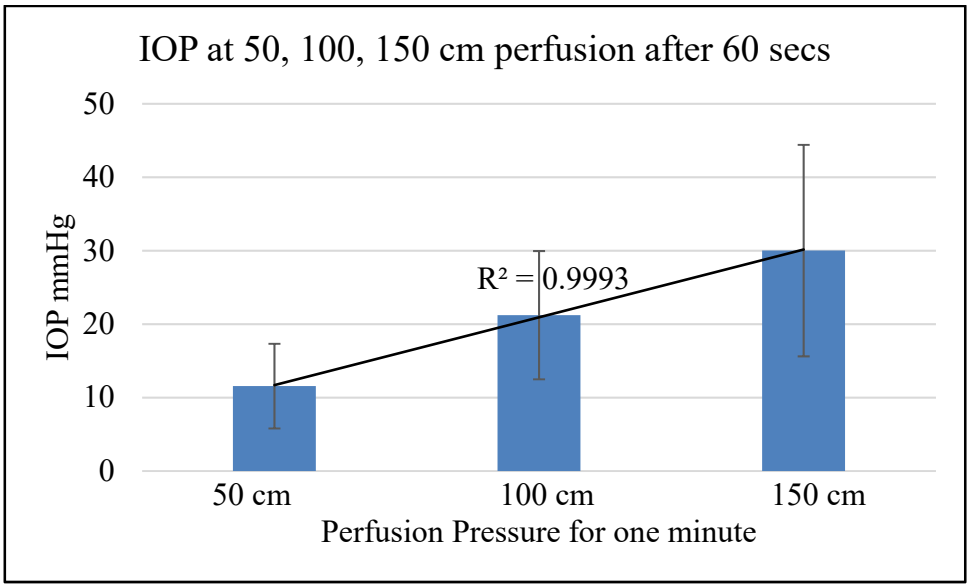


Figure 3.11 Perfusion at 50, 100 and 150 cms serum pressure after 60 seconds within each individual site. Pearson correlation R2=0.9993. Error bars SD, n=15 feet.

Experiment 6 IOP rise and fall with perfusion

There was a rise in IOP with perfusion for about a minute and a fall with cessation of perfusion as shown in Figure 3.12. Where there had been no previous perfusion during experimental set up, the first part of the filling curve represents an initial filling or charging of the system. Subsequent emptying and refilling cycles at minute intervals have symmetrical curves indicating that once filled the system is 'elastic'. The filling and emptying pressures on application and removal of a tourniquet at minute intervals were also symmetrical over a physiological pressure range.

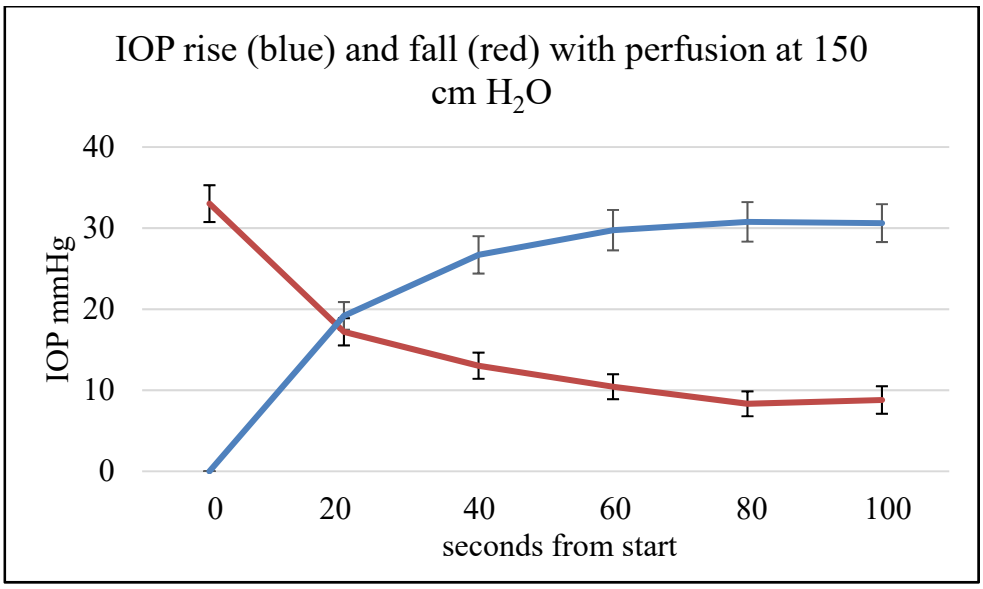


Figure 3.12 Relative rates of rise and fall with perfusion at 150 cm serum, n=15 Error bars SEM.

Experiment 7 IOP filling curves in fresh and old feet

There were differences in IOP filling curves between feet less than four hours old and feet more than 4 hours old. Under low pressure perfusion fresh feet had a significantly lower IOP for the same perfusion pressure than equivalent feet more than 4 hours old. The difference was less marked at higher perfusion pressures and with 60 or more seconds of perfusion as in Table 3.1 and Figures 3.12 and 3.13.

Difference between fresh and old feet IOP at different perfusion pressures

	20 sec	**40 sec**	**60 sec**	**80 sec**	**100 sec**
150 cm	P=0.40	P=0.13	P=0.26	P=0.58	P=0.57
100 cm	P=0.02	P=0.10	P=0.24	P=0.16	P=0.10
50 cm	P=0.0001	P=0.01	P=0.02	P=0.03	P=0.0001

Table 3.1 At 150 cm perfusion pressure the fresh feet showed no significant difference in IOP from 60 to 100 seconds (32.4 mmHg to 29.8 mmHg, p= 0.4).

Fresh feet appeared to stabilise their IOP after about one minute as in Figure 3.13.

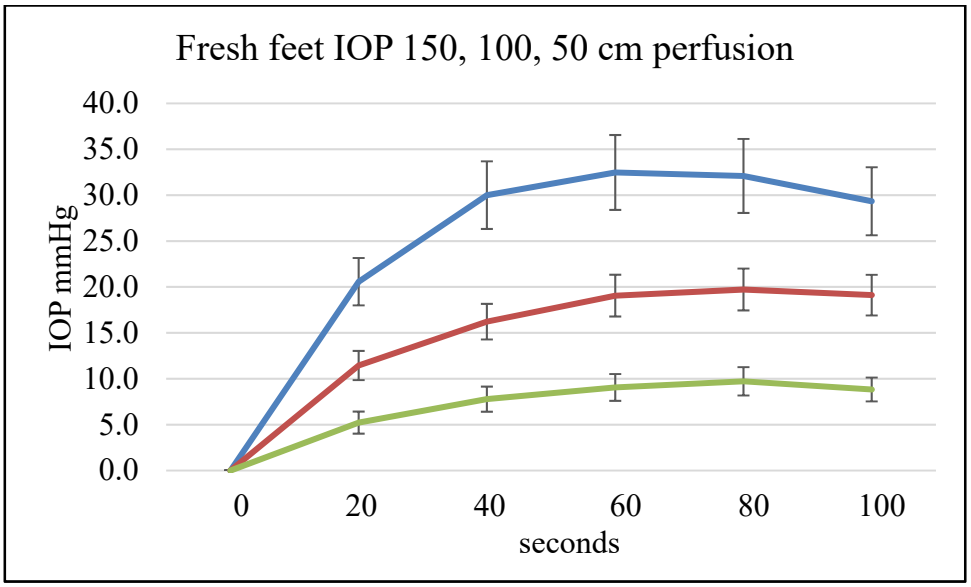


Figure 3.13 For fresh feet IOP peaked at about one minute with no further increase up to 100 seconds (t-test $p<0.4$). Blue=150 cm, Red=100 cm, Green=50 cm perfusion pressure, N=8, Error bars SEM.

Older feet at lower perfusion pressures had higher IOPs than fresh feet. Continued perfusion caused an indefinite slow rise in IOP. The old feet gradually became oedematous. From 60 to 100 seconds older feet showed a continuing rise in IOP (27.3 mmHg to 32.4 mmHg, $p<0.002$) as in Figure 3.14.

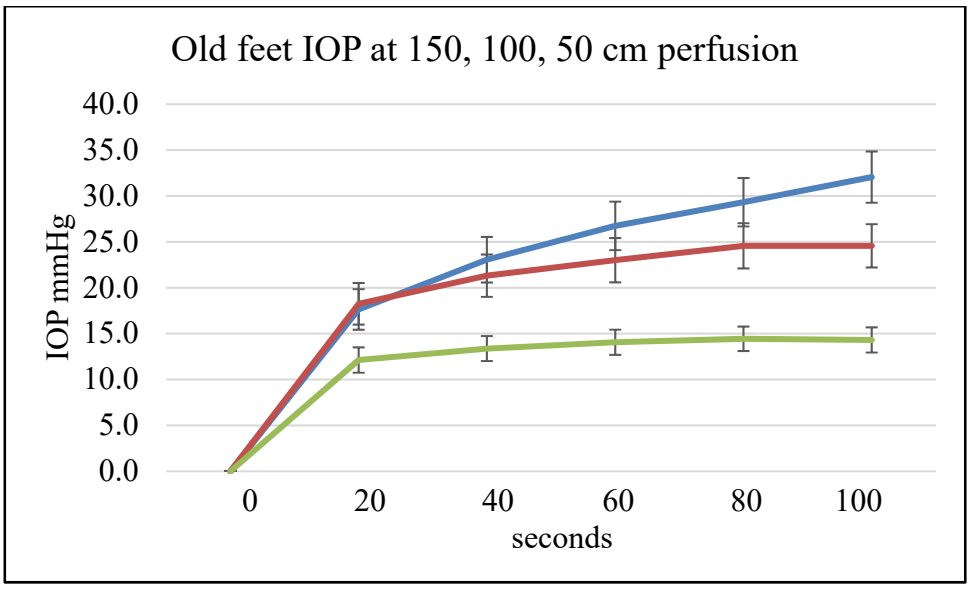


Figure 3.14 Older feet had a different filling curve profile with continued perfusion. They become increasingly oedematous with no obvious IOP end point. Blue=150 cm, Red=100 cm, Green=50 cm perfusion pressure, N=7, Error bars SEM

The combined fresh / old feet filling profiles were as shown in Figure 3.13.

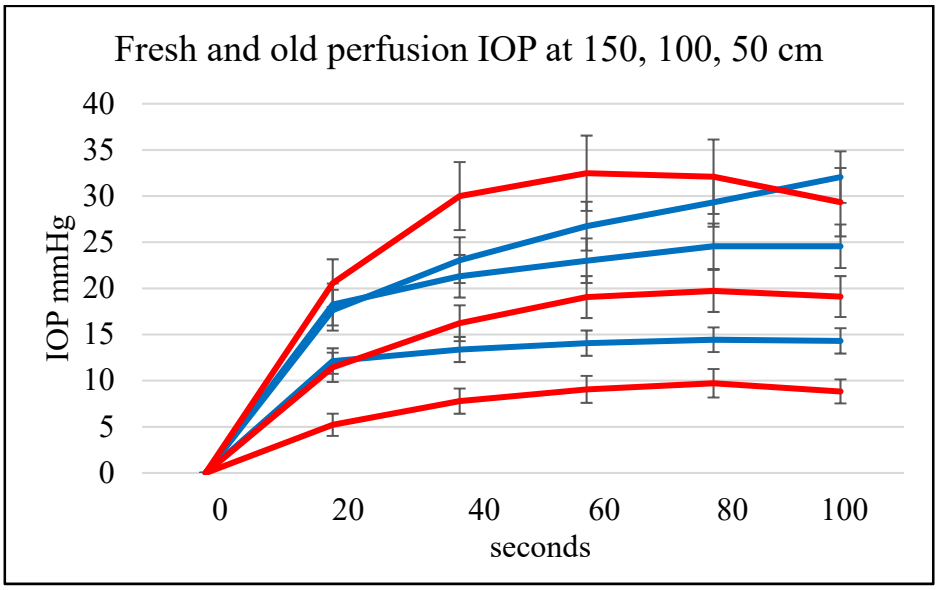


Figure 3.15 The different patterns in filling curves for fresh and old feet at different perfusion pressures. Red – eight fresh feet perfused at 50 cm, 100 cm and 150 cm pressure: Blue – seven older feet perfused at 50 cm, 100 cm and 150 cm pressure. Error bars SEM

3.5. Discussion (1-7)

The discussion follows the experimental sequence described in 1-7 above.

Experiment 1 Baseline IOP

This experiment demonstrates again the wide variation found in single IOP measurements obtained under apparently similar circumstances. This was discussed more fully in Chapter 2, experiments 1, 6, 7, 8 and 12. Other authors have struggled to identify a normal IOP (Salzman 2017). It was generally held that bone has an IOP which is a constant, present throughout the bone and in normal bone is approximately 30 mmHg. The variation is due not to some significant physiological difference between subjects or within bones but to the nature of the vessels contacted at the needle tip blood pool even by a standardised needle insertion. It is surprising that for several decades it has been assumed that cancellous bone has an intrinsic or constant background IOP and that the IOP may be measured by inserting a needle into a solid organ. It is only in bone that it has been assumed that a needle tip will give a reliable pressure reading representative of what is going on throughout that organ.

In this model the proximal end of the specimen was effectively open at the amputation site. It is assumed that each bone is a relatively enclosed and rigid structure lying within the softer perfused bag of forefoot tissue. Even with the open proximal end of the foot a reasonable IOP is generated inside the bone within a minute or so. There is probably primary filling of the foot soft tissues and secondary filling of the bone contained within. In order for a pressure to be recorded at all there must be some resistance or obstruction to free exit of the perfusing serum. It remains uncertain in this model what proportion

of the recorded IOP is due to arterial supply pressure and what proportion represents venous back pressure.

Experiment 2 Site differences

Site differences appeared to be minimal. In the calf there is an epiphyseal plate between the metacarpal diaphysis and the epiphysis. There is little or no flow across the epiphyseal plate. The two areas are likely to be functionally isolated from each other in a vascular sense. With respect to the proximal phalanx, although there is a single proximal epiphysis, the needles were placed in the mid shaft or diaphysis cancellous bone region. In effect, in this forefoot model there are three separate bones each with their own circulation. However each of the bones lay within the same envelope of soft tissue. For the purposes of this work the different sites produced no significant difference in IOP. The similar IOPs at different sites allows pooling of results from all sites for further analysis of physiology. While variation in IOP between subjects was considerable, at any single needle in any one subject there was a close correlation between IOP and the perfusion pressure as shown in experiment 5 below. Even though there is a wide range of starting pressures the model is reliable in terms of testing perfusion effects on IOP at an individual needle tip level. The injection study shown in Figure 3.8 demonstrates that the whole bone is perfused through the artery as expected and that there is little or no cross flow between the metaphysis and epiphysis.

Experiment 3 Perfusion pressures

The starting or initial IOP was always zero. There was no evidence of a background intrinsic pressure or tissue turgor even in very fresh specimens. In order to register an IOP the foot required initial ‘filling’ or charging with serum. The results show that

perfusion for about a minute was generally sufficient, given the dimensions of the tissues in this model, to load or charge the foot soft tissues and the bone contained within. This applied whatever the eventual perfusion pressure, as in Figure 3.8. While pressures of 50 cm and 100 cm water equivalent to 37 mmHg and 74 mmHg were tested it seems that the 150 cm height perfusion equivalent to 110 mmHg is the most physiological pressure to use in this model. As the graphs show the perfusion filling time was about a minute for all perfusion pressures and this was taken as a reasonable duration of observation before recording results both with these perfusion and tourniquet measurements and for the later loading experiments.

Experiment 4 Tourniquet effects

When a tight proximal venous tourniquet is applied while perfusion continues through the unobstructed artery, the IOP rises to a new steady level after about a further minute. It is not clear to what extent the new higher IOP is due to venous back pressure or the arterial supply. Probably both contribute to IOP in different proportions. If the initial IOP is based mainly on arterial supply it might be expected that after application of a tourniquet the limb would fill to nearly 150 cm IOP in all areas. This is not the case. An explanation might be that in any vascular ‘tree’ the pressure will fall or decrease further down the tree. There is a ‘stepping down’ in pressure through to the smaller vessels as described in Chapter 2, experiments 7 and 8. Even if the venous outflow is completely obliterated there is no compelling reason for back pressure to ever fully achieve the arterial filling pressure. Much the same applies to venous drainage or back pressure with loss of the perfusion. The IOP never quite reaches zero. This indicates that after perfusion there is a residual tissue or fluid load or charge and some modest resistance to out flow even in these amputated specimens.

However, the model is potentially more complex. For this work bone is understood to be a relatively rigid structure or enclosed box which has a relatively low blood content compared to the surrounding soft tissues. There might be almost instant filling of the bone itself if it could be directly connected to the arterial supply or nutrient vessels. But in this model the bone lies in a surrounding bag of forefoot tissue. The arterial catheter tip lies outside the bone approximately level with the mid-metacarpal. The soft tissues take the majority of the blood flow and require an appreciable time to fill and empty. The time taken to fill the average amputated foot specimen may well be dependent on other factors such as the perfusion height or pressure, the viscosity of serum, the diameter and length of the IV lines, and the dimensions of any taps, catheters and obstructions. Throughout this work these extrinsic parameters remained constant. The observed IOP is therefore secondary to the pressures in the surrounding soft tissues. Pressure in the soft tissues was not directly measured other than at the arterial supply point in the radial artery.

Experiment 5 Individual site response

At any individual needle tip site there is a close relationship between IOP and the perfusion pressure in spite of the wide range of initial values encountered as shown in Figure 3.9. This is perhaps unsurprising and confirms that the IOP needle is dealing with a sampling of an individual point along a vascular tree with IOP reflecting pressure in the serum pool at the needle tip rather than measuring a constant pressure for the whole tissue or organ. At each individual measurement site IOP was closely correlated with perfusion pressure ($r= 0.999$). Filling and emptying curves with perfusion and a tourniquet were similar indicating that the amputated foot model offers a simple ‘elastic’ environment.

Experiment 6 IOP rise and fall with perfusion

If a model demonstrates equal 'filling' and 'emptying' curves one could assume that the system is 'elastic'. During the initial experimental set up perhaps an hour or two post-mortem and post amputation and post irrigation with K-H saline, any fluid in the vessels had fully drained away. The first filling or charging of the limb with serum results in a slightly longer filling curve than subsequent filling curves where the limb has already been filled or charged. Thereafter filling and emptying curves were very similar. Similarly once the perfused limb was in a steady state and a tourniquet was applied for 60 seconds the further tourniquet 'filling' curve was very similar to the 'emptying' curve on removal of the tourniquet. After use of a tourniquet and perfusion at 150 cm for 60 seconds there was a virtually full recovery on removal of the tourniquet within a further 60 seconds. This implies that once initially charged the model is hydrodynamically 'elastic' over the range of pressures encountered by perfusion up to 150 cm.

Experiment 7 IOP filling curves in fresh and old feet

There was a difference between feet in terms of filling curves depending on their age or presumed viability. Feet up to 4 hours post-mortem filled as expected but after 60-80 seconds exhibited a static IOP as in Figure 3.12. This contrasts with the pressure curves seen in older probably non-viable feet as in Figure 3.13.

Autoregulation is the biological process by which certain organs such as the brain, kidney and heart can adjust their blood flow in the face of changing arterial supply pressures. The mechanism may include local chemical, hormonal, neurological or other unknown means. As blood supply to the organ is reduced, vasoconstriction is relaxed

allowing blood flow to be maintained and vice versa. Skin and muscle have less capacity for autoregulation. It is not known if bone has that property at all.

Experiments typically began within 2 hours post mortem and lasted for an hour or two. All the fresh specimens showed a rise in IOP with static perfusion and then an otherwise unexplained stabilising or fall in IOP after about 60 seconds of static perfusion. This appears to be 'autoregulation' in the absence of any other explanation. The effect was never seen in older specimens. The effect could be blocked in fresh specimens by the prior injection of formalin. The perfusion curve then resembled that in the older limbs. In formalin treated feet or feet older than 6 hours, perfusion led to a gradual increase in IOP without an obvious end point, no matter how long the duration of perfusion. In summary it seems likely that the amputated limb perfused with warmed serum retains some biological activity or power of autoregulation for a few hours post mortem.

However, this model is not an isolated bone but an amputated limb. Although IOP was measured in the bone, that bone was contained in a surrounding bag of distensible soft tissue. There seems to be no obvious reason for bone to require its own autoregulation mechanism. In any event it is not possible to exclude the possibility that regulation, if present, might be occurring in the surrounding soft tissues. Older feet did not show the same regulation as in Figure 3.13. In the older feet IOP continued to rise slowly even after 500 seconds but never reached arterial supply pressure. After prolonged perfusion the feet became visibly oedematous. In this model there was no significant difference between fresh and old feet after one minute of perfusion with serum at 150 cm pressure. Although the shapes of the filling curves differed between the fresh and older specimens, the absolute values were similar at 60 seconds of perfusion.

We therefore took the IOP at 60 seconds as the point for basal measurements and for subsequent analysis. As in previous in vivo work there were substantial differences in

recorded IOP between and within individual specimens. These did not appear to be site specific. Other than the autoregulation phenomenon there was no obvious difference between fresh and old feet for the rest of the work.

The object of this part of the study was to derive a model fit for further loading experiments. Perfusion at 150 cm pressure for 60 seconds seemed an appropriate and usable starting point for loading studies. Both fresh and older feet were therefore used in the following Chapter 4 onperfusion, tourniquet, static loading and dynamic loading or 'walking' studies.

Limitations

There are several possible limitations in this work. The calves were all male Friesian breed animals of similar but not identical age and weight. They were probably more similar than any group of patients might be. They were otherwise healthy but the bone was of a juvenile pattern with cartilaginous epiphyses present. The forefeet often came in pairs. Although the specific pairing was not recorded, there seemed to be no uniformity in IOP values between same animal forefeet or different animal feet. The calf has a fused third and fourth metacarpal which becomes bifid at the distal metacarpal and for the remaining phalanges and hoof. There is no direct human equivalent but the specimens otherwise approximately resembled the human forearm and wrist in size, weight and bone strength.

The feet were catheterised through the equivalent of the radial artery and were rinsed out with two hand flushes of Krebs-Henseleit saline solution. The irrigation pressure was not controlled. Serum rinsing may have been preferable top K-H solution in physiological terms. The use of whole blood would have required more complex formal anticoagulation and probably oxygenation. Initial tests were carried out using a pulsatile flow device but it proved difficult to record stable IOP values and the system consumed

excessive amounts of perfusate. It is not clear from the literature whether or not for normal capillary Starling type exchange a steady state flow has any physiological advantage or disadvantage compared with pulsatile flow (Koning 2012). Neither is it clear to what degree bone capillaries, which are known to be fenestrated, might be affected by non-pulsatile flow and whether or not mixed serum from a number of calves who may not be genetically identical might cause an immunological reaction to the serum.

The exact depth of insertion of the catheter varied but was to about 6" or well into the proximal third of the metacarpal. Flushing was carried out immediately using a 60 ml Luer lock syringe and two fills of warmed Krebs Henseleit solution by hand. The emerging perfusate was almost but never completely clear of blood. Needle insertion was by hand and the sites could not be identical. Placement within a few millimetres of the subchondral surface or the central diaphysis was achievable. In spite of practice with insertion, connection and setting up of the pressure transducers the experiment took time and could not be guaranteed to work on every occasion.

A doubled string tourniquet was applied at the level of the carpus. The tourniquet did not crush the polythene catheter which lay within the artery. The tourniquet was essentially a venous tourniquet but one applied tightly.

The colour of the perfused serum varied between batches from straw colour to a medium haemoglobin pink. Of all attempted recordings some 60-80% were successful. Needle leakage, obstruction, bubbles and unknown pressure transducer, recorder and data storage failures account for most of the others. In the analysis all useable records for each experiment were included. No outliers were excluded.

It was found that static perfusion even in old or dead feet gave consistent results without developing oedema for the duration of these experiments.

3.6. Conclusion

The object of this work was to develop a reliable in vitro model based on the calf foot to explore IOP and bone perfusion physiology. That was achieved. Earlier in vivo findings of IOP variability were confirmed. IOP variation is due to differing conditions at the needle tip rather than there being a significant physiological difference. Site differences appear to be minimal but there are differences in the IOP response to perfusion in fresh and old feet. These were minimal at the chosen experimental pressures and times parameters. The model shows that subchondral cancellous bone behaves as a perfused tissue and demonstrates the expected 'elastic' responses to hydrodynamic changes and the use of a tourniquet. This inexpensive in vitro model fulfilled the 3Rs of animal research (Replace, Reduce and Refine) and offered a basis for the further work on bone perfusion physiology with loading described in Chapter 4.

4. CALF FOOT IN VITRO MODEL FOR IOP WITH LOADING

4.1. Background

Intraosseous pressure (IOP) measurement has been of historic interest in osteoarthritis, osteonecrosis and bone pain but of limited clinical value. The skeleton is clearly adapted to support activity but little is known about subchondral perfusion during activity. In the previous chapter a new in vitro calf foot model was developed to comply with the 3Rs of animal research and to check and repeat earlier in vivo work. Baseline perfusion physiology values were established. This study aimed to use that model for testing IOP with combinations of vascular occlusion and loading. The object of this study was to explore the effects of perfusion and loading on IOP at different loads and with different loading regimes from static to more dynamic loading to resemble that experienced by the joint during life when walking.

4.2. Development of set up and methods

Model preparation

The foot acquisition, preparation and setup were as described in Chapter 3.

Loading method

Initial attempts to create a loading jig involved concentric spring loaded tubes much as those used in Chapter 2. These failed because they obstructed access for the IOP needles. Eventually two different forms of loading were used. The first involved skeletal

loading through an external fixator (Ex-fix). This avoided movement of the joints and compression of the soft tissues. The second involved the foot being loaded in a 'standing' posture by hoof tip pressure. Counter pressure was against the flexed carpal joint on the side of the water bath. A kneeling calf takes weight through the same flexed carpal surface.

External Fixator Skeletal Loading

For the external fixator, loading screws were drilled across the middle of the metacarpal diaphysis and the phalanx as in Figure 4.1 and 4.2.

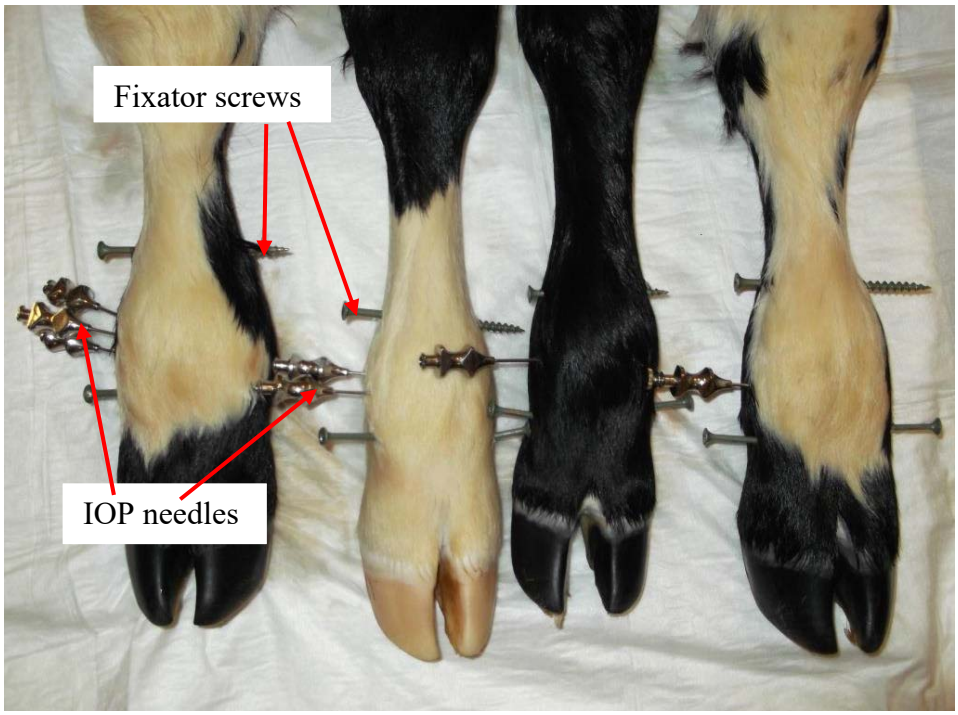


Figure 4.1 Calf feet with various arrangements of fixator screws and IOP needles in position.

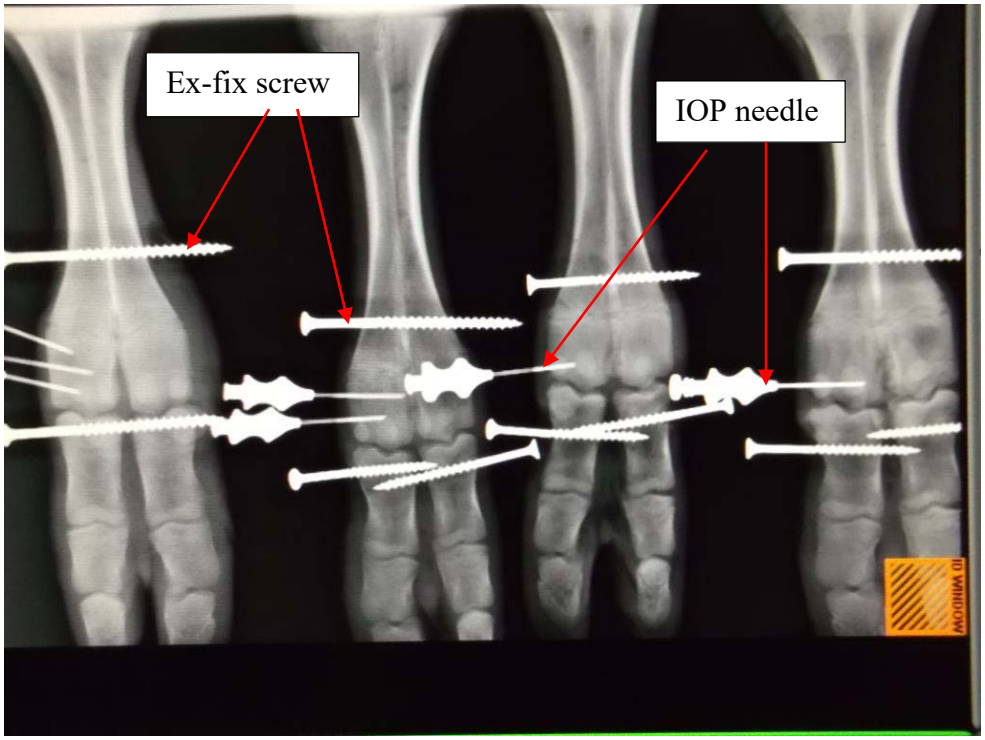


Figure 4.2 X-ray of calf feet above showing bifid metacarpal, phalanges and hoof and typical location of Ex-fix screws and IOP needles.

A simple 'fixator' was made in the form of two large pairs of scissors. Flat metal strips 45 cm in length were connected through a hinge or bolt at the 10 cm point. Screws were passed through the limb transversely in the mid metacarpal area and middle phalanx. The screw ends passed through the distal tips of the fixator. The "scissor" fixator was attached to the screws on both sides of the foot. Compression was applied by squeezing the opposite ends of the scissors as in Figure 4.3. For loading a calibrated 0 - 20 kg fisherman's weighing spring was attached to one of the Ex-fix arms and physically pulled towards or against the other arm by hand at the required force. The bone screw to hinge distance was 10 cm and the hinge to lever arm distance was 35 cm. A ratio or multiplication factor for the force across the joint was therefore 3.5 times that applied to the ends of the fixator scissors. Where external fixator loading was used the force across the joint was purely skeletal without additional loading, joint movement,

distortion or compression of the soft tissues. Providing that the screws were inserted at the mid thickness of the metacarpal (MC) and the middle phalanx (MP), the fixator controlled and prevented flexion and extension at the MCP joint.

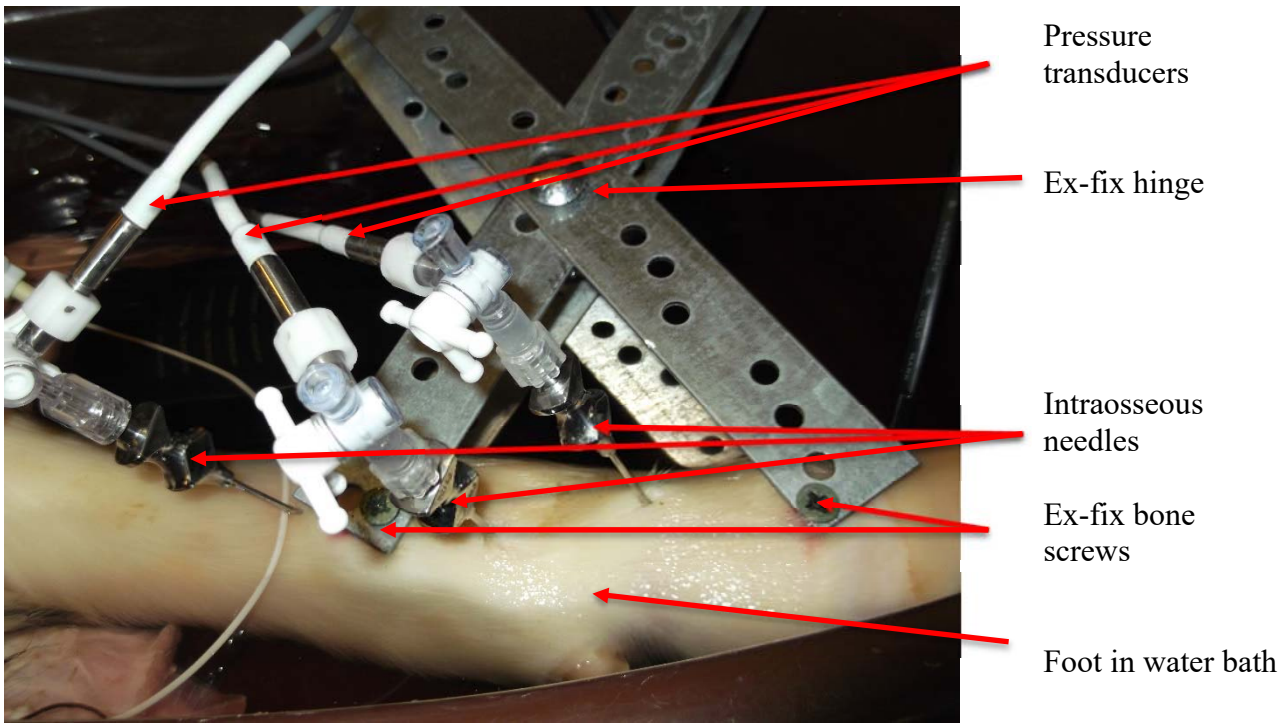


Figure 4.3 Calf foot in water bath with scissor type Ex-fix applied. Fixator held by transverse screws through distal third of metacarpal and middle phalanx. IOP needles in metacarpal diaphysis, distal subchondral epiphysis and diaphysis of proximal phalanx.

Standing Posture Loading

When 'standing' loading was used, pressure was applied to the tip of the hoof through a simple pusher. That caused the foot MCP, PIP and DIP joints to adopt a posture of slight hyperextension as seen in the natural standing posture of the calf as in Figure 4.4. Counter pressure was from the flexed carpal joint kneeling or pressing against the side of the water bath. The posture during this manner of loading was stable with the wrist or carpal joint in a flexed position effectively 'kneeling' against the side of the water

bath as a counter force to the applied load. The polythene catheter within the radial artery adopts an 'S' shape behind the flexed knee, much as the popliteal artery flexes but does not obstruct in man when kneeling fully. The foot could continue to be perfused and the tourniquet could be applied as needed for the experiment without compromising the arterial supply. The line of weight bearing force lies in front of the MCP joint and IP joints. The force through the joint is a factor of the distance from the articulation centre to the posterior restraining structure and the distance from the centre of articulation to the weight bearing line.

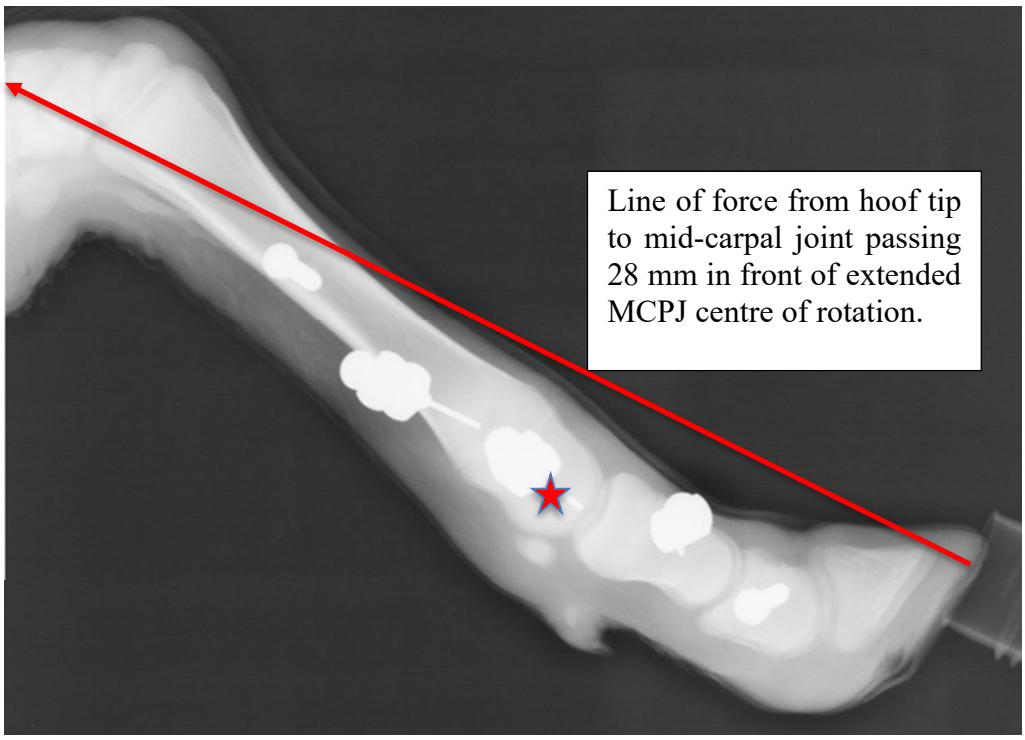


Figure 4.4 showing the posture during 'standing' load. (External fixator screws are seen in the mid metacarpal and proximal phalangeal positions and the intraosseous needles are seen in the metacarpal diaphysis, metacarpal subchondral epiphysis and proximal phalanx positions). The line of weight bearing passes from the tip of the hoof to the carpal joint centre. At the MCP joint the line lies approximately 3 cm in front of the centre of rotation of the MCP joint marked by a red star.

The load applied across the joint was calculated by estimating the distance from the centre of rotation of the MCP joint hinge indicated by a red star in Figure 4.4 to the restraining or tensioned elements of the capsule and posterior ligaments. There is a sesamoid bone behind the MCPJ, as seen in Figure 4.4. The centre of the sesamoid bone was taken as the centre of the posterior stabilising ligament. The anterior lever arm distance was from the centre of the joint to the line of force which lay in front of the hyperextended MCP joint.

By x-ray and by direct measurement the distance from the centre of rotation to the centre of the posterior elements was 14 mm and the distance from the centre of rotation to the weight bearing line calculated on a stress x-ray was 28 mm. That point lay in a plane anterior to the hinge type MCP joint on a line of force running from the tip of the hoof to the centre of the carpus. A factor of twice the applied longitudinal load was thereby transmitted across the joint surfaces as in Figure 4.4. The same proportional formula applied whatever the size of the foot.

With a ‘standing’ load the posterior ligaments and soft tissues at the MCP, PIP and DIP joints are put under tension. The joint hyperextends and the venous sinuses behind the foot and in the hoof are compressed as in real life standing.

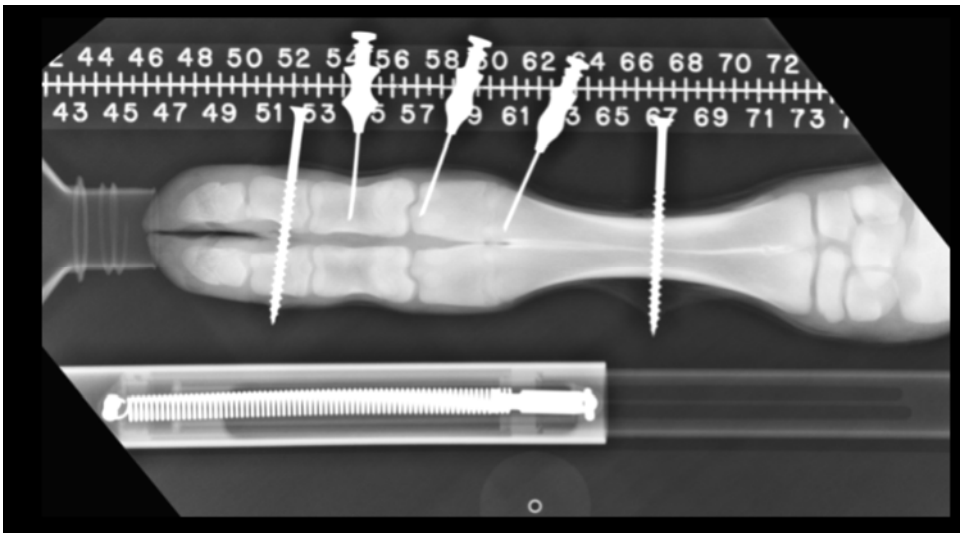


Figure 4.5 Radiograph showing the transverse external fixator screws in the metacarpal diaphysis and the IOP needles in the metacarpal metaphysis, subchondral epiphysis and middle of the proximal phalanx. A centimetre scale is seen above and the manual compression loading pusher is seen below with its calibrated internal spring.

Experimental plan

Part 1 - Static loading experiments 1-3

Static loading was defined as a steady load for 10 seconds continuously with a 10 second rest interval before the next 10 second load period.

Experiment 1 Static loads and perfusion variation

Ex-fix loading was carried out with non-perfusion, perfusion at 150 cm pressure and perfusion at 150 cm with a venous tourniquet applied. The effect of a static 10 kg load on IOP was tested.

Experiment 2 Static load and weight variation

Weights of 5, 10, 15, and 20 kg were tested at different perfusion pressures.

Experiment 3 Repeat static load

IOP was recorded during repeated static loading at different perfusion pressures.

Part 2 –Dynamic loading experiments 4-5

Dynamic loading was defined as one load per second for ten seconds followed by a 10 second rest period. This was designed to simulate the animal walking.

Experiment 4 Dynamic walking load

Dynamic loading was carried out with one load per second for 10 'steps' with different weights. IOP was recorded during activity to test for drops to below initial levels on removal of the load. The loads used were 5, 10, 15 and 20 kg. These were multiplied x 3.5 for the ex-fix loading and x 2 for the 'standing' loading regime.

Experiment 5 Dynamic load 'swing' and 'drop'

Walking type loading with and without perfusion was carried out to explore the 'swing' and 'drop' effect in IOP with walking at different weights and with different perfusion states.

Statistics

Results were expressed as means, standard deviations and ranges. Student's t-test was used to determine if there were significant differences. When each subject was used as its own control, paired t-tests were used. Otherwise unpaired tests were used. The Pearson test was used to assess correlations and $p<0.05$ was considered to be statistically significant.

4.3. Results Part 1 – Static loading

Experiment 1 – Static loads and perfusion variation

Static loading increased subchondral IOP whether the bone was non-perfused, perfused or perfused and with a tourniquet. Examples of Ex-fix loading are seen in Figures 4.6, 4.8, 4.11 and 4.12. Figure 4.6 shows a typical trace during loading with perfusion and a tourniquet, perfusion alone and loading without perfusion.

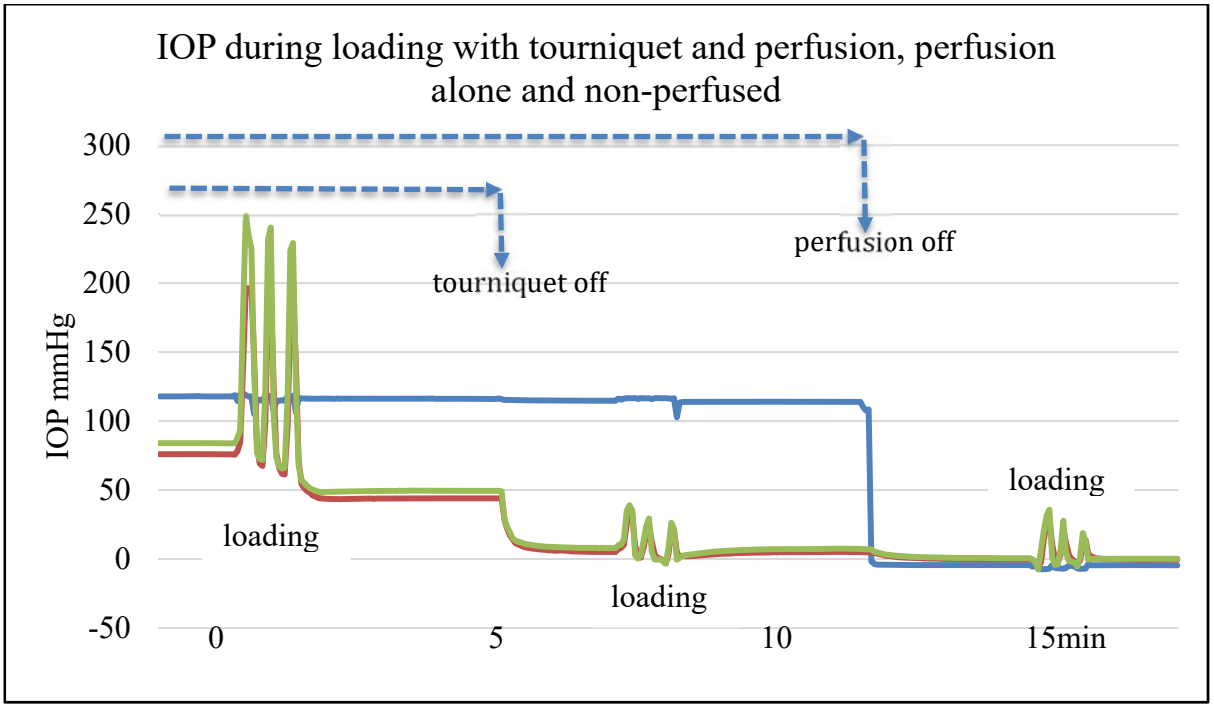


Figure 4.6 (Foot 187) showing IOP with standing type loading of 10 kg for 10 seconds with 10 seconds intervals x 3 during perfusion with a tourniquet, removal of the tourniquet at 5 minutes, loading during perfusion alone at 7 minutes, removal of perfusion at 12 minutes, and loading non-perfused at 15 minutes. Blue - serum perfusion pressure, Red - metacarpal diaphysis IOP, Green - metacarpal epiphyseal IOP.

In a group of nine separate feet the effect on IOP of a static Ex-fix load to 10 kg was as shown in Figure 4.7. There was a significant rise in IOP whatever the perfusion condition ($p<0.0001$) for all pairs.

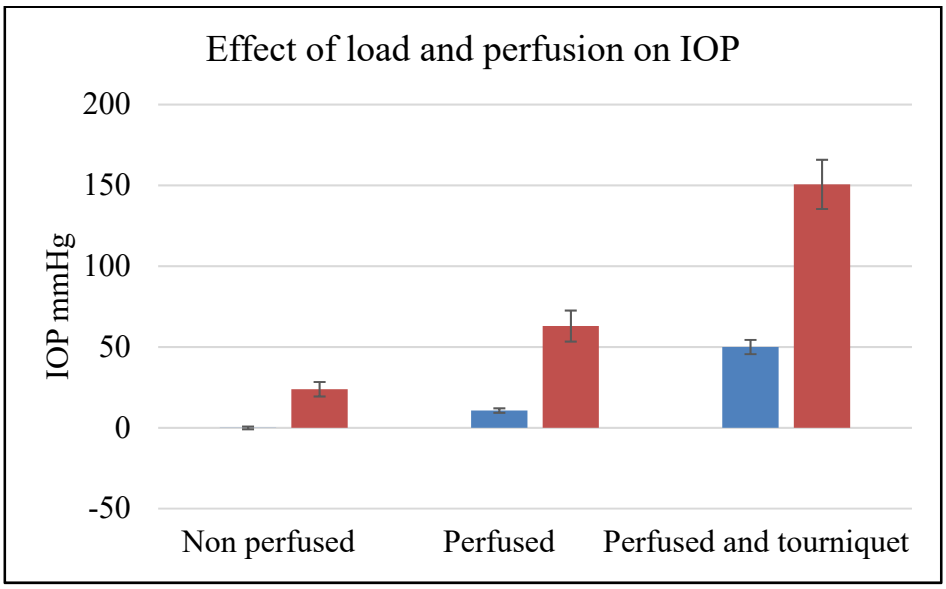


Figure 4.7 showing the effect of a 10 kg static load on IOP. Blue no load, Red 10 kg load, n=9. Error bars SEM

Experiment 2 – Static load and weight variation

Loads of 5, 10, 15 and 20 kg caused a proportionate increase in IOP from the background whether non-perfused or perfused. Figure 4.8 shows a typical graph with Ex-fix loading at 5, 10, 15 and 20 kg for 10 seconds with perfusion and without perfusion.

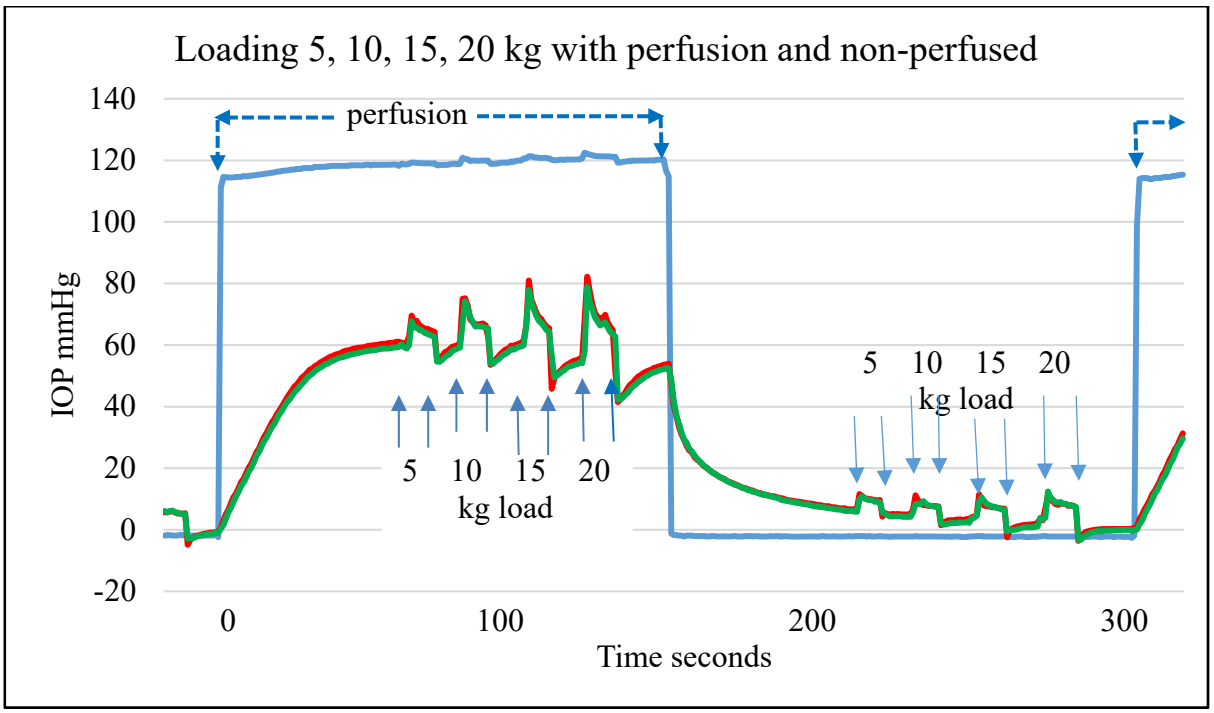


Figure 4.8 (Foot 143) Blue - perfusion pressure, Red - Metacarpal diaphysis IOP, Green - Metacarpal epiphysis IOP. Perfusion for 60 seconds, then Ex-fix type loading for 10 seconds at each weight, 5, 10, 15 and 20 kg with 10 seconds between as between blue arrows, perfusion off for 60 seconds and repeat load pattern.

The intraosseous pressures achieved were proportional to the applied load as shown in Figure 4.9 with correlation as in Figure 4.10.

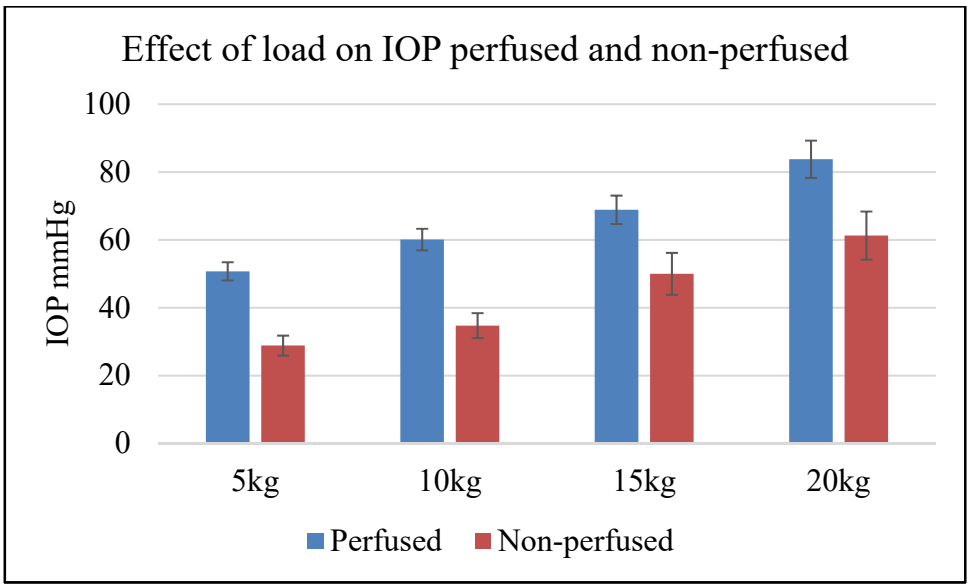


Figure 4.9 showing that the IOP is proportional to the applied load whether the bone is perfused (Blue) or not perfused (Red).

Although there was a wide variation in the initial IOP, at any one site there was a close correlation between the load applied and the rise in IOP in both perfused and non-perfused feet as shown in Figure 4.10.

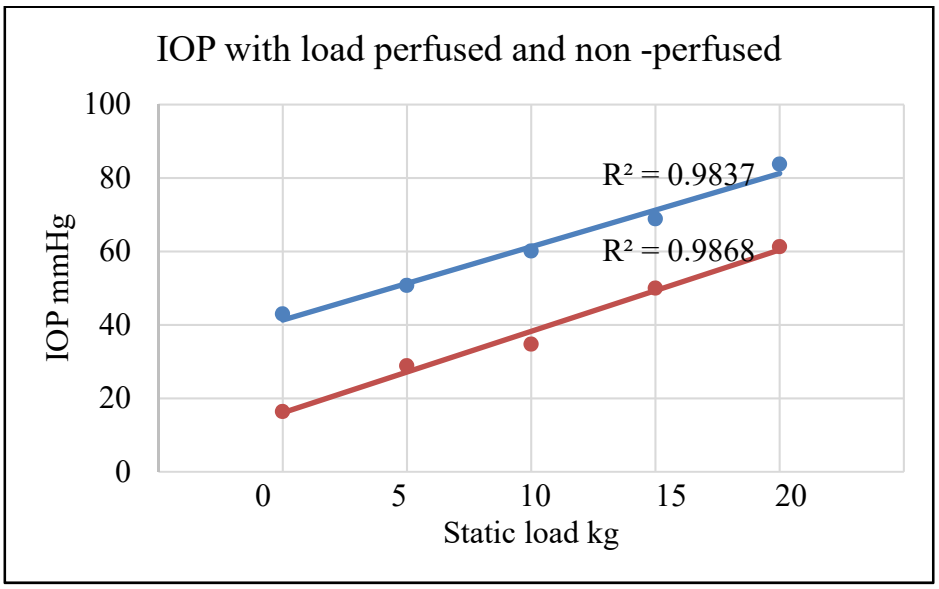


Figure 4.10 The change or gain in IOP is well correlated with the applied load in both non-perfused (Red) and perfused (Blue) bone, Pearson correlation R^2=0.984, n=22.

Experiment 3 - IOP Repeat static load

An example of a trace with perfusion and loading of 10 kg for 10 seconds with and without a proximal venous tourniquet is shown in Figure 4.11. IOP may exceed the perfusion pressure as seen in Figures 4.6, 4.11 and 4.12.

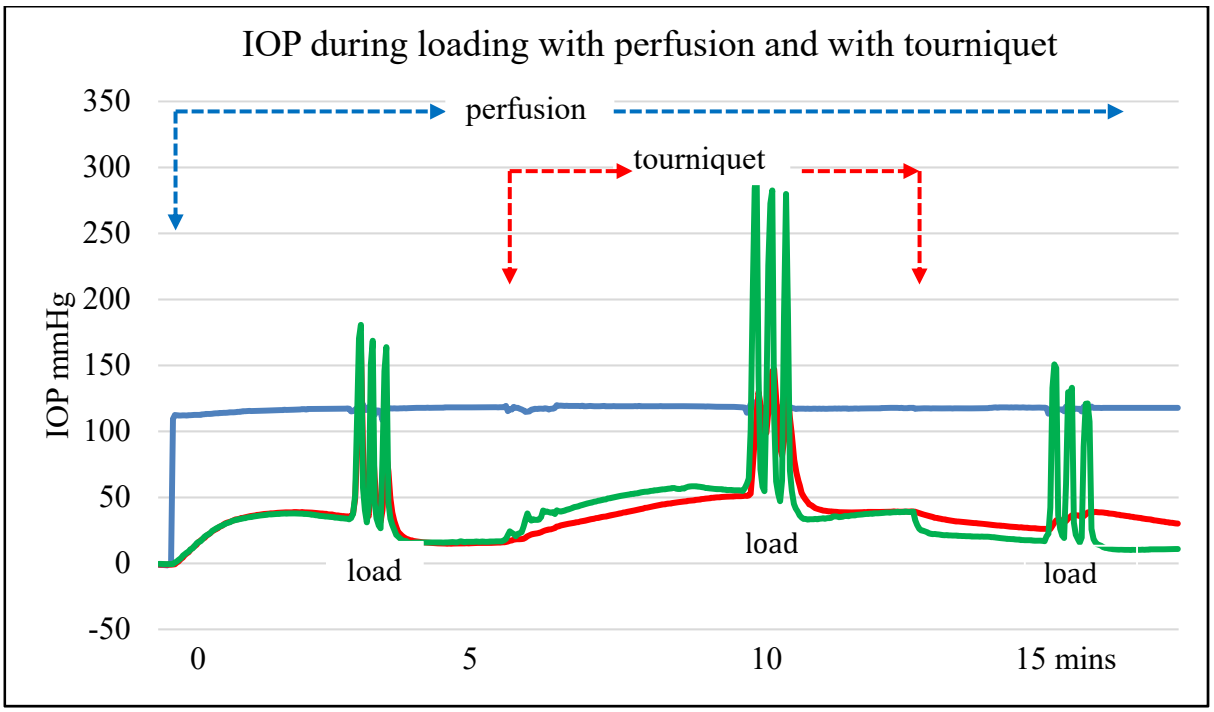


Figure 4.11 (Foot 186) showing an example of IOP with standing type loading during perfusion (left group), with perfusion and tourniquet (central group) and perfusion alone (right group). Blue – serum perfusion pressure, Red – metacarpal diaphysis IOP, Green – metacarpal epiphysis IOP. Each group shows the effect of a static load of 10 kg applied for 10 seconds with 10 second intervals x 3. The tourniquet was applied at 6 minutes and removed at 12 minutes (dotted red line).

On removal of a static standing load, IOP falls to below the starting IOP whether perfused with a tourniquet, perfused alone or non-perfused as shown in Figures 4.11 and 4.12 Whatever the perfusion state loading appears to squeeze fluid out of the bone resulting in a lowered IOP or 'drop' after repeated static loads. With repeated walking type loading there appears to be a 'pump out' or IOP lowering effect.

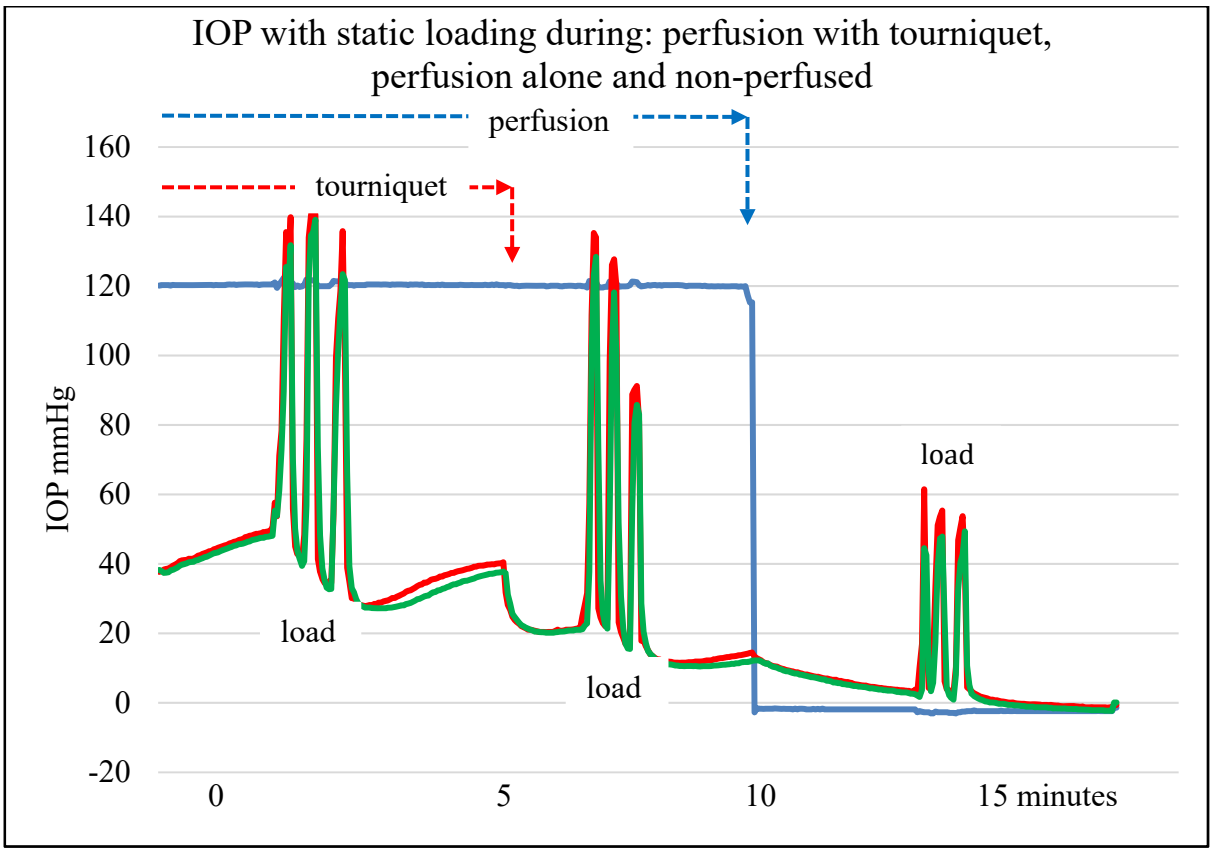


Figure 4.12 (Foot 177) Example showing effect of three sets of 10 kg static standing type load for 10 seconds with 10 second intervals. Left group - perfused with tourniquet, tourniquet removed at 5 minutes, central group - perfused only and right group - non-perfused. Blue – serum perfusion, Red – metacarpal diaphysis, Green – metacarpal epiphysis. There is a progressive fall in IOP with repeat load in all three perfusion states.

4.4. Results Part 2 - Dynamic loading

Dynamic loading was defined as a loading one per second for 10 seconds with a 10 second interval before the next 10 seconds of loading. This was designed to simulate short walks.

Experiment 4 – Dynamic walking load

Repetitive dynamic or walking type loading at one load per second for 10 seconds is demonstrated in Figures 4.13 and 4.14 for different weights and different perfusion states.

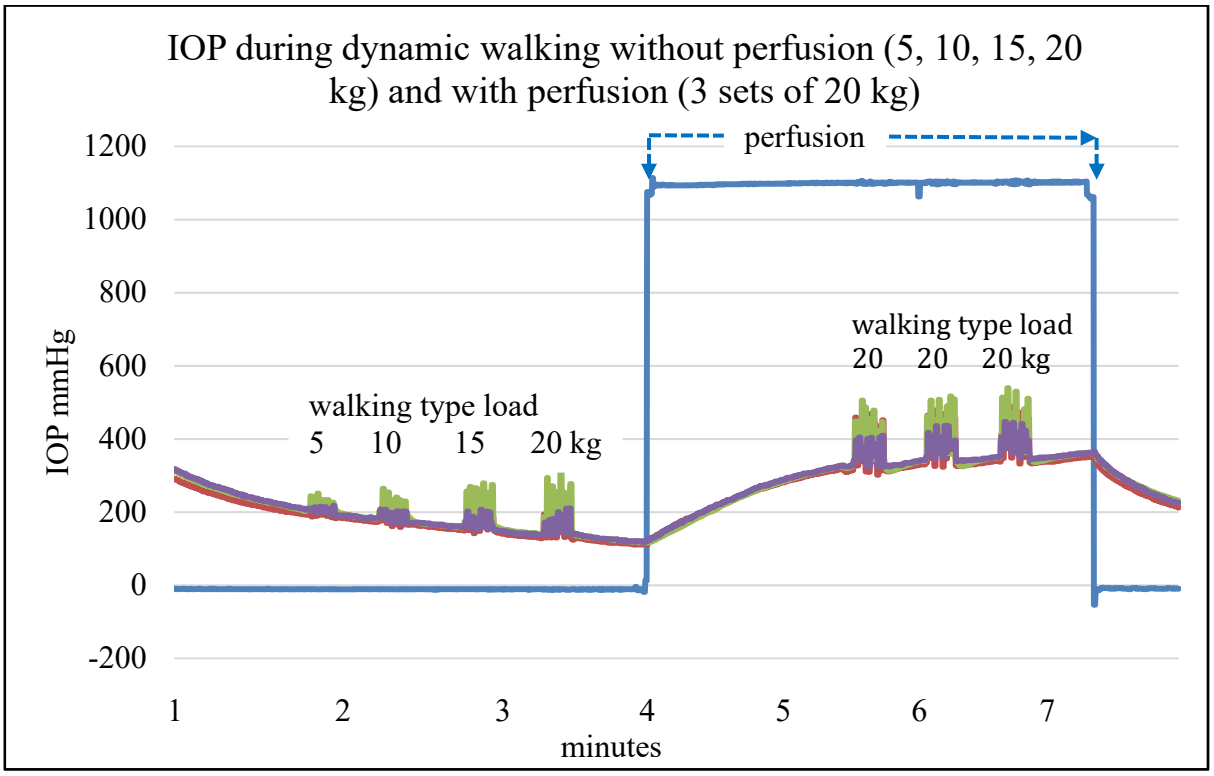


Figure 4.13 (Foot 142b) showing a typical dynamic Ex-fix type load trace. Left side non-perfused, right side perfused. Left side 5, 10, 15, 20 kg load x 10 steps in 10 seconds, right side 20 kg x 10 steps in 10 seconds, three groups. Blue – perfusion pressure 0 - 150 cm, Red – metacarpal diaphysis IOP, Green – metacarpal subchondral IOP, Purple – proximal phalanx diaphysis IOP.

Repetitive loading in the standing posture was applied, with and without perfusion. The IOP fluctuated or 'swung' through a greater range with greater loads whether perfused or not as in the example shown in Figure 4.13.

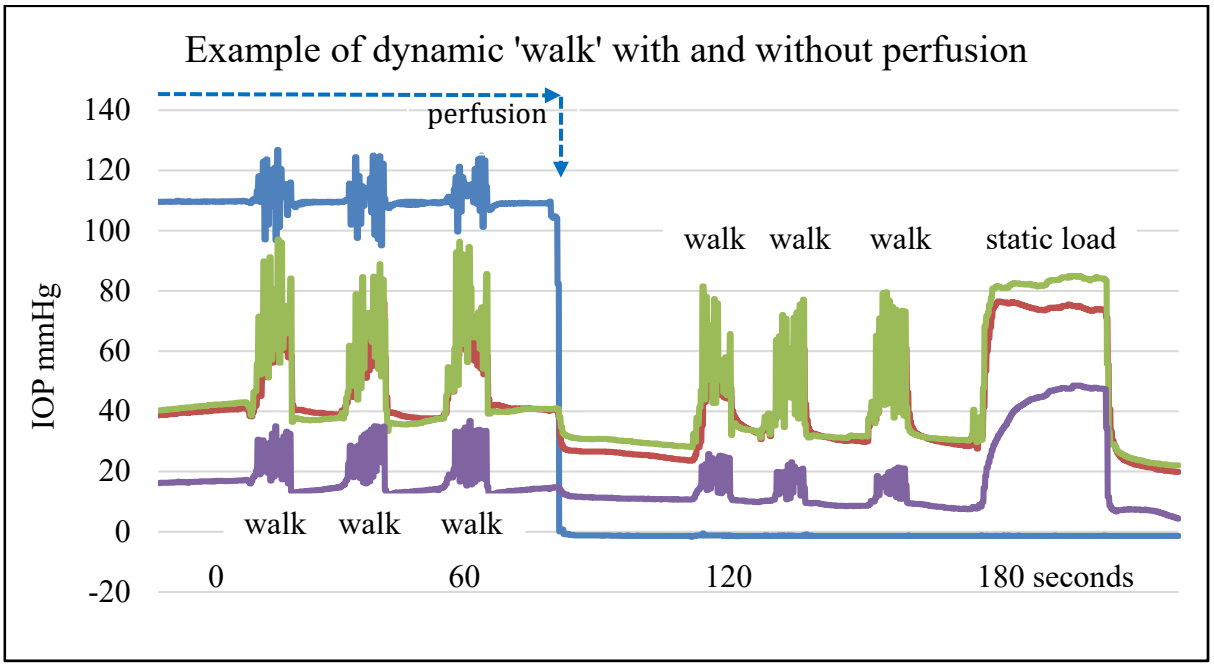


Figure 4.14 (Foot 141b) showing the effect of dynamic Ex-fix type loading on IOP. Each set of steps is of 20 kg load x 10 steps in 10 seconds. The sequence shows from the left three sets of 20 kg x 10 steps in 10 seconds during perfusion at 150 cms. Perfusion was stopped at 80 seconds and a further three sets of 20 kg x 10 steps in 10 seconds follows. The load applied at 180 seconds was a steady 20 kg for 20 seconds. Blue – perfusion pressure, Red - metacarpal diaphysis IOP, Green - metacarpal epiphysis IOP, Purple - proximal phalanx diaphysis IOP.

Experiment 5 - Dynamic load ‘swing’ and ‘drop’

Loading to simulate walking at one second intervals for 10 seconds produced a fluctuating IOP with or without perfusion which was proportional to the applied load as shown in Figure 4.13 and 4.14. These experiments were carried out using the physiological hoof tip loading and the physiological walking pattern of one load per second for 10 steps with a ten second rest interval.

Swing

The 'swing' or fluctuation with load was compared in the perfused and non-perfused state in 24 sites among 11 feet, six fresh and 5 old. With 10 'steps' there was a swing proportional to the load.

Drop

A drop or reduced IOP was found after removal of a physiological or hoof tip load in virtually all traces whether static loading as in Figure 4.11 or after dynamic loading as in Figure 4.13 and 4.14. The drop after loading appeared proportional to the applied load as in Figure 4.15.

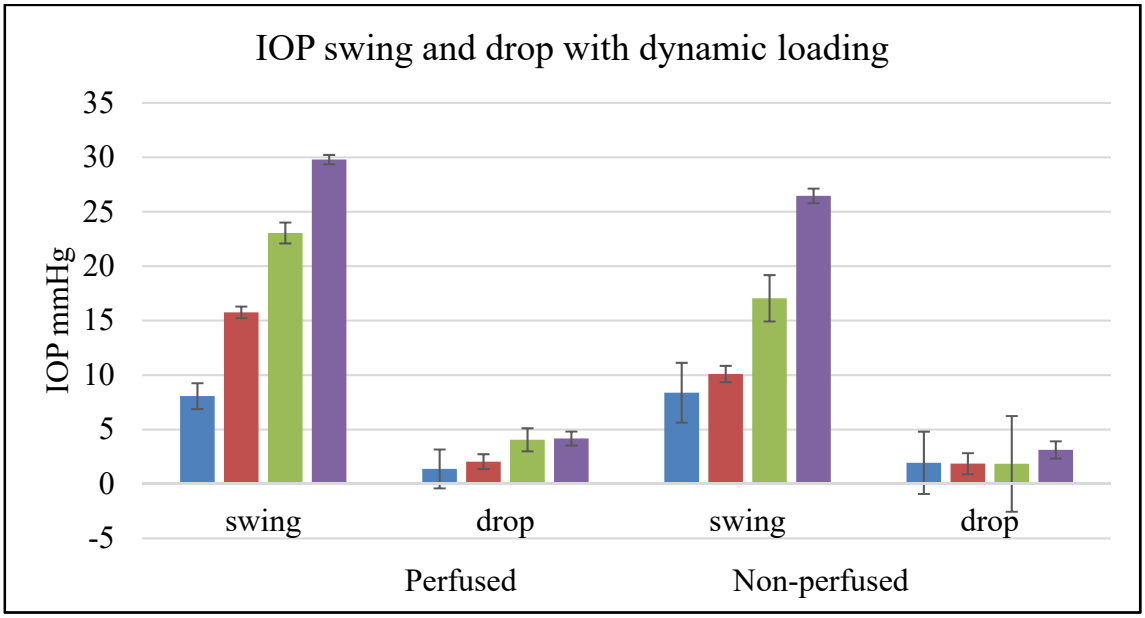


Figure 4.15 IOP fluctuation with loading, Blue – 5 Kg, Red – 10 Kg, Green – 15 Kg, and Purple - 20 Kg loads, 10 steps in 20 seconds and associated drop in IOP post exercise for perfused and non-perfused feet, n=25 sites in 11 feet, error bars SEM.

4.5. Discussion

The discussion follows the experiments as numbered 1 to 5 in the results above.

Part 1 - Static loading experiments 1 - 3

Experiment 1 Static loads and perfusion variation

In the previous chapter the IOP response to changes in perfusion while at rest was described. Based upon those experiments the standard used for all feet in this series was for perfusion at 150 cm pressure for 60 seconds before loading. After a tourniquet was used there was a further delay of 60 seconds before loading. Where a tourniquet was removed or perfusion was discontinued there was another delay of 60 seconds before loads were applied.

In all loading experiments the rise in IOP with loading is virtually instantaneous whereas changes to IOP with stopping or starting perfusion occur more gradually over a minute or so in this model. A rise in IOP with loading was found under all three perfusion states as seen in Figure 4.6. The greater rise was during perfusion with a proximal venous tourniquet. The least rise was with no perfusion. The explanation appears to be that subchondral bone flexes or is compressed slightly by loading. The subchondral area is a relatively contained or enclosed space. Loading instantly leads to a raised IOP as a result.

The differences in IOP seen for the same weights is proportional to the fluid fill or ‘charge’ present in the tissue before the application of load. Where the subchondral bone is ‘charged’ or full and under more pressure because of a proximal venous tourniquet the same load will cause a greater rise in IOP than when there is less or no pressure in

the subchondral bone. Previously it was generally considered that load was directly borne by the trabeculae. The instant rise in IOP with loading appears to show that some of the load is being transmitted by hydraulic force through the soft subchondral fatty and haemopoetic tissues. Although previous authors have considered the possibility that bone might be hydraulically strengthened they discounted the idea. But they were using non-physiological tests. This model is much closer to the situation in vivo. Furthermore, loading increased IOP whether applied by an Ex-fix through the skeleton alone or by the more physiological 'standing' load with pressure on the end of the hoof.

Experiment 2 - Static load and weight variation

Over the range tested here the IOP rise appears to be proportional to the load applied irrespective of the starting IOP. If a simple hydraulic pressure transfer is the mechanism whereby most load is transferred from the subchondral plate to the trabeculae and cortical shaft it might be expected that with physiological loads there would be a proportionate response as demonstrated here. It has long been recognised that up to five times body weight may be transferred across the hip in man during the stance phase (Denham 1959). It would be difficult to determine the exact load across joints in this animal in vivo. Much would depend on the posture and speed of load application or the shock wave generated if the foot is suddenly stamped.

Experiment 3 - Repeat static load

Others have calculated that pressures of over 3 MPa, (mega Pascals) or 20,000 mmHg might be expected at the joint surface during activity (Fukubayashi 1980). In this work the maximum load which could be comfortably applied by hand was 20 kg when compressing a loading spring through the Ex-fix. This gave a probable total load across

the MCP joint of 3.5 x 20 kg or about 70 kg. The animal weights were estimated to be between 50 and 80 kg. If the cross sectional area of the MCP joint, as shown in Figures 6.16 and 6.17, is 5 cm x 2 cm or 10 cm square a force of some 7 kg per square cm might be produced. One atmosphere is about 1 kg per cm square or 760 mmHg. The MCP joint surface pressure load in this experiment may therefore have been 7 x 760 or over 5,000 mmHg. It is likely that IOP is greatest immediately under the subchondral plate and diminishes further away as the soft tissues transfer pressure from one cell to the next and onto the adjacent fine trabeculae (Simkin 2018). The trabeculae in turn transfer the load down to larger trabeculae and the cortical shaft. The process is probably reversed at the next joint. Pressures of 5,000 or even 20,000 mmHg far exceed likely circulation pressures in vivo. There must be anatomical features which protect the relatively delicate thin walled fat cells, haemopoetic tissues, capillaries and red cells from those very high pressures during acute loading and yet allow the usual circulating blood to flow at very much lower pressures when the load is removed or the animal is at rest. Anatomical and histological evidence for specialised subchondral perfusion arrangements is discussed in Chapters 5 and 6.

Part 2 - Dynamic loading experiments 4 - 5

Experiment 4 - Dynamic walking load

Dynamic loading was designed to reflect the likely walking pattern of the animal for 10 steps in 10 seconds with 10 second rest intervals. As seen in Figure 4.13 and 4.14 in spite of a range of different starting values the IOP traces respond in a similar manner to walking type loads. There is a proportionately greater IOP fluctuation with higher initial IOP starting points and with greater loads.

As seen in Figures 4.11 and 4.12, on removal of static load applied in a 'standing' posture, IOP falls to below the starting IOP whether perfused and with a tourniquet, perfused alone or non-perfused. In fact it was found that on removal of the load in virtually all the standing load traces the IOP dropped to below the initial pre-load pressure. This was unexpected.

The fall or 'drop' was defined as the difference in IOP from the point at which the load was applied to the IOP after removal of the load.

The rise with loading and fall with removal of load was virtually instantaneous. The fall in IOP after removal of a tourniquet or ceasing perfusion was more gradual and there was no evidence of an overshoot or reduction to below the starting IOP.

The fall to below the starting IOP after standing loading appeared to be greater if the foot was non-perfused. With repeated standing type loading the drop was cumulative. This 'drop' was not seen with skeletal type Ex-fix loading either with static 10 second loads or dynamic one load per second loading. An explanation is required.

If the load bearing system is hydraulic and fully elastic, removal of the load would be expected to result in a fall in pressure but only to around the starting point. Furthermore any loss in hydraulic elasticity should in fact result in a lesser fall in IOP, that is, to above the start point.

With hoof tip standing or more physiological type of loading other factors come into play such as possible joint and muscle movement and stretching of posterior structures. There is a potential 'calf muscle' type of venous return pump in the calf foot.

This may be augmented by the hoof venous sinus which is compressed and 'pumps' out blood during the stance phase as described in the horse. None of these apply with use of the skeletal compression produced by the Ex-fix.

Up to this point it was accepted that the cancellous metaphysis was a relatively enclosed space capable of bearing hydraulic compression load without leakage. This is difficult to reconcile with the idea that the blood is squeezed out and somehow empties more between each compression with a falling IOP as seen on these traces.

Perhaps the answer is that a load applied physiologically through the hoof stretches the posterior compartment of the foot at the same time as the separate high pressure subchondral hydraulic compression is taking place. The extra osseous blood is being squeezed and returned up the posterior 'calf muscle' type pump. This is not seen with skeletal compression alone. As a result of the soft tissue 'pump' the extra osseous venous pressure falls. When the load is removed there is a reduced back pressure seen in the IOP needle which reflects the reduced extra osseous pressure.

In any event the serum or perfusing fluid appears to be 'pumped' out of the bone with repeated physiological rather than Ex-fix loading cycles and more so when the foot is not being perfused. The somewhat greater fall in IOP after repeated loading in the non-perfused state compared to the perfused state supports the concept that blood is being actively pumped out of the bone. 'Topping-up' of the system can take place between steps when perfusion is present but not where perfusion is absent. This seems to confirm the idea that while normal low pressure circulation is required to keep the system 'charged' very much higher pressures can then operate by subchondral hydraulic force transfer.

It is probably an extra osseous 'calf muscle venous blood pump' type of process that results in an apparently falling IOP after repeated standing but not Ex-fix loading. All of this probably assists bone blood flow during activity in real life. A falling IOP with exercise will encourage better osseous filling by the arterial system just as there is better

cardiac filling during inspiration and presumably better still with exercise hyperventilation.

These observations raise the possibility of a third hydrodynamic system being in operation. The first is the ordinary circulation seen in all tissues at rest. The second is the subchondral hydraulic cushion and load transfer which is the main subject of this research. The third is the 'calf muscle blood pump' or equivalent of that seen in man which assists venous blood back to the heart. More research would be needed to achieve a better understanding and to quantify those components. It is recognised that in legs with chronic venous insufficiency and a failed calf muscle blood pump that there are secondary osseous changes on plain x-ray (List-Hellwig 1999).

The subchondral area must have anatomical features to allow the different fluid pressure systems to function. There is a basic resting circulation which has been well described. In Chapter 5 and 6 a search was made for other factors which might offer evidence for the existence of an additional specialised subchondral circulation.

Experiment 5 Dynamic load 'swing' and 'drop'

In dealing with these observations on fluctuating load and IOP the terms 'swing' and 'drop' are proposed as they describe the findings most effectively. All traces showed a substantial 'swing' with both Ex-fix skeletal and hoof type physiological loading whether for a static 10 seconds or for the faster one per second pattern of loading.

The 'drop' or additional fall in IOP was seen only after physiological type loading, both static for 10 seconds and faster one per second loads. The conclusion must be that the physiological type of loading causes some other, probably extra osseous, factor to function thereby causing a greater drop in blood pressure in the surrounding foot soft tissue. It is this which is seen as the 'drop' in intraosseous pressures after physiological

hoof compression loading. There is clearly scope for the future study of subchondral hydraulic force transmission in joints during activity. The calf foot model would be suitable for further work.

Limitations

There are several possible limitations in this work. In addition to those limitations listed in Chapter 3, the loading methods used here were relatively crude. The application of an external fixator screw though the foot might be expected to alter pressures within the bone. For this reason a bone was 'skipped' from the distal metacarpal diaphysis to the middle phalanx for the distal Ex-fix attachment. IOP was then tested in the virtually unscathed metacarpal epiphysis and proximal phalanx. However, it could be argued that any penetration of the skin and bone with screws or drills was damaging to the integrity of the specimen. However, when no drill or screw penetration was used, such as in the more physiological dynamic loading on the hoof tip, the IOP results and responses were very similar to those with an Ex-fix in place.

It is recognised that there is a network of veins behind the foot, deep to the flexors which is akin to the human calf muscle venous plexus. There is also a plexus of veins within the hoof which empties during the stance phase. Both may cause an additional back pressure change in IOP. The loading by 'standing' probably causes an additional pressure during the stance phase in the surrounding foot soft tissue. Figure 14.4 shows fluctuating back pressure affecting the perfusion trace during rapid 'walking'. This temporary rise in pressure with stretching of the posterior foot tissues and venous sinuses in the hoof occurs much as in man the calf muscle and sole of foot venous blood pump function during walking (Gardner 1989). As soon as the 'stance' phase is over there would be a lower pressure in the surrounding soft tissues until inflow of arterial

blood or the next cycle of stance and weight bearing occurs. The equipment used in this experiment recorded pressures up to around 300 mmHg at a maximum rather than the 5,000 mmHg which might have been expected. Beyond 300 mmHg an overload occurred. Further efforts to load to higher pressures were avoided in order to prevent damage to the delicate pressure transducer membrane. The speed of response of the equipment to pressure change was fast but not known exactly. For the registration of acute loading 'shock waves' a more advanced and sensitive method would be required.

4.6. Conclusion

In conclusion, a new in vitro model to explore the effect of loading and vascular occlusion on IOP is demonstrated. There is a close correlation between subchondral IOP and load. Whether non-perfused, perfused or perfused and with a venous tourniquet, high subchondral pressures are generated by load. The force is dissipated from the subchondral region to the shaft cortex partly by hydraulic pressure. Anatomy must exist to allow and perhaps enhance circulation during activity. After repeated physiological loading IOP falls, probably due to a soft tissue venous blood pump. This work opens a new field of dynamic subchondral joint physiology from a vasculo-mechanical perspective. Failure of that vasculo-mechanical mechanism may offer a simple pathological explanation for, and an understanding of, bone diseases such as osteoarthritis.

Further work to identify and explore vascularisation in the subchondral region was therefore undertaken in Chapter 5.

5. UPPER TIBIAL VASCULAR MARKS, K-L GRADE AND OA [2]

5.1. Introduction – Part 1

In previous chapters the possibility that there was a specialised subchondral circulation capable of transferring load by hydraulic force was explored. Further supporting evidence was sought. As an orthopaedic surgeon I had often noticed longitudinal white marks on MRI scans around most joints in the general subchondral region. These seemed to attract little interest. A literature search returned no references or previous papers when using key words including MRI, tibia, subchondral, intraosseous, vessel or vein. The marks were usually visible on T2 or water bright scans. They could best be seen in axial plane upper tibial scans as shown in Figure 5.1 and Figure 5.2 (Beverly 2018).

An initial study of 60 pairs of x-rays and MRI scans was undertaken to assess the frequency, distribution and pattern of occurrence of the white marks and to compare those with the Kellgren-Lawrence grade of their contemporary plain x-rays. In terms of scoring plain x-rays the Kellgren-Lawrence system, though relatively crude, has stood the test of time. It was used here because of its direct applicability to the plain x-rays available. There were no other comparable upper tibial plain x-ray scoring systems

[2]Work in this chapter has been published in

Upper tibial MRI vascular marks lost in early osteoarthritis. Beverly M, Stamm G, Hamilton TW, Murray DW, Pandit HG. J. Orthop Surg Res. 2018 Nov 12;13(1):281. doi: 10.1186/s13018-018-0991-(Beverly, 2018)

which could be used with the same ease where large numbers of films were to be scored (Kellgren 1957, Kiapour 2019). After analysing 60 pairs of x-rays and upper tibial MRI scans there was an opportunity to carry out a second study with a larger group of patients with closer matching of the time between x-ray and scan.

In Part 2 of this Chapter a further group of 200 paired x-rays and scans was undertaken. This included MRI slices from the distal femur. In the second study the aim was to confirm the previous findings and to explore the general incidence and distribution of the vessels and their association with arthritis. A further aim of the second part of this work was to include the femoral condylar vascular marks.

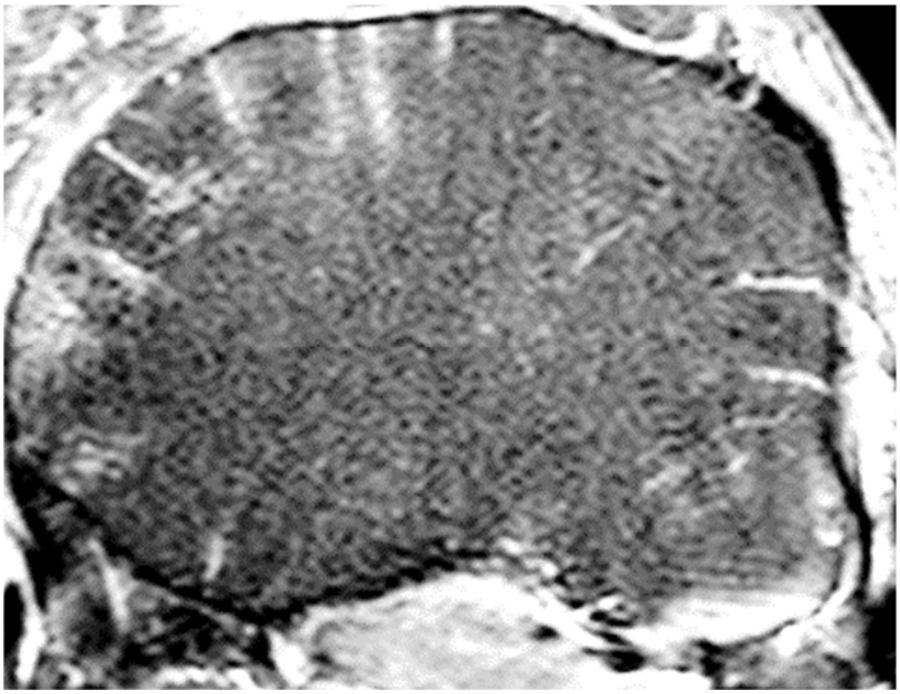


Figure 5.1 Left upper tibial PD_SPAIR MRI scan. Third slice down from tibial surface.

5.2. Method – Part 1

Material

Oxford knee clinic anonymised pairs of x-ray and MRI images were obtained. Subchondral radiating marks were observed in the proximal tibia on PD_SPAIR water bright or fat suppressed axial MRI scans of the knee.

A pilot audit study used 20 pairs of anonymised x-rays and MRI scans to see if the marks were present and what their distribution was. It quickly became apparent that the marks were visible in the axial plane of the upper tibia of most knees. They appeared to be in the subchondral area covered by the local scanning protocol. With ethical committee consent a formal study of 60 pairs of x-rays and MRI scans was therefore undertaken. The study had University and NHS ethical approval (OUH R&D Ref 12541). Anonymised films of 60 sequential patients who attended a knee clinic over a six month period in a University Teaching Hospital were reviewed. All patients who had a plain standing antero-posterior (A-P) x-ray of the knee and an MRI scan of the same knee within a 12 month period were included. Patients were excluded if their x-ray or MRI scan showed previous significant surgery such as partial or total knee replacement or internal fixation for trauma, ligament repair or other significant pathology. There remained 27 male and 29 female patients. There were 28 left knees and 28 right knees. The patients ranged in age from 22 - 85 years old with a mean age of 53.1 years. Their weight and BMI were known from the MRI data set. The MRI sequences were from a standard knee protocol used in routine clinical practice at our institution. In a 3 Tesla machine the protocol included axial Proton Density Spectral Attenuated Inversion Recovery (PD_SPAIR) images.



Figure 5.2 A typical MRI left upper tibial PD_SPAIR slice at level of third slice from upper tibial plateau. Radial vascular marks are evident in all quadrants. The popliteal artery contents are dark while the superficial veins, periosteal veins and proximal tibio fibular joint fluid are bright.

Two researchers, one an experienced orthopaedic surgeon and the other a medical student, assessed all the x-rays on a standard computer monitor. On standing plain AP knee films the medial and lateral compartments were independently scored for osteoarthritis using the Kellgren-Lawrence (K-L) (Kellgren 1957) classification as described below and in Figure 5.3.

Kellgren-Lawrence Grading Scale

Grade 0: Normal

Grade 1: doubtful narrowing of joint space, possible osteophytic lipping

Grade 2: definite osteophytes, definite narrowing of joint space

Grade 3: moderate multiple osteophytes, definite narrowing of joint space, some sclerosis and possible deformity of bone contour

Grade 4: large osteophytes, marked narrowing of joint space, severe sclerosis and definite deformity of bone contour



Figure 5.3 Kellgren-Lawrence grade reference sheet. These are computer generated teaching images from the internet (osteoarthritis classification WikiDoc). They give more uniform scoring examples rather than clinical radiographs.

The same researchers also assessed the MRI scans. They were blinded as to the K-L grade of the x-rays and as to each other's findings. In addition, radiographs and MRI scans were reassessed by both observers three weeks after the initial measurements in

order to calculate inter- and intra-observer variability. The observers were blind as to their previous results.

MRI scoring method

The MRI images were reviewed one slice per full screen on the same viewing monitor without changing the brightness, contrast or magnification. The first tibial slice or layer was taken as the most proximal axial slice of the knee to show only tibial bone. The scanning protocol was for slices 3.0 mm thick spaced 0.3 mm apart. The total scanned depth was therefore 16.5 mm from the centre of the first slice to the centre of the sixth slice or 19.5 mm in all. The axial scans were divided into quadrants vertically and horizontally at their maximum diameter as in Figure 5.4. The vascular marks were counted by layer and by quadrant. A vascular mark was defined as a radiating white line which reached the outside edge of the tibia. Vascular marks were not counted if they did not reach the outer edge of the tibia or if they were less than 5 mm long.

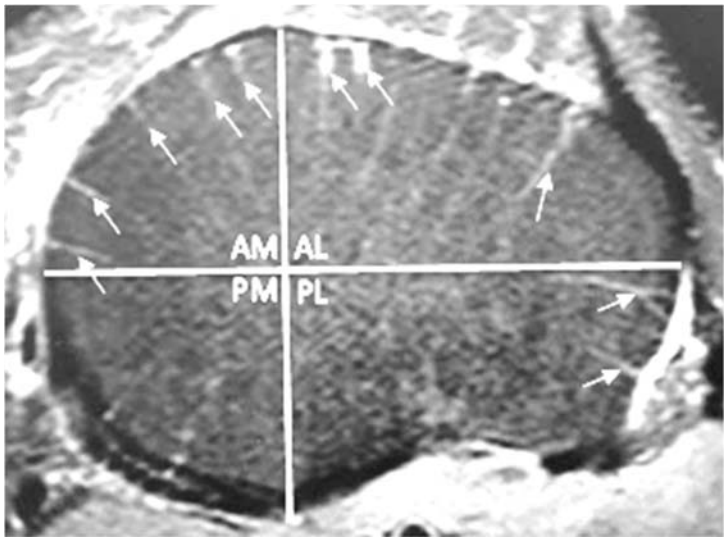


Figure 5.4 showing the same level 3 MRI slice seen in Figure 5.2 with scoring marks. This slice scored 5, 0, 2, 3 for Anteromedial, Posteromedial, Posterolateral and Anterolateral quadrants.

Statistical methods

Inter- and intra-observer agreement for Kellgren-Lawrence grade and number of veins on MRI was determined using a weighted kappa assessment for ordinal data. Inspection of the data revealed both Kellgren-Lawrence grade and number of veins to be skewed and as such non-parametric analysis was performed. To assess the association between location based on analysis of four quadrants of the proximal tibia and the number of veins observed, a Kruskal Wallis test was performed with Mann Whitney U post-hoc testing to assess for differences between individual quadrants. Where post-hoc tests were performed, a Bonferroni correction was applied to the significance level to account for multiple testing. To assess the association with age, a Spearman Rank test was performed with Mann Whitney U tests performed to assess for associations with gender and left and right knees. To assess for association with BMI and weight, Spearman Rank tests were performed. To assess for an association with grade of osteoarthritis a Spearman Rank test was performed. To assess for differences in vessels within grade of osteoarthritis Mann Whitney U tests were performed.

All analyses were performed using SPSS Version 22 (IBM Corporation, Armonk, New York). Statistical significance was set at $p< 0.05$.

5.3. Results - Part 1

Time between x-ray and MRI

The mean time interval between AP radiographs and MRI scans of the ipsilateral knee was 3.65 months (SD: 3.21, range: 0.03 – 11.87).

Inter- and intra-observer reliability

There was close agreement between the graders. Inter- and intra-observer reliability was moderate to excellent. Inter-observer agreement for Kellgren-Lawrence Grade and total number of vessels was 0.73 and 0.82 respectively. Intra-observer agreement for Kellgren-Lawrence Grade and total number of vessels was 0.89 and 0.93 respectively.

Pattern of osteoarthritis

The plain x-ray Kellgren-Lawrence distribution of osteoarthritis grades between the knees was as in Table 5.1 and Figure 5.5. There was more osteoarthritis medially than laterally. The great majority of the patients had lower grades of osteoarthritis, K-L 0-2.

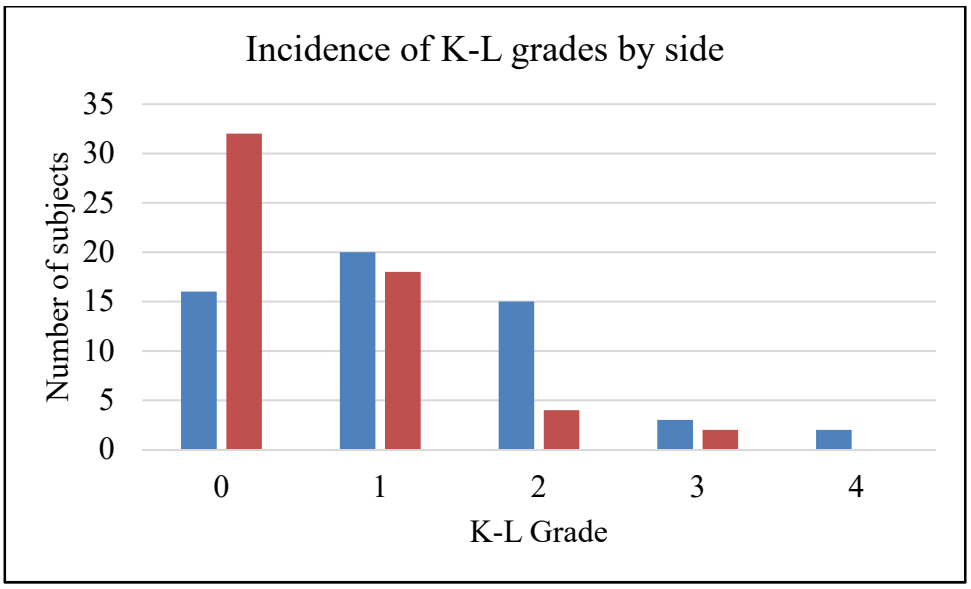


Figure 5.5 The distribution of K-L grades among 56 subjects by severity and side, Blue medial, Red lateral. There was more osteoarthritis medially, p<0001, n=56.

A Kellgren-Lawrence score of 0 equates to a normal knee x-ray. The patients attending the knee clinic had a range of potential diagnoses, not necessarily osteoarthritis. Those with obvious or severe osteoarthritis would probably not have been sent for MRI scans. Those with obvious meniscal or soft tissue problems may not have been sent for plain x-rays. Nevertheless there was a reasonable number of patients who had both investigations within 12 months.

K-L grade	Numbers of patients with each K-L grade medially, n=56	Numbers of patients with each K-L grade laterally, n=56
0	16	32
1	20	18
2	15	4
3	3	2
4	2	0
Mean K-L score	1.2	0.57

Table 5.1 Distribution of patients at each K-L grade. There was proportionately more osteoarthritis medially. There were more patients in the lower grades.

Vascular mark position below surface

Vascular marks appeared in the first subchondral tibial layer, increased in number in the second and third layer and virtually disappeared by the sixth as in Figure 5.6 and 5.7.

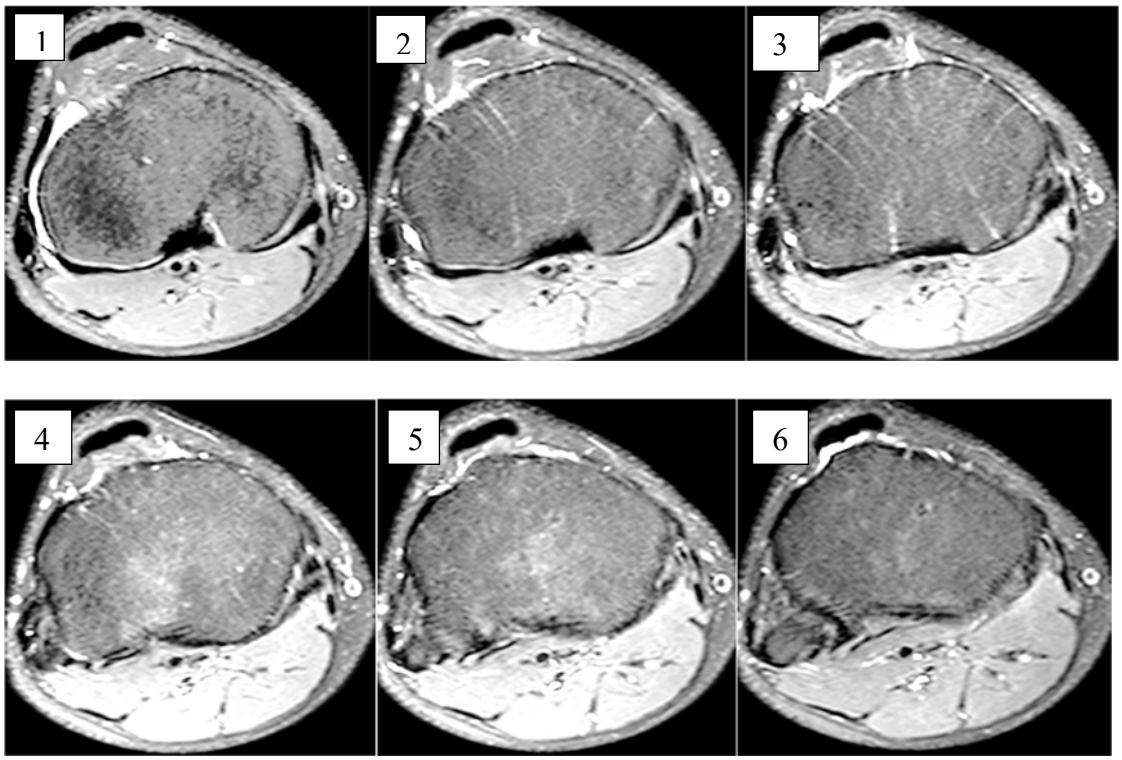


Figure 5.6 Example of six consecutive axial PD_SPAIR MRI slices from one upper tibia showing vessel frequency and distribution.

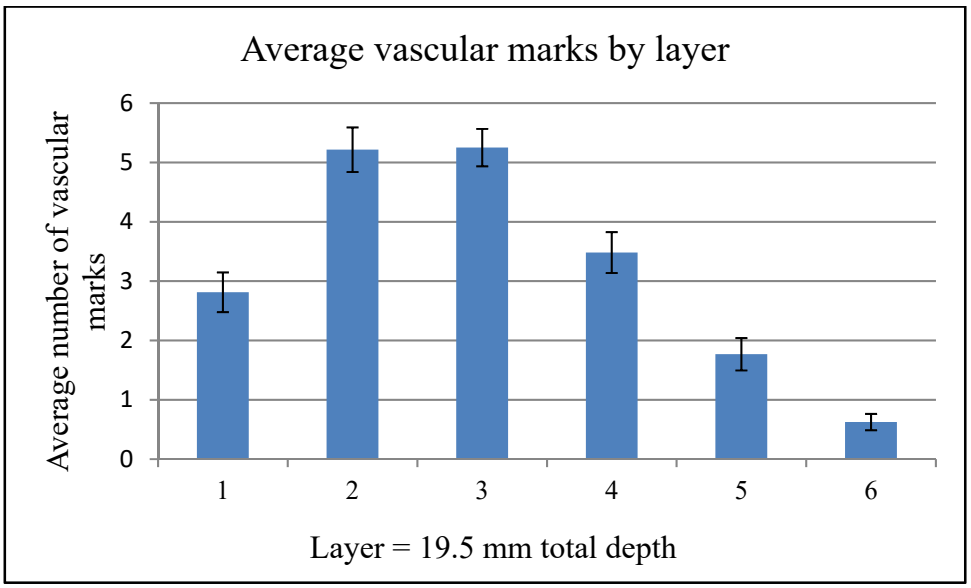


Figure 5.7 Vascular marks by layer for the first six axial layers below the upper tibial articular surface. Scans slices were 3.0 mm thick and 0.3 mm apart giving a depth of 16.5 mm from the middle of slice 1 to the middle of slice 6 or total depth of 19.5 mm. Error bars SEM, N=56.

Distribution

The distribution between the quadrants was analysed. The distribution of vessels was found to differ significantly between different quadrants ($p<0.001$) with the antero-lateral quadrant containing the most vessels and the postero-medial quadrant the fewest. Post-hoc testing revealed a significantly higher number of vessels anteriorly compared to posteriorly in both the medial ($p<0.001$) and lateral compartments ($p<0.001$) and a significantly higher number of vessels laterally compared with medially across both the anterior ($p<0.001$) and posterior quadrants ($p<0.001$) as in Figure 5.8.

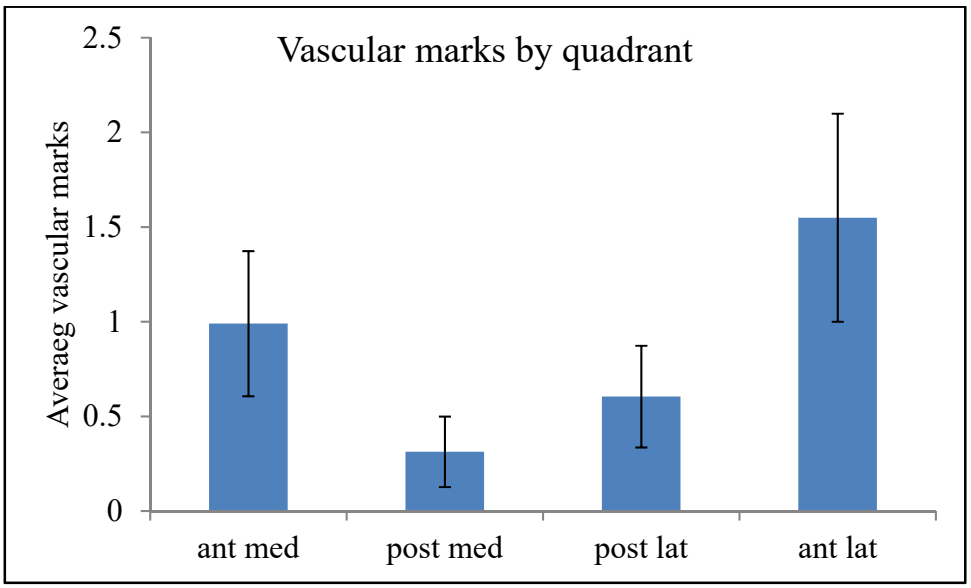


Figure 5.8 The distribution of vascular marks was as shown with most in the anterolateral quadrant and fewest in the posteromedial quadrant, $p<0.001$ for all.

Age and left and right knees

No association between age and total number of vessels was detected ($p=0.3$). No association between left and right knees and total number of vascular markings was detected ($p=0.10$).

BMI and weight

There was no association between the total number of vascular markings and a patient's BMI ($p=0.50$) or their body weight ($p=0.87$).

Gender

Fewer vessels were seen in females compared to males ($p<0.001$). Females had more osteoarthritis with a mean K-L score for females of 1.83 medially (SD: 0.83) and 1.43 laterally (SD: 0.73). The mean K-L score for males was 1.54 medially (SD: 0.78) and 1.20 laterally (SD: 0.40).

Correlation with OA

Analysis showed a negative correlation between the grade of osteoarthritis and the number of tibial vessels in both the medial (Spearman rho -0.31, $p<0.001$) and the lateral (Spearman rho -0.29, $p<0.002$) compartments of the knee. There were differences in vessels within the OA grades between medial and lateral. Mann Whitney U tests at each K-L grade showed significant differences between the two compartments in grade 0 ($p<0.001$) and 1 ($p<0.005$) but no significant difference at K-L grade 2 ($p=0.271$) as in Figure 5.9.

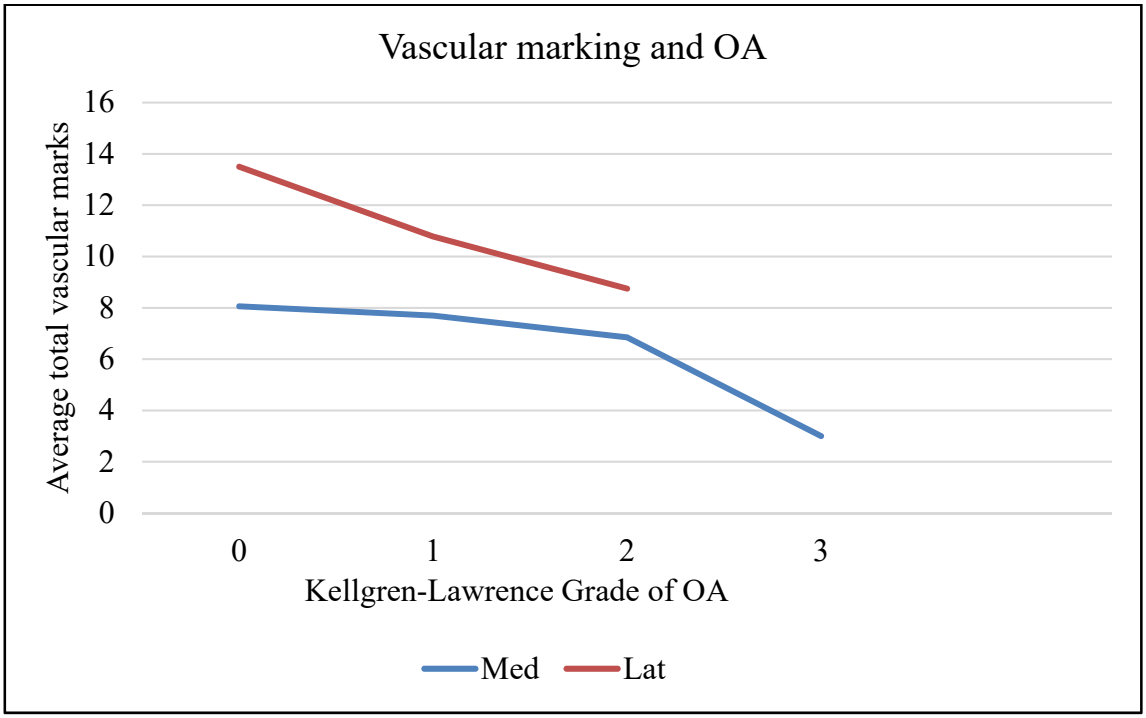


Figure 5.9 showing the reduction in vascular marks with increasing K-L grade. There were insufficient numbers for comparison in grades 3 and 4.

The loss in vascular mark loss was often confined to one side as shown in the example in Figure 5.10

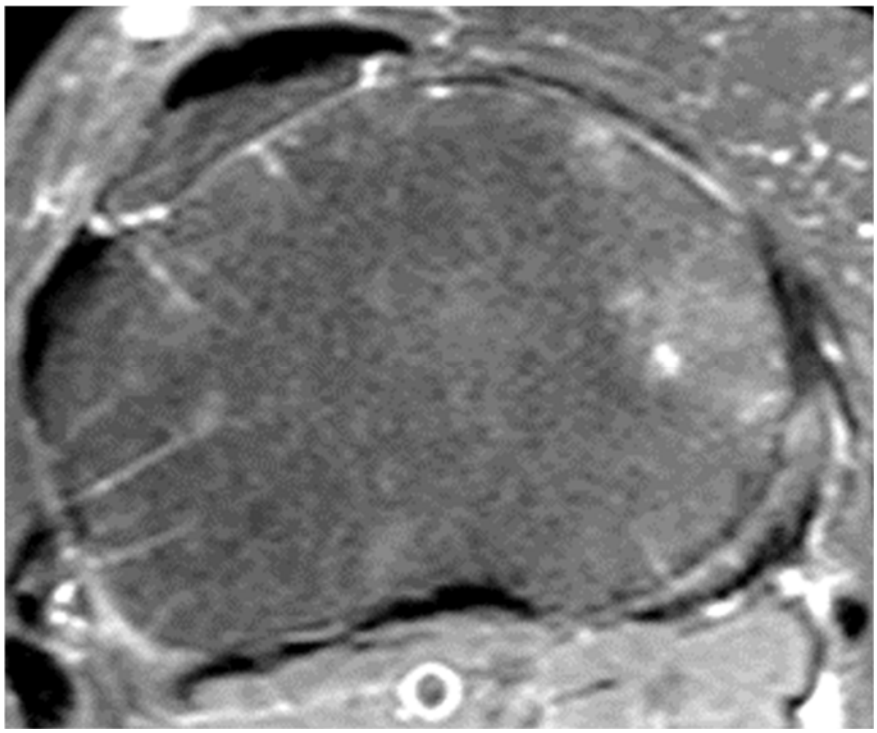


Figure 5.10 showing a typical right upper tibial MRI slice at level 3 of the right knee with K-L grade 2 osteoarthritis medially and K-L grade 0 laterally on plain x-ray. The medial vascular marks have been lost while the lateral marks remain.

5.4. Introduction - Part 2

Following encouraging results from the first study a set of 200 paired knee plain x-ray and MRI scans was obtained. In the second study the aim was to confirm the previous findings and to explore the general incidence and distribution of the vessels and their association with arthritis. A further aim of the second part of this work was to include the femoral condyle vascular marks.

5.5. Method – Part 2

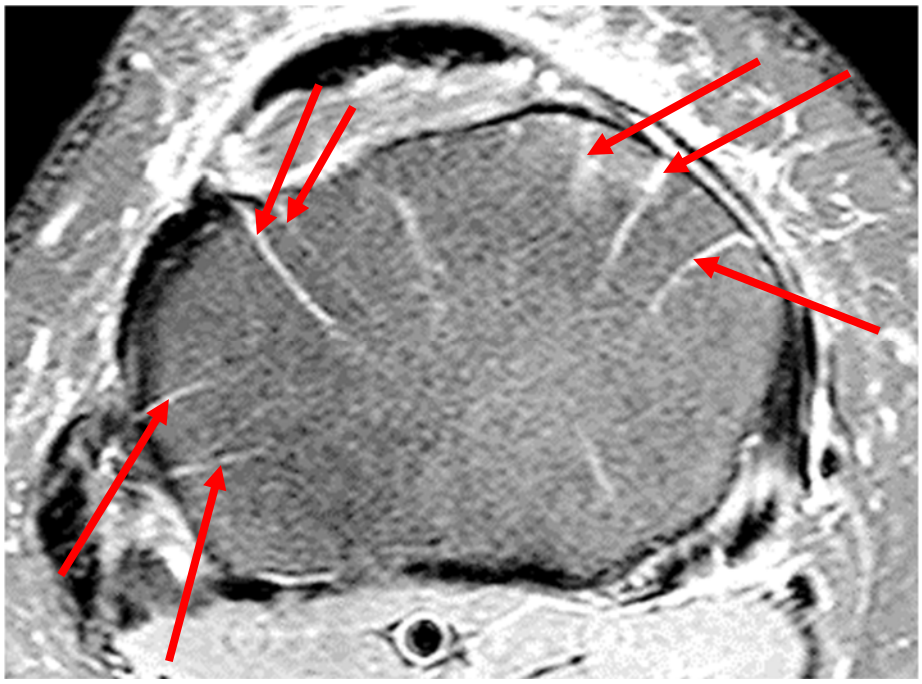


Figure 5.11 Left upper tibial axial slice showing the radiating vascular marks (red arrows) in a typical PD_SPAIR scan at layer 2.

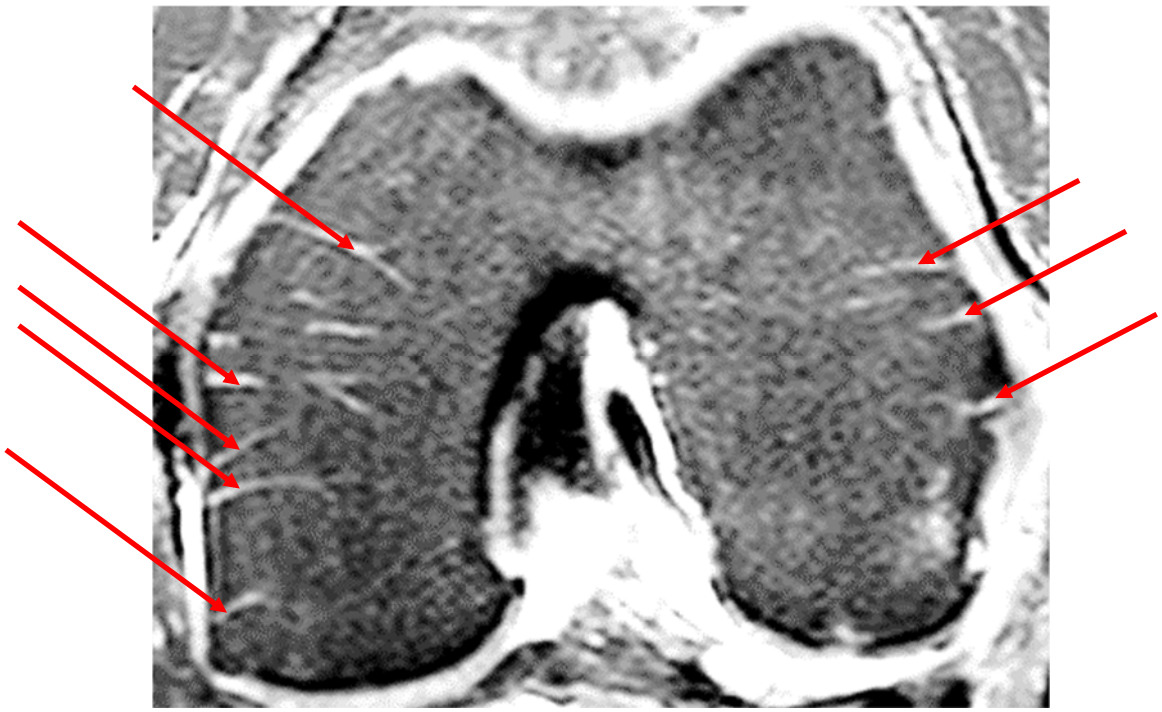


Figure 5.12 Left femoral PD_SPAIR slice sixth from joint surface showing vascular marks as indicated.

Material

For this study with ethical consent (OUH PID 12541) the anonymised films of 200 sequential patients were obtained. They included all those in sequence who had attended a University Teaching Hospital and had had a plain x-ray of the knee and an MRI scan of the same knee within a 6 month period. Patients were excluded if their x-ray or MRI showed previous significant knee surgery such as partial or total knee replacement, internal fixation for trauma, ligament repair or other significant pathology.

Their mean age was 55 years (range 18 - 81) with 100 males and 100 females. The medial and lateral compartments of each knee x-ray were scored for osteoarthritis (OA) using the Kellgren-Lawrence (K-L) classification as outlined in Part 1.

X-ray scoring method

The Kellgren-Lawrence (K-L) method of scoring for OA was used as above and based on images taken from a set of teaching images. The images were consulted for each x-ray grade assessment. Blocks of 20 x-rays were scored independently before switching to grading the associated MRI images in order to prevent observer bias.

All the plain antero-posterior knee x-rays were scored for K-L grade of osteoarthritis in the medial and lateral compartment on a standard PACS computer monitor.

MRI scoring method upper tibia

The MRI sequences were from a standard knee protocol used in our clinic in a 3 Tesla machine and included axial PD_SPAIR images. The MRI images were reviewed one slice per full screen on the same standard viewing monitor without changing the brightness, contrast or magnification. The first layer of the tibia was taken as the most proximal subchondral axial MRI slice of the knee to show only tibial bone. The scanning protocol was for slices 3.0 mm thick spaced 0.3 mm apart. The total scanned depth amounted to 16.5 mm from the centre of the first slice to the centre of the sixth slice or 19.5 mm in all for the upper tibia.

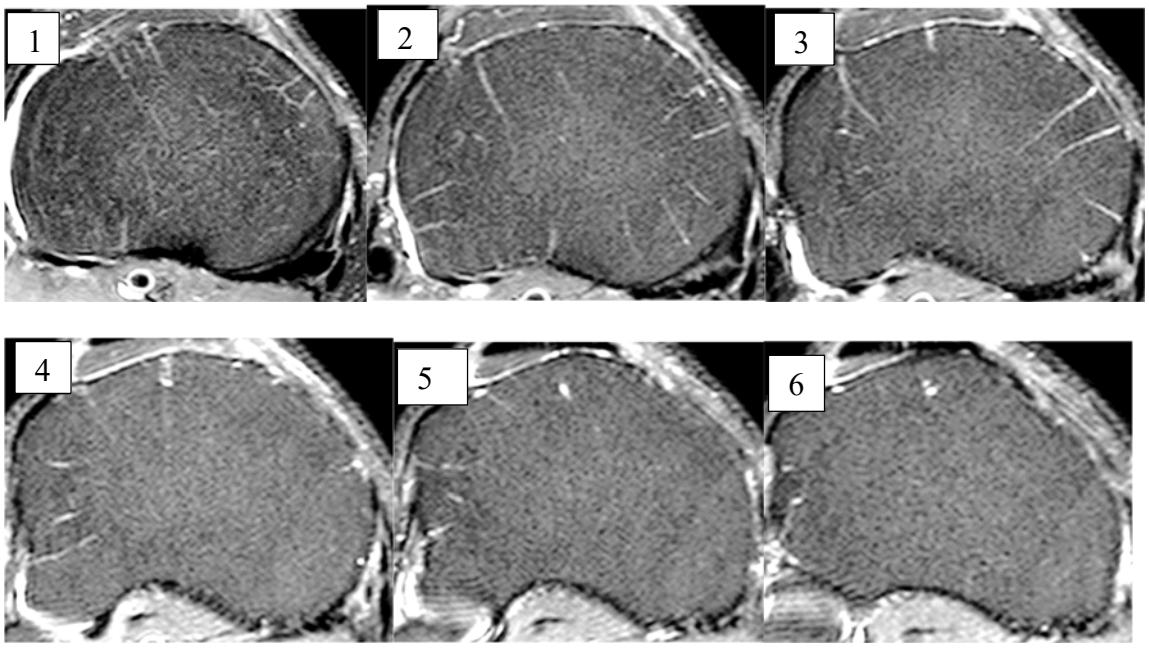


Figure 5.13 Six sequential PD_SPAIR MRI slices from the upper tibia of a right knee. Vascular marks are evident from slice 1 to slice 5.

The axial scans were divided vertically into medial and lateral halves at their maximum diameter. The vessels were counted by layer and by side, medial or lateral of the midline. A vessel was defined as a radiating white line of more than 0.5 cm in length which reached the outer edge of the tibia as shown in Figure 5.11. Each observer was blinded as to each x-ray or MRI score by processing the images in blocks of 20.

Slice number	1	2	3	4	5	6
Medial	2	4	2	3	2	0
Lateral	2	6	4	1	0	0

Table 5.2 showing the vascular marks score for the above six slices by layer and medial or lateral side.

MRI scoring method for distal femur

There were similar vascular marks evident on the distal femoral axial slices. The marks ran transversely from the intercondylar notch to the medial and lateral femoral cortices. Taking the first slice as being that which showed cancellous bone from both femoral condyles, the first 10 slices were scored by counting vascular marks as transverse longitudinal white lines which reached the cortical surface and were more than 0.5 cm long. The distal femur was included in all the MRI scans within the same protocol. The protocol was the same as that for the tibial slices, 3.0 mm thick and 0.3 mm apart giving a total scanned depth of femoral bone of 33 mm. Femoral vessels were counted both medially and laterally over the first 10 slices from the joint surface proximally. An example of the marks is shown in Figure 5.14.



Figure 5.14 An example of a left distal femoral axial slice at level 5 showing 2 transverse white lines medially and 5 laterally.

Statistical methods

Data was loaded directly into an Excel (Microsoft Corporation, Redmond, US) spreadsheet. Results were expressed as means, standard deviations and ranges. Student's t-test was used to determine if there were significant differences. For paired data paired t-tests were used. Otherwise unpaired t-tests were used. The Pearson test was used to assess correlations. $P<0.05$ was considered to be statistically significant.

5.6. Results – Part 2

The mean time interval between AP radiographs and MRI scans of the ipsilateral knee was 65.8 days (SD: 46.2 range: 0 - 181 days).

There were 100 male and 100 female patients. There were 105 left knees and 95 right knees. The females were older (57.8 years, range 24 - 80, SD 14.3) than men (52.5 years, range 18 - 81 SD 13.8). The men were heavier (85.4 kg, range 55 - 120, SD 13.7) than the women (72.8 kg, range 42 - 124, SD 15.0).

K-L score and Age, Weight and Left and Right knees

There was no significant correlation between age and increasing K-L score ($p=0.143$), weight and K-L score ($p=0.98$) and between left and right knees ($p=0.43$). Weight and age were not correlated ($p=0.999$). Females had combined total K-L scores of 208 (average 2.08) and men of 195 (average 1.95) but this was not significant ($p=0.17$).

K-L scores Medial and Lateral

There was a significant difference between the total tibial K-L scores medially (mean 1.54) and laterally (mean 0.69), $p<0.0001$.

Vascular mark depth and Medial or Lateral side

Vascular marks appeared in the first subchondral tibial layer, increased in number in the second and third layer and virtually disappeared by the sixth as in Figure 5.15.

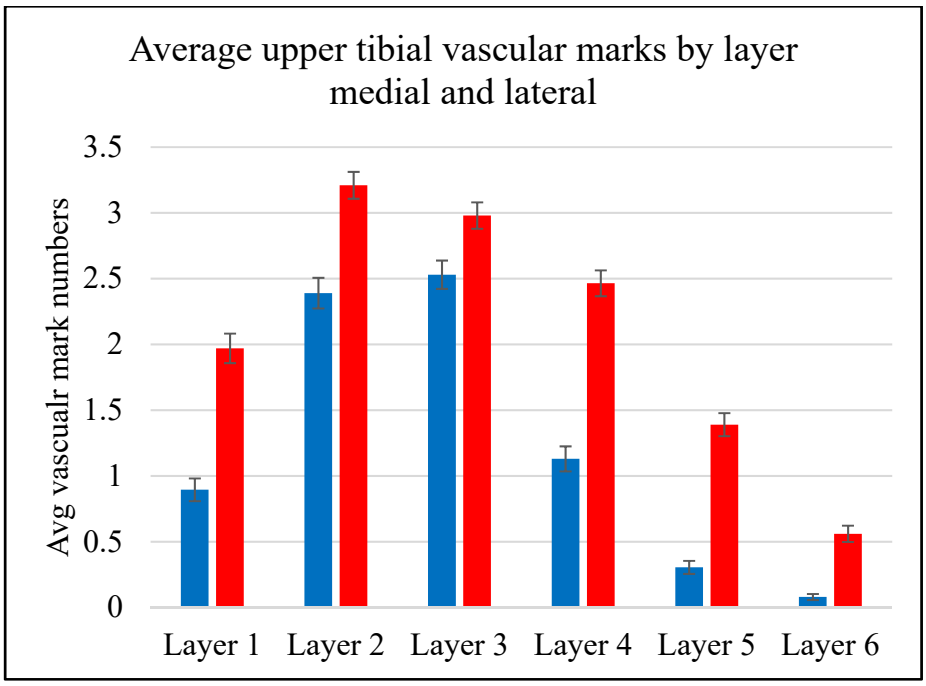


Figure 5.15 Average vascular mark numbers by layer from the upper tibial surface on the medial and lateral sides, Blue – medial, Red – lateral. The distance from the centre of layer 1 to the centre of layer 6 is 16.5 mm. Error bars are SEM.

Vascular marks medial/lateral distribution

There were more vascular marks laterally. The vascular marks distribution between the medial and lateral sides was analysed at each level and was found to differ significantly between medial and lateral sides as in Figure 5.15 and Table 5.3.

	Average medial vascular marks	Average lateral vascular marks	p value
Layer 1	0.895	1.97	p<0.0001
Layer 2	2.39	3.21	p<0.0001
Layer 3	2.53	2.98	p<0.003
Layer 4	1.13	2.465	p<0.0001
Layer 5	0.305	1.39	p<0.0001
Layer 6	0.08	0.56	p<0.0001
All layers	**1.047**	**2.096**	**p<0.0001**

Table 5.3 There was a significant difference in average vascular mark numbers between the medial and lateral sides of the tibia at all levels as set out above.

Vascular marks score and Age, Weight and Left/Right knees

There was no significant correlation between vascular marks and increasing age (p=0.94), vascular mark numbers and weight (p=0.85) and between vascular marks and left and right knees (p=0.43). Females had combined total vascular mark scores of 1771 and men of 2210 and this was significant (p<0.0001).

Correlation between K-L grade of osteoarthritis and vascular mark loss

Analysis showed a negative correlation between grade of osteoarthritis and the number of tibial vascular marks in the medial side between early (Grade 0 and 1) and late (Grade 2 and 3) knees, (p<0.001). On the lateral side there was a loss in vascular marks with increasing K-L grade between early (Grade 0 and 1) and late (Grade 2 and 3), (p<0.002) osteoarthritis of the knee. There were differences in vascular marks within the OA grades between medial and lateral sides in grade 0 (p<0.001) and grade 1 (p<0.005) but no significant difference at grade 2 (p=0.271) as in Figures 5.16 and 5.17.

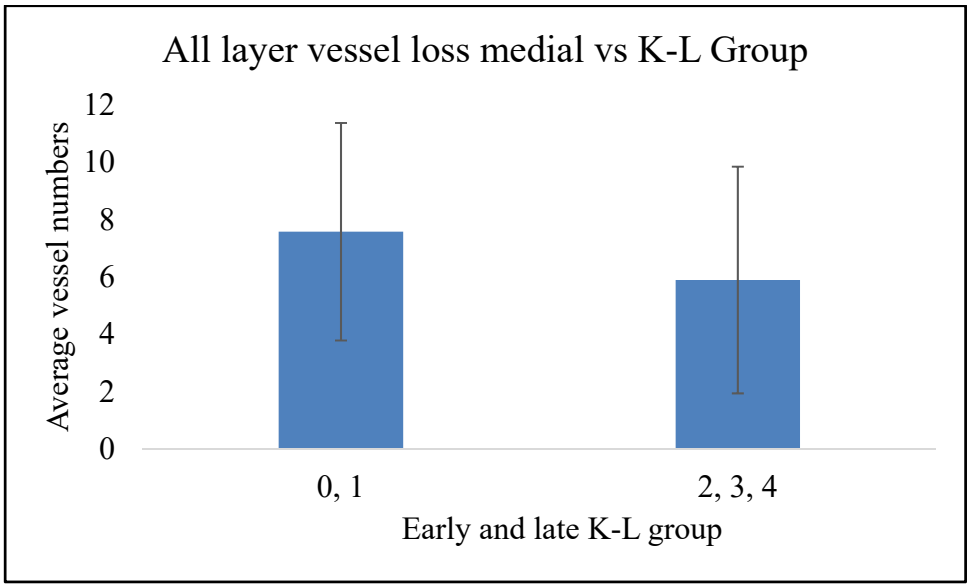


Figure 5.16 There was a loss in vascular marks medially with increasing K-L grade, p<0.001. Error bars =SD.

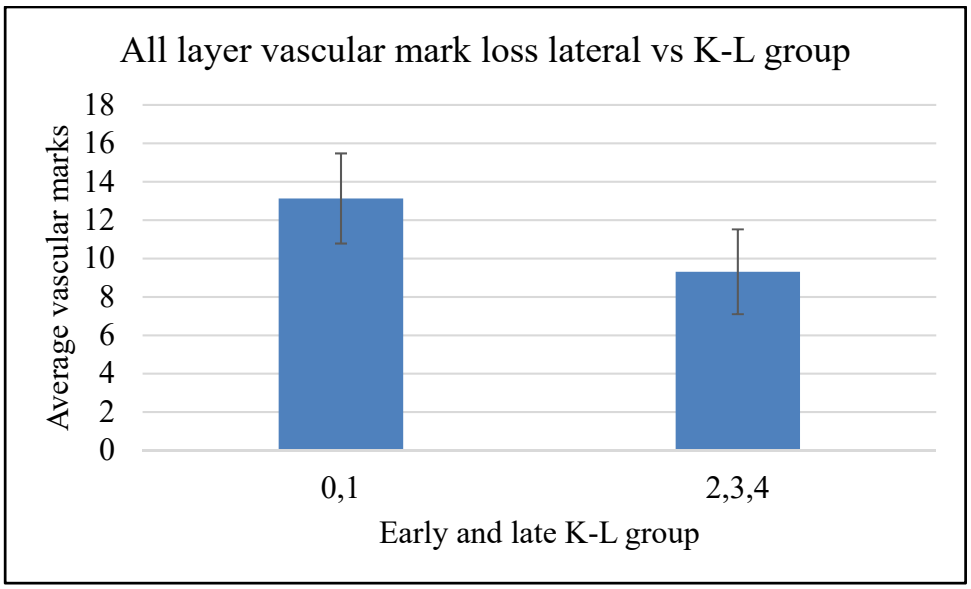


Figure 5.17 There was a loss in vascular marks laterally with increasing K-L grade, p<0.002. Error bars=SD.

When the medial and lateral combined average vascular mark for all layers in each joint were compared with their respective K-L grade there was an inverse correlation as in Figure 5.18.

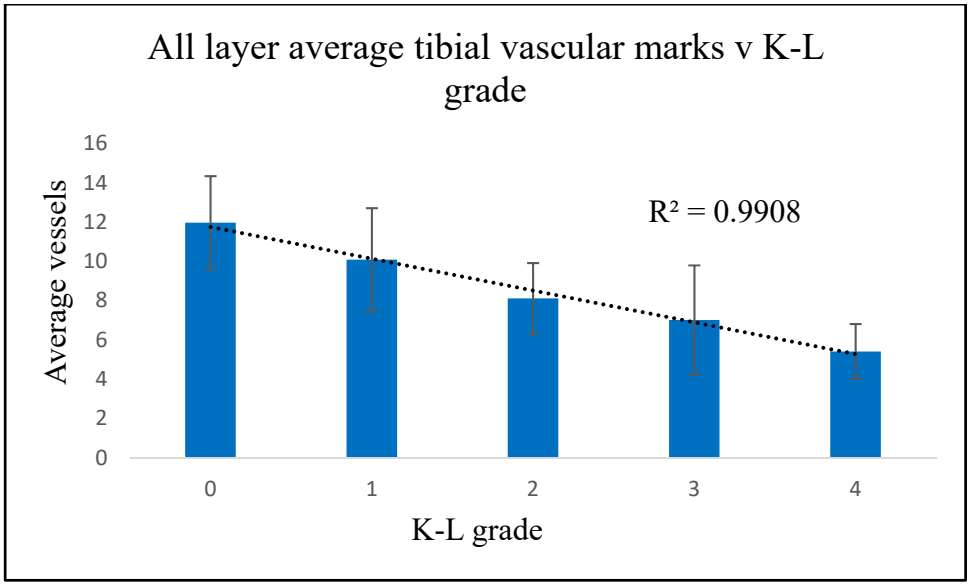


Figure 5.18 The tibial average total vascular marks decreased with increasing K-L grade, $p<0.0001$, error bars=SD.

Femoral vascular marks

Axial femoral slices were 3 mm thick at 0.3 mm intervals giving a total from the centre of slice one to the centre of slice ten of 29.7 mm.

The overall distribution of the femoral vascular marks is shown in Figure 5.19.

There was a significant difference in the numbers of vessels present in the medial and lateral femoral condyles, $p<0.0001$.

Because the distal femur is curved as opposed to the upper tibia which is flat, the area of bone seen in the femoral slices increased rapidly and continued to increase over the full 3 cm scanned. The vascular mark count was reducing from about 1.5 cm depth onwards.

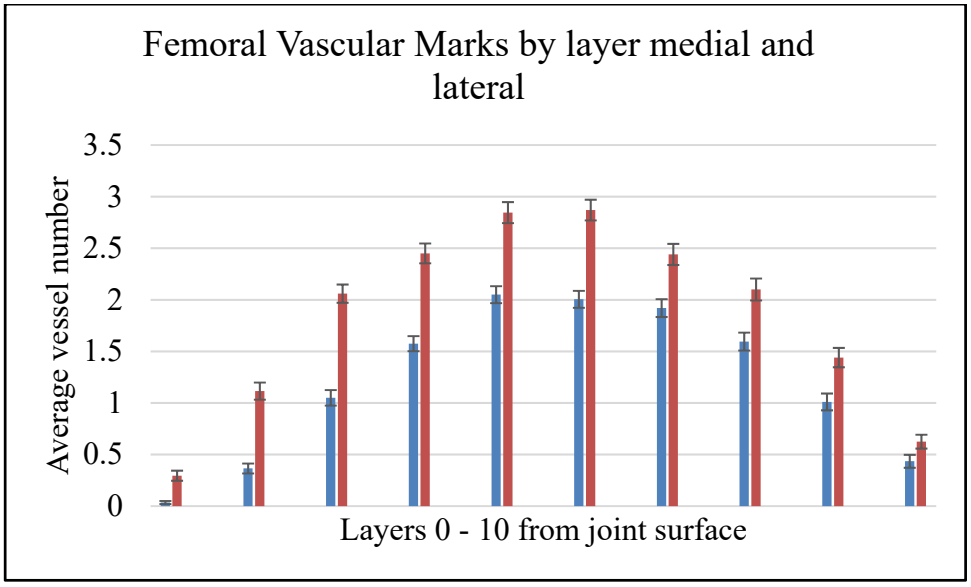


Figure 5.19 The first 10 axial slices from the distal femur showing the average numbers of vascular marks by layer and medial (blue) or lateral (red) side. The total depth covered is 30 mm. There were more vessels laterally $p<0.0001$. Error bars=SEM.

Although there were femoral transverse subchondral vascular marks as demonstrated above there was no significant loss of vessels with increasing K-L grade as shown in Figure 5.20.

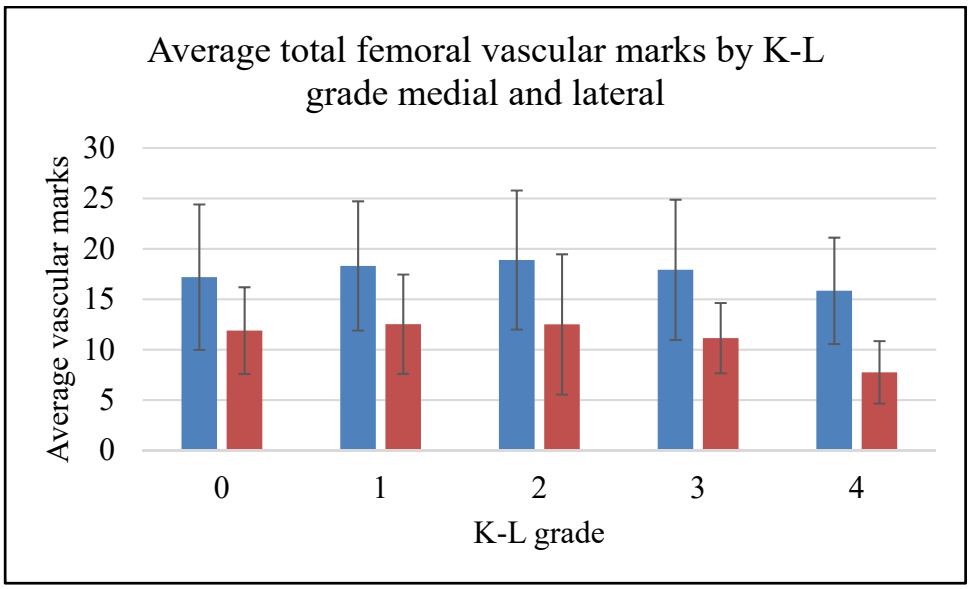


Figure 5.20 Vascular mark numbers by K-L grade and medial (Blue) or lateral (Red). Error bars = SD.

5.7. Discussion - Part 1

MRI vascular marks

Previously undescribed radial vascular markings on MRI scans of the upper tibia are presented. It is surprising that these vessels which are usually present in T2 and PD_SPAIR MRI scans of joints have attracted so little attention. Such vessels are apparent in virtually all water bright T2 MRI scans of joints and appear to lie mainly in the subchondral plane. The most likely explanation for their not having been previously described is that orthopaedic pathology has usually been sought at the joint surface. Subchondral vascular structures have not received much interest and the result is that scans of that area are generally ignored. In any event most joint surfaces have a curved profile making any subchondral vascular marks more difficult to observe over any length in flat MRI slices.

Fortunately the upper tibia is relatively flat and lies in an axial plane in an MRI scanner. Axial scans in the subchondral plane therefore allow good visualisation of the vascular marks in single slices. The vessels are best seen in axial T2 or PD_SPAIR scans. Consultant radiological opinion was that these marks are vascular and probably venous. Reasons given include that they are longitudinal channels, water enhancing, often in tributary form, increase in size as they reach the periphery, penetrate the cortex and appear to link with periosteal vessels. There is a slow flow rate in these vessels during MRI scanning in the recumbent patient. Arteries are generally narrower and their higher flow rate makes their contents less visible. The contents of the popliteal artery in Figures 5.2, 5.4, 5.6, 5.10 and 5.11 are dark as a result of flow during the period of data collection for each slice. The superficial veins in the same slices remain bright as their high water contents barely move during the image acquisition period of a second or more.

Anatomy

Hunter (Hunter 1861) described a vascular ‘mesentery’ in the subchondral region and Nelson and Crock described axial plane radiating upper tibial arteries in post-mortem injection studies in their papers of the early 1960s but there has been little interest in subchondral vessels subsequently (Nelson 1960, Crock 1962). No reference to the loss of those vessels with the onset of osteoarthritis could be found and no reference to such changes being observed on MRI scans exists. The possibility that there might be a specialised subchondral circulation does not appear to feature in any contemporary anatomy books. Other than Nelson and Crock, few anatomists have injected then sectioned weight bearing bone in the axial subchondral plane. Most descriptions of the anatomy of the blood supply are as a result of arterial injection studies followed by clearance of the calcified tissues and then describing bone circulation in the sagittal and coronal plane perpendicular to the joint.

It is technically difficult to inject the osseous venous system for several reasons. Limb veins are thin walled and difficult to catheterise. Pressure injection of contrast leads to bursting and leaks. While there is often a single main artery supplying the limb there are usually multiple superficial veins draining the limb. Veins have valves preventing retrograde flow. There are frequently anastomoses and sinuses rather than an injectable tree or tributary pattern such as exists on the arterial side. As a result the popular view which has been adopted is that illustrated in Gray’s Anatomy (Standring 2016). The venous pattern is depicted as a reciprocal or mirror image of the arterial supply. That may be true in some organs but, as will be shown in Chapter 6, is not likely to be the case in weight-bearing long bones.

Kellgren-Lawrence

The Kellgren-Lawrence (K-L) method of grading osteoarthritis of the knee on plain AP x-rays was used because of its simplicity and widespread current use. It classifies osteoarthritis in the upper tibia (Schiphof 2008, Park 2013, Culvenor 2015, Kohn 2016, Taguchi 2017). Other more complex grading systems for osteoarthritis on plain x-rays are available (Ahlback 1968, Collins 2011) but were not used because of their complexity or requirement for patient questionnaire data (Collins 2011) or their focus mainly on MRI scans (Hunter 2008, Felson 2010, Alizai 2014, Ronga 2014, Hafezi-Nejad 2015).

The majority of our patients had rankings in the lower K-L grades from 0 (normal with no sign of osteoarthritis to 3 (moderate joint space reduction). In the clinic very few patients with severe osteoarthritis would be sent for an MRI scan. The original publication by Kellgren and Lawrence gives example x-rays which are of poor quality and of different size and x-ray penetration. Most studies have therefore used standardised computer generated teaching images such as those above obtained from the internet.

MRI imaging

MRI analyses the signal given off by hydrogen atoms as they return to random positions from their previous alignment after a magnetic field is removed. MRI image quality depends on many variables including, but not limited to, the strength of the magnetic field, the protocol used, slice thickness and spacing, the timing of analysis of the emitted signal, intensity, windowing, brightness, fat suppression, presence of other metallic bodies, the position of the limb within the field and the imaging screen resolution. The MRI knee scanning protocol here was that used routinely in our institution on a 3 Tesla machine.

Medial side osteoarthritis

The medial side is generally the more frequent site for primary knee OA. Patients presenting in the clinic had more medial osteoarthritis. The loss of vessels on MRI appears potentially to be as useful in detecting early OA as K-L grading. Further analysis or quantification of the MRI vessel loss may give a quantifiable score in osteoarthritis or help with prognosis. In this preliminary study of a mixed group with varying degrees of early osteoarthritis there were fewer vessels on the medial side generally and this was associated with more advanced K-L scores. Although generally having smaller knees, females had fewer vessels than males with higher mean K-L scores for osteoarthritis both medially and laterally. Findlay suggests that osteoarthritis is associated with reduced blood flow. He does not speculate on the possible reasons for that and does not consider that force is transferred by hydraulic means across the joint or that osteoarthritis might be a vasculo-mechanical disease or that there is a specialized anatomy and vasculature involved in weight bearing (Findlay 2007).

Limitations

There are several possible limitations in this work. For analysis a standard PC screen such as those found on any ward-based PACS system was used to view the images. It is acknowledged that much of the image quality is lost in those images compared with the optimal conditions on specialised screens available in the darkened rooms of an x-ray department.

The study is cross-sectional rather than longitudinal. Although there is an inverse correlation between the presence of vascular markings in the proximal tibia and the presence and severity of early osteoarthritis, it is not possible to comment on cause and effect. The first study was based on an unselected but sequential series of 60 patients referred to the Knee Clinic in a University Teaching Hospital. The only exclusions were those with significant previous trauma and surgery to the joint. It is not claimed that the remaining patients represent a typical

adult population or that they all had osteoarthritis. The data was anonymised and clinical information such as pain or function scores for these patients were not available. It is accepted that there is often a difference between the radiological findings of knee osteoarthritis and a patient's symptoms. A further limitation at this stage was the need to prove that the MRI marks are blood vessels. However, a literature search failed to identify any other description of these marks on MRI scans and local consultant radiological opinion was that they fulfil the MRI criteria for veins or vessels. Histology was therefore carried out to identify the marks and the results are presented in Chapter 6.

Conclusion

In conclusion this seems to be the first study to describe upper tibial subchondral radiating vascular marks on MRI scans and to identify an inverse relationship between the marks and the presence and distribution of knee osteoarthritis. At this stage it was not possible to say whether the loss in vessels causes the osteoarthritis or if osteoarthritis causes the loss of vessels but there is clearly an association. The loss of marks on MRI may be a means of diagnosing or predicting the development of osteoarthritis. The first study of 60 pairs of x-rays and MRI scans offered support to the hypothesis that there is a loss in vascularity associated with osteoarthritis. A second study was therefore undertaken to confirm the original findings and to look at the femoral side of the joint.

5.8. Discussion - Part 2

MRI scoring

The second study looked at a larger group of patients and included their femoral scans. The same method of counting, scoring and analysis was used for both groups. The Kellgren-

Lawrence method to grade osteoarthritis of the knee on plain AP x-rays was used because of its simplicity and access to the corresponding MRI scans. More complex methods of MRI grading osteoarthritis are available such as Whole Organ MR Scoring (WORMS) and Boston-Leeds Osteoarthritis Knee Scoring (BLOKS). Neither method counts the obvious vascular marks discussed here. Both are methods for semi-quantitatively assessing structural changes of OA from knee MRIs. They are time consuming and were unsuitable for use in this study where large numbers of films were reviewed for the presence of vascular marks rather than to accurately grade the osteoarthritis in a particular part of the joint. It is acknowledged that MRI image quality depends on many variables some of which are listed above.

Patient selection

This sequential group of 200 patients had x-rays and MRI scans in the department for a variety of different reasons. They came from a range of clinics and GP referrals. They were not selected for osteoarthritis or in any other way. The whole group of sequential studies was included. There was no access to their diagnoses. Because the medial side is the more common site for primary knee OA it is likely that any large group of patients would have more early medial osteoarthritis. As in the previous study there were generally fewer upper tibial vascular marks medially and this was associated with more advanced K-L scores. In addition females had fewer vessels than males and a higher mean score for OA in both compartments.

Distal femur

The upper tibial analysis generally confirmed the earlier study findings. The femoral condyle vascular mark count has a number of potential difficulties. The tibia is flat and of essentially the same surface area over the first six slices. The femoral slice area increases considerably over the first two or three centimetres or about six slices from the joint. That alone may account for more vessels being seen. Over the next 2 - 3 cm the femoral slice area continues to increase

in area but the vascular count fell significantly. The femoral condyles are curved especially in the anteroposterior plane. Each condyle is also curved in the coronal plane. Curved subchondral vessels would not be revealed in these flat transverse slices. Fortunately there were vascular marks which appeared to run from the inner aspect of the intercondylar notch transversely outwards to the medial and lateral cortices. These were visible on all scans and in most slices as illustrated.

The increasing area of the femoral slices could nevertheless possibly mask an effect such as that seen in the upper tibia where vessel numbers were inversely proportional to K-L grade. This was not fully explored as calculating the femoral slice area was not feasible.

It was apparent from this study that the transverse vascular marks also have a subchondral distribution which appears to increase over the first centimetre or two before diminishing 2-3 cm deep to the articular surface. This does not appear to have been described previously. In this study it was not possible to show an association between K-L grade and vascular mark loss in the distal femur. In any event K-L grading appears to apply mainly to the tibial surface rather than the much larger femoral articular surface. However, it is interesting to note that even on the femoral side there were more vascular marks laterally and less arthritis laterally, with fewer marks medially and more arthritis medially. The Findlay paper suggests that osteoarthritis is associated with reduced blood flow. He does not speculate on the possible reasons for that and does not consider that force is transferred by hydraulic means across the joint or that osteoarthritis might be a vasculo-mechanical disease or that there is a specialized anatomy and vasculature involved in weight bearing.

It is tempting to speculate that the vascular marks are in the subchondral region for a reason. That reason may have something to do with nutrition and perhaps reflects a circulation modified to cope with hydraulic cushioning of weight bearing impacts to the joint. That speculation is reinforced by their apparent loss in OA.

Articular surface areas

K-L grading is usually applied to the knee joint in an antero-posterior x-ray. The tibial joint surface is well profiled while only a tangential view of the curved femoral articular surface is possible. The size of the articulating surface area of the femoral condyle is considerably more than the articulating surface area of the upper tibia, perhaps 2 to 3 times greater. That may lead to earlier OA changes on the tibia rather than on the femur. Even if both show equivalent changes, the femoral curve may obscure them on the antero-posterior x-ray.

Limitations

There are potential limitations to this study. The study is cross-sectional and therefore although an inverse correlation appears to exist between the presence of vascular markings in the proximal tibia and the presence and severity of OA, it is not possible to comment on cause and effect. In addition the study is based on an unselected but sequential series of patients who had had both an x-ray and an MRI scan of the same knee within six months. They may not represent a typical adult population. Diagnoses, pain, functional scores and cardiovascular condition were not available for these patients. A further potential limitation is proof that the vascular marks are in fact blood vessels. Chapter 6 addresses that point.

Conclusion

These studies appear to be the first to describe commonly seen subchondral vascular marks in both the femoral and tibial side of the joint. An inverse relationship between the marks and the presence and distribution of knee OA is demonstrated. Whether the loss in vessels causes the OA or OA causes the loss of vessels is not clear but there appears to be an association. The loss of vascular marks on MRI may be a means of diagnosing or predicting the development of OA

more accurately than by plain x-ray alone. Osteoarthritis may be a partly vascular or vasculo-mechanical disease.

In Chapter 6 histology was carried out in order to confirm these findings and to look for other vascular features which might support the existence of a specialised subchondral circulation capable of transferring load partly by hydraulic force.

6. SUBCHONDRAL BONE ANATOMY AND HISTOLOGY

6.1. Background

Some aspects of the history of bone circulation were described in Chapter 1. Because of the findings of vascular marks on MRI scans of the subchondral plane and the possible subchondral hydraulic pressure transfer with loading, the anatomy and vascular histology in the axial subchondral plane was explored, looking for features that might support a dynamic or pressure tolerating environment. The tissues available included foot calf metacarpal, normal human proximal tibia and arthritic human proximal tibia. This histological study was firstly designed to confirm that the marks seen on MRI scans are vascular and secondly to seek to identify any other features that might support the concept of a specialised subchondral circulation with hydraulic load transmission in normal and arthritic bone.

6.2. Objectives

Macroscopic anatomy

1. The gross anatomy of the proximal calf metacarpal and upper human tibia were compared.
2. The results of dye injection into the arterial supply was studied.
3. The effect of physical compression of the injected bone was tested.
4. Whole bone slices of human and calf bone were reviewed macroscopically and compared with the equivalent MRI slices
5. Macroscopic slices of decalcified bone were compared with the MRI slices.

Histology

6. Bone histology was carried out on the available material to look for the subchondral vessels in the axial plane.
7. The cortical bone adjacent to the joint was examined to look for possible valve or choke features.
8. The subchondral bone in the vertical plane in normal healthy bone and early arthritic bone was examined for the presence of subchondral capillaries in normal and arthritic bone.

6.3. Method

Calf

Freshly culled male calf fore feet were obtained from an abattoir. The calves were aged one to two weeks and weighed between 50 and 80 kg. The fore feet were amputated proximal to the carpus. The radial artery was catheterised with a 16 G 12" Teflon catheter (E-ZCath, Deseret Pharmaceutical Co, Inc, Sandy Utah 84070). The artery was injected with 200 ml 10% Formalin and the metacarpal bone was dissected free of soft tissues. For the purposes of this study the relatively flat proximal metacarpal was used. This is effectively a single bone. The calf bone was of a juvenile type with cartilaginous epiphyses present. The cortex was partially ossified.

Human

Specimens of human knee tissue were obtained from the Oxford Musculoskeletal Biobank and were collected with informed donor consent in compliance with national and institutional ethical requirements, the United Kingdom Human Tissue Act, and the Declaration of Helsinki

(HTA Licence 12217 and Oxford REC C 09/H0606/11). Four samples came from patients undergoing knee replacement for osteoarthritis. One was a whole knee amputation specimen for sarcoma proximal to the knee. There was no sign of metastatic disease in the knee joint itself. The human bone was mature and fully ossified. The bone was cut transversely into 5 mm thick sections deep to the medial and lateral sides of the proximal tibia and distal femur.

Histology

Slide preparation

Following decalcification the samples were tissue processed (Leica ASP300S) overnight and embedded (Leica EG1140H) in paraffin wax blocks and chilled. Sections were cut on a Leica RM2125 RTS microtome. Experience showed that sections 10 microns thick were obtainable. Sections were mounted from a water bath on to slides and these were placed on a 60 °C hot plate for an hour and incubated overnight at 37 °C. In preparation for staining, the sections were dewaxed and rehydrated by successive immersion in Histoclear, graded ethanol and water. The sections were then stained with Haematoxylin and Eosin (H+E), Masson's trichrome, Goldner's trichrome or Van Gieson's stain. H+E is good for general detail staining producing nuclei dark blue, red cells red and other tissues pink/blue. Masson's trichrome stains nuclei dark purple-red, cytoplasm pink and connective tissue blue. Goldner's trichrome stains nuclei brown/black, cytoplasm red, red cells orange, muscle red and collagen green. Van Gieson stains elastin black or dark brown.

Light microscopy

The slides were examined with a power x 2 and x 4 lens using an Olympus BX40 microscope connected to an AxioCam MRc to allow image capture by Zen 2012 software. Other images

were obtained with a digital camera Fujifilm Corporation Digital camera JV500, an iPhone SE or from images captured from MRI scans using RadiAnt DICOM Viewer 4.2.1 (64bit).

Experimental plan

1. Images of the tibial articular surface and proximal calf metacarpal surface were compared.
2. Twenty millilitres of two percent Evans Blue in 10% formalin was injected into the calf foot radial artery. The distal end was sectioned transversely with a fine saw and photographed for the presence of a subchondral plexus.
3. The bone was placed in a work bench vice, squeezed in the coronal plane and the cut surface was photographed.
4. Sections of human distal femur and proximal tibia were photographed and compared with the MRI scan images prior to decalcification.
5. Bone samples were fixed in 10% formalin overnight and decalcified in 5% nitric acid. After initial tests 12 hours was found to be adequate for calf decalcification. For the human bone slices 48 hours with a change of nitric acid at 24 hours gave acceptable results. Decalcification was tested for manually by flexing the specimen and with a needle for penetration. Plain x-rays were used to confirm decalcification of some specimens. Specimens were photographed after decalcification to show the presence of axial plane radial subchondral vessels.
6. Human and calf subchondral axial slices were examined histologically for the presence of radiating vascular structures and images were photographed.
7. Human and calf cortical slices in the vertical and transverse planes were examined for possible valves or choke mechanisms and photographed.
8. Vertical slices of bone from joints were examined for the presence of subchondral vessels in normal and early arthritic bone and photographed.

6.4. Results

1. The proximal articular surface of the metacarpal closely resembles the human tibial plateau in form and function as in Figure 6.1. The articular surface at the calf carpo-metacarpal joint is flat and similar to the human tibia in cross section but without menisci.



Figure 6.1 Left - human upper tibial articular surface and right - calf proximal metacarpal articular surface. The calf metacarpal is a fused third and fourth metacarpal. (This example was perfused with Evans blue).

2. When injected with dye through the radial artery there is clearly a zone of subchondral filling as shown in Figure 6.2



Figure 6.2 Calf metacarpal after arterial injection with Evans Blue. Subchondral capillary vessels filling is evident.

3 When healthy bone is injected with dye through the artery then compressed in a vice the subchondral plexus or Hunter's mesentery is seen to ooze blood as in Figure 6.3.

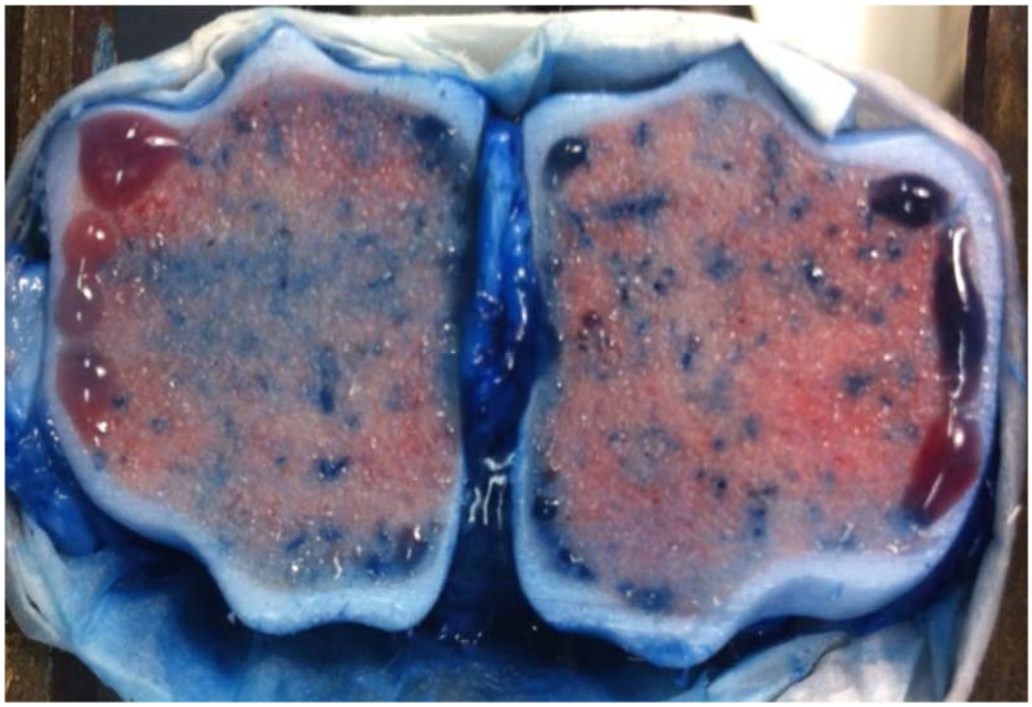


Figure 6.3 Calf metacarpal injected with dilute Evans Blue and squeezed in a vice. The subchondral plexus oozes Evans blue stained blood**.**

4 Photographs of the proximal tibia showed vessels resembling the vascular marks seen on the MRI slices of the same area of the tibia Figure 6.4.

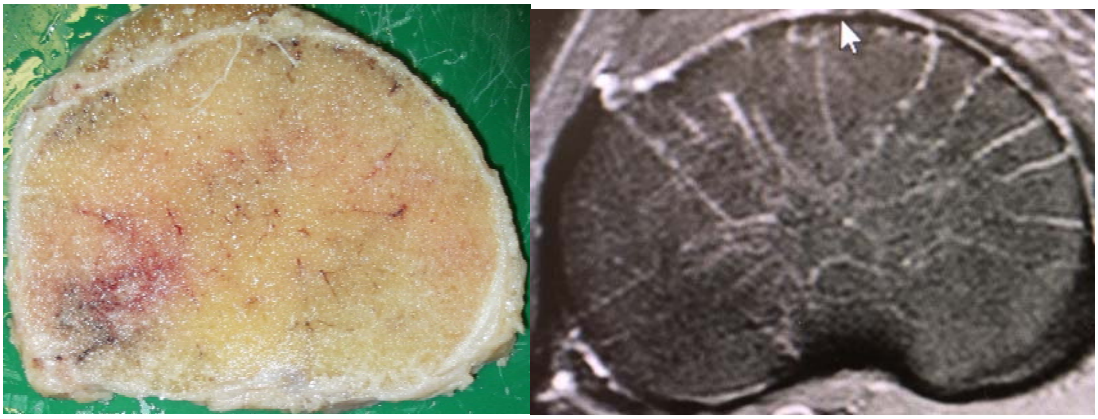


Figure 6.4 Slice of normal human upper tibia showing radiating vascular marks as in an equivalent PD_SPAIR MRI scan.

Photographs of the cut normal distal femoral condyles showed vascular marks equivalent to those in the PD_SPAIR axial distal femoral MRI scan as in Figure 6.5

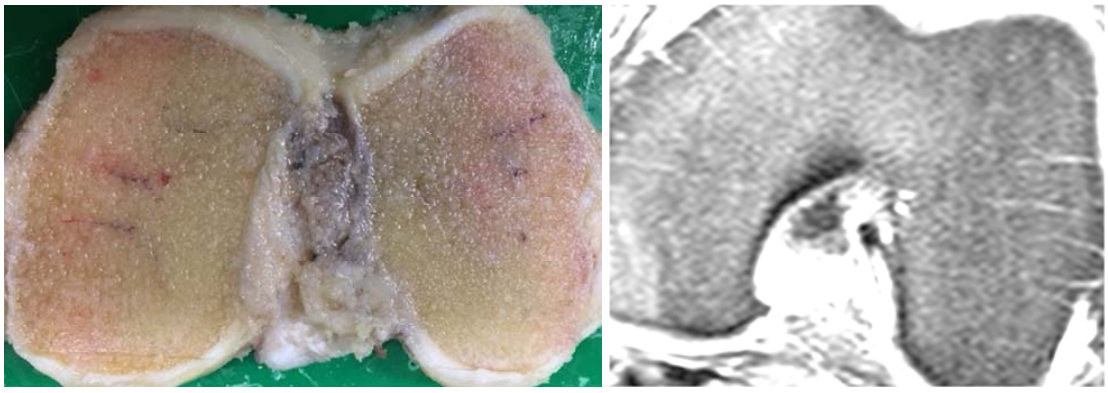


Figure 6.5 Slice of human normal distal femur showing transverse vascular marks as in an equivalent PD_SPAIR MRI scan.

5 Macroscopically after decalcification there were vessels visible to the naked eye lying in the subchondral plane in the upper tibia as shown in Figure 6.6



Figure 6.6 Photograph of decalcified subchondral section of human upper tibia prior to tissue processing and embedding. Cortical surface left edge in all images. Specimen size 1 x 3 cm.

6 Calf subchondral bone

Histological sections of healthy subchondral bone were obtained from the flat articular surface of calf metacarpal joint. Axial slices within a few millimetres of the surface showed radiating vessels as in the examples shown in Figure 6.7. The vascular marks consist of an artery and vein pair in most cases. All images are shown with the cortex to the left.

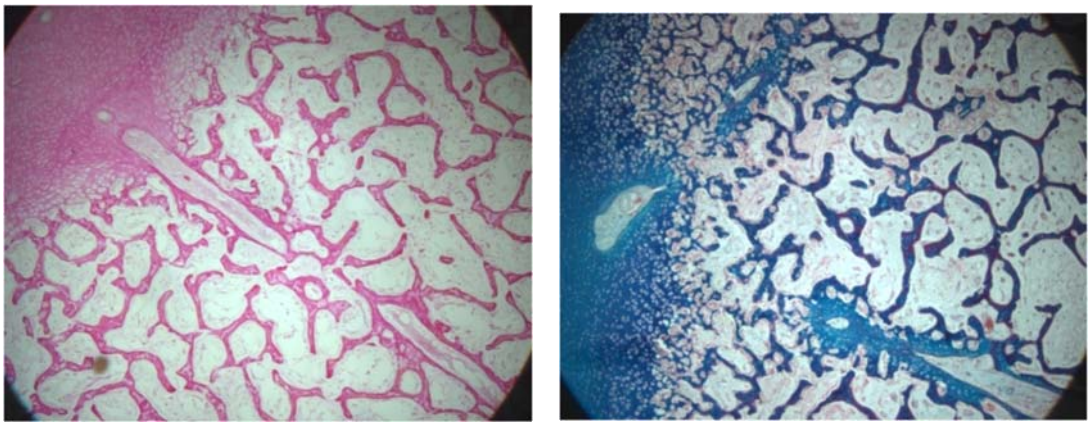


Figure 6.7 Left - calf axial subchondral proximal metacarpal bone. Stain Van Gieson trichrome, x 20 Right – calf axial subchondral proximal metacarpal bone. Goldner's, x 20. Subchondral vessels running towards the juxta articular cortex which is still cartilaginous in the calf at this age. Cortex to the left in all images.

Human subchondral bone

Similar patterns of subchondral axial plane radiating vessels were found in human upper tibial slices as in figure 6.8

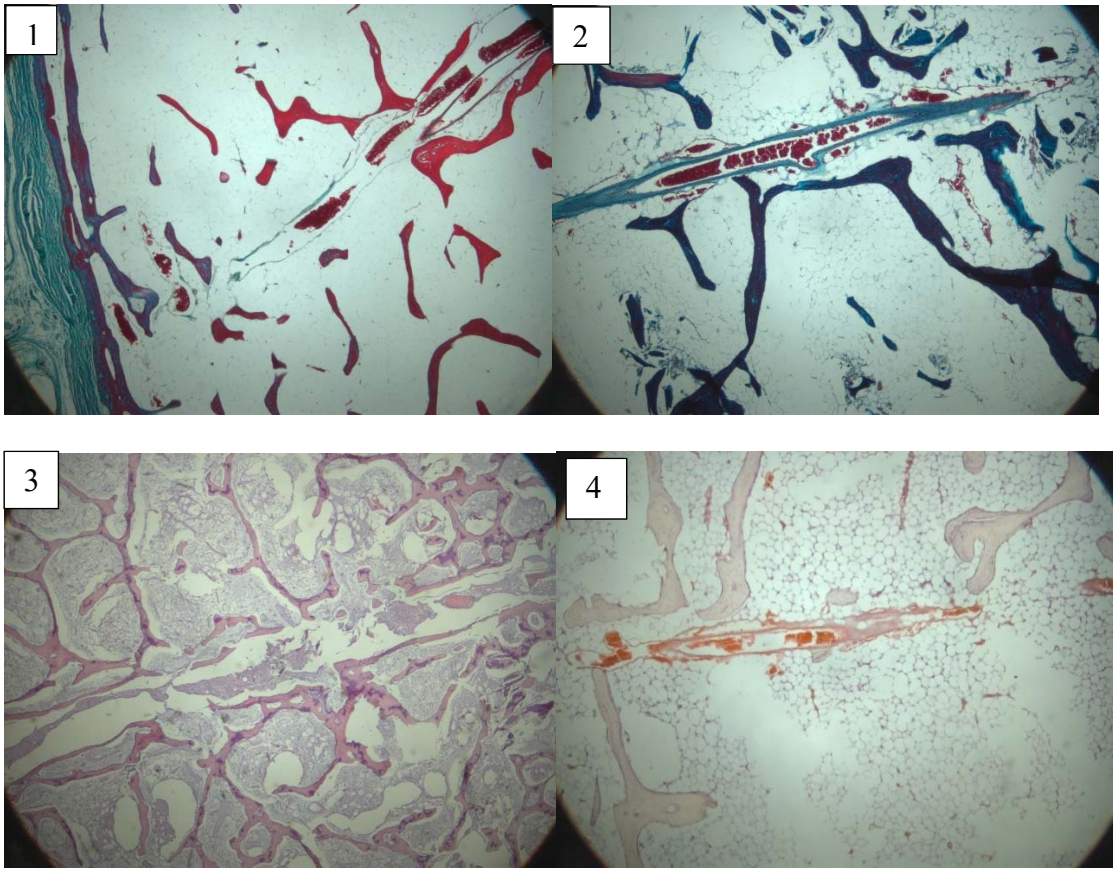


Figure 6.8 Low power human subchondral bone in the axial plane. Cortex to left in all images. Axial plane - vein and artery pairs are seen.
1 Human upper tibia Goldners trichrome x 20
2 Human upper tibia Masson's trichrome x 20
3 Human upper tibia H&E x 20.
4 Human upper tibia Van Gieson trichrome x 20

7 The vessels appear to be artery and vein pairs measuring 1-2 cm length as in the composite low power image in Figure 6.9. In all cases the vessel bundle angulates as it enters the cortex. After leaving the medulla the vessel bundles are seen angulating before traversing the cartilaginous cortex towards surface.

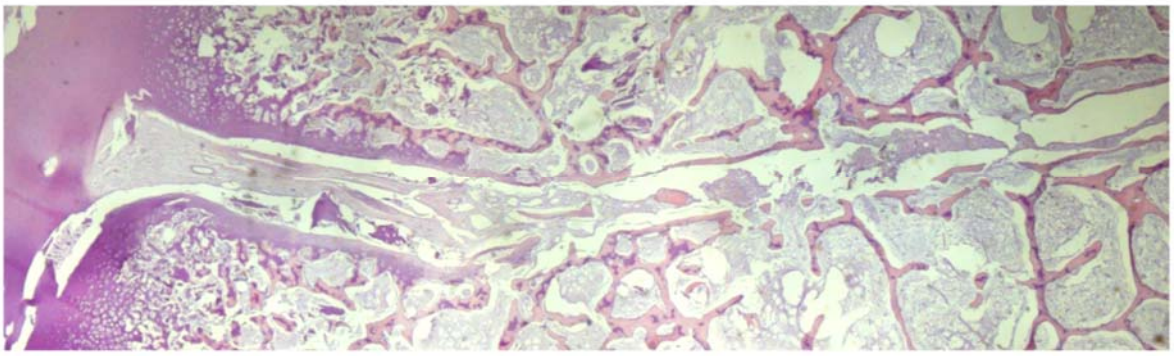


Figure 6.9 A composite image from three calf axial subchondral proximal metacarpal low power H&E images demonstrating the length of the vessel bundle of approximately 2 cm running in the subchondral plane. The vascular channels run straight towards the cortex but bend or kink at the margin.

As the vessels enter and traverse the cortical cartilage they usually bend through a right angle

as in figure 6.10

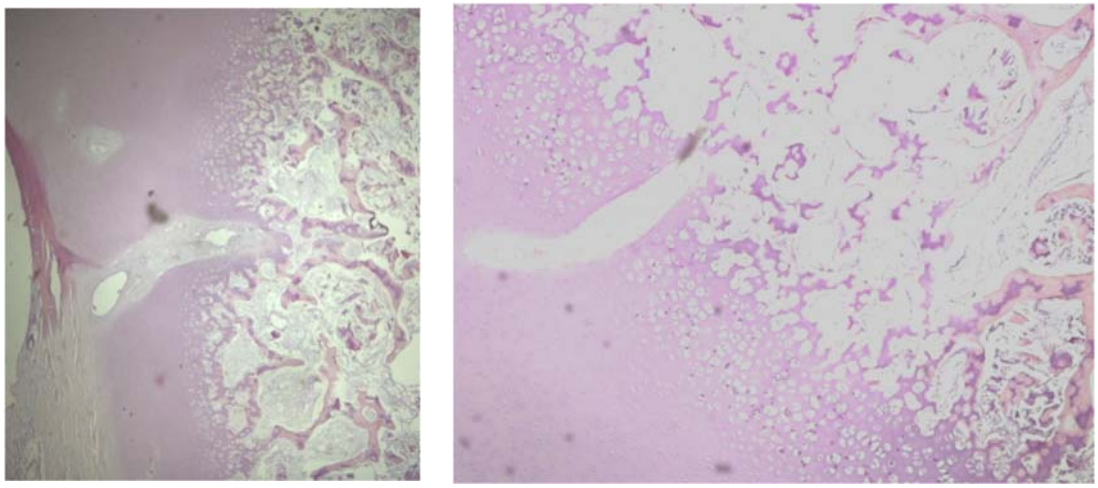


Figure 6.10 Both images show calf axial subchondral proximal metacarpal bone, H&E, x 20 showing vessels angulating as they exit the medulla and enter the cartilaginous cortex.

Vessels are seen frequently in the cortex or cartilaginous cortex at this age in the calf. They appear to bend or angulate as they enter the cartilaginous cortex and do not appear to run in the axial subchondral plane as they traverse as seen in Figure 6.11.

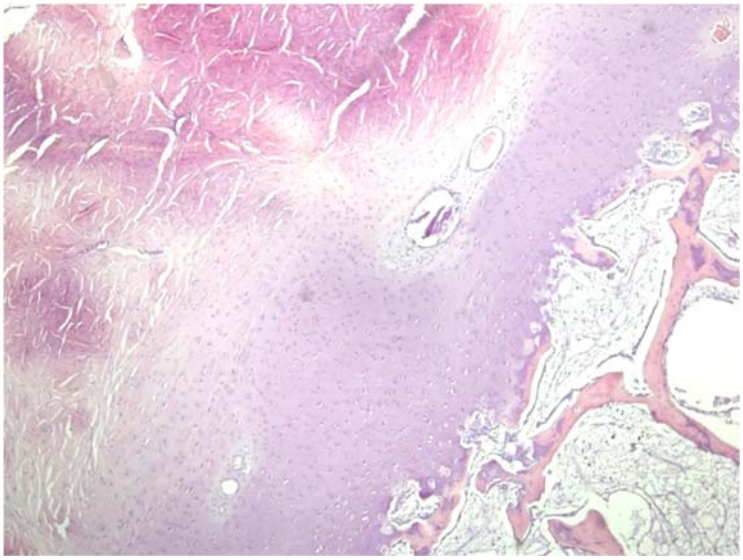


Figure 6.11 The image shows calf axial plane subchondral proximal metacarpal bone, H&E, x 20. Example of vascular channels traversing the cartilaginous cortex.

As the vessels approach the cortex they become angulated or distorted as seen in Figure 6.12

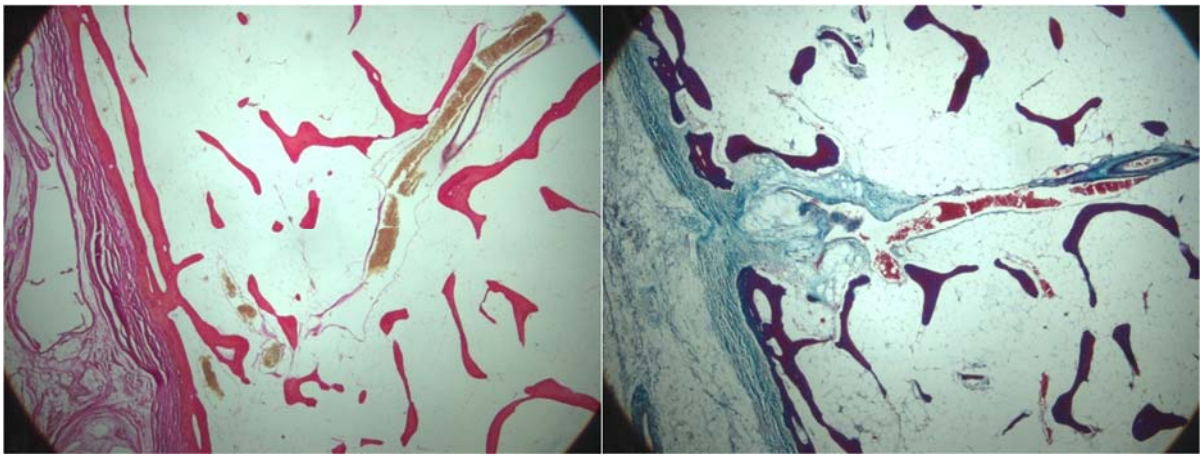


Figure 6.12 Both slides show normal human upper tibial axial subchondral longitudinal vessels running towards the cortex. As the vessels approach the cortex they become convoluted and distorted. Left - Van Gieson trichrome. Right - Goldner's, x 20.

In the sub cortical region as the axial vessel bundles prepare to exit the medulla and while still surrounded by cancellous bone and fatty tissue they develop convoluted or distorted paths as shown in Figure 6.12, 6.13 and 6.14. These structures may act as choke valves when compressed by the surrounding fatty tissue.

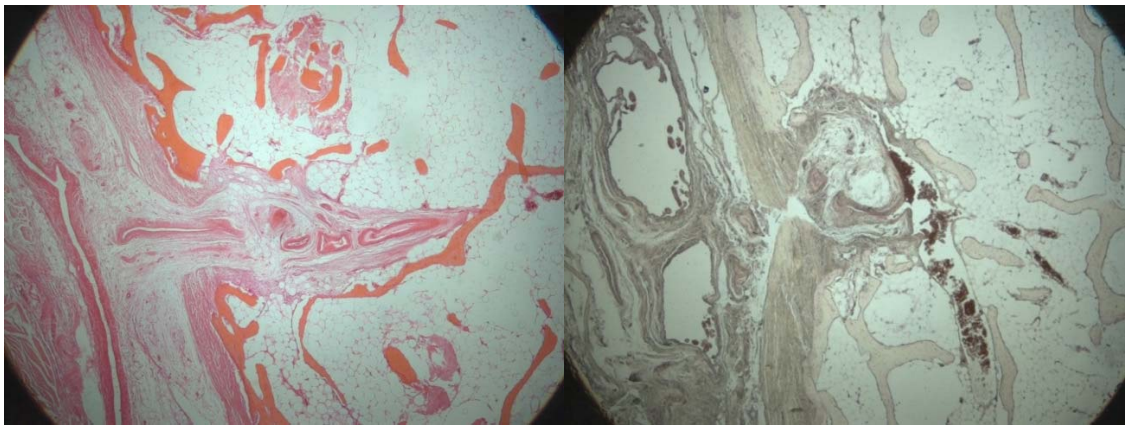


Figure 6.13 Both images show axial subchondral vessels reaching the cortex in normal human upper tibial slices. Complex angulation and distortion develops. Left - H&E, Right – Goldner's, x 20.

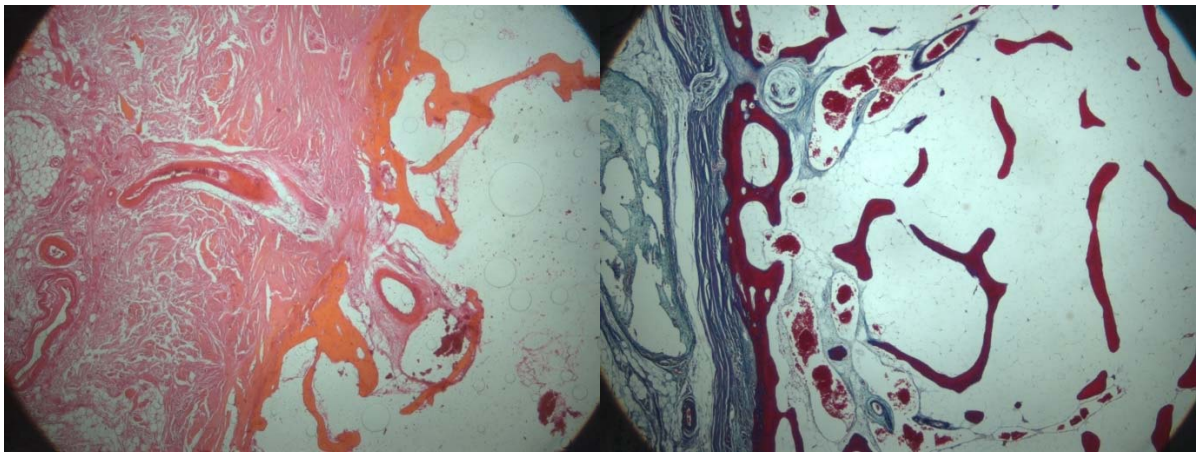


Figure 6.14 Both images show axial subchondral vessels reaching the cortex in normal human upper tibial slices. Complex angulation and distortion develops. Left - H&E, Right – Masson's trichrome, x 20.

The vascular convolutions or distortions in the vessels next to the cortex are seen at a higher power in Figure 6.15.

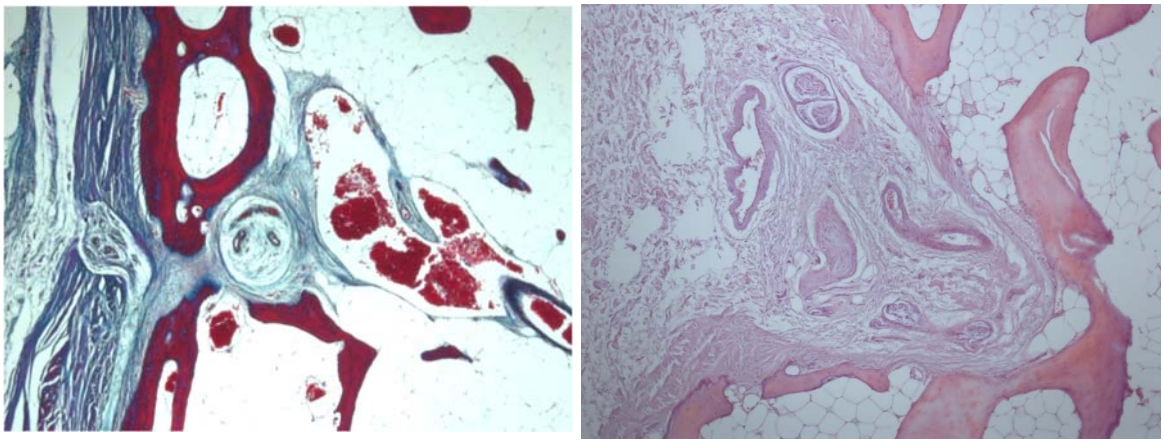


Figure 6.15 Higher power view of normal human upper tibia axial plane sections with vascular distortions at the cortex. Left Masson's trichrome, right H&E x 40.

8. **Subchondral capillaries**

In addition to the larger axial plane vessels described above underlying healthy articular cartilage there is a well-defined subchondral mesh of capillaries in the immediate subchondral region as shown in Figure 6.16. These fine capillaries are not seen underlying the cortex in early osteoarthritis.

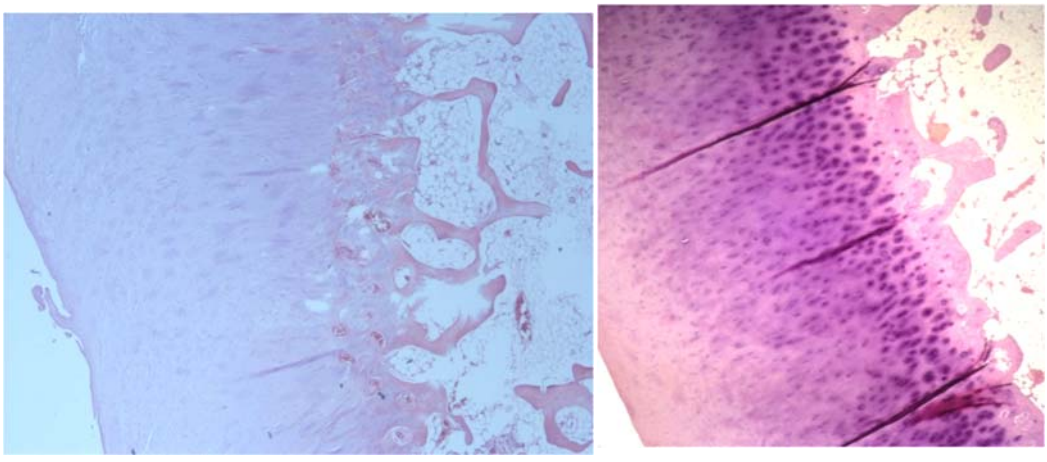


Figure 6.16 Two sections of healthy human articular surface cartilage in sagittal section showing fine capillaries in the subchondral region. H&E x 20.

The subchondral capillaries are absent in early osteoarthritis. In Figure 6.17 the example shown has very few subchondral vessels. The overlying cartilage is ischaemic and poorly nourished and the cartilage at the joint surface is beginning to fibrillate and break down. The arthritic human bone slices did not have the subchondral longitudinal vessels or the subchondral capillary plexus seen in healthy bone.

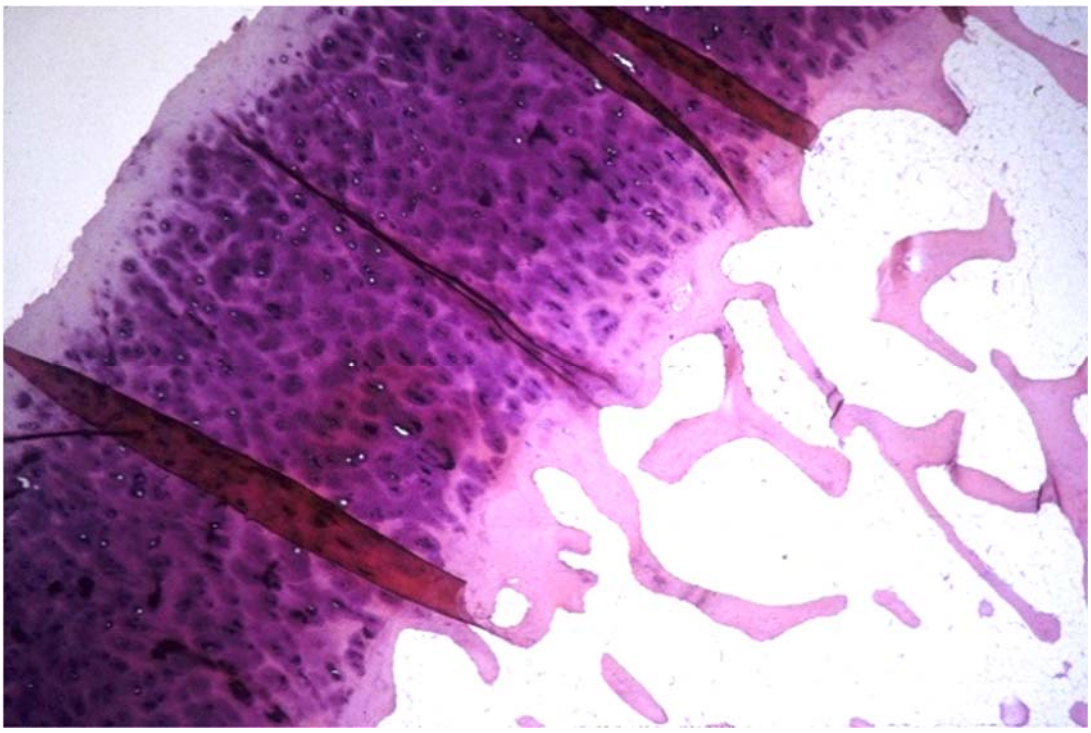


Figure 6.17 Section of human upper tibia with early osteoarthritis in sagittal section showing a lack of subchondral vascular features, unhealthy overlying cartilage and early surface fibrillation beginning. H&E x 20.

6.5. Discussion

Previous chapters showed that during activity IOP fluctuates. Chapter 5 suggests that there is probably a specialised subchondral circulation to deal with those pressures. Calf proximal metacarpal and the human proximal tibia are strikingly similar. Both have essentially flat weight bearing articular surfaces. This Chapter used calf and human

tissue to look for the presence of the subchondral vessels and also to look for features which might support the possibility that the subchondral circulation is designed to withstand high intraosseous pressures. Osteoarthritic bone was also examined for the presence of the vessels. None were found.

The vessels were easily seen macroscopically and histologically in the subchondral plane. No other structures of those dimensions were found in that plane and there appears to be no other explanation for these MRI marks other than that they are vascular. In most cases there appeared to be a pair of vessels, one vein and a smaller artery. Red cells were visible in the lumen of both. Slices of proximal tibia from arthritic patients undergoing knee replacement were also examined but contained no vessels.

Subchondral vessels

The calf proximal metacarpal articular surface and the human upper tibia are curiously similar in form and function. In this study subchondral vessels which run parallel and deep to the subchondral surface are confirmed. In both the calf proximal metacarpal and the human proximal tibia, veins and arteries exist and run in a radiating pattern much as described by Crock and Nelson in their barium and ink injection studies nearly 60 years ago. The pattern is very similar to the previously undescribed marks seen on PD_SPAIR MRI scans of the proximal tibia described in Chapter 5. The vessels may be of considerable length, up to 2 - 3 cm long, crossing up to half of the diameter of the articular surface. They generally consist of an artery and one or more adjacent thin walled veins or sinusoids. They run directly to and from the cortex. The histological appearances are qualitative rather than quantitative. All the stains used appear to show vessels. The images are at low power in order to demonstrate the length of the vessels. No other examples of histological sections taken transversely in the upper tibial

subchondral plane were available. No other long structures were found in that subchondral axial plane. All the bundles of radiating vessels appear to reach and penetrate the cortex. They angulate as they do so. The reasons are not known. It could be that with high intraosseous pressures during loading the vessels 'kink' and close off thereby preventing harmful high velocity flows both antegrade and retrograde within the small vessels.

Cortical anatomy

Where vessels traverse directly into juvenile cartilage they appear to have an angulation or constriction. This could act as a flap or valve like when the surrounding intraosseous pressure increase with loading.

Cortical valve

During the stance phase of gait a raised IOP is found in the subchondral upper tibia. The subchondral tissues are relatively delicate, particularly the fat cells or adipocytes and capillaries. Significant pressure rises in the subchondral area might result in forced ante grade or retrograde flow of blood along vessels. Semi liquid fat cells and other soft tissues could easily be damaged by those high pressures. But the soft or semi liquid nature of the fat and haemopoetic tissues might equally act as a medium for hydraulic pressure transmission. It appears possible that the complex distorted vascular structures at the cortical transition zone which are shown here could act as choke valves. This would allow forces on the cartilage and subchondral plate to be transferred by hydraulic force to the trabeculae and along those trabeculae ultimately to the cortical shaft. At the next joint the process would be reversed. Once the stance phase pressure wave has

passed or during the swing phase of gait or at rest, circulation at normal pressures resumes.

Joint anatomy therefore appears to be modified to cope with brief high pressures in at least four ways.

1. The soft hydrophilic cartilage and the thin endplate bone flex to cushion impact.
2. As hydrophilic cartilage is physically squeezed it exudes water from its articulating surface against the opposing articular surface and the joint is thus supplied with nearly perfect water on water lubrication. After load is removed the exuded fluid is taken up again by the hydrophilic cartilage.
3. Soft subchondral fatty adipocytes and haemopoetic tissues transmit force by hydraulic pressure to the trabeculae and on to the cortex.
4. At the cortex adjacent to the joint there are vascular convolutions which when subject to raised intraosseous pressure from the surrounding semi liquid fat, distort and closes off the artery and vein preventing violent flow from the subchondral high pressure area to the extra osseous low pressure region.

Burkhardt listed a number of features in normal bone for which he offered no explanation. They may have a part to play in pressure transfer. These are described more fully below in Chapter 7 (Burkhardt 2012).

Subchondral capillaries - Hunter's mesentery

In all healthy articular bone examined, in the sagittal sections there were fine capillaries present in the immediate subchondral layer. These resemble Hunter's mesentery, first described by William Hunter more than 250 years ago (Hunter 1743) but also demonstrated here in Figure 6.2, 6.3 and 6.16.

Veins

Drainage from the calf foot is mainly by a subcutaneous web of veins. There are several additional deeper veins which are valved and therefore difficult to catheterise. They appear to form a web or mesh rather than there being a specific longitudinal vessel path or mirror image of the arterial supply. In addition there is a subungual or hoof venous plexus. There are also venous plexuses which lie posteriorly between the phalangeal bones, capsules and ligaments and anterior to the tendons and soft tissues. Reliable venous catheterisation proved impossible. Both the hoof and posterior soft tissues are compressed during the natural stance phase and probably function much as the foot venous pump and calf muscle blood pump in man (Gardner 1989).

Osteoarthritis

Several sections from the osteoarthritic human specimens were examined. There were none of the longitudinal subchondral vessels and none of the valve-like distortions. The arthritic specimens had no evidence of the fine subchondral capillary network and all the arthritic bone examined was essentially avascular.

Bone blood flow during exercise

Bone receives only a small part (5 - 10%) of cardiac output or 5 - 20 ml/min/100 g of bone. Direct flow measurement during activity is difficult (McCarthy 2006). Tondevold used microspheres in exercising dogs and found that general bone blood flow in dogs doubled during exercise after an hour or more. He suspected a metabolic mechanism. He did not consider a mechanical effect. Although it might be possible to regulate flow within bone by vasoconstriction or vasodilation, each bone appears to be a closed space making internal volume change difficult to accommodate. As far as it is known there

are no lymphatics available to allow volume change (Edwards 2008). It seems possible at least that Tondevold was seeing the effects of augmented blood flow because of the osseous 'pump' or increased subchondral flow with activity proposed here (Tondevold 1983). Any future assessment of bone blood flow during exercise should probably be looking at a subchondral level rather than the 'whole bone level'.

Limitations

This preliminary work is qualitative. Possible objections to the findings might include the lack of a larger numbers of specimens, the definition of the structures identified and the interpretation of their function. If there is some form of vascular modification present to cope with fluctuating high IOP it would be present in all weight bearing subchondral bone, juvenile and adult. The vessels were found in both. The bones chosen in this study are from essentially flat articular surfaces making it easier to follow subchondral vessels over a reasonable distance. Both the upper tibia and the calf metacarpal had been used in the earlier work. In terms of identification, routine stains at low power gave acceptable results. Access to specific vascular endothelium stains was not available.

There was insufficient material and resources to carry out formal histological counting. The interpretation of the function of the structures identified remains open but given the previous findings of a raised and fluctuating IOP during activity, the MRI observation of possible vessel patterns and their loss in early osteoarthritis and the obligation to account in some way for the pressures likely to be found in active subchondral bone, it seems that this interpretation may hold.

It may be that future work accepts that there is probably a vasculo-mechanical interpretation of joint physiology and explores the possibility that osteoarthritis is a

disease caused by a failure of the vasculo-mechanical environment (Beverly 2012) (Beverly 2015).

6.6. Conclusion

There are radiating axial plane vessels in the subchondral region. They have modifications at the cortical margin which may act as valves preventing venous blood from being forced out of the bone under load and increased IOP thus protecting delicate subchondral tissues from high pressure damage. There are fine immediately subchondral capillaries which may supply cartilage with nutrition. The absence of the axial vessels and subchondral capillaries in osteoarthritis suggests that OA may be a vasculo-mechanical disease.

7. SUPPORTING EVIDENCE

For any novel hypothesis such as that advanced here to be justified and defended, it would seem reasonable to offer other supporting observations, even if they were not the result of work directly covered in the experiments described. Several areas of interest which may support the central thesis are therefore presented.

1 Man walking

There have been very few attempts to measure IOP in man during activity though the means to do so has been available for some time (McDermott 1986, Pooley 1987). A limited number of IOP recordings were obtained in volunteers in a private hospital in Germany in 1986 under the guidance of the surgeon in charge, Dr Joseph Pflug, a colleague at the RPMS Hammersmith Hospital and vascular surgeon from Goppingen, Germany. At his request IOP was measured in the leg veins and sub fascial space and upper tibia in conscious walking volunteers. Qualitative results showed a fluctuating IOP in response to walking at various speeds as shown in Figures 7.1 and 7.2. The results were published as an appendix in 'The Return of Blood to the Heart, 1989 (Gardner 1989). It was evident that with walking, fluctuating IOP in the upper tibial subchondral region was present and that the pressure fluctuation was over a greater pressure range than any possible circulation pressures. Figure 7.2 also demonstrates the 'drop' phenomenon described in Chapter 4 with repeated loading whereby the IOP falls during exercise.



Figure 7.1 Volunteer walking during measurement of pressure in dorsal foot vein, subcutaneous calf tissue and upper tibial intraosseous pressure.

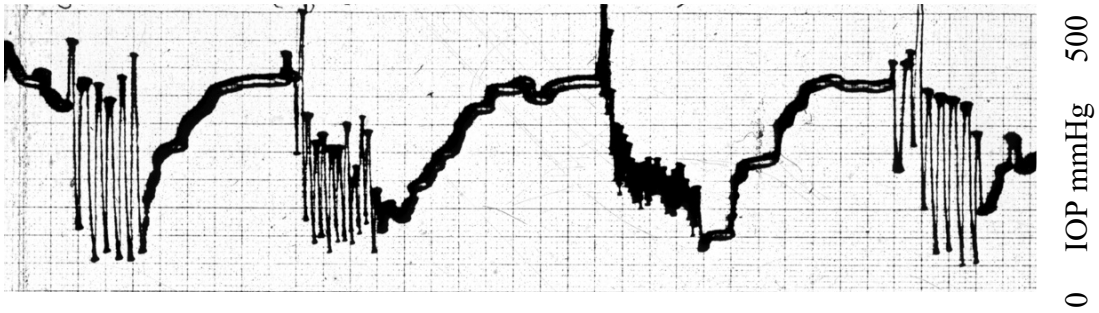


Figure 7.2 IOP trace showing upper tibial IOP recording from subject taking 10 slow steps, 20 fast steps, running on the spot and 10 slow steps, each with 20 second rest interval between exercises. Vertical scale 0 - 500 mmHg. Large square 0.5 cm or 3 secs.

2 Dry bone

Although vascular channels which penetrate the cartilage are described, the substantial apertures adjacent to the articular cartilage of most long bones do not seem to have attracted much attention (Clark 1990).

Macroscopic inspection of any dried long bone shows that while there are a few well defined oblique mid shaft apertures for the nutrient arteries, there are many mainly perichondral or juxta articular exiting straight apertures which are probably venous as seen in Figure 7.3. Recently these vessels appear to have been re-discovered (Grüneboom 2019). The flow in an actively exercising long bone might be mainly inwards at the diaphyseal oblique nutrient artery and outwards at the metaphyseal juxta articular exit veins shown in Figure 7.3. This was not formally tested in this work but Tondevold found increased cancellous blood flow with microspheres in exercising dogs (Tondevold 1983).

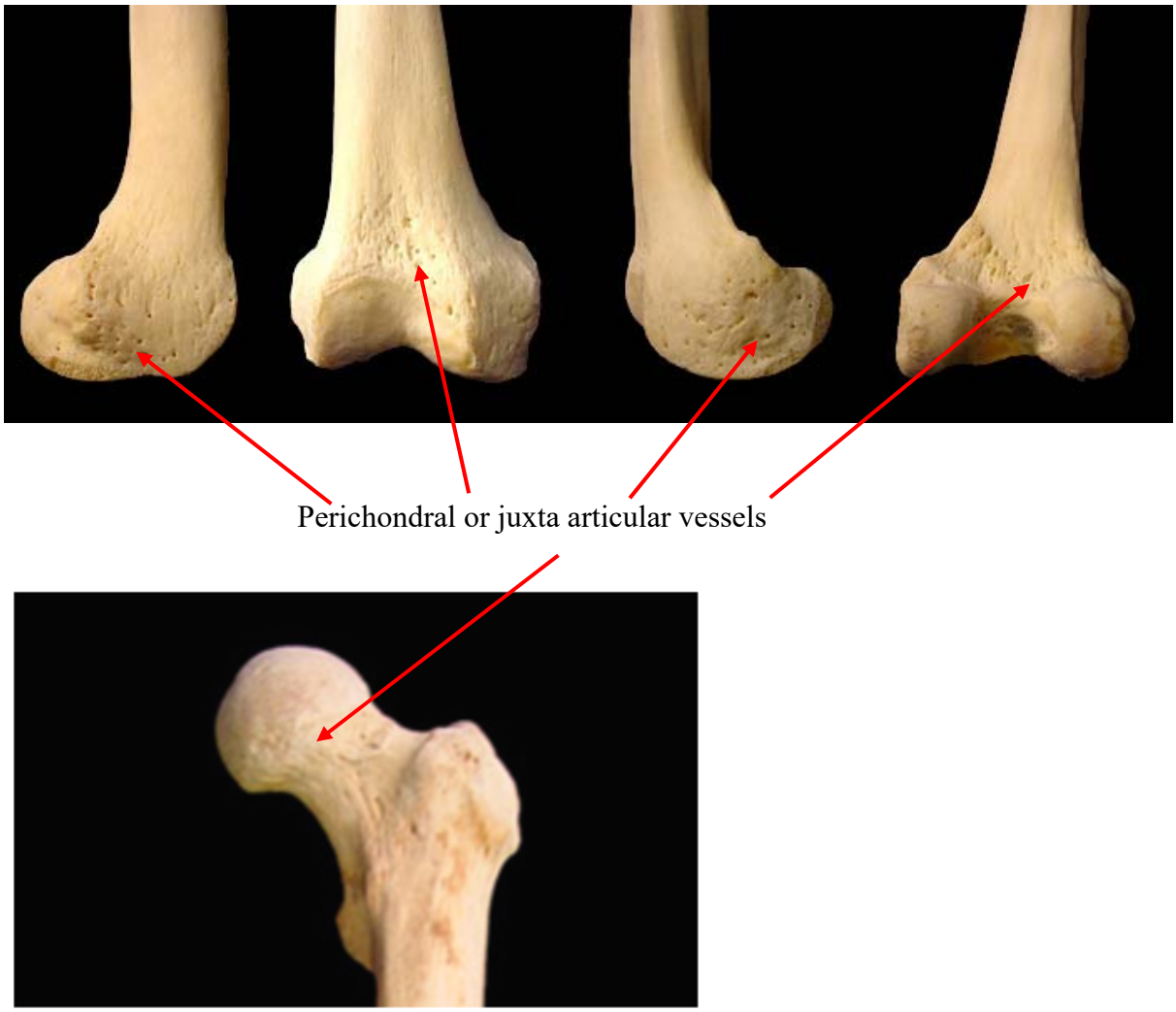


Figure 7.3 Images of femora from the internet (anatomycorner.com) showing the articular margin holes which may be venous exit channels.

3 Liquid fat

Orthopaedic surgeons are well aware that during surgery when a bone is fractured, cut or drilled, fat pours out in liquid form. High speed drills or saws cause a spray of fat from bone but not from other tissues. Bone fat at body temperature is similar to olive oil in texture (personal observation) rather than being solid, soft and greasy as are other

adipose tissues. Fractures seen on horizontal x-rays often have a blood / fat interface layer with the fat floating on the blood, for example, around elbow fractures. Bone fat is the only fat in the body which appears liquid at body temperatures. This requires an explanation. Although the metabolism and hormonal aspects of bone marrow fat have been studied, there appear to be few if any references to the fat in bone marrow being effectively liquid at body temperature (Scheller 2019). Liquid bone fat within the adipocytes could act as a hydraulic fluid or pressure transfer medium even if there is no actual flow in vivo.

4 Adipocytes

Although bone marrow adipocyte response to vibration has been studied there appear to be no references dealing with the reaction of fat adipocytes to loading (Tirkkonen 2011). Bone fat lies in thin walled adipocytes. One might have expected bony tissues to be of more robust composition. Surprisingly these delicate cells are not destroyed by the forces of weight bearing and fluctuating IOP. Together the thin walled fat cells and other haemopoetic tissues are effectively oily or liquid in vivo. While they do not actually flow they may nevertheless act as a hydraulic pressure transfer medium.

5 Fat embolism

Under certain conditions fat from bone embolises throughout the vascular system (fat embolism). No other body fat has ever been implicated in this phenomenon (Blokhuis 2017). Steroids have been tried in order to ameliorate the effects of embolism (Silva 2013). Surgeons impacting cement and femoral components into patients during hip replacement or intramedullary nailing are often asked to warn the anaesthetist in advance in order to deal with the expected shower of fat emboli. It would seem that

bone fat, though usually constrained within the skeleton, is physically released by trauma and is then able to travel throughout the body in the vascular system. It impacts in lung, neurological and dermatological tissues and is recognised as fat embolism (Newbigin 2016). Apart from blood and blood borne products and occasionally air, no other tissue or fat has the property of embolisation.

6 Starvation

Bone fat is virtually liquid. The carbon chains are shorter and have more double bonds than other body fat. Such lipids would be normally be more easily metabolised than heavier, longer chain and more saturated body fats. But in starvation bone fat is preserved or even proportionately increased while body fat and muscle are metabolised (Bathija 1979, Devlin 2011). There may be a mechanism whereby the body recognises the vital role played by fat in bone for locomotion and therefore preserves bone fat in the face of starvation.

7 Caisson disease

The Decompression Sickness Central Registry in Newcastle (McCallum 1984) described osteonecrotic lesions in bone in workers who had suffered decompression accidents while working in compressed air, such as in the Mersey and Dartford tunnels and in deep water, such as in the North Sea oil industry. Those who had been decompressed in air suffered twelve times as much femoral head necrosis as those decompressed in a weightless environment. It is likely that microbubbles arise in circulating blood during decompression. They are more likely to impact in bone which is being subjected to cycles of compression and decompression in the walking or weight bearing air pressure tunnellers than in the effectively ‘weightless’ divers. The

weightless divers suffer a more generalised pattern of caisson disease. (McCallum 1968, McCallum 1984, Beverly 1987). Elsewhere in the skeleton the patterns of osteonecrosis are similar. Microbubbles within blood have other interesting properties. They impact in both hard tissues (bone osteonecrosis and nerve paralysis) and soft tissues (lung and brain) giving the classical picture of the bends with pain, paralysis, ‘chokes’ and strokes respectively. The gas involved is said to be nitrogen but simple desk top experiments indicate that it is probably carbon dioxide. Carbon dioxide is a far more volatile gas. It is usually the gas used in fizzy, drinks partly for that reason. Carbon dioxide is present in the circulation and easily dissociates when blood is decompressed (Beverly, Pflug et al. 1987).

8 Diving mammals

Seals, walruses, whales and other mammals are capable of diving to great depths, sometimes in excess of 2,000 metres. Pressures there are more than 200 atmospheres. Because the whole animal is evenly pressurised there are no ill effects. Their blood gases are only exchanged at atmospheric pressure. Similarly the subchondral region in man can tolerate brief exposure to great pressures (perhaps up to 20,000 mmHg or 20 atmospheres) provided that the gas saturation environment remains intact. There is no significant fluid flow and no cavitation or microbubble formation. The subchondral area may well be under great pressure but ‘shuts down’ or closes off briefly during hydraulic load transfer (Fukubayashi 1980). The valve like folds or contortions in the cortical region vessels described in Chapter 6 may be closed off on loading to protect the cellular environment from fluid shifts while distributing hydraulic force to the cortical shaft.

9 Osteoarthritis and osteoporosis.

Orthopaedic surgeons have removed femoral heads for decades. They fall into two groups which are nearly mutually exclusive (Bultink 2013, Geusens 2016). Those with osteoporotic femoral neck fractures usually have pristine articular surfaces and rarely any sign of osteoarthritis. The osteoarthritic hips rarely fracture and are removed with more difficulty as they have hard or sclerotic bone with osteophytes, capsular thickening and an arthritic head. It may be that in those with osteoporosis the thinner trabeculae in the subchondral region remain slightly more flexible to ordinary body weight. They therefore flex more and 'pump' or circulate more blood through the subchondral vessels thereby enhancing cartilage nutrition. The osteoarthritic subject might possibly have a reduced blood supply secondary to any of the well-recognised associated conditions. Smoking, vascular disease, obesity, metabolic and embolic disease, inactivity or even excessive activity or sports with heavy but restricted range usage all lead to reduced subchondral circulation and reduced cartilage nutrition. It is recognised that any tissue with a restricted blood supply will respond by becoming harder, sclerotic, fibrotic or even ossified. In the subchondral bone this in turn leads to more sclerosis and a further reduction in blood supply.

Although fibrillation and superficial wear are seen first on the surface of a joint in early osteoarthritis, that wear appears not as a result of synovial fluid or surface irritation but is secondary to the loss of vasculo mechanical flexibility in the subchondral region which leads in turn to poor cartilage nutrition. Degeneration is seen first on the articular surface because it is furthest from the subchondral vessels and capillary network source of nutrition. This offers a simple explanation for the widely recognised and nearly mutually exclusive patterns of osteoporotic and osteoarthritic femoral heads seen in orthopaedics.

10 Patterns of osteoarthritis

A vasculo mechanical approach would help to explain the different patterns of osteoarthritis seen in clinical practice (Brandt 2008) (Favre 2017). If there is a slow reduction in blood supply to the joint generally, then a general sclerosis takes place in the subchondral region leading to a slow onset of a generalised and sclerotic pattern of disease. The bone become less flexible and the subchondral 'pump' fails, leading to progression in OA over some years. If at any point there is a more acute loss of blood supply in a smaller vessel, the area supplied by that small vessel dies or infarcts and is later recognised on x-ray as a bone cyst. If a larger area loses blood supply more rapidly, the pattern is more one of generalised osteonecrosis. Combinations may occur. At the periphery the periosteal blood supply is not affected. Marginal bone attempts to support the adjacent sclerotic area by hypertrophy, recognised on x-ray as an osteophyte (Wong 2016) (Mathiessen 2017). This vasculo mechanical theory would help to explain the four cardinal signs of osteoarthritis seen on x-ray, namely sclerosis, cysts, loss of joint space and osteophytes.

More recently Tse has used a dual CT technique to explore subchondral perfusion and others are coming to recognise the link between subchondral bone and osteoarthritis (Funck-Brentano 2015).

11 Bone pain

Bone is recognised to have a rich periosteal nerve supply but only a relatively poor intraosseous nerve supply (Mach 2002). That supply seems to have no recognised efferent function. Bone has no known lymphatics (Edwards 2008). There seems to be no reason for an efferent nerve supply to bone as the vessels are unlikely to be able to

expand or contract significantly in a closed environment. The afferent function appears to be sensitive, mainly to pressure. They appear to transmit an aching or bursting sensation. Pressure lesions within bone may cause severe pain such as in osteomyelitis. The aching pain described in osteoarthritis is a unique pain in so far as it is aggravated by prolonged immobility and relieved by activity while at the same time it is aggravated by activity and relieved by rest. A vasculo mechanical 'disequilibrium' may explain this pattern of discomforts (Dieppe 2005). It may be that as the patient develops circulatory problems the subchondral vasculo mechanical equilibrium is disturbed and functions less efficiently. As soon as the delicate balance is disturbed for example by swelling from infection or micro fractures or oedema or vascular insults the joint cannot function effectively. Great pain may then arise and can often be relieved by reducing the intraosseous pressure with osteotomy or simply drilling the affected area. This is recognised to be particularly effective in osteonecrosis which responds well to 'forage' (page 12/13) and other pressure relieving methods (Samy 2016).

12 Weather pain

It is widely recognised by patients and their doctors that bones and joints ache in certain weather conditions. This has been the subject of several studies (Ferreira 2016) but the results have been variable (Wilder 2003). None of the studies appear to have looked specifically at large populations as the barometric pressure fell. If atmospheric pressure changes from perhaps 1025 millibars to 975 millibars as the weather passes from a high to low pressure system it is perhaps not surprising that bone, a relatively enclosed space with a precarious circulation in the older patient might be sensitive to these weather mediated pressure changes of around 5%. Reduced circulation may result in either a

direct pressure mediated pain where a ‘proportional’ or relative rise in IOP as external pressure falls, or a secondary ischaemic change. The former seems more likely. It is generally agreed that the pain is induced by a falling barometric pressure or with the onset of bad weather rather than during a persistent low and that the approach of good weather or a rising barometric pressure relieves the pain long before a high has actually arrived or the weather itself has significantly changed (Steffens 2014).

13 Burkhardt

Burkhardt described other microscopic features including ‘choke cells’ or cuffs on smaller capillaries and 90 ° capillary junctions within cancellous bone. He offered no explanation for those observations. Potentially they might act as a reverse flow or back pressure limiting device. If a hydraulic load is suddenly applied to the capillaries in the subchondral area it would be useful if acute high pressure did not cause damaging back or forward flow in the capillaries. Such a cuff or choke or 90 ° step down in the capillaries may assist. Burkhardt also described thick muscle cuffs at the periosteal level on the exit vein sinuses (Burkhardt 2012). These might act as pressure retaining devices which close and maintain subchondral pressure rises with acute loading and yet allow ordinary circulation to continue at other times. Chapter 6 above describes other features which might support hydraulic pressure transfer in load bearing.

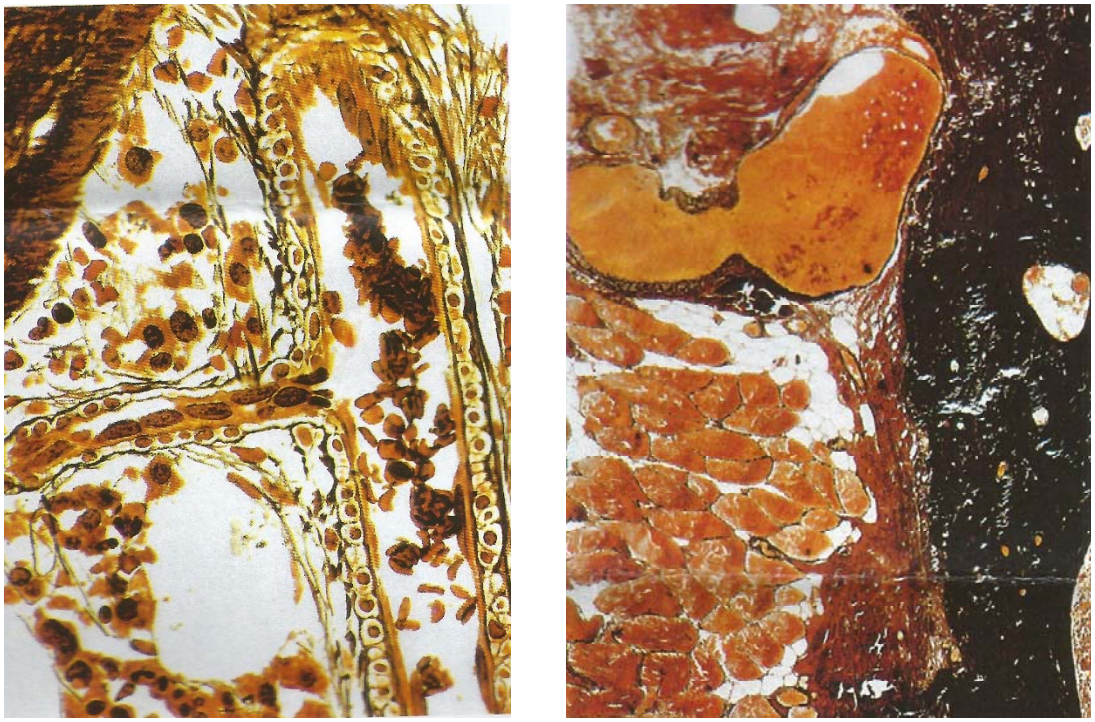


Figure 7.4 Left – 90 ° capillary/arteriole junction with thickened cuff of cells at junction. Gomori x 560. Right – cortical bone surface showing vein with circular muscle constriction. Gomori x 150. Taken from Burkhardt 1975.

14 Subchondral capillaries

While injection studies show a branching vascular tree in mature bone, sagittal histological sections of healthy joints show quite a different pattern of vessels as in Figures 6.16 and 6.17. The rich subchondral capillary network or Hunter's mesentery, probably requires dynamic or repeated compression rather than simple arterial supply pressure to fill. The slowly moving blood in subchondral capillary loops has been proposed as the reason that circulating bacteria or metastatic cells tend to deposit in the subchondral area. In any event the vascular tree has generally been defined by 'vessel chasing' techniques or by injection of the arterial supply. Retrograde injection of the venous side is much more difficult and may be nearly impossible. If there is a secondary or alternative type of circulation between the arterial and venous systems dependent to a degree on physical activity, that part of the circulation will be invisible to mere

antegrade or retrograde injection studies. It might be more obvious with loading or compression as in Figure 6.2 and 6.3.

The subchondral capillaries shown in Figures 6.16 are intimately connected to the chondral base plate. They are different to and some distance away from the subchondral vessels described in Chapters 5 and 6 which in the knee are a centimetre or more from the joint surface (Imhof 1997, Brookes 2012).

15 Joint mechanics

In healthy bone the thicker the cartilage the more obvious is the subchondral plexus (personal observation) as in Figure 6.16. In normal joints the subchondral capillaries probably supply fluid and nutrients to the overlying cartilage. Fluid is squeezed from the hydrophilic cartilage surface under load to provide perfect fluid on fluid joint surface lubrication (Jahn 2016). The greater the load the more fluid is squeezed out much as for a skate on ice. Although tritiated hydrogen and other substances in synovial fluid penetrate cartilage and although loose pieces of bone and cartilage remain viable within the joint, the conclusion that cartilage normally receives its nutrition from synovial fluid may be questioned. Much research effort has been directed at looking for factors in synovial fluid which cause arthritis. In disease there are of course breakdown products in synovial fluid from cartilage but cause and effect may be confused. It is more likely that in a healthy joint cartilage receives nutrition from the subchondral bone. Physical activity stimulates an increase in flow through enhanced circulation in the subchondral bone. Where there is vascular disease or if the joint is otherwise diseased, fractured, under or overused the subchondral plexus of vessels is less effective. The cartilage no longer receives adequate nutrition. The joint surface is furthest from the subchondral source of nutrition and is subject to the most wear. Superficial fibrillation appears first

on the cartilage surface and is held to be the earliest sign of arthritis. Research has frequently been directed at synovial fluid products and the cartilage surface rather than at the subchondral vascular layer, possibly the source of the problem in most osteoarthritis.

16 Joint size

If there is a common means of transferring force across joints there might be a commonality in the proportions or metrics of the joints involved. Cells of various types have evolved to be of much the same order of magnitude whatever the size of the animal. For example, mouse red blood cells are much the same size as those in an elephant because they have a common purpose. The size of joints differs widely with the size of the animal but the proportional sizes are similar possibly allowing for a similar basic common hydraulic force transfer mechanisms to operate in all synovial joints (Alexander 1980, Biewener 1983).

17 Epidemiology

Activity seems to be important for healthy joints. Joint immobilisation is known to promote arthritis (Nomura 2017). Different occupations and ethnic groups exhibit different patterns of arthritis possibly dependent on different work, prayer or sitting habits (Chokkhanchitchai 2010). All these factors may have a bearing on the development of osteoarthritis if the cartilage requires regular compression through a full range of movement to maintain health. Western man rarely squats fully and may develop OA in the hips and knees partly from disuse. Other cultures which do not own chairs or who habitually sit or squat for toilet or prayer have different patterns and usually less hip and knee osteoarthritis (Jordan 1996). While it is possible that osteoarthritis is

associated with genetic predisposition, vascular disease, smoking and weight gain (Nevitt 1995, Conaghan 2005), it is also possible that osteoarthritis is partly a vasculo-mechanical disease, mediated at the subchondral level. The final common pathway for all the predisposing diseases may lie at the subchondral vascular level and be partly dependent on physical activity 'working' a subchondral 'pumped'circulation.

18 Other Pathology

In osteonecrosis, acute obstruction of larger proximal vessels produces wider avascular necrosis or may involve the whole metaphysis if it is effectively an end organ such as the femoral head. Cellular swelling and venous obstruction may also play a part. In addition embolic diseases such as sickle cell disease and caisson disease and clumps of platelets after bypass surgery produce patterns of arthritis of a more acute onset and cystic or osteonecrotic type (Mallet 2018).

Perthes disease, osteochondritis dissecans, avascular necrosis and infarction due to embolic phenomena often have a similar end stage histological pattern. For whatever reason the loss of blood supply to the subchondral plexus results in infarction and a splitting osteochondral fracture. There may be a final common vascular failure pathway in those conditions. Histopathologists evidently have some difficulty in separating the conditions without other clinical information.

19 Treatment – forage / osteotomy

Forage is very successful in relieving bone pain (Sultan 2019). It probably works by decompressing the ischaemic area. In those on steroids or immunosuppressants the effect is long lasting while in otherwise well patients with osteoarthritis the pain relief is of shorter duration, typically several months rather than several years.

The reason may lie in the arthritic bone ‘healing’ once the blood supply is enabled whereas in the poorly healing bone of the other patients the effect continues.

20 Compartment syndromes

The logical exploration of perfusion within a closed space as set out in Chapter 2 is probably of use in other organs and soft tissues with compromised circulation. Examples might include situations such as compartment syndromes, typically though not exclusively seen with closed tibial fractures. The differential pressure technique may possibly be further developed for research on bone itself. The simple use of IOP combined with differential tourniquet pressure may allow exploration of bone perfusion at the needle tip level. It may be possible to manipulate the intraosseous environment by drugs or other means to relieve or treat osteoarthritis and osteonecrosis as described in Chapter 8.

Conclusion

In summary these several observations may support the ‘vasculo-mechanical’ model of subchondral bone perfusion. That model offers a new understanding of osteoarthritis and other bone pathology and in due course may offer other means of treatment.

8. CONCLUSION

8.1. The Problem

Bone circulation has been studied for a century but there was no clear understanding of the links between bone circulation and bone disease. Previous IOP studies had offered a glimpse into a possible understanding of bone circulation but the findings were confusing and little progress was made. Though joints were recognised to tolerate huge forces there was no clear understanding of how that was achieved. Hydraulic force transfer had been discounted. Vascular anatomical studies had focused on injection methods under static or post mortem conditions rather than in vivo. There was no indication that intraosseous pressure and circulation in vivo might be modified or specialised under joint surfaces. As a result bone diseases such as osteoarthritis and osteonecrosis were not generally thought to have a vascular basis. There was no appreciation of a specialised subchondral physiology.

8.2. The Hypothesis

There is a specialised vasculo-mechanical subchondral environment which allows load to be transferred partly by hydraulic force. Subchondral anatomy is modified to cope with high pressures. Vessels are lost in early osteoarthritis. Osteoarthritis may be a partly vasculo-mechanical disease.

8.3. The Objectives

- CHAPTER 1 introduced the project.
- CHAPTER 2 explored and re-analysed previous in vivo IOP studies.

- CHAPTER 3 developed an in vitro model to test IOP perfusion regimes.
- CHAPTER 4 used the model to test IOP with different loading regimes.
- CHAPTER 5 analysed subchondral vascular marks on MRI scans of knees and compared them with Kellgren-Lawrence grading of osteoarthritis.
- CHAPTER 6 explored subchondral upper tibial vascular histology.
- CHAPTER 7 lists other evidence which may support the thesis.
- CHAPTER 8 summarises the work and points to future research.

8.4. The Findings

CHAPTER 1

Introduced the project from a historical perspective in terms of bone circulation, IOP measurement and the clinical background for this thesis.

CHAPTER 2

Demonstrated that:

1 There is a wide range of IOP values in healthy bone rather than a single value.

2 IOP is significantly affected by the method of measurement and needle clearance.

3 IOP is not much affected by weight, gender, site or size of needle used.

4 Saline injection damages the micro circulation at the needle tip. Clearance by aspiration is preferable.

5 IOP records have cardiac, respiratory and circulation time waves.

6 IOP fluctuates with systemic circulation pressure changes.

7 IOP is proportional to BP confirming a that it is a measure of arterial supply rather than a venous or other back pressure.

8 Pulse pressure is proportional to IOP confirming that there is a physiological link which can be manipulated as below.

9. IOP measurement itself can be suficient to monitor anaesthesia.

10 Proximal arterial occlusion reduces IOP and obliterates the pulse pressure.

11 Proximal venous occlusion increases IOP with preservation of the pulse pressure.

12 A better means of assessing needle tip perfusion might be by subtraction IOPv-IOPa.

13. This subtraction technique could be used clinically for example to measure bone health at the needle tip and in compartment syndromes.

14 Physical loading increases IOP

15 Loading during arterial occlusion gives a smaller rise in IOP.

16 Loading during proximal venous occlusion gives an augmented rise in IOP.

17 Load is transferred partly by hydraulic pressure from the subchondral region to the trabeculae.

18 Each bone behaves as a relatively enclosed space.

19 Joints act as hydraulic barriers.

20 Steroids in this model increase IOP, PP and the occlusion and loading values.

21 Steroids have little effect on needle tip perfusion range by the subtraction method.

22 Steroids in this model raise IOP by reducing fat cell volume thereby improving perfusion.

23 Two fluid systems exist, one for low pressure circulation and one for high pressure hydraulic force transfer.

24 There must be anatomical and histological modifications to cope with both.

The majority of these findings appear to be novel observations.

Chapter 2 therefore indicates limits as to the usefulness of IOP as a measure of bone perfusion in itself. IOP measurements assess only the pressure in the blood pool at the needle tip from the largest arteriole. Nevertheless, a fresh interpretation of subchondral bone perfusion and IOP physiology is offered, specifically that there is a specialised vasculo-mechanical subchondral environment which allows load to be transferred partly by hydraulic force. A new means of assessing perfusion in bone at the needle tip by a subtraction technique is suggested. Loading raises IOP whatever the perfusion state. Steroids raise IOP but by a different method, at least in this model. The work opens the door to a new vasculo-mechanical understanding of the physiology of bone circulation. A further study was therefore undertaken in Chapter 3 to develop an in vitro model to confirm the perfusion findings.

CHAPTER 3

1. Developed an inexpensive 3Rs compliant in vitro model using the calf foot.

2 Tested surgical technique, water bath, perfusion fluids, pressures, IOP needles, pressure transducers and recording software.

3. Results confirmed earlier perfusion physiology but demonstrated differences between live and old specimens. Symmetrical elasticity in filling and emptying with and without a tourniquet was shown.

4. Established parameters for future use in loading work.

In Chapter 3 a reliable in vitro model based on the calf foot was developed to explore IOP and bone perfusion physiology. Earlier in vivo findings of IOP variability were confirmed. IOP variation is due to differing conditions at the needle tip rather than there being a significant physiological difference. The model shows that subchondral cancellous bone behaves as a perfused tissue and demonstrates 'elastic' responses to hydrodynamic changes with filling and emptying and the use of a tourniquet. The model offered a basis for further work on bone perfusion physiology with loading as described in Chapter 4.

CHAPTER 4

1. Developed and applied two different methods of loading, pure skeletal Ex-fix loading and 'physiological' standing type loading.

2. Explored loading in both static and dynamic patterns, single and repetitive.

3. Confirmed that IOP may exceed perfusion pressure.

4. Confirmed that subchondral load is transferred partly by hydraulic force.

5. Postulated a likely additional soft tissue blood pump,

6. Indicated that there must be anatomical features to support subchondral load bearing by hydraulic force.

In Chapter 4 the new in vitro model was used to explore the effect on IOP of loading and vascular occlusion. A close correlation between subchondral IOP and load whether non-perfused, perfused or perfused and with a venous tourniquet, was demonstrated. High subchondral pressures are generated by load. The force is dissipated from the subchondral region to the shaft cortex partly by hydraulic pressure. After physiological loading IOP falls to below the pre-load level, probably due to an extra osseous soft

tissue venous blood pump. Anatomy must exist to allow and perhaps enhance circulation during activity**.**

Further work to identify and explore vascularisation in the subchondral region was therefore undertaken in Chapter 5.

CHAPTER 5

1. Identified previously unrecognised vascular marks present on MRI scans.

2 Showed that they were distributed over the first 2 cm below the tibial joint surface.

3. Showed that there were more marks laterally and less osteoarthritis.

4 Showed that there was a loss in vascular marks with increasing K-L grade.

5 Suggested further study as in Chapter 5 part 2

6 Part 2 confirmed correlation between tibial OA and loss of vascular marks.

7 Showed similar vascular marks in the femoral subchondral area.

8 In the femur correlation with OA failed perhaps due to the curved anatomy of the condyle.

Chapter 5 describes upper tibial subchondral vascular marks on MRI scans and identifies an inverse relationship between the marks and the presence and distribution of knee osteoarthritis. A second study confirmed the original findings and found a similar distribution of vascular marks on the femoral condyles. Femoral anatomy prevented correlation between K-L grades of osteoarthritis and vascular marks but that does not exclude the relationship. It was not possible to say if vessel loss leads to OA or vice versa but there appears to be an association. The loss of vascular marks on MRI may be a means of diagnosing or predicting the development of OA. Osteoarthritis may

therefore be a partly vascular disease. Chapter 6 sought better histological evidence for the existence of the subchondral vessels and other features which might support a specialised subchondral circulation capable of transferring load by hydraulic force.

CHAPTER 6

1 Demonstrated macroscopic vessels in the subchondral axial plane from both calf and human and showed longitudinal radiating vessels consistent with those seen on MRI scans. These vessels were distributed over the first 2 cm below the joint.

2 There were none in arthritic human bone.

3 The vessels appear to angulate on entering or leaving the cortex.

4 There are complex convolutions or distortions just as the vessels approach the cortex. These could be valves which close when pressure in the surrounding subchondral area rises.

5 Immediately under healthy cartilage and separate from the vessels described above there is a well-developed capillary network. This is compressed during load bearing and is probably the main source of nutrients to the cartilage.

6 The subchondral capillary network is also lost in early osteoarthritis.

Chapter 6 demonstrates previously undescribed vessels in the subchondral region. They have modifications at the cortical margin which may act as valves preventing high pressure damage to the delicate subchondral tissues. The absence of the vessels in osteoarthritis suggests that OA may be a vasculo-mechanical disease. This is further supported by the loss of the subchondral capillary plexus in early osteoarthritis. Chapter 7 sets out and references evidence which may support the primary hypothesis.

CHAPTER 7

Chapter 7 lists other evidence which may support the thesis.

These referenced observations offer support for the 'vasculo-mechanical' model of subchondral perfusion. Collectively they suggest a new model or understanding for bone perfusion and subchondral physiology in active joints and point the way to a better understanding of joint disease such as osteoarthritis.

8.5. Research Relevance

This work explores a new field of subchondral physiology. This needs to be further explored, confirmed and quantified and developed into clinically useful tests and treatments. The project potentially offers a better understanding of the pathogenesis of osteoarthritis.

8.6. Clinical Relevance

IOP studies in their present form are shown to be flawed. However, by applying the physiological understanding outlined above, the use of IOP in the clinical situation, both for the study of bone disease and also perhaps compartment syndromes, has a promising future.

It is evident that the forced injection of saline has potentially serious consequences for the local micro circulation. There are other means of delivering fluids in emergency situations such as nasogastric, rectal and intraperitoneal routes which may be preferable.

8.7. Treatment of Painful Bone

The treatment of bone pain by forage drilling, osteotomy or decompression seems safe and justifiable especially in steroid taking or immunocompromised patients.

8.8. The Future

The discovery of the circulation by Harvey allowed a better understanding of cardiovascular physiology and pathology and in due course led to better treatments. It is hoped that a better understanding of bone and joint circulation and the physiology of the subchondral region in active joints would lead in turn to better prevention and treatment of osteoarthritis. This work may play a part in that and may ultimately be of wider benefit.

Further work is required in the following areas:

Using the present or similar model:

1 To check and confirm the IOP physiological findings and to use the model to look for evidence of much higher IOP during loading. This will require better IOP transducers.

2 To check and test the 'subtraction theory' to see if that or IOP measurement alone is a better technique and which may be transferable to the clinical setting to assess bone perfusion and viability before and after treatment.

Histology:

3 To formally look for other features in normal bone that would confirm the existence of a specialised subchondral physiology.

4 To confirm and count vessel numbers in relation to cartilage thickness and health.

5 To examine vessel distribution in relation to osteoarthritis in both the immediate subchondral capillaries and the larger radial axial plane subchondral vessels.

6 To examine subchondral bone for the incidence and distribution of pressure sensitive nerve endings within bone and to test their response to pressure, lactic acid, heat or other potential stimuli which may explain bone pain.

Compartment Syndromes:

6 To obtain consent for a clinical trial to use the subtraction method in the diagnosis of compartment syndromes.

7 It may be possible to develop a disposable kit to use in emergency rooms to diagnose compartment syndromes.

Bone pain:

8 To obtain consent to use IOP differential measurement in patients with bone pain and to then apply forage or drilling to relieve bone pain for example following total knee replacement where no other cause of pain can be found.

9 It may be possible to develop an implant such as a plastic tube to prevent closure of the forage channel by healing bone and thus allow a more permanent IOP reduction or a ‘bone pain drain’.

10 To apply the same technique to the treatment of arthritic vertebral spinal bone pain.

11 To carry out a mass population study of weather associated bone pain taking care to examine the correlation between falling barometric pressure and the onset of pain.

Epidemiology:

12 If vascular disease underlies the arthritic process, epidemiological evidence should be studied to assess its possible association with statin use and other potentially vascular affecting drugs such as aspirin or anticoagulants and lipid profiles, exercise and other population data.

13 Further epidemiological studies are indicated looking at the use of NSAIDS, corticosteroids and lipid modulating drugs in relation to osteoarthritis.

Drugs:

14 If bone fat cell volume and intraosseous circulation are capable of manipulation such as that achieved in the steroid treated model in Chapter 2, there may be possible therapeutic means of developing treatments for osteoarthritis possibly by improving subchondral or bone circulation.

Other investigation:

15 Isotope bone scans, MRI, PET and SPECT scans could be employed to assess subchondral perfusion preferably in active load bearing joints to understand better the physiology of the subchondral region.

8.9. Summary

The main and most important conclusions from this work are that:

- IOP measurement in isolation is not useful. It measures pressure only at the needle tip and effectively relates to the largest punctured arteriole. By adding selective proximal vascular occlusion more can be learned.
- IOP is influenced by several external factors related to blood pressure.
- Loads are transmitted across the subchondral region partly by hydraulic pressure through flexible soft tissues.
- There is a specialised subchondral vascular anatomy visible on MRI scans and histologically. There appear to be possible valve like structures which stop blood being forced out of subchondral cancellous bone when loaded.
- In osteoarthritis there is a loss of subchondral vascularity.
- Osteoarthritis may have a vasculo-mechanical basis.
- This understanding may open the door to further research and better treatment for osteoarthritis.

REFERENCES

Aaron, R. K. and J. Racine (2013). "Pathogenesis and epidemiology of osteoarthritis." Rhode Island Medical Journal **96**(3): 19.

Abramson, S. B. and M. Attur (2009). "Developments in the scientific understanding of osteoarthritis." Arthritis research & therapy **11**(3): 227.

Afoke, N. Y., P. D. Byers and W. C. Hutton (1987). "Contact pressures in the human hip joint." J Bone Joint Surg Br **69**(4): 536-541.

Aglietti, P., J. Insall, R. Buzzi and G. Deschamps (1983). "Idiopathic osteonecrosis of the knee. Aetiology, prognosis and treatment." The Journal of bone and joint surgery. British volume **65**(5): 588-597.

Ahlback, S. (1968). "Osteoarthrosis of the knee. A radiographic investigation." Acta Radiol Diagn (Stockh): Suppl 277:277-272.

Albinus, B. S. (1761). Academicarum annotationum ll. VIII, Apud J. & H. Verbeek.

Alexander, R. M. (1980). "Forces in animal joints." Engineering in Medicine **9**(2): 93-97.

Alizai, H., W. Virayavanich, G. B. Joseph, L. Nardo, F. Liu, H. Liebl, M. C. Nevitt, J. A. Lynch, C. E. McCulloch and T. M. Link (2014). "Cartilage lesion score: comparison of a quantitative assessment score with established semiquantitative MR scoring systems." Radiology **271**(2): 479-487.

Allen, K. D. and Y. M. Golightly (2015). "Epidemiology of osteoarthritis: state of the evidence." Current opinion in rheumatology **27**(3): 276.

Amiel, D., M. F. Abel, J. B. Kleiner, R. L. Lieber and W. H. Akeson (1986). "Synovial fluid nutrient delivery in the diathrial joint: an analysis of rabbit knee ligaments." Journal of Orthopaedic research **4**(1): 90-95.

Arlet, J., R. P. Ficat and D. S. Hungerford (1984). Bone circulation, Williams & Wilkins.

Arnoldi, C. C., J. C. Djurhuus, J. Heerfordt and A. Karle (1980). "Intraosseous phlebography, intraosseous pressure measurements and 99mTC-polyphosphate scintigraphy in patients with various painful conditions in the hip and knee." Acta Orthop Scand **51**(1): 19-28.

Arnoldi, C. C., H. Linderholm and H. Müssbichler (1972). "Venous engorgement and intraosseous hypertension in osteoarthritis of the hip." The Journal of bone and joint surgery. British volume **54**(3): 409-421.

Åström, J. (1975). "Peroperative effect of fenestration upon intraosseous pressure in patients with osteoarthritis of the hip." Acta Orthopaedica Scandinavica **46**(6): 963-967.

Azuma, H. (1964). "Intraosseous pressure as a measure of hemodynamic changes in bone marrow." Angiology **15**(9): 396-406.

Babhulkar, S. (2013). Osteonecrosis, JP Medical Ltd.

Baksi, D. (1991). "Treatment of osteonecrosis of the femoral head by drilling and muscle-pedicle bone grafting." The Journal of bone and joint surgery. British volume **73**(2): 241-245.

Barclay, A. E. (1947). "Micro-arteriography." Br J Radiol **20**(238): 394-404.

Barr, A. J., T. M. Campbell, D. Hopkinson, S. R. Kingsbury, M. A. Bowes and P. G. Conaghan (2015). "A systematic review of the relationship between subchondral bone

features, pain and structural pathology in peripheral joint osteoarthritis." Arthritis Research & Therapy **17**(1): 228.

Bashir, A., M. Gray, J. Hartke and D. Burstein (1999). "Nondestructive imaging of human cartilage glycosaminoglycan concentration by MRI." Magnetic Resonance in Medicine: An Official Journal of the International Society for Magnetic Resonance in Medicine **41**(5): 857-865.

Bathija, A., S. Davis and S. Trubowitz (1979). "Bone marrow adipose tissue: response to acute starvation." American journal of hematology **6**(3): 191-198.

Beverly, M. (2012). "Arthritis is a vasculo-mechanical disease." Bone **50**: S191-S191.

Beverly, M., D. Murray, J. Urban and P. Winlove (2015). "The Possible Role of Vasculo-Mechanical Factors in Joint Patho-Physiology." Osteoarthritis and Cartilage **23**: A270-A270.

Beverly, M., J. Pflug and R. Mathie (1987). Bone - a flexible perfused sponge. J Bone Joint Surg Br. **69:** 494-494.

Beverly, M., G. Stamm, T. W. Hamilton, D. W. Murray and H. G. Pandit (2018). "Upper tibial MRI vascular marks lost in early knee osteoarthritis." J Orthop Surg Res **13**(1): 281.

Beverly, M., J. Urban and D. Murray (2016). "Factors Affecting Physiology of Intraosseous Pressure Measurement." Osteoarthritis and Cartilage **24**: S343-S343.

Beverly, M. C. (1987). "Cancellous Bone Perfusion, Intraosseous Pressure and the Bone Blood Pump." International Journal of Microcirculation-Clinical and Experimental **5**(4): 388-388.

Beverly, M. C. and J. J. Pflug (1987). "Radiological Types of Caisson Disease and Microbubble Formation." British Journal of Radiology **60**(716): 845-845.

Beverly, M. C., J. J. Pflug and T. Gourlay (1987). "Circulating Microbubble Induction and Caisson Disease." International Journal of Microcirculation-Clinical and Experimental **6**(1): 92-92.

Beverly, M. C., J. J. Pflug and R. T. Mathie (1987). "Cancellous Bone as a Blood Pump - Physiological, Anatomical and Pathological Evidence." Annals of the Royal College of Surgeons of England **69**(5): 245-245.

Biewener, A. A. (1983). "Allometry of quadrupedal locomotion: the scaling of duty factor, bone curvature and limb orientation to body size." Journal of Experimental Biology **105**(1): 147-171.

Blokhuis, T. J., H. C. Pape and J. P. Frolke (2017). "Timing of definitive fixation of major long bone fractures: Can fat embolism syndrome be prevented?" Injury **48 Suppl 1**: S3-s6.

Boskey, A., C. Raggio, P. Bullough and J. Kinnett (1983). "Changes in the bone tissue lipids in persons with steroid-and alcohol-induced osteonecrosis." Clinical orthopaedics and related research(172): 289-295.

Boss, J. H. and I. Misselevich (2003). "Osteonecrosis of the femoral head of laboratory animals: the lessons learned from a comparative study of osteonecrosis in man and experimental animals." Vet Pathol **40**(4): 345-354.

Bourne, G. H. (1972). The Biochemistry and Physiology of Bone Vol 2: Physiology and Pathology, Elsevier.

Bouteiller, G., J. Arlet, A. Blasco, F. Vigoni and A. Elefterion (1983). "Is osteonecrosis of the femoral head avascular? Bone blood flow measurements after long-term treatment with corticosteroids." Metab Bone Dis Relat Res **4**(5): 313-318.

Brandt, K. D., P. Dieppe and E. L. Radin (2008). "Etiopathogenesis of Osteoarthritis." Rheumatic Disease Clinics of North America **34**(3): 531-559.

Breusch, S. (2000). "A New Concept in the Treatment of Anterior Knee Pain: Patellar Hypertension Syndrome." UNE **23**(6).

Brookes, M. and W. J. Revell (1998). Blood supply of bone : scientific aspects. London, Springer.

Brookes, M. and W. J. Revell (2012). Blood supply of bone: scientific aspects, Springer Science & Business Media.

Brorson, S. (2009). "Management of fractures of the humerus in Ancient Egypt, Greece, and Rome: an historical review." Clinical Orthopaedics and Related Research® **467**(7): 1907-1914.

Bryant, J. D. (1983). "The Effect of Impact on the Marrow Pressure of Long Bones Invitro." Journal of Biomechanics **16**(8): 659-&.

Bultink, I. E. and W. F. Lems (2013). "Osteoarthritis and osteoporosis: what is the overlap?" Curr Rheumatol Rep **15**(5): 328.

Burkhardt, R. (2012). Bone marrow and bone tissue: color atlas of clinical histopathology, Springer Science & Business Media.

Burrows, H. J. (1952). "Leonardo da Vinci and Nicholas Andry on Posture." The Journal of bone and joint surgery. British volume **34**(4): 541-544.

Camp, J. F. and J. C. Colwell (1986). "Core decompression of the femoral head for osteonecrosis." The Journal of bone and joint surgery. American volume **68**(9): 1313-1319.

Cardoso, L., S. P. Fritton, G. Gailani, M. Benalla and S. C. Cowin (2013). "Advances in assessment of bone porosity, permeability and interstitial fluid flow." J Biomech **46**(2): 253-265.

Chokkhanchitchai, S., T. Tangarunsanti, S. Jaovisidha, K. Nantiruj and S. Janwityanujit (2010). "The effect of religious practice on the prevalence of knee osteoarthritis." Clinical rheumatology **29**(1): 39.

Chryssanthou, C. P. (1978). "Dysbaric osteonecrosis. Etiological and pathogenetic concepts." Clinical orthopaedics and related research(130): 94-106.

Clark, J. M. (1990). "The structure of vascular channels in the subchondral plate." Journal of anatomy **171**: 105.

Collins, N. J., D. Misra, D. T. Felson, K. M. Crossley and E. M. Roos (2011). "Measures of knee function: International Knee Documentation Committee (IKDC) Subjective Knee Evaluation Form, Knee Injury and Osteoarthritis Outcome Score (KOOS), Knee Injury and Osteoarthritis Outcome Score Physical Function Short Form (KOOS-PS), Knee Outcome Survey Activities of Daily Living Scale (KOS-ADL), Lysholm Knee Scoring Scale, Oxford Knee Score (OKS), Western Ontario and McMaster Universities Osteoarthritis Index (WOMAC), Activity Rating Scale (ARS), and Tegner Activity Score (TAS)." Arthritis Care Res (Hoboken) **63 Suppl 11**: S208-228.

Conaghan, P. G., H. Vanharanta and P. A. Dieppe (2005). "Is progressive osteoarthritis an atheromatous vascular disease?" Ann Rheum Dis **64**(11): 1539-1541.

Conklin, J., P. Alderson, T. Zizic, D. Hungerford, J. Densereaux, A. Gober and H. Wagner (1983). "Comparison of bone scan and radiograph sensitivity in the detection of steroid-induced ischemic necrosis of bone." Radiology **147**(1): 221-226.

Cooper, A. (1973). "A treatise on dislocations and on fractures of the joints: fractures of the neck of the thigh-bone." Clinical Orthopaedics and Related Research® **92**: 3-5.

Cooper, C., M. Steinbuch, R. Stevenson, R. Miday and N. B. Watts (2010). "The epidemiology of osteonecrosis: findings from the GPRD and THIN databases in the UK." Osteoporos Int **21**(4): 569-577.

Crock, H. V. (1962). "The arterial supply and venous drainage of the bones of the human knee joint." Anat Rec **144**(3): 199-217.

Cruess, R. L., D. Ross and E. Crawshaw (1975). "The etiology of steroid-induced avascular necrosis of bone. A laboratory and clinical study." Clin Orthop Relat Res(113): 178-183.

Culvenor, A. G., C. N. Engen, B. E. Oiestad, L. Engebretsen and M. A. Risberg (2015). "Defining the presence of radiographic knee osteoarthritis: a comparison between the Kellgren and Lawrence system and OARSI atlas criteria." Knee Surg Sports Traumatol Arthrosc **23**(12): 3532-3539.

D'Lima, D. D., B. J. Fregly, S. Patil, N. Steklov and C. W. Colwell, Jr. (2012). "Knee joint forces: prediction, measurement, and significance." Proc Inst Mech Eng H **226**(2): 95-102.

Dabiri, Y. and L. P. Li (2013). "Altered knee joint mechanics in simple compression associated with early cartilage degeneration." Comput Math Methods Med **2013**: 862903.

Davidson, J. K. (1975). "Proceedings. Basm Scottish Area—Inverclyde House, Largs. April 23rd and 24th 1975: Dysbaric Osteonecrosis." British journal of sports medicine **9**(3): 144.

Day, W. H., S. A. Swanson and M. A. Freeman (1975). "Contact pressures in the loaded human cadaver hip." J Bone Joint Surg Br **57**(3): 302-313.

De Lorenzo, R. A., J. A. Ward, B. S. Jordan and C. E. Hanson (2014). "Relationships of intraosseous and systemic pressure waveforms in a Swine model." Acad Emerg Med **21**(8): 899-904.

Denham, R. A. (1959). "Hip mechanics." J Bone Joint Surg Br **41-B**: 550-557.

Devlin, M. J. (2011). "Why does starvation make bones fat?" American Journal of Human Biology **23**(5): 577-585.

Devlin, M. J. and C. J. Rosen (2015). "The bone–fat interface: basic and clinical implications of marrow adiposity." The Lancet Diabetes & Endocrinology **3**(2): 141-147.

Dieppe, P. (1999). "Subchondral bone should be the main target for the treatment of pain and disease progression in osteoarthritis." Osteoarthritis and cartilage **7**(3): 325-326.

Dieppe, P. A. and L. S. Lohmander (2005). "Pathogenesis and management of pain in osteoarthritis." The Lancet **365**(9463): 965-973.

Downey, D. J., P. A. Simkin, W. L. Lanzer and F. A. Matsen, 3rd (1988). "Hydraulic resistance: a measure of vascular outflow obstruction in osteonecrosis." J Orthop Res **6**(2): 272-278.

Downey, D. J., P. A. Simkin and R. Taggart (1988). "The effect of compressive loading on intraosseous pressure in the femoral head in vitro." J Bone Joint Surg Am **70**(6): 871-877.

Drescher, W., M. H. Bunger, K. Weigert, C. Bunger and E. S. Hansen (2004). "Methylprednisolone enhances contraction of porcine femoral head epiphyseal arteries." Clin Orthop Relat Res(423): 112-117.

Drescher, W., H. Li, S. D. Jensen, J. Ingerslev, E. S. Hansen, E. M. Hauge and C. Bunger (2002). "The effect of long-term methylprednisolone treatment on the femoral head in growing pigs." J Orthop Res **20**(4): 662-668.

Drescher, W., D. Varoga, T. R. Liebs, J. Lohse, T. Herdegen, J. Hassenpflug and T. Pufe (2006). "Femoral artery constriction by norepinephrine is enhanced by methylprednisolone in a rat model." J Bone Joint Surg Am **88 Suppl 3**: 162-166.

Dyke, J. P., M. Synan, P. Ezell, D. Ballon, J. Racine and R. K. Aaron (2015). "Characterization of bone perfusion by dynamic contrast-enhanced magnetic resonance imaging and positron emission tomography in the Dunkin-Hartley guinea pig model of advanced osteoarthritis." J Orthop Res **33**(3): 366-372.

Edwards, J. R., K. Williams, L. G. Kindblom, J. M. Meis-Kindblom, P. C. Hogendoorn, D. Hughes, R. G. Forsyth, D. Jackson and N. A. Athanasou (2008). "Lymphatics and bone." Human pathology **39**(1): 49-55.

Elliott, K. G. and A. J. Johnstone (2003). "Diagnosing acute compartment syndrome." J Bone Joint Surg Br **85**(5): 625-632.

Favre, J., J. C. Erhart-Hledik, K. Blazek, B. Fasel, G. E. Gold and T. P. Andriacchi (2017). "Anatomically Standardized Maps Reveal Distinct Patterns of Cartilage Thickness With Increasing Severity of Medial Compartment Knee Osteoarthritis." J Orthop Res **35**(11): 2442-2451.

Felson, D. T., J. Lynch, A. Guermazi, F. W. Roemer, J. Niu, T. McAlindon and M. C. Nevitt (2010). "Comparison of BLOKS and WORMS scoring systems part II. Longitudinal assessment of knee MRIs for osteoarthritis and suggested approach based on their performance: data from the Osteoarthritis Initiative." Osteoarthritis Cartilage **18**(11): 1402-1407.

Fernandes, G. S. and A. M. Valdes (2015). "Cardiovascular disease and osteoarthritis: common pathways and patient outcomes." Eur J Clin Invest **45**(4): 405-414.

Ferreira, M. L., Y. Zhang, B. Metcalf, J. Makovey, K. L. Bennell, L. March and D. J. Hunter (2016). "The influence of weather on the risk of pain exacerbation in patients with knee osteoarthritis - a case-crossover study." Osteoarthritis Cartilage **24**(12): 2042-2047.

Ficat, R. P. (1985). "Idiopathic bone necrosis of the femoral head. Early diagnosis and treatment." J Bone Joint Surg Br **67**(1): 3-9.

Findlay, D. M. (2007). "Vascular pathology and osteoarthritis." Rheumatology **46**(12): 1763-1768.

Frascone, R. J., J. P. Jensen, K. Kaye and J. G. Salzman (2007). "Consecutive field trials using two different intraosseous devices." Prehosp Emerg Care **11**(2): 164-171.

Frascone, R. J., J. G. Salzman, A. B. Adams, P. Bliss, S. S. Wewerka and D. J. Dries (2015). "Evaluation of intraosseous pressure in a hypovolemic animal model." J Surg Res **193**(1): 383-390.

Frascone, R. J., J. G. Salzman, P. Bliss, A. Adams, S. S. Wewerka and D. J. Dries (2013). "Decreasing Intraosseous Pressure and Increasing Respiratory Variability Track Fluid Volume Reduction in a Porcine Hypovolemia Model." Circulation **128**(22).

Fukubayashi, T. and H. Kurosawa (1980). "The contact area and pressure distribution pattern of the knee: a study of normal and osteoarthrotic knee joints." Acta Orthopaedica Scandinavica **51**(1-6): 871-879.

Fukushima, W., M. Fujioka, T. Kubo, A. Tamakoshi, M. Nagai and Y. Hirota (2010). "Nationwide epidemiologic survey of idiopathic osteonecrosis of the femoral head." Clin Orthop Relat Res **468**(10): 2715-2724.

Funck-Brentano, T. and M. Cohen-Solal (2015). "Subchondral bone and osteoarthritis." Curr Opin Rheumatol **27**(4): 420-426.

Gardner, A. and R. Fox (1989). The return of blood to the heart: venous pumps in health and disease, Libbey.

Geusens, P. P. and J. P. van den Bergh (2016). "Osteoporosis and osteoarthritis: shared mechanisms and epidemiology." Curr Opin Rheumatol **28**(2): 97-103.

Glade, M. J. and L. Krook (1982). "Glucocorticoid-induced inhibition of osteolysis and the development of osteopetrosis, osteonecrosis and osteoporosis." Cornell Vet **72**(1): 76-91.

Goetz, J. E., T. R. Derrick, D. R. Pedersen, D. A. Robinson, M. G. Conzemius, T. E. Baer and T. D. Brown (2008). "Hip joint contact force in the emu (Dromaius novaehollandiae) during normal level walking." J Biomech **41**(4): 770-778.

Gold, E. W., O. D. Fox, S. Weissfeld and P. H. Curtiss (1978). "Corticosteroid-induced avascular necrosis: an experimental study in rabbits." Clin Orthop Relat Res(135): 272-280.

Gosling, D. C., W. F. Sampson, M. MacLeod, A. M. Hanby and M. Slapak (1987). "Susceptibility of the rabbit and the rat to steroid osteonecrosis--an experimental study." Transplantation **43**(5): 751-753.

Gronlund, J., H. Kofoed and E. Svalastoga (1984). "Effect of increased knee joint pressure on oxygen tension and blood flow in subchondral bone." Acta Physiol Scand **121**(2): 127-131.

Grüneboom, A., I. Hawwari, D. Weidner, S. Culemann, S. Müller, S. Henneberg, A. Brenzel, S. Merz, L. Bornemann, K. Zec, M. Wuelling, L. Kling, M. Hasenberg, S. Voortmann, S. Lang, W. Baum, A. Ohs, O. Kraff, H. H. Quick, M. Jäger, S. Landgraeber, M. Dudda, R. Danuser, J. V. Stein, M. Rohde, K. Gelse, A. I. Garbe, A. Adamczyk, A. M. Westendorf, D. Hoffmann, S. Christiansen, D. R. Engel, A. Vortkamp, G. Krönke, M. Herrmann, T. Kamradt, G. Schett, A. Hasenberg and M. Gunzer (2019). "A network of trans-cortical capillaries as mainstay for blood circulation in long bones." Nature Metabolism.

Hafezi-Nejad, N., B. Zikria, J. Eng, J. A. Carrino and S. Demehri (2015). "Predictive value of semi-quantitative MRI-based scoring systems for future knee replacement: data from the osteoarthritis initiative." Skeletal Radiol **44**(11): 1655-1662.

Han, N., Z. Q. Yan, C. A. Guo, F. Shen, J. Liu, Y. X. Shi and Z. Y. Zhang (2010). "Effect of rifampicin on the risk of steroid-induced osteonecrosis of the femoral head." Orthop Surg **2**(2): 124-133.

Handley, R. and J. Pooley (1991). "The venous anatomy of the scaphoid." Journal of anatomy **178**: 115.

Harvey, W. (1628). "De Motu Cordis (On the Motion of the Heart and Blood)."

Havers, C. (1691). Osteologia Nova or some New Observations of the Bones and the Parts belonging to them, and the manner of their accretion and nutrition, Samuel Smith.

Hejgaard, N. and C. C. Arnoldi (1984). "Osteotomy of the patella in the patellofemoral pain syndrome." International orthopaedics **8**(3): 189-194.

Hietala, S. O. and J. Astrom (1977). "The effect of fenestration on intraosseous drainage in osteoarthritis of the hip." Acta Orthop Scand **48**(1): 80-85.

Hirano, K., M. Tada, H. Isayama, H. Yagioka, T. Sasaki, H. Kogure, Y. Nakai, N. Sasahira, T. Tsujino and H. Yoshida (2007). "Long-term prognosis of autoimmune pancreatitis without and with corticosteroid treatment." Gut.

Ho, K. Y., H. H. Hu, P. M. Colletti and C. M. Powers (2014). "Running-induced patellofemoral pain fluctuates with changes in patella water content." Eur J Sport Sci **14**(6): 628-634.

Holm, I. E., H. Ewald, J. Bulow and C. Bunger (1990). "Vasoactive substances in subchondral bone of the dog knee." J Orthop Res **8**(2): 205-212.

Hungerford, D. S. and D. W. Lennox (1985). "The importance of increased intraosseous pressure in the development of osteonecrosis of the femoral head: implications for treatment." Orthop Clin North Am **16**(4): 635-654.

Hunter, D. J., G. H. Lo, D. Gale, A. J. Grainger, A. Guermazi and P. G. Conaghan (2008). "The reliability of a new scoring system for knee osteoarthritis MRI and the validity of bone marrow lesion assessment: BLOKS (Boston Leeds Osteoarthritis Knee Score)." Ann Rheum Dis **67**(2): 206-211.

Hunter, D. J., D. Schofield and E. Callander (2014). "The individual and socioeconomic impact of osteoarthritis." Nat Rev Rheumatol **10**(7): 437-441.

Hunter, J. (1861). Essays and observations on natural history, anatomy, physiology, psychology and geology: Being his posthumous papers on those subjects arranged and revised, with notes: to which are added the introductory lectures on the Hunterian collection of fossil remains, delivered... by Richard Ossen. II, John van Voorst.

Hunter, W. (1743). "VI. Of the structure and diseases of articulating cartilages." Philosophical Transactions **42**(470): 514-521.

Hwa, H. J. (2004). "Could the intraosseous fluid in cancellous bone bear external load significantly within the elastic range?" Proc Inst Mech Eng H **218**(6): 375-379.

Hwang, J., W. C. Bae, W. Shieu, C. W. Lewis, W. D. Bugbee and R. L. Sah (2008). "Increased hydraulic conductance of human articular cartilage and subchondral bone plate with progression of osteoarthritis." Arthritis Rheum **58**(12): 3831-3842.

Ikeuchi, K., Y. Hasegawa, T. Seki, Y. Takegami, T. Amano and N. Ishiguro (2015). "Epidemiology of nontraumatic osteonecrosis of the femoral head in Japan." Mod Rheumatol **25**(2): 278-281.

Imhof, H., M. Breitenseher, F. Kainberger and S. J. S. R. Trattnig (1997). "Degenerative joint disease: cartilage or vascular disease?" **26**(7): 398-403.

Inoue, S., M. Horii, T. Asano, M. Fujioka, T. Ogura, M. Shibatani, W.-C. Kim, M. Nakagawa, T. Tanaka and Y. Hirota (2003). "Risk factors for nontraumatic osteonecrosis of the femoral head after renal transplantation." Journal of orthopaedic science **8**(6): 751-756.

Jahn, S., J. Seror and J. Klein (2016). "Lubrication of Articular Cartilage." Annu Rev Biomed Eng **18**: 235-258.

Jones, J. P. (1993). Pathophysiology of osteonecrosis. Bone circulation and vascularization in normal and pathological conditions, Springer**:** 249-261.

Jones, L. C. and M. R. Allen (2011). "Animal models of osteonecrosis." Clinical Reviews in Bone and Mineral Metabolism **9**(1): 63.

Jones, L. C. and D. S. Hungerford (2004). "Osteonecrosis: etiology, diagnosis, and treatment." Curr Opin Rheumatol **16**(4): 443-449.

Jordan, J. M., G. Luta, J. B. Renner, A. Dragomir, M. C. Hochberg and J. G. Fryer (1996). "Ethnic differences in self-reported functional status in the rural south: the Johnston County Osteoarthritis Project." Arthritis Care Res **9**(6): 483-491.

Kafka, V. (1983). "On hydraulic strengthening of bones." Biorheology **20**(6): 789-793.

Kawai, K., A. Tamaki and K. Hirohata (1985). "Steroid-induced accumulation of lipid in the osteocytes of the rabbit femoral head. A histochemical and electron microscopic study." J Bone Joint Surg Am **67**(5): 755-763.

Keck, S. W. and P. J. Kelly (1965). "The Effect of Venous Stasis on Intraosseous Pressure and Longitudinal Bone Growth in the Dog." J Bone Joint Surg Am **47**: 539-544.

Kellgren, J. H. and J. S. Lawrence (1957). "Radiological assessment of osteo-arthrosis." Ann Rheum Dis **16**(4): 494-502.

Kenzora, J., R. Steele, Z. Yosipovitch and M. Glimcher (1978). "Experimental osteonecrosis of the femoral head in adult rabbits." Clinical Orthopaedics and Related Research®(130): 8-46.

Kerachian, M. A., C. Seguin and E. J. Harvey (2009). "Glucocorticoids in osteonecrosis of the femoral head: a new understanding of the mechanisms of action." J Steroid Biochem Mol Biol **114**(3-5): 121-128.

Keynes, G. (1966). The Life of William Harvey, Oxford University Press.

Kiapour, A. M., D. S. Yang, G. J. Badger, N. P. Karamchedu, M. M. Murray, P. D. Fadale, M. J. Hulstyn, R. M. Shalvoy and B. C. Fleming (2019). "Anatomic Features of the Tibial Plateau Predict Outcomes of ACL Reconstruction Within 7 Years After Surgery." Am J Sports Med: 363546518823556.

Kim, J., H. H. Lee, Y. Kang, T. K. Kim, S. W. Lee, Y. So and W. W. Lee (2017). "Maximum standardised uptake value of quantitative bone SPECT/CT in patients with medial compartment osteoarthritis of the knee." Clin Radiol **72**(7): 580-589.

King, W., R. Ruttencutter, H. N. Nagaraja, V. Matkovic, J. Landoll, C. Hoyle, J. R. Mendell and J. T. Kissel (2007). "Orthopedic outcomes of long-term daily corticosteroid treatment in Duchenne muscular dystrophy." Neurology **68**(19): 1607-1613.

Klenerman, L., S. A. Swanson and M. A. Freeman (1967). "Mechanical and physiological properties of bone." Proc R Soc Med **60**(9): 850-854.

Kofoed, H. (1986). "Positive correlation between osteoarthritic ankle pain and bone marrow pressure." J Rheumatol **13**(4): 801-803.

Kogan, F., A. P. Fan, E. J. McWalter, E. H. G. Oei, A. Quon and G. E. Gold (2017). "PET/MRI of metabolic activity in osteoarthritis: A feasibility study." J Magn Reson Imaging **45**(6): 1736-1745.

Kohn, M. D., A. A. Sassoon and N. D. Fernando (2016). "Classifications in Brief: Kellgren-Lawrence Classification of Osteoarthritis." Clin Orthop Relat Res **474**(8): 1886-1893.

Koning, N. J., A. B. Vonk, L. J. van Barneveld, A. Beishuizen, B. Atasever, C. E. van den Brom and C. Boer (2012). "Pulsatile flow during cardiopulmonary bypass preserves postoperative microcirculatory perfusion irrespective of systemic hemodynamics." J Appl Physiol (1985) **112**(10): 1727-1734.

Koo, K.-H., M. A. Mont and L. C. Jones (2014). Osteonecrosis, Springer.

Koshino, T. (1982). "The treatment of spontaneous osteonecrosis of the knee by high tibial osteotomy with and without bone-grafting or drilling of the lesion." The Journal of bone and joint surgery. American volume **64**(1): 47-58.

Kremer, R. and V. Gilsanz (2015). "Fat and Bone: An Odd Couple." Front Endocrinol (Lausanne) **6**: 190.

Kuribayashi, M., M. Fujioka, K. A. Takahashi, Y. Arai, M. Ishida, T. Goto and T. Kubo (2010). "Vitamin E prevents steroid-induced osteonecrosis in rabbits." Acta Orthop **81**(1): 154-160.

Laroche, M. (2002). "Intraosseous circulation from physiology to disease." Joint Bone Spine **69**(3): 262-269.

Larsen, R. M. (1938). "Intramedullary pressure with particular reference to massive diaphyseal bone necrosis: experimental observations." Annals of surgery **108**(1): 127.

Lausten, G. S. and B. Mathiesen (1990). "Core decompression for femoral head necrosis: Prospective study of 28 patients." Acta orthopaedica Scandinavica **61**(6): 507-511.

Learmonth, I., S. Maloon and G. Dall (1990). "Core decompression for early atraumatic osteonecrosis of the femoral head." The Journal of bone and joint surgery. British volume **72**(3): 387-390.

Lemperg, R. K. and C. C. Arnoldi (1978). "Significance of Intraosseous Pressure in Normal and Diseased States with Special Reference to Intraosseous Engorgement-Pain Syndrome." Clinical Orthopaedics and Related Research(136): 143-156.

Lexer, E., P. Kuliga and W. Türk (1904). Untersuchungen über Knochenarterien mittelst Röntgenaufnahmen injizierter knochen und ihre bedentung für einzelne pathologische vorgänge am knochensystenie, A. Hirschwald.

List-Hellwig, E. and H. Meents (1999). Magnetic resonance imaging and computed tomography in advanced chronic venous insufficiency. Management of leg ulcers, Karger Publishers. **27:** 109-113.

Liu, S. L. and T. C. Ho (1991). "The role of venous hypertension in the pathogenesis of Legg-Perthes disease. A clinical and experimental study." J Bone Joint Surg Am **73**(2): 194-200.

Livingston, M. (1988). "Hippocratic principles in orthopaedics." Orthopaedic review **17**(11): 1122, 1124, 1127-1122, 1124, 1127.

Loeser, R. F., S. R. Goldring, C. R. Scanzello and M. B. Goldring (2012). "Osteoarthritis: A disease of the joint as an organ." Arthritis & Rheumatism **64**(6): 1697-1707.

Mach, D. B., S. D. Rogers, M. C. Sabino, N. M. Luger, M. J. Schwei, J. D. Pomonis, C. P. Keyser, D. R. Clohisy, D. J. Adams, P. O'Leary and P. W. Mantyh (2002). "Origins

of skeletal pain: sensory and sympathetic innervation of the mouse femur." Neuroscience **113**(1): 155-166.

Mallet, C., A. Abitan, C. Vidal, L. Holvoet, K. Mazda, A. L. Simon and B. Ilharreborde (2018). "Management of osteonecrosis of the femoral head in children with sickle cell disease: results of conservative and operative treatments at skeletal maturity." J Child Orthop **12**(1): 47-54.

Marti-Carvajal, A. J., I. Sola and L. H. Agreda-Perez (2016). "Treatment for avascular necrosis of bone in people with sickle cell disease." Cochrane Database Syst Rev(8): CD004344.

Mathiessen, A., B. Slatkowsky-Christensen, T. K. Kvien, I. K. Haugen and H. Berner Hammer (2017). "Ultrasound-detected osteophytes predict the development of radiographic and clinical features of hand osteoarthritis in the same finger joints 5 years later." RMD Open **3**(2): e000505.

Matsui, M., S. Saito, K. Ohzono, N. Sugano, M. Saito, K. Takaoka and K. Ono (1992). "Experimental steroid-induced osteonecrosis in adult rabbits with hypersensitivity vasculitis." Clin Orthop Relat Res(277): 61-72.

McCallum, R. (1968). "Decompression sickness: a review." British journal of industrial medicine **25**(1): 4.

McCallum, R. (1984). "Bone necrosis due to decompression." Phil. Trans. R. Soc. Lond. B **304**(1118): 185-191.

McCallum, R. I. and A. Petrie (1984). "Optimum weights for commercial divers." Br J Ind Med **41**(2): 275-278.

McCarthy, I. (2006). "The Physiology of Bone Blood Flow: A Review." JBJS **88**(suppl_3): 4-9.

McDermott, A. G., R. H. Yabsley and J. L. Leahey (1986). "A new method to measure intraosseous pressures." Clin Orthop Relat Res(208): 25-27.

McQueen, M. M. and C. M. Court-Brown (1996). "Compartment monitoring in tibial fractures. The pressure threshold for decompression." J Bone Joint Surg Br **78**(1): 99-104.

Miyanishi, K., T. Yamamoto, T. Irisa, G. Motomura, S. Jingushi, K. Sueishi and Y. Iwamoto (2005). "Effects of different corticosteroids on the development of osteonecrosis in rabbits." Rheumatology (Oxford) **44**(3): 332-336.

Miyanishi, K., T. Yamamoto, T. Irisa, A. Yamashita, S. Jingushi, Y. Noguchi and Y. Iwamoto (2002). "Bone marrow fat cell enlargement and a rise in intraosseous pressure in steroid-treated rabbits with osteonecrosis." Bone **30**(1): 185-190.

Morscher, E. and R. Feinstein (1984). Results of intertrochanteric osteotomy in the treatment of osteoarthritis of the hip. The Intertrochanteric Osteotomy, Springer**:** 169-177.

Mukisi, M. M., K. Bashoun and F. Burny (2009). "Sickle-cell hip necrosis and intraosseous pressure." Orthop Traumatol Surg Res **95**(2): 134-138.

Nelson, G. E., Jr., P. J. Kelly, L. F. Peterson and J. M. Janes (1960). "Blood supply of the human tibia." J Bone Joint Surg Am **42-A**(4): 625-636.

Nevitt, M. C., N. E. Lane, J. C. Scott, M. C. Hochberg, A. R. Pressman, H. K. Genant and S. R. Cummings (1995). "Radiographic osteoarthritis of the hip and bone mineral density." Arthritis & Rheumatism **38**(7): 907-916.

Newbigin, K., C. A. Souza, C. Torres, E. Marchiori, A. Gupta, J. Inacio, M. Armstrong and E. Pena (2016). "Fat embolism syndrome: State-of-the-art review focused on pulmonary imaging findings." Respir Med **113**: 93-100.

Nomura, M., N. Sakitani, H. Iwasawa, Y. Kohara, S. Takano, Y. Wakimoto, H. Kuroki and H. Moriyama (2017). "Thinning of articular cartilage after joint unloading or immobilization. An experimental investigation of the pathogenesis in mice." Osteoarthritis Cartilage **25**(5): 727-736.

Okazaki, S., S. Nagoya, K. Tateda, R. Katada, K. Mizuo, S. Watanabe, T. Yamashita and H. Matsumoto (2012). "Weight bearing does not contribute to the development of osteonecrosis of the femoral head." Int J Exp Pathol **93**(6): 458-462.

Osunkwo, I. (2013). "An update on the recent literature on sickle cell bone disease." Curr Opin Endocrinol Diabetes Obes **20**(6): 539-546.

Paget, S. J. (1966). "On a form of chronic inflammation of bones (osteitis deformans)." Clinical Orthopaedics and Related Research® **49**: 3-16.

Park, D. Y., L. H. Jin, B. H. Min, K. S. Kwack, Y. S. An and Y. J. Kim (2017). "Subchondral bone scan uptake correlates with articular cartilage degeneration in osteoarthritic knees." Int J Rheum Dis **20**(10): 1393-1402.

Park, H. J., S. S. Kim, S. Y. Lee, N. H. Park, J. Y. Park, Y. J. Choi and H. J. Jeon (2013). "A practical MRI grading system for osteoarthritis of the knee: association with Kellgren-Lawrence radiographic scores." Eur J Radiol **82**(1): 112-117.

Pasley, J., C. H. Miller, J. J. DuBose, S. A. Shackelford, R. Fang, K. Boswell, C. Halcome, J. Casey, M. Cotter, M. Matsuura, N. Relph, N. T. Tarmey and D. M. Stein (2015). "Intraosseous infusion rates under high pressure: a cadaveric comparison of anatomic sites." J Trauma Acute Care Surg **78**(2): 295-299.

Pedersen, M., A. Moghaddam, K. Bak and J. Koch (1995). "The effect of bone drilling on pain in gonarthrosis." International orthopaedics **19**(1): 12-15.

Petty, W. (1986). "Osteonecrosis." JBJS **68**(9): 1311-1312.

Ponseti, I. V. (1991). "History of orthopaedic surgery." The Iowa orthopaedic journal **11**: 59.

Pooley, J. and T. R. Davis (1987). "Intraosseous pressure changes during simulated dives: fact or transducer artifact?" Undersea Biomed Res **14**(4): 343-346.

Prisby, R. D. (2017). "Mechanical, hormonal and metabolic influences on blood vessels, blood flow and bone." J Endocrinol **235**(3): R77-r100.

Rendina-Ruedy, E. and C. J. Rosen (2017). "Bone-Fat Interaction." Endocrinol Metab Clin North Am **46**(1): 41-50.

Reynolds, S. (1948). "Morphological determinants of the flow-characteristics between an artery and its branch, with special reference to the ovarian spiral artery in the rabbit." Cells Tissues Organs **5**(1-2): 1-16.

Roentgen, W. (1959). "On a new kind of ray (first report)." Munchener medizinische Wochenschrift (1950) **101**: 1237-1239.

Ronga, M., G. Angeretti, S. Ferraro, D. E. F. G, E. A. Genovese and P. Cherubino (2014). "Imaging of articular cartilage: current concepts." Joints **2**(3): 137-140.

Saag, K. G., R. Koehnke, J. R. Caldwell, R. Brasington, L. F. Burmeister, B. Zimmerman, J. A. Kohler and D. E. Furst (1994). "Low dose long-term corticosteroid

therapy in rheumatoid arthritis: an analysis of serious adverse events." The American journal of medicine **96**(2): 115-123.

Salzman, J. G., N. M. Loken, S. S. Wewerka, A. M. Burnett, A. E. Zagar, K. R. Griffith, P. L. Bliss, B. K. Peterson, C. J. Ward and R. J. Frascone (2017). "Intraosseous Pressure Monitoring in Healthy Volunteers." Prehosp Emerg Care **21**(5): 567-574.

Samy, A. M. (2016). "Management of osteonecrosis of the femoral head: A novel technique." Indian J Orthop **50**(4): 359-365.

Savic, D., V. Pedoia, Y. Seo, J. Yang, M. Bucknor, B. L. Franc and S. Majumdar (2016). "Imaging Bone-Cartilage Interactions in Osteoarthritis Using [(18)F]-NaF PET-MRI." Mol Imaging **15**: 1-12.

Scheller, E. L., S. Khandaker, B. S. Learman, W. P. Cawthorn, L. M. Anderson, H. A. Pham, H. Robles, Z. Wang, Z. Li, S. D. Parlee, B. R. Simon, H. Mori, A. J. Bree, C. S. Craft and O. A. MacDougald (2019). "Bone marrow adipocytes resist lipolysis and remodeling in response to beta-adrenergic stimulation." Bone **118**: 32-41.

Schiphof, D., M. Boers and S. M. Bierma-Zeinstra (2008). "Differences in descriptions of Kellgren and Lawrence grades of knee osteoarthritis." Ann Rheum Dis **67**(7): 1034-1036.

Sen, R. K., S. K. Tripathy, S. Aggarwal, N. Marwaha, R. R. Sharma and N. Khandelwal (2012). "Early results of core decompression and autologous bone marrow mononuclear cells instillation in femoral head osteonecrosis: a randomized control study." The Journal of arthroplasty **27**(5): 679-686.

Sharma, L., F. Eckstein, J. Song, A. Guermazi, P. Prasad, D. Kapoor, S. Cahue, M. Marshall, M. Hudelmaier and D. Dunlop (2008). "Relationship of meniscal damage, meniscal extrusion, malalignment, and joint laxity to subsequent cartilage loss in osteoarthritic knees." Arthritis & Rheumatism **58**(6): 1716-1726.

Sheng, H., C. J. Sheng, X. Y. Cheng, G. Zhang, K. M. Lee, K. S. Leung, S. Qu and L. Qin (2013). "Pathomorphological changes of bone marrow adipocytes in process of steroid-associated osteonecrosis." Int J Clin Exp Pathol **6**(6): 1046-1050.

Shih, C. H., W. E. Yang, Z. L. Lee, Y. L. Kao, S. Hsueh and J. S. Wei (1991). "Effect of long-term alcohol ingestion on the femoral head of rabbit." J Formos Med Assoc **90**(5): 443-447.

Silva, D. F., C. V. Carmona, T. R. Calderan, G. P. Fraga, B. Nascimento and S. Rizoli (2013). "The use of corticosteroid for the prophylaxis of fat embolism syndrome in patients with long bone fracture." Rev Col Bras Cir **40**(5): 423-426.

Simkin, P. A. (2004). Bone pain and pressure in osteoarthritic joints. Novartis Foundation Symposium, Chichester; New York; John Wiley; 1999.

Simkin, P. A. (2018). "Marrow fat may distribute the energy of impact loading throughout subchondral bone." Rheumatology (Oxford) **57**(3): 414-418.

Solomon, L. (1981). "Idiopathic necrosis of the femoral head: pathogenesis and treatment." Can J Surg **24**(6): 573-578.

Stabley, J. N., N. C. Moningka, B. J. Behnke and M. D. Delp (2014). "Exercise training augments regional bone and marrow blood flow during exercise." Med Sci Sports Exerc **46**(11): 2107-2112.

Standring, S. (2016). "Gray's Anatomy." Book(41st Edition).

Steffens, D., C. G. Maher, Q. Li, M. L. Ferreira, L. S. Pereira, B. W. Koes and J. Latimer (2014). "Effect of weather on back pain: results from a case-crossover study." Arthritis Care Res (Hoboken) **66**(12): 1867-1872.

Steinke, H. and W. Wolff (2001). "A modified Spalteholz technique with preservation of the histology." Ann Anat **183**(1): 91-95.

Sultan, A. A. and M. A. Mont (2019). "Core Decompression and Bone Grafting for Osteonecrosis of the Talus: A Critical Analysis of the Current Evidence." Foot Ankle Clin **24**(1): 107-112.

Suominen, P., E. Nurmi and K. Lauerma (2015). "Intraosseous access in neonates and infants: risk of severe complications–a case report." Acta Anaesthesiologica Scandinavica **59**(10): 1389-1393.

Swanson, S. A. and M. A. Freeman (1966). "Is bone hydraulically strengthened?" Med Biol Eng **4**(5): 433-438.

Taguchi, K., K. Chiba, N. Okazaki, Y. Kido, T. Miyamoto, A. Yonekura, M. Tomita, M. Uetani and M. Osaki (2017). "Characterization of cartilage defects detected by MRI in Kellgren-Lawrence grade 0 or 1 knees." J Orthop Sci **22**(5): 868-873.

Tannenbaum, J. and B. T. Bennett (2015). "Russell and Burch's 3Rs then and now: the need for clarity in definition and purpose." J Am Assoc Lab Anim Sci **54**(2): 120-132.

Taylor, C. C. and N. Clarke (2011). "Amputation and intraosseous access in infants." BMJ: British Medical Journal (Online) **342**.

Taylor, C. C. and N. M. Clarke (2011). "Amputation and intraosseous access in infants." BMJ **342**: d2778.

Temmerman, O. P., P. G. Raijmakers, R. Kloet, G. J. Teule, I. C. Heyligers and A. A. Lammertsma (2013). "In vivo measurements of blood flow and bone metabolism in osteoarthritis." Rheumatol Int **33**(4): 959-963.

Termansen, N. B. and K. Okholm (1976). "Intraosseous pressure in the femoral head and greater trochanter before and 1-3 years after osteotomy for osteoarthritis of the hip joint." Acta Orthop Scand **47**(1): 96-100.

Termansen, N. B., P. S. Teglbjaerg and K. H. Sorensen (1981). "Primary osteoarthritis of the hip. Interrelationship between intraosseous pressure, X-ray changes, clinical severity and bone density." Acta Orthop Scand **52**(2): 215-222.

Tian, L., X. Q. Dang, C. S. Wang, P. Yang, C. Zhang and K. Z. Wang (2013). "Effects of sodium ferulate on preventing steroid-induced femoral head osteonecrosis in rabbits." J Zhejiang Univ Sci B **14**(5): 426-437.

Tirkkonen, L., H. Halonen, J. Hyttinen, H. Kuokkanen, H. Sievanen, A. M. Koivisto, B. Mannerstrom, G. K. Sandor, R. Suuronen, S. Miettinen and S. Haimi (2011). "The effects of vibration loading on adipose stem cell number, viability and differentiation towards bone-forming cells." J R Soc Interface **8**(65): 1736-1747.

Tondevold, E. and J. Bulow (1983). "Bone Blood-Flow in Conscious Dogs at Rest and during Exercise." Acta Orthopaedica Scandinavica **54**(1): 53-57.

Tøndevold, E. and J. Bülow (1983). "Bone blood flow in conscious dogs at rest and during exercise." Acta Orthopaedica Scandinavica **54**(1): 53-57.

Trueta, J. and A. X. Caladias (1964). "A Study of the Blood Supply of the Long Bones." Surg Gynecol Obstet **118**(3): 485-498.

van Leeuwenhoek, A. (1700). "Part of a letter from Mr Antony van Leeuwenhoek, concerning the worms in sheeps livers, gnats, and animalcula in the excrements of frogs." Philosophical Transactions (1683-1775) **22**: 509-518.

Verbruggen, S. W., T. J. Vaughan and L. M. McNamara (2014). "Fluid flow in the osteocyte mechanical environment: a fluid-structure interaction approach." Biomech Model Mechanobiol **13**(1): 85-97.

Wang, G. J., S. S. Dughman, S. I. Reger and W. G. Stamp (1985). "The effect of core decompression on femoral head blood flow in steroid-induced avascular necrosis of the femoral head." J Bone Joint Surg Am **67**(1): 121-124.

Wang, G. J., S. L. Hubbard, S. I. Reger, E. D. Miller and W. G. Stamp (1983). "Femoral head blood flow in long-term steroid therapy: study of rabbit model." South Med J **76**(12): 1530-1532.

Wang, L., N. Wang, M. Li and K. Wang (2010). "To investigate the role of the nervous system of bone in steroid-induced osteonecrosis in rabbits." Osteoporos Int **21**(12): 2057-2066.

Warner, J. J., J. H. Philip, G. L. Brodsky and T. S. Thornhill (1987). "Studies of nontraumatic osteonecrosis. Manometric and histologic studies of the femoral head after chronic steroid treatment: an experimental study in rabbits." Clin Orthop Relat Res(225): 128-140.

Wilder, F. V., B. J. Hall and J. P. Barrett (2003). "Osteoarthritis pain and weather." Rheumatology (Oxford) **42**(8): 955-958.

Wilkes, C. H. and M. B. Visscher (1975). "Some Physiological Aspects of Bone-Marrow Pressure." Journal of Bone and Joint Surgery-American Volume **A 57**(1): 49-57.

Wong, S. H., K. Y. Chiu and C. H. Yan (2016). "Review Article: Osteophytes." J Orthop Surg (Hong Kong) **24**(3): 403-410.

Yang, L., K. Boyd, S. C. Kaste, L. Kamdem Kamdem, R. J. Rahija and M. V. Relling (2009). "A mouse model for glucocorticoid-induced osteonecrosis: effect of a steroid holiday." J Orthop Res **27**(2): 169-175.

Yoon, B. H., Y. W. Kim and H. K. Yoon (2013). "Patterns of isotope uptake in sequential postoperative bone scan in undisplaced femoral-neck fractures." Int Orthop **37**(8): 1541-1545.

Zhang, D., S. Weinbaum and S. C. Cowin (1998). "Estimates of the peak pressures in bone pore water." J Biomech Eng **120**(6): 697-703.

Zizic, T. M., C. G. Lewis, C. Marcoux and D. S. Hungerford (1989). "The predictive value of hemodynamic studies in preclinical ischemic necrosis of bone." J Rheumatol **16**(12): 1559-1564.

Zizic, T. M., C. Marcoux, D. S. Hungerford and M. B. Stevens (1986). "The early diagnosis of ischemic necrosis of bone." Arthritis Rheum **29**(10): 1177-1186.

Appendix 1

A PubMed search of MEDLINE databases from inception to 2018 was searched for the key words listed below, both individually and in groups appropriate to each chapter. PubMed was searched in all fields for the terms ‘intraosseous pressure’ or ‘intra osseous pressure’. No limits were applied to the search. Secondary references were retrieved from reviews. It was not always possible to survey the whole literature for each term for example, ‘intraosseous pressure’ or ‘osteoarthritis’. Some key words combinations produced no relevant references for example ‘MRI’ and ‘venous or vascular marks’. While it is acknowledged that the traditional key word approach to reference searching has a potential for more bias than a full systematic review or meta-analyses, an attempt to be inclusive and open-minded and to seek the opinion and advice of other orthopaedic surgeons, rheumatologists, radiologists, cardiologists, physiologists and anaesthetists was made. Bodleian Library staff kindly reviewed theses held by the University. These included open access theses from the Medical Sciences Division as well as those from NDORMS to examine the previous standard and pattern in terms of DPhil thesis literature reviews. According to them most theses do not mention searching databases, search terms, PubMed, or even the phrase “literature review”. Nevertheless for this work a further formal review was undertaken.

The Primary key word was ‘intraosseous pressure’. PubMed produced 435 references. Secondary key word groups included: (number of references for this pair of keywords in PubMed in brackets)

- Bone circulation (64), artery (42), vein (50), capillary (11), blood vessel (54), bone perfusion (14), blood flow (77), venous back pressure (3) and tourniquet (6).

- Loading (16), weight bearing (13), hydraulic pressure (4), force (7), bone marrow (87), fat liquid (0) and adipocytes (5).
- MRI 36), vascular marks (0), Kellgren-Lawrence (0), bone scan (20) and osteoarthritis (38).
- Anatomy (169), subchondral (19), histology (164), subcortical (0), endplate (2), bone cartilage (15) and interface (4).
- Disease (96), osteoarthritis (38), osteonecrosis (65), osteoporosis (7), bone pain (56), avascular necrosis (69) and embolic bone disease (16).
- Treatment (280), surgery (180), forage (0), decompression (39) and osteotomy (22).

From more than a thousand references some 500 references were down loaded, reviewed and saved to Endnote X9 of which some 200 are quoted here. The work done in 1985 resulted in several minor presentations and abstracts but no formal papers. Nevertheless that grey literature is quoted here where relevant.